Density Model for Humpback Whale (*Megaptera novaeangliae*) for the U.S. East Coast: Supplementary Report

Duke University Marine Geospatial Ecology Lab[*]

Model Version 9.4 - 2016-04-21

Citation

When referencing our methodology or results generally, please cite our open-access article:

Roberts JJ, Best BD, Mannocci L, Fujioka E, Halpin PN, Palka DL, Garrison LP, Mullin KD, Cole TVN, Khan CB, McLellan WM, Pabst DA, Lockhart GG (2016) Habitat-based cetacean density models for the U.S. Atlantic and Gulf of Mexico. Scientific Reports 6: 22615. doi: 10.1038/srep22615

To reference this specific model or Supplementary Report, please cite:

Roberts JJ, Best BD, Mannocci L, Fujioka E, Halpin PN, Palka DL, Garrison LP, Mullin KD, Cole TVN, Khan CB, McLellan WM, Pabst DA, Lockhart GG (2016) Density Model for Humpback Whale (*Megaptera novaeangliae*) for the U.S. East Coast Version 9.4, 2016-04-21, and Supplementary Report. Marine Geospatial Ecology Lab, Duke University, Durham, North Carolina.

Copyright and License

Revision History

Version	Date	Description of changes
1	2013-05-03	Initial version.
2	2013-05-08	Figures regenerated with improved label placement.
3	2014-03-01	Switched from four seasonal models to two. Reformulated density model using a Horvitz-Thompson estimator. Eliminated GAM for group size (consequence of above). Added group size as a candidate covariate in detection functions (benefit of above). Added survey ID as a candidate covariate in NOAA NARWSS detection functions. Took more care in selecting right-truncation distances. Fitted models with contemporaneous predictors, for comparison to climatological. Switched SST and SST fronts predictors from NOAA Pathfinder to GHRSST CMC0.2deg L4. Changed SST fronts algorithm to use Canny operator instead of Cayula-Cornillon. Switched winds predictors from SCOW to CCMP (SCOW only gives climatol. estimates.) Added DistToEddy predictors, based on Chelton et al. (2011) eddy database. Added cumulative VGPM predictors, summing productivity for 45, 90, and 180 days. Added North Atlantic Oscillation (NAO) predictor; included 3 and 6 month lags. Transformed predictors more carefully, to better minimize leverage of outliers. Implemented hybrid hierarchical-forward / exhaustive model selection procedure. Model selection procedure better avoids concurvity between predictors. Allowed GAMs to select between multiple formulations of dynamic predictors. Adjusted land mask to eliminate additional estuaries and hard-to-predict cells.

[*]For questions, or to offer feedback about this model or report, please contact Jason Roberts (jason.roberts@duke.edu)

4	2014-05-14	Added discussion of acoustic monitoring studies to text. Eliminated accidentally-included off-effort sighting at Cape Lookout (2006-04-20 14:14:00). Refitted summer model.
5	2014-05-20	Fixed bug in temporal variability plots. Density models unchanged.
6	2014-09-02	Added surveys: NJ-DEP, Virginia Aquarium, NARWSS 2013, UNCW 2013. Extended study area up Scotian Shelf. Added SEAPODYM predictors. Switched to mgcv estimation of Tweedie p parameter (family=tw()).
7	2014-10-15	Added Palka (2006) survey-specific g(0) estimates. Removed distance to eddy predictors and wind speed predictor from all models; they were not ecologically justified. Fixed missing pixels in several climatological predictors, which led to not all segments being utilized. Eliminated Cape Cod Bay subregion.
8	2014-11-11	Reconfigured detection hierarchy and adjusted NARWSS detection functions based on additional information from Tim Cole. Removed CumVGPM180 predictor. Updated documentation.
9	2014-12-03	Fixed bug that applied the wrong detection function to segments NE_narwss_1999_widgeon_hapo dataset. Refitted models. Updated documentation.
9.1	2015-03-05	Updated the documentation. No changes to the model.
9.2	2015-05-14	Updated calculation of CVs. Switched density rasters to logarithmic breaks. No changes to the model.
9.3	2015-09-26	Updated the documentation. No changes to the model.
9.4	2016-04-21	Switched calculation of monthly 5% and 95% confidence interval rasters to the method used to produce the year-round rasters. (We intended this to happen in version 9.2 but I did not implement it properly.) Updated the monthly CV rasters to have value 0 where we assumed the species was absent, consistent with the year-round CV raster. No changes to the other (non-zero) CV values, the mean abundance rasters, or the model itself.

Survey Data

Survey	Period	Length (1000 km)	Hours	Sightings
NEFSC Aerial Surveys	1995-2008	70	412	174
NEFSC NARWSS Harbor Porpoise Survey	1999-1999	6	36	9
NEFSC North Atlantic Right Whale Sighting Survey	1999-2013	432	2330	2461
NEFSC Shipboard Surveys	1995-2004	16	1143	41
NJDEP Aerial Surveys	2008-2009	11	60	5
NJDEP Shipboard Surveys	2008-2009	14	836	7
SEFSC Atlantic Shipboard Surveys	1992-2005	28	1731	0
SEFSC Mid Atlantic Tursiops Aerial Surveys	1995-2005	35	196	4
SEFSC Southeast Cetacean Aerial Surveys	1992-1995	8	42	1
UNCW Cape Hatteras Navy Surveys	2011-2013	19	125	6
UNCW Early Marine Mammal Surveys	2002-2002	18	98	3
UNCW Jacksonville Navy Surveys	2009-2013	66	402	2
UNCW Onslow Navy Surveys	2007-2011	49	282	1
UNCW Right Whale Surveys	2005-2008	114	586	11
Virginia Aquarium Aerial Surveys	2012-2014	9	53	7
Total		895	8332	2732

Table 2: Survey effort and sightings used in this model. Effort is tallied as the cumulative length of on-effort transects and hours the survey team was on effort. Sightings are the number of on-effort encounters of the modeled species for which a perpendicular sighting distance (PSD) was available. Off effort sightings and those without PSDs were omitted from the analysis.

Season	Months	Length (1000 km)	Hours	Sightings
Winter	Dec Jan Feb Mar	274	2099	149
Summer	Apr May Jun Jul Aug Sep Oct Nov	622	6234	2583

Table 3: Survey effort and on-effort sightings having perpendicular sighting distances, summarized by season.

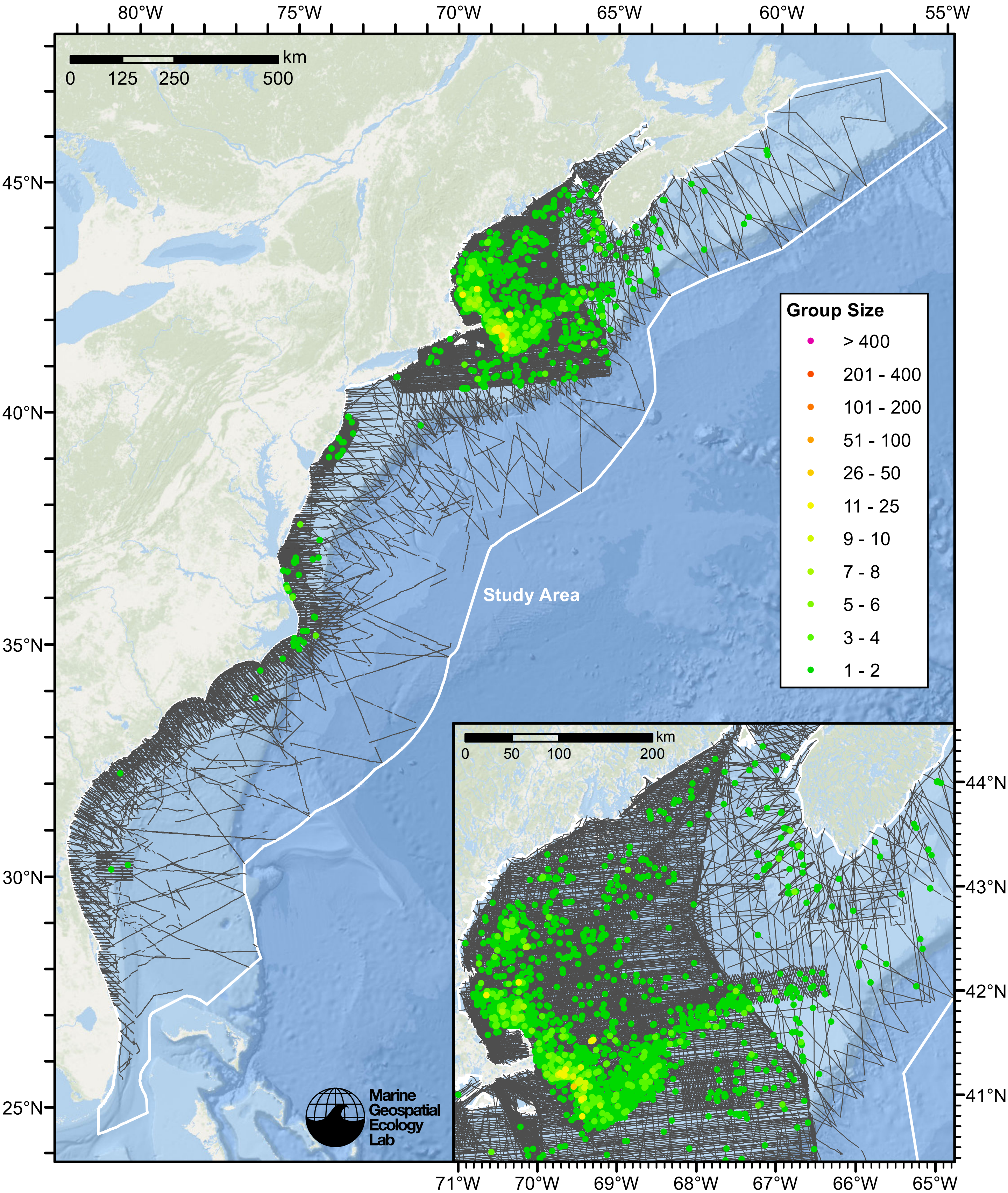

Figure 1: Humpback whale sightings and survey tracklines.

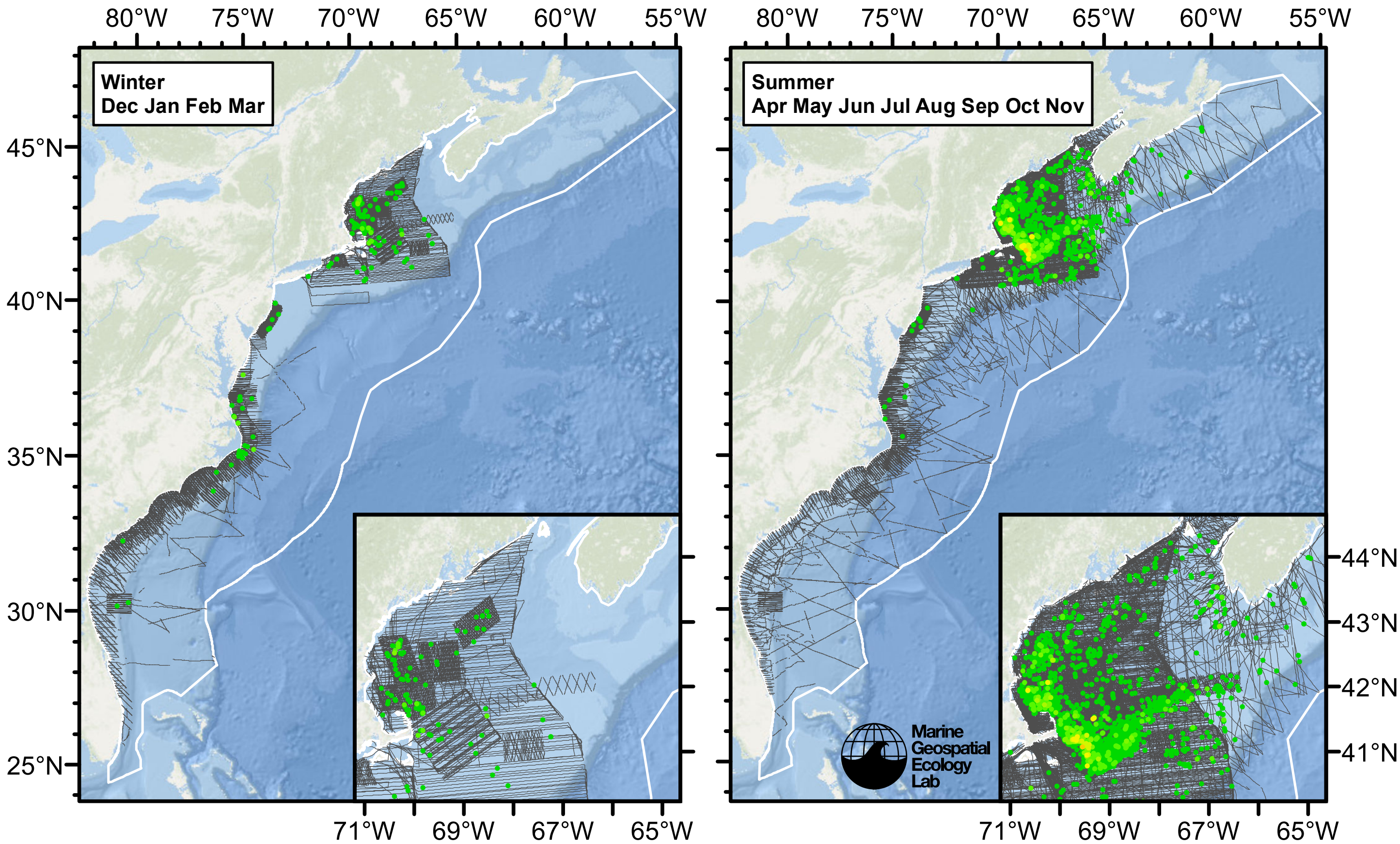

Figure 2: Humpback whale sightings and survey tracklines, by season. Sighting colors are the same as the previous figure.

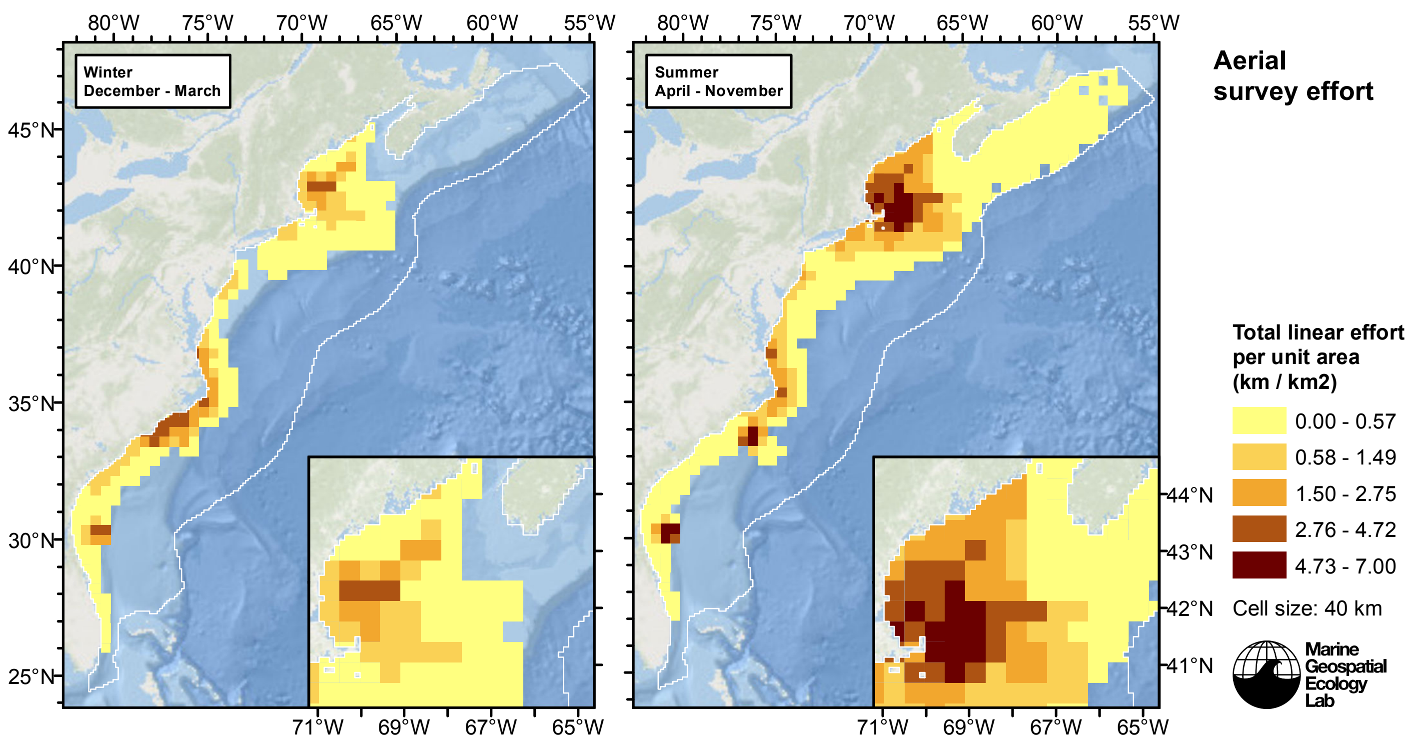

Figure 3: Aerial linear survey effort per unit area.

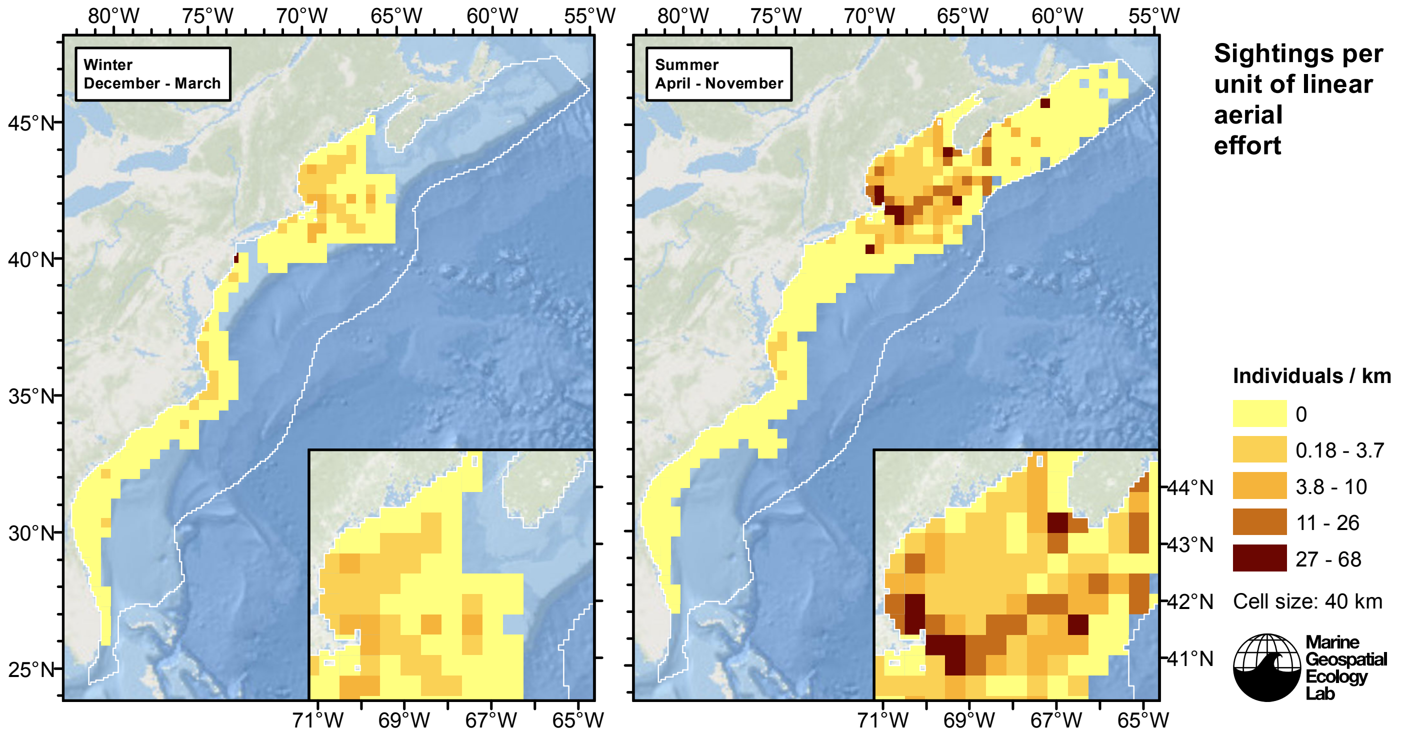

Figure 4: Humpback whale sightings per unit aerial linear survey effort.

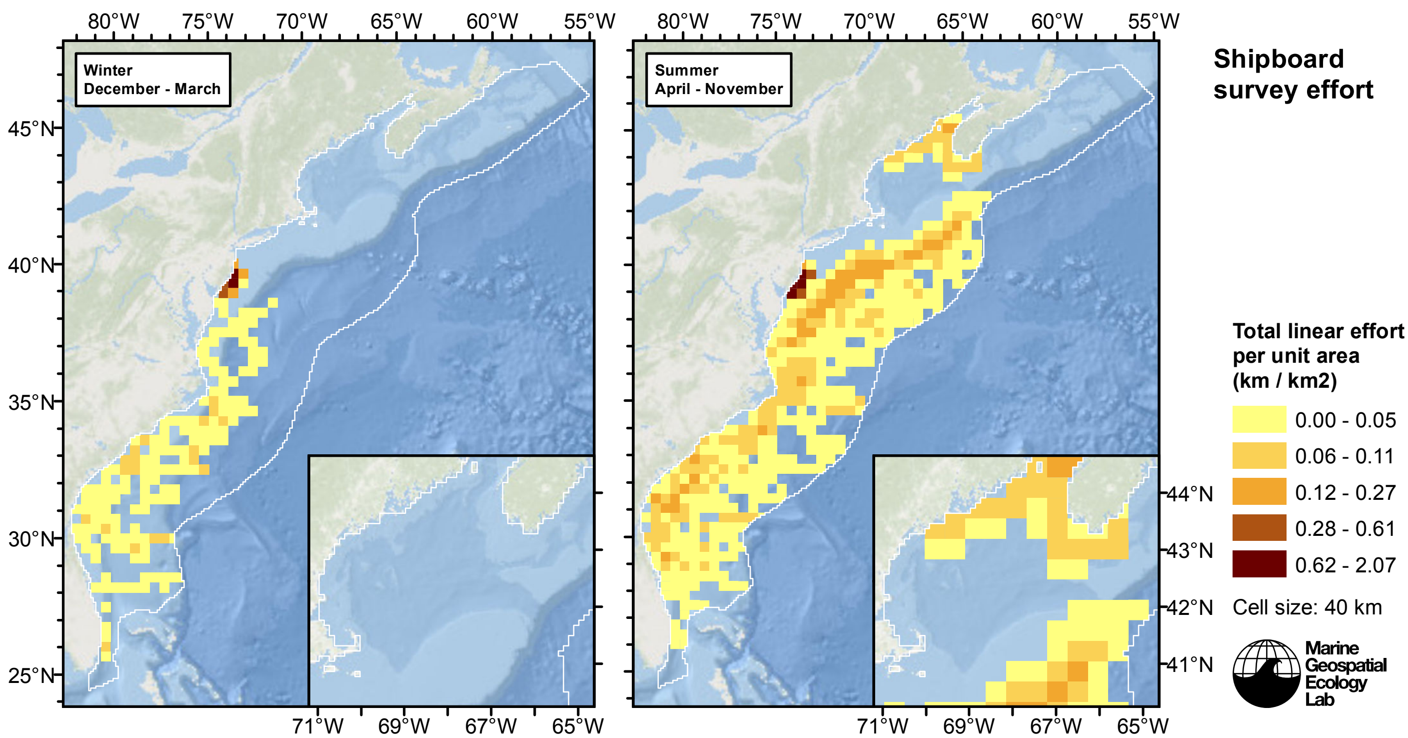

Figure 5: Shipboard linear survey effort per unit area.

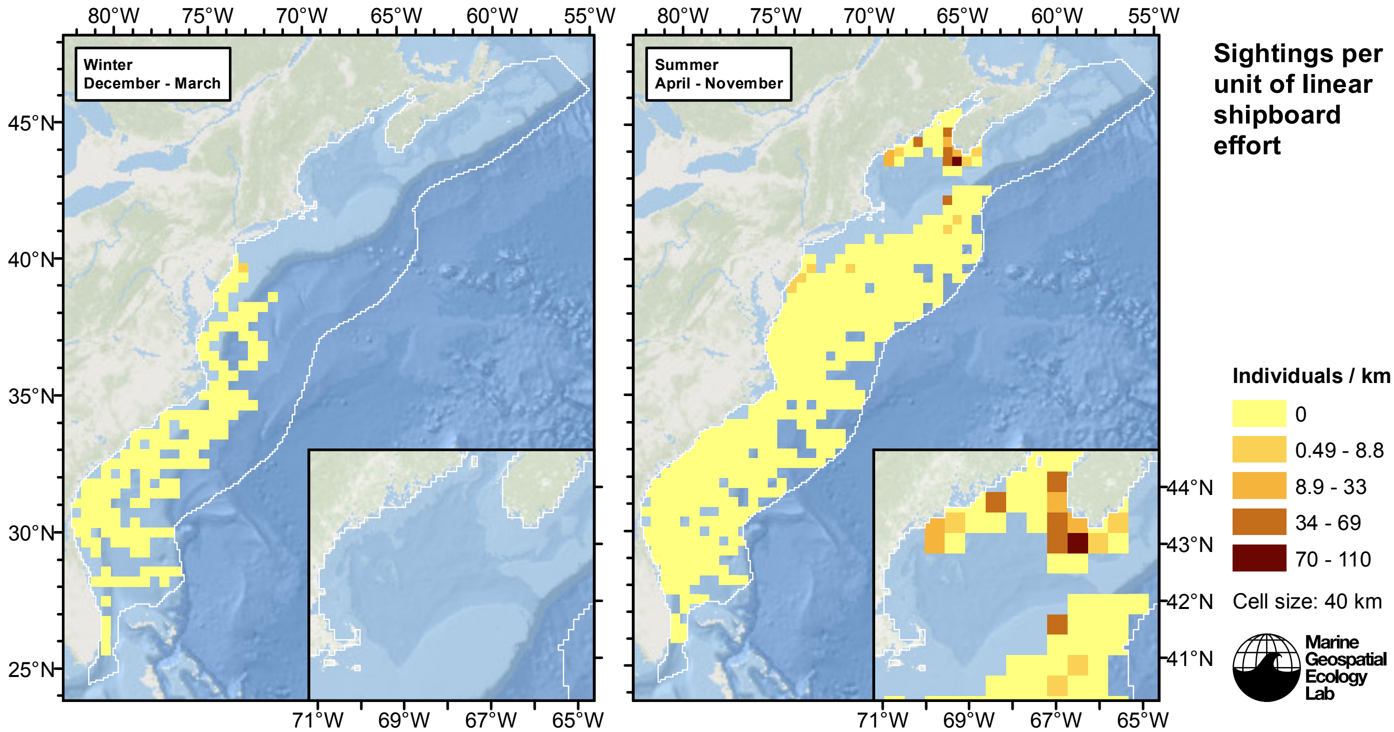

Figure 6: Humpback whale sightings per unit shipboard linear survey effort.

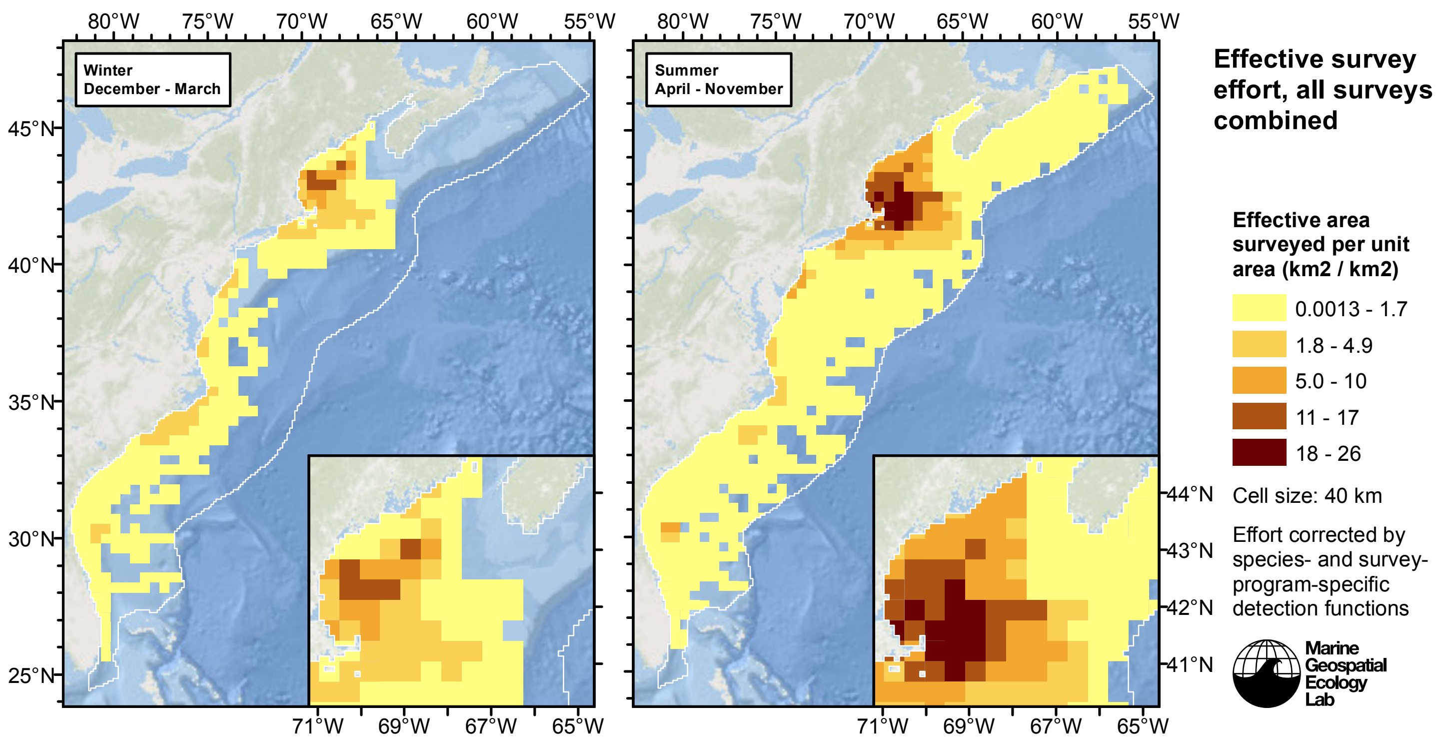

Figure 7: Effective survey effort per unit area, for all surveys combined. Here, effort is corrected by the species- and survey-program-specific detection functions used in fitting the density models.

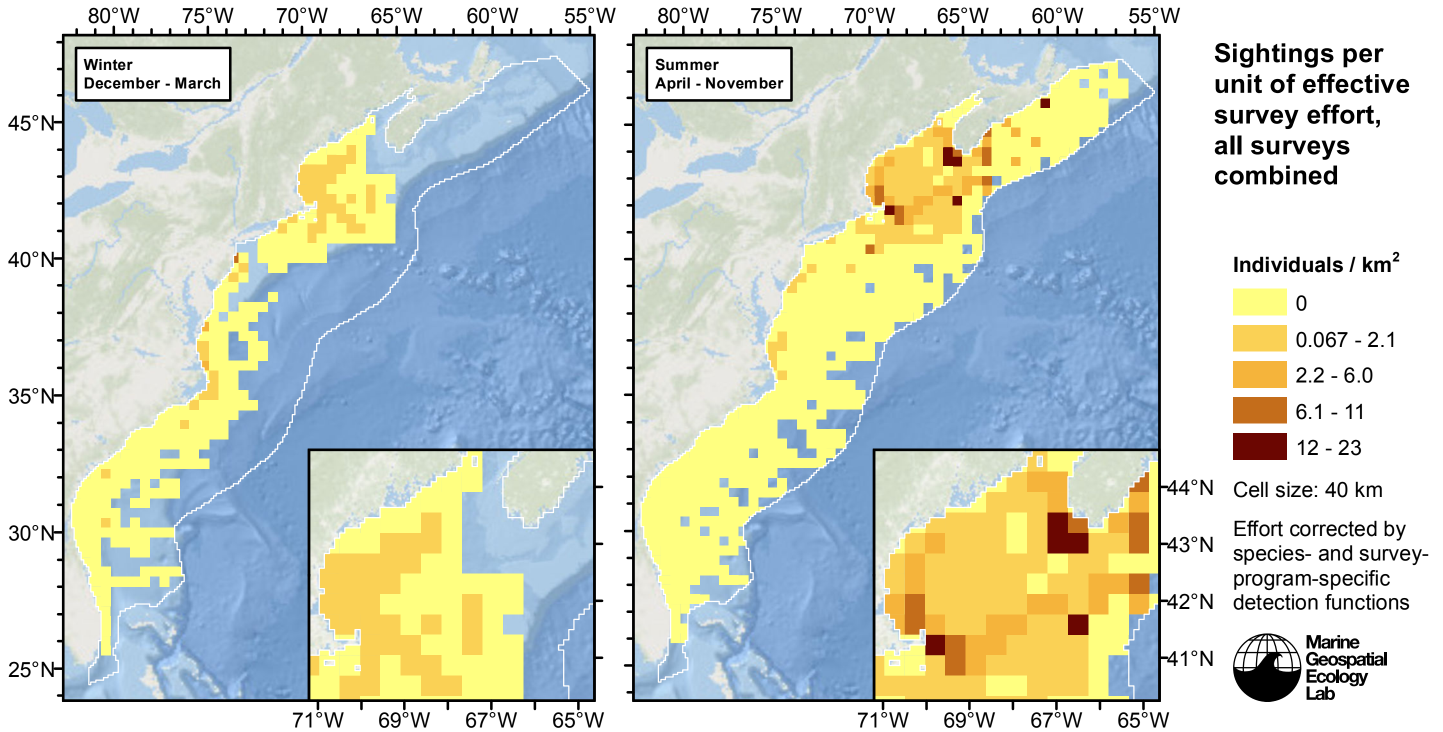

Figure 8: Humpback whale sightings per unit of effective survey effort, for all surveys combined. Here, effort is corrected by the species- and survey-program-specific detection functions used in fitting the density models.

Detection Functions

The detection hierarchy figures below show how sightings from multiple surveys were pooled to try to achieve Buckland et. al's (2001) recommendation that at least 60-80 sightings be used to fit a detection function. Leaf nodes, on the right, usually represent individual surveys, while the hierarchy to the left shows how they have been grouped according to how similar we believed the surveys were to each other in their detection performance.

At each node, the red or green number indicates the total number of sightings below that node in the hierarchy, and is colored green if 70 or more sightings were available, and red otherwise. If a grouping node has zero sightings–i.e. all of the surveys within it had zero sightings–it may be collapsed and shown as a leaf to save space.

Each histogram in the figure indicates a node where a detection function was fitted. The actual detection functions do not appear in this figure; they are presented in subsequent sections. The histogram shows the frequency of sightings by perpendicular sighting distance for all surveys contained by that node. Each survey (leaf node) recieves the detection function that is closest to it up the hierarchy. Thus, for common species, sufficient sightings may be available to fit detection functions deep in the hierarchy, with each function applying to only a few surveys, thereby allowing variability in detection performance between surveys to be addressed relatively finely. For rare species, so few sightings may be available that we have to pool many surveys together to try to meet Buckland's recommendation, and fit only a few coarse detection functions high in the hierarchy.

A blue Proxy Species tag indicates that so few sightings were available that, rather than ascend higher in the hierarchy to a point that we would pool grossly-incompatible surveys together, (e.g. shipboard surveys that used big-eye binoculars with those that used only naked eyes) we pooled sightings of similar species together instead. The list of species pooled is given in following sections.

Shipboard Surveys

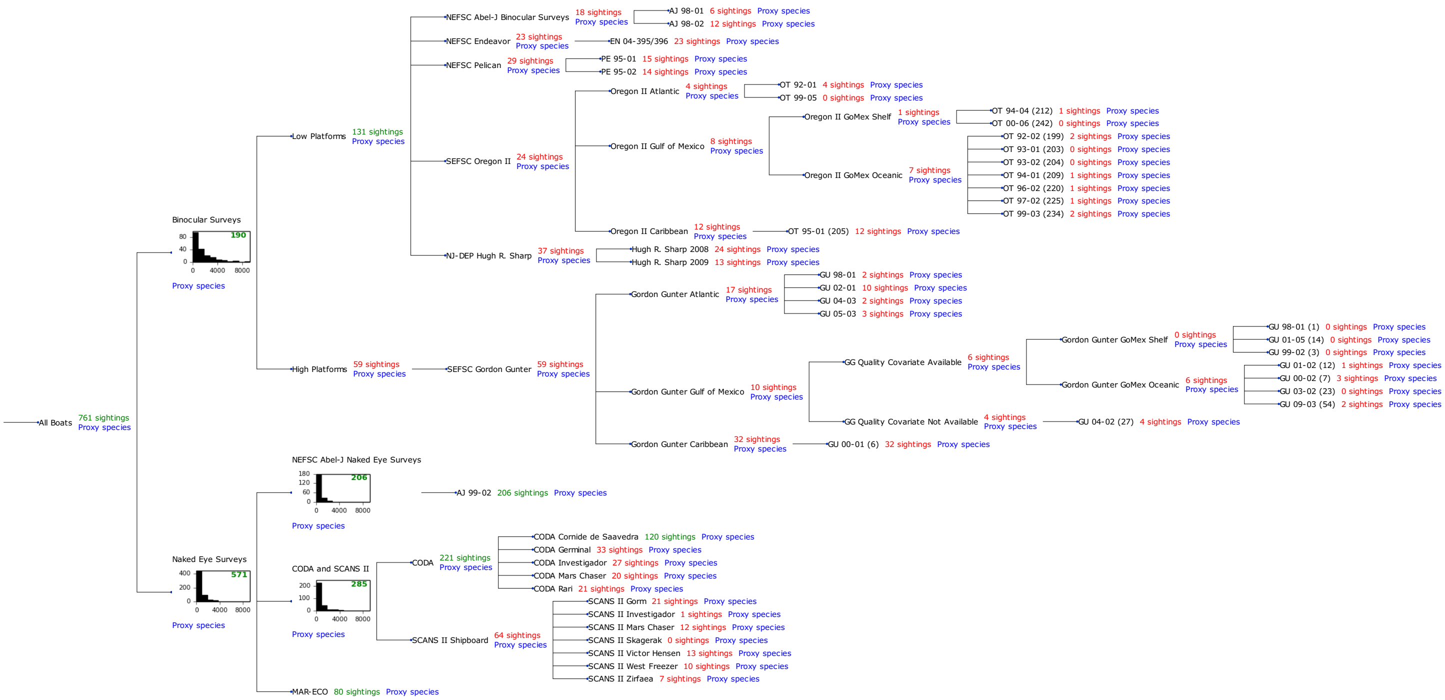

Figure 9: Detection hierarchy for shipboard surveys

Binocular Surveys

Because this taxon was sighted too infrequently to fit a detection function to its sightings alone, we fit a detection function to the pooled sightings of several other species that we believed would exhibit similar detectability. These "proxy species" are listed below.

Reported By Observer	Common Name	n
Balaenoptera	Balaenopterid sp.	8
Balaenoptera acutorostrata	Minke whale	4
Balaenoptera borealis	Sei whale	4
Balaenoptera borealis/edeni	Sei or Bryde's whale	6
Balaenoptera borealis/physalus	Fin or Sei whale	0
Balaenoptera edeni	Bryde's whale	21
Balaenoptera musculus	Blue whale	0
Balaenoptera physalus	Fin whale	98
Eubalaena glacialis	North Atlantic right whale	4
Eubalaena glacialis/Megaptera novaeangliae	Right or humpback whale	0
Megaptera novaeangliae	Humpback whale	46
Total		191

Table 4: Proxy species used to fit detection functions for Binocular Surveys. The number of sightings, n, is before truncation.

The sightings were right truncated at 5500m.

Covariate	Description
beaufort	Beaufort sea state.
size	Estimated size (number of individuals) of the sighted group.
vessel	Vessel from which the observation was made. This covariate allows the detection function to account for vessel-specific biases, such as the height of the survey platform.

Table 5: Covariates tested in candidate "multi-covariate distance sampling" (MCDS) detection functions.

Key	Adjustment	Order	Covariates	Succeeded	Δ AIC	Mean ESHW (m)
hr	poly	4		Yes	0.00	1354
hr			size	Yes	0.31	1757
hr				Yes	0.33	1542
hn	cos	2		Yes	1.52	1802
hr			beaufort, size	Yes	2.17	1780
hr			beaufort	Yes	2.24	1553
hr	poly	2		Yes	2.33	1542
hr			size, vessel	Yes	5.84	1920
hr			vessel	Yes	6.42	1605
hr			beaufort, size, vessel	Yes	7.56	1952
hr			beaufort, vessel	Yes	8.03	1675
hn	cos	3		Yes	9.44	1787
hn			size	Yes	11.39	2317
hn			beaufort, size	Yes	13.21	2319
hn			size, vessel	Yes	14.82	2298
hn			vessel	Yes	17.10	2301
hn				Yes	17.13	2311
hn			beaufort	Yes	18.72	2311
hn	herm	4		Yes	18.78	2306
hn			beaufort, vessel	No		
hn			beaufort, size, vessel	No		

Table 6: Candidate detection functions for Binocular Surveys. The first one listed was selected for the density model.

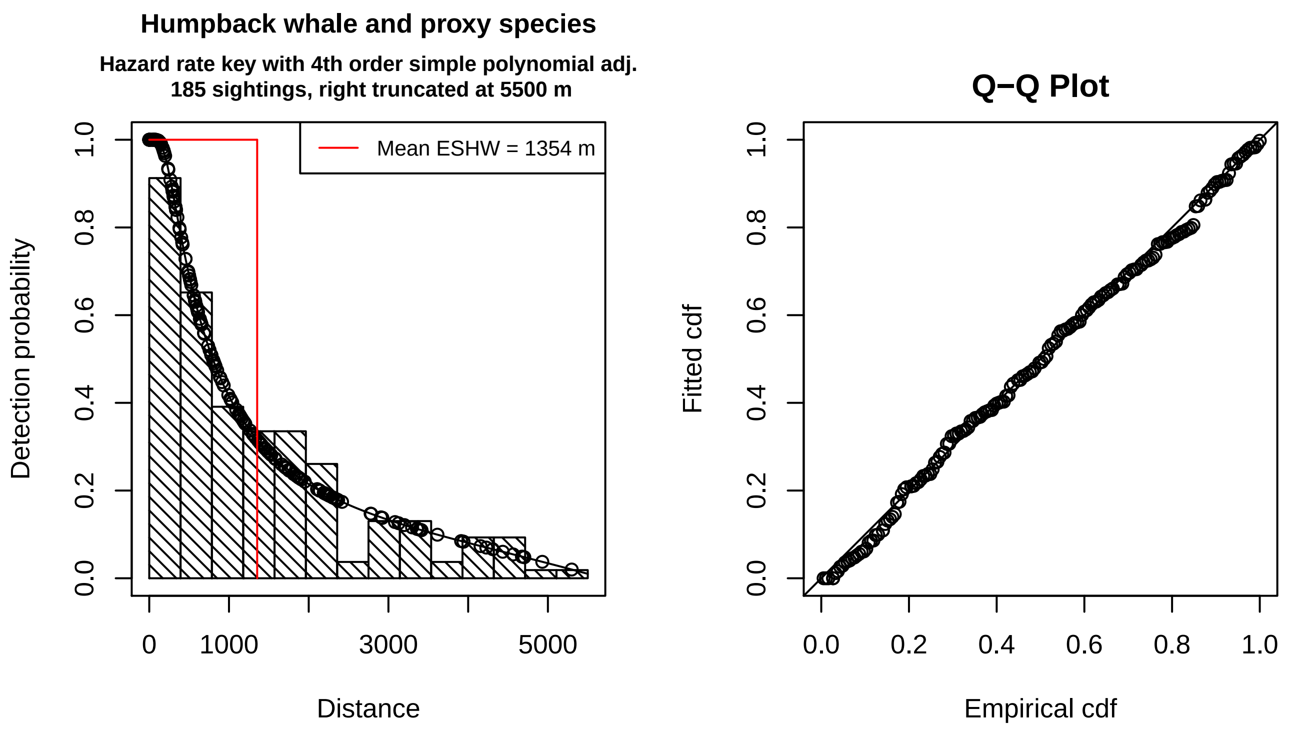

Figure 10: Detection function for Binocular Surveys that was selected for the density model

Statistical output for this detection function:

```
Summary for ds object
Number of observations :  185
Distance range         :  0  -  5500
AIC                    :  3030.414

Detection function:
 Hazard-rate key function with simple polynomial adjustment term of order 4

Detection function parameters
Scale Coefficients:
            estimate        se
(Intercept) 6.355815 0.3367864

Shape parameters:
             estimate        se
(Intercept) 0.1193933 0.1815256

Adjustment term parameter(s):
                  estimate        se
poly, order 4 -0.8663169 0.2837938


Monotonicity constraints were enforced.
                       Estimate          SE        CV
Average p             0.2460911   0.03962055 0.1609995
N in covered region 751.7541457 130.19901860 0.1731936

Monotonicity constraints were enforced.
```

Additional diagnostic plots:

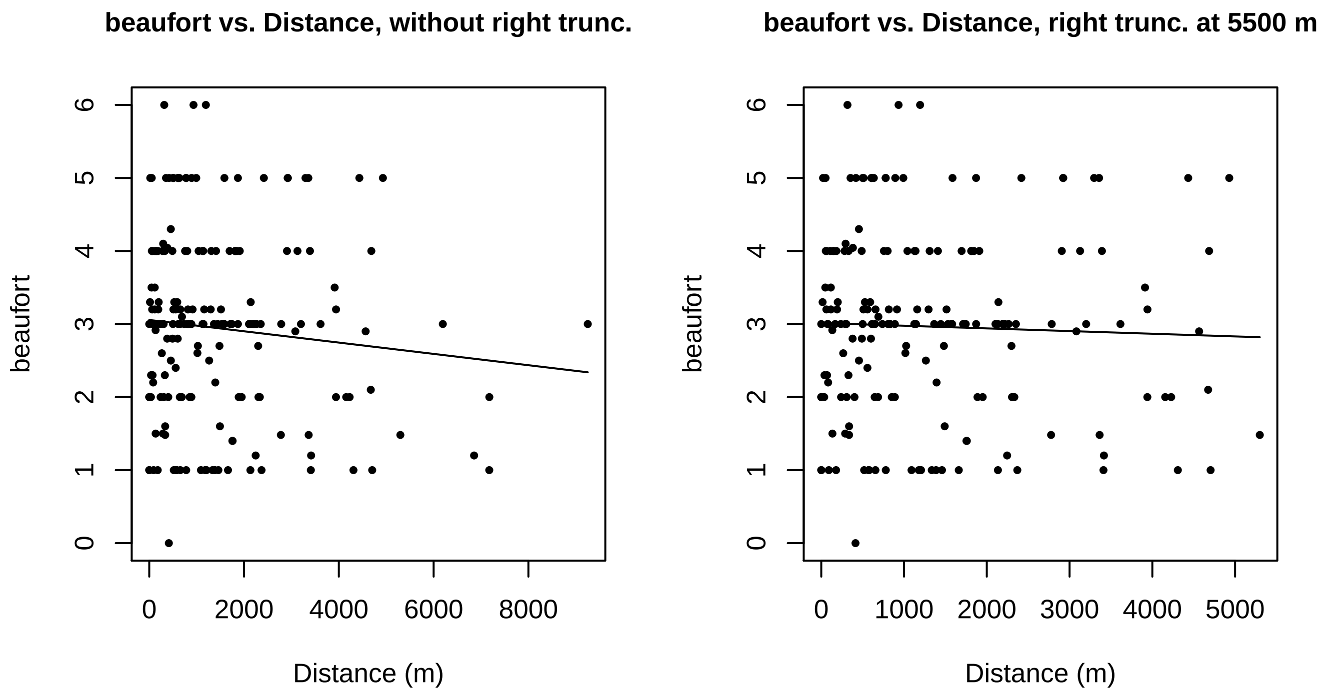

Figure 11: Scatterplots showing the relationship between Beaufort sea state and perpendicular sighting distance, for all sightings (left) and only those not right truncated (right). The line is a simple linear regression.

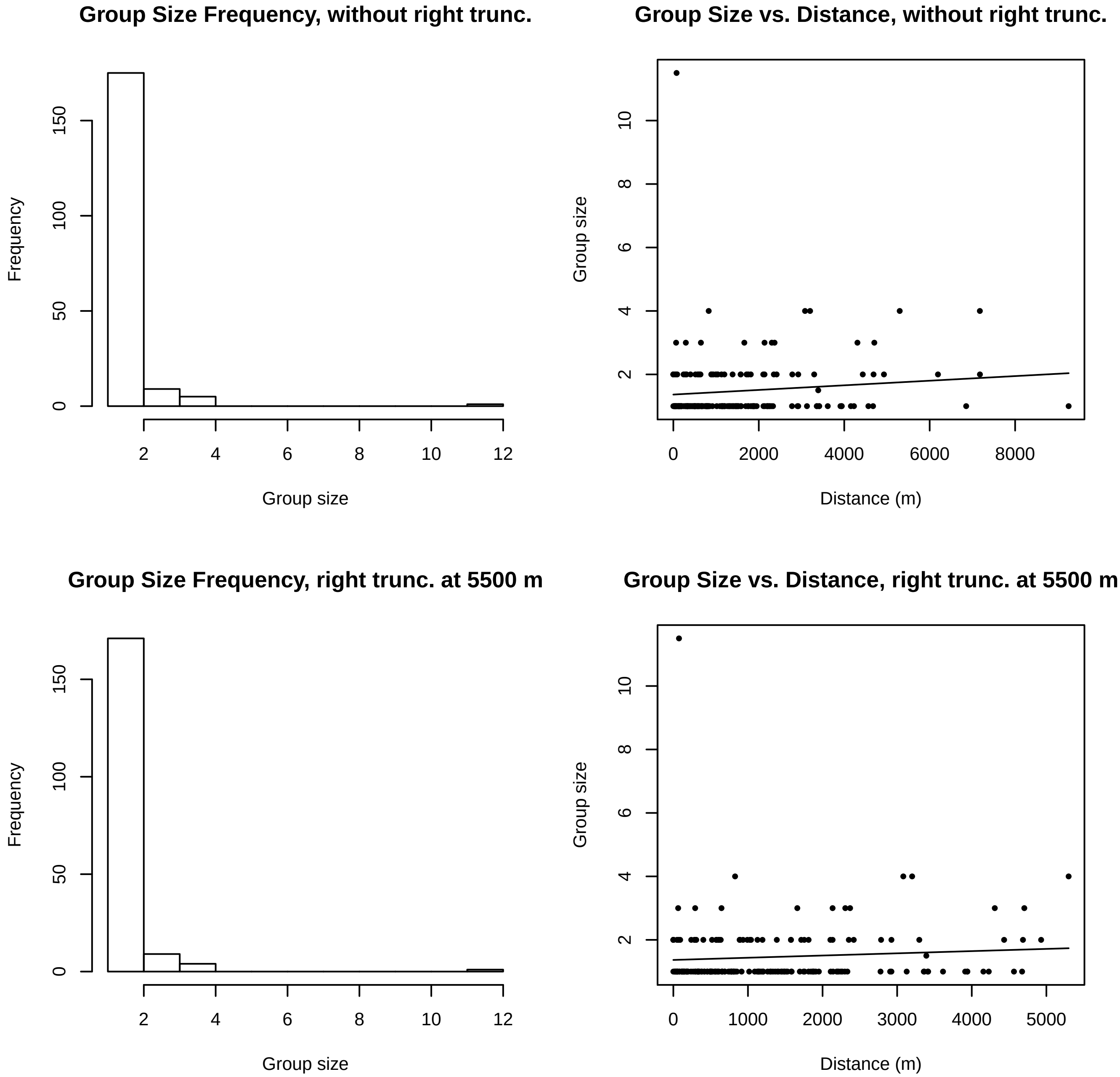

Figure 12: Histograms showing group size frequency and scatterplots showing the relationship between group size and perpendicular sighting distance, for all sightings (top row) and only those not right truncated (bottom row). In the scatterplot, the line is a simple linear regression.

Naked Eye Surveys

Because this taxon was sighted too infrequently to fit a detection function to its sightings alone, we fit a detection function to the pooled sightings of several other species that we believed would exhibit similar detectability. These “proxy species” are listed below.

Reported By Observer	Common Name	n
Balaenoptera	Balaenopterid sp.	7
Balaenoptera acutorostrata	Minke whale	177

Balaenoptera borealis	Sei whale	68
Balaenoptera borealis/edeni	Sei or Bryde's whale	0
Balaenoptera borealis/physalus	Fin or Sei whale	4
Balaenoptera edeni	Bryde's whale	1
Balaenoptera musculus	Blue whale	5
Balaenoptera physalus	Fin whale	261
Eubalaena glacialis	North Atlantic right whale	10
Eubalaena glacialis/Megaptera novaeangliae	Right or humpback whale	0
Megaptera novaeangliae	Humpback whale	38
Total		571

Table 7: Proxy species used to fit detection functions for Naked Eye Surveys. The number of sightings, n, is before truncation.

The sightings were right truncated at 2500m.

Covariate	Description
beaufort	Beaufort sea state.
size	Estimated size (number of individuals) of the sighted group.

Table 8: Covariates tested in candidate "multi-covariate distance sampling" (MCDS) detection functions.

Key	Adjustment	Order	Covariates	Succeeded	Δ AIC	Mean ESHW (m)
hn	cos	2		Yes	0.00	788
hr			size	Yes	0.23	881
hr	poly	2		Yes	4.00	802
hr	poly	4		Yes	4.09	816
hr				Yes	5.53	844
hn	cos	3		Yes	12.95	774
hn			size	Yes	17.09	953
hn			beaufort, size	Yes	19.06	953
hn				Yes	28.40	951
hn	herm	4		Yes	29.75	950
hn			beaufort	Yes	30.12	951
hr			beaufort	No		
hr			beaufort, size	No		

Table 9: Candidate detection functions for Naked Eye Surveys. The first one listed was selected for the density model.

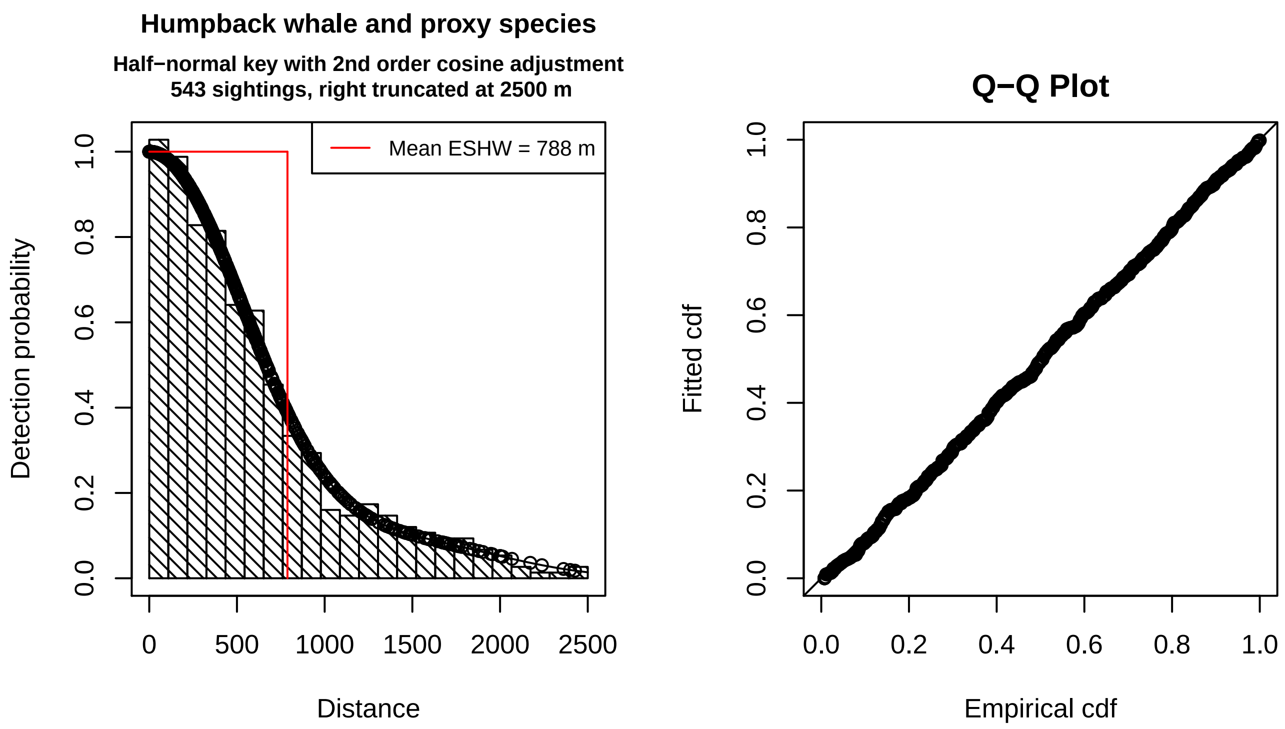

Figure 13: Detection function for Naked Eye Surveys that was selected for the density model

Statistical output for this detection function:

```
Summary for ds object
Number of observations :  543
Distance range         :  0  -  2500
AIC                    :  7957.87

Detection function:
 Half-normal key function with cosine adjustment term of order 2

Detection function parameters
Scale Coefficients:
            estimate         se
(Intercept) 6.752184 0.03908018

Adjustment term parameter(s):
             estimate         se
cos, order 2 0.410427 0.07032538


Monotonicity constraints were enforced.
                        Estimate          SE         CV
Average p              0.3152031  0.01193739 0.03787208
N in covered region 1722.6990344 89.43828822 0.05191754

Monotonicity constraints were enforced.
```

Additional diagnostic plots:

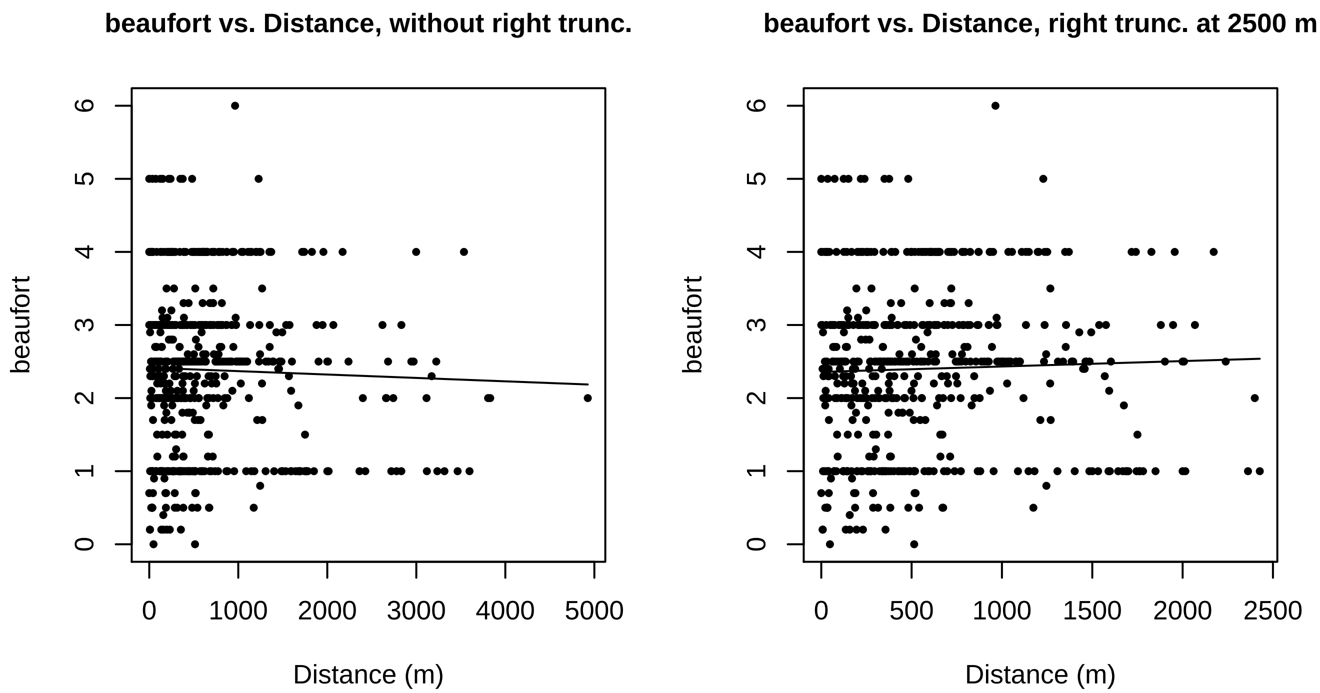

Figure 14: Scatterplots showing the relationship between Beaufort sea state and perpendicular sighting distance, for all sightings (left) and only those not right truncated (right). The line is a simple linear regression.

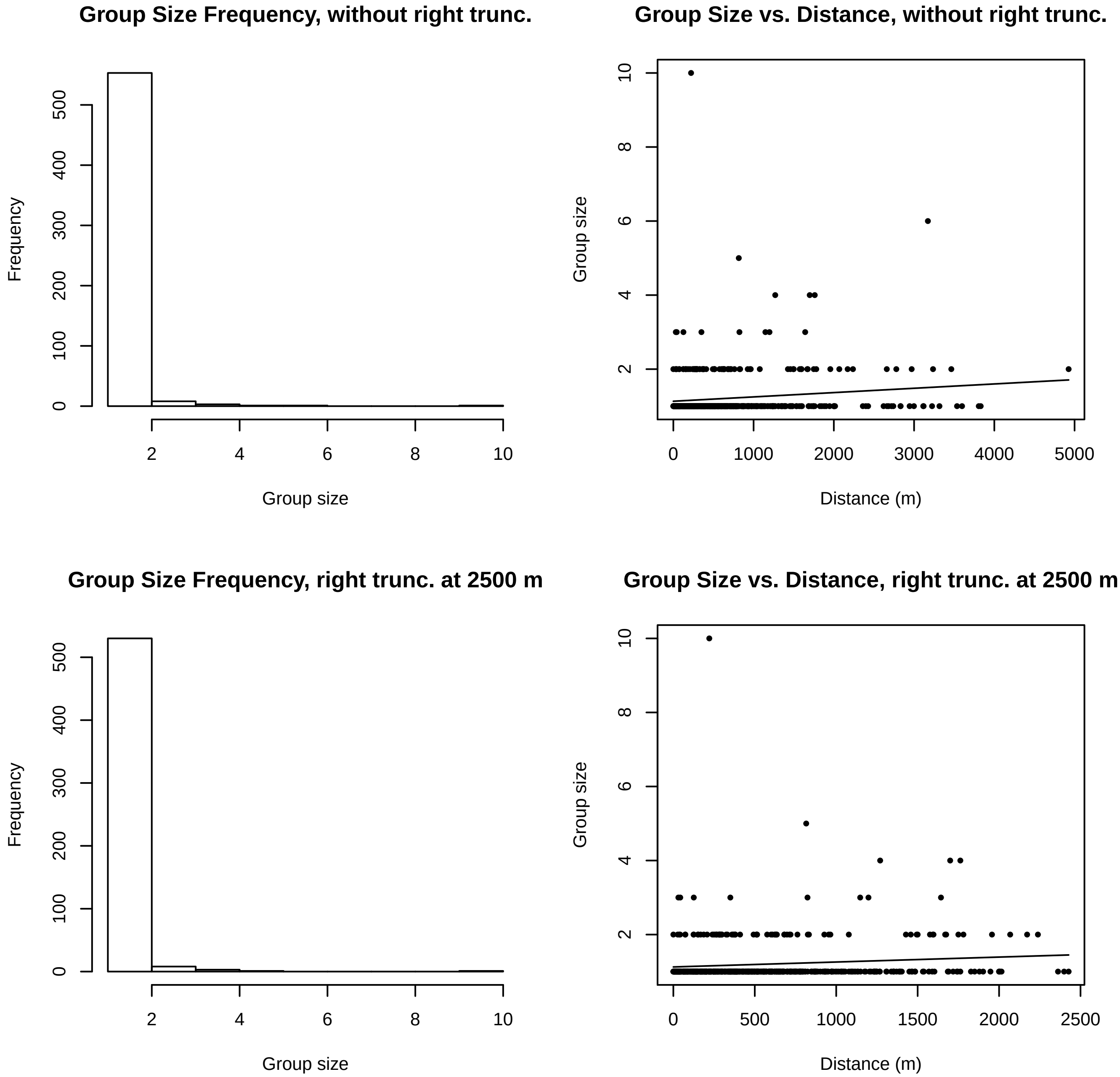

Figure 15: Histograms showing group size frequency and scatterplots showing the relationship between group size and perpendicular sighting distance, for all sightings (top row) and only those not right truncated (bottom row). In the scatterplot, the line is a simple linear regression.

NEFSC Abel-J Naked Eye Surveys

Because this taxon was sighted too infrequently to fit a detection function to its sightings alone, we fit a detection function to the pooled sightings of several other species that we believed would exhibit similar detectability. These "proxy species" are listed below.

Reported By Observer	Common Name	n
Balaenoptera	Balaenopterid sp.	0
Balaenoptera acutorostrata	Minke whale	100

Balaenoptera borealis	Sei whale	2
Balaenoptera borealis/edeni	Sei or Bryde's whale	0
Balaenoptera borealis/physalus	Fin or Sei whale	0
Balaenoptera edeni	Bryde's whale	0
Balaenoptera musculus	Blue whale	0
Balaenoptera physalus	Fin whale	57
Eubalaena glacialis	North Atlantic right whale	10
Eubalaena glacialis/Megaptera novaeangliae	Right or humpback whale	0
Megaptera novaeangliae	Humpback whale	37
Total		206

Table 10: Proxy species used to fit detection functions for NEFSC Abel-J Naked Eye Surveys. The number of sightings, n, is before truncation.

The sightings were right truncated at 2500m.

Covariate	Description
beaufort	Beaufort sea state.
quality	Survey-specific index of the quality of observation conditions, utilizing relevant factors other than Beaufort sea state (see methods).
size	Estimated size (number of individuals) of the sighted group.

Table 11: Covariates tested in candidate "multi-covariate distance sampling" (MCDS) detection functions.

Key	Adjustment	Order	Covariates	Succeeded	Δ AIC	Mean ESHW (m)
hn	cos	2		Yes	0.00	714
hr			size	Yes	0.04	799
hr				Yes	0.63	760
hr	poly	4		Yes	0.75	741
hr	poly	2		Yes	1.11	728
hn	cos	3		Yes	2.84	669
hn			size	Yes	5.19	854
hn			quality, size	Yes	6.85	854
hn				Yes	10.43	845
hn			quality	Yes	12.24	845
hn	herm	4		Yes	12.25	844
hr			beaufort	No		
hn			beaufort	No		
hr			quality	No		
hr			beaufort, quality	No		

hn	beaufort, quality	No
hr	beaufort, size	No
hn	beaufort, size	No
hr	quality, size	No
hr	beaufort, quality, size	No
hn	beaufort, quality, size	No

Table 12: Candidate detection functions for NEFSC Abel-J Naked Eye Surveys. The first one listed was selected for the density model.

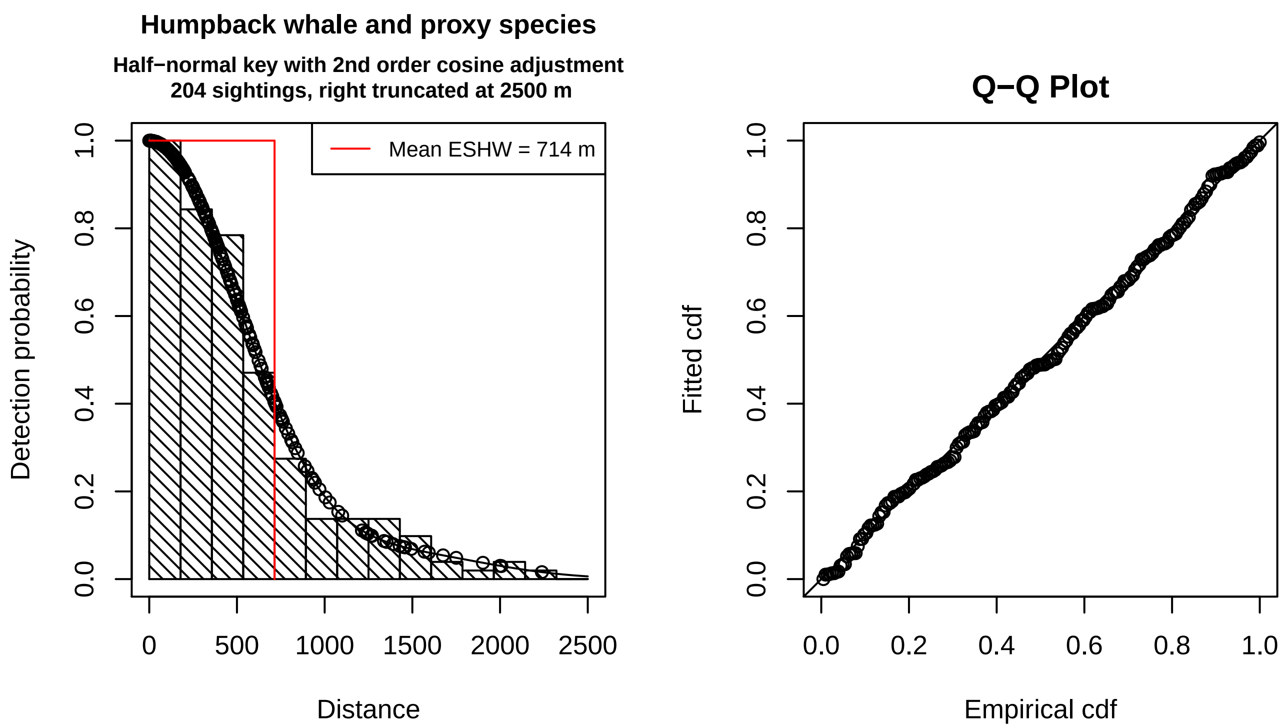

Figure 16: Detection function for NEFSC Abel-J Naked Eye Surveys that was selected for the density model

Statistical output for this detection function:

```
Summary for ds object
Number of observations :  204
Distance range         :  0  -  2500
AIC                    :  2944.665

Detection function:
 Half-normal key function with cosine adjustment term of order 2

Detection function parameters
Scale Coefficients:
            estimate         se
(Intercept) 6.665111 0.06962658

Adjustment term parameter(s):
```

```
              estimate        se
cos, order 2 0.4654074 0.1236342


Monotonicity constraints were enforced.
                       Estimate          SE         CV
Average p             0.2857526  0.01551915 0.05430975
N in covered region 713.9042227 57.33838325 0.08031663

Monotonicity constraints were enforced.
```

Additional diagnostic plots:

Figure 17: Scatterplots showing the relationship between Beaufort sea state and perpendicular sighting distance, for all sightings (left) and only those not right truncated (right). The line is a simple linear regression.

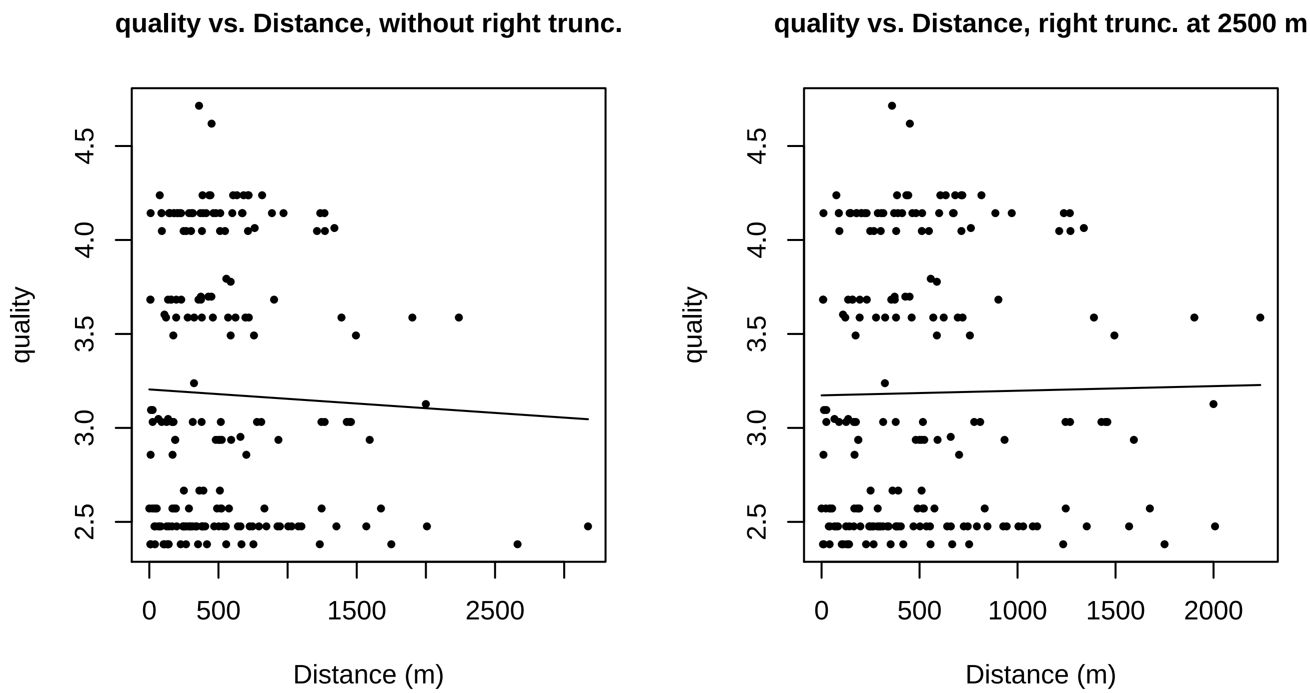

Figure 18: Scatterplots showing the relationship between the survey-specific index of the quality of observation conditions and perpendicular sighting distance, for all sightings (left) and only those not right truncated (right). Low values of the quality index correspond to better observation conditions. The line is a simple linear regression.

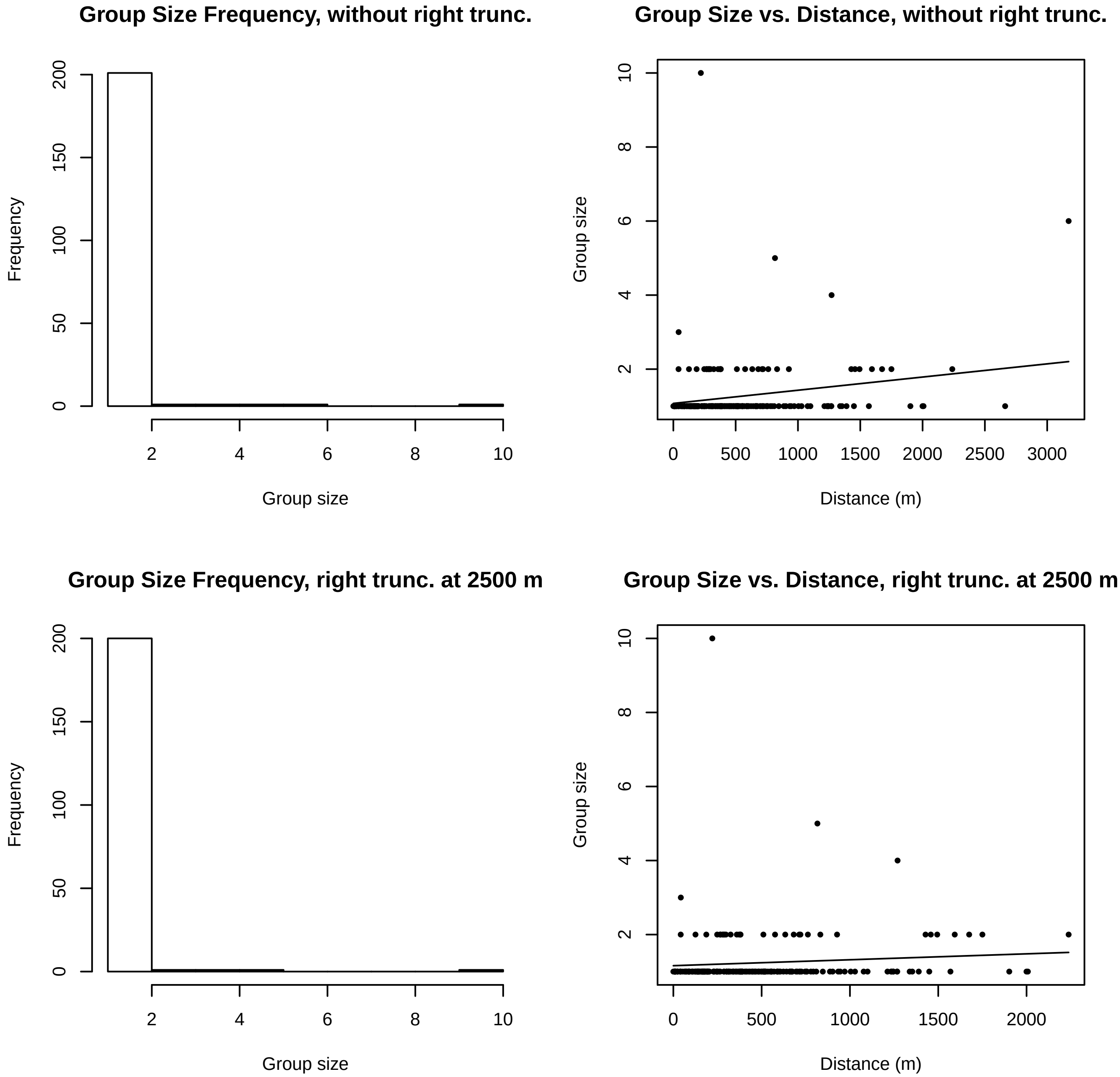

Figure 19: Histograms showing group size frequency and scatterplots showing the relationship between group size and perpendicular sighting distance, for all sightings (top row) and only those not right truncated (bottom row). In the scatterplot, the line is a simple linear regression.

CODA and SCANS II

Because this taxon was sighted too infrequently to fit a detection function to its sightings alone, we fit a detection function to the pooled sightings of several other species that we believed would exhibit similar detectability. These “proxy species” are listed below.

Reported By Observer	Common Name	n
Balaenoptera	Balaenopterid sp.	0
Balaenoptera acutorostrata	Minke whale	76

Balaenoptera borealis	Sei whale	12
Balaenoptera borealis/edeni	Sei or Bryde's whale	0
Balaenoptera borealis/physalus	Fin or Sei whale	4
Balaenoptera edeni	Bryde's whale	0
Balaenoptera musculus	Blue whale	1
Balaenoptera physalus	Fin whale	192
Eubalaena glacialis	North Atlantic right whale	0
Eubalaena glacialis/Megaptera novaeangliae	Right or humpback whale	0
Megaptera novaeangliae	Humpback whale	0
Total		285

Table 13: Proxy species used to fit detection functions for CODA and SCANS II. The number of sightings, n, is before truncation.

The sightings were right truncated at 2500m.

Covariate	Description
beaufort	Beaufort sea state.
quality	Survey-specific index of the quality of observation conditions, utilizing relevant factors other than Beaufort sea state (see methods).
size	Estimated size (number of individuals) of the sighted group.

Table 14: Covariates tested in candidate "multi-covariate distance sampling" (MCDS) detection functions.

Key	Adjustment	Order	Covariates	Succeeded	Δ AIC	Mean ESHW (m)
hn	cos	2		Yes	0.00	796
hn			size	Yes	3.86	900
hn				Yes	4.25	901
hn	cos	3		Yes	4.27	815
hr				Yes	5.06	929
hn	herm	4		Yes	6.02	899
hr			size	Yes	7.05	931
hr	poly	4		Yes	7.06	929
hr	poly	2		Yes	7.06	929
hr			beaufort	No		
hn			beaufort	No		
hr			quality	No		
hn			quality	No		
hr			beaufort, quality	No		
hn			beaufort, quality	No		

hr	beaufort, size	No
hn	beaufort, size	No
hr	quality, size	No
hn	quality, size	No
hr	beaufort, quality, size	No
hn	beaufort, quality, size	No

Table 15: Candidate detection functions for CODA and SCANS II. The first one listed was selected for the density model.

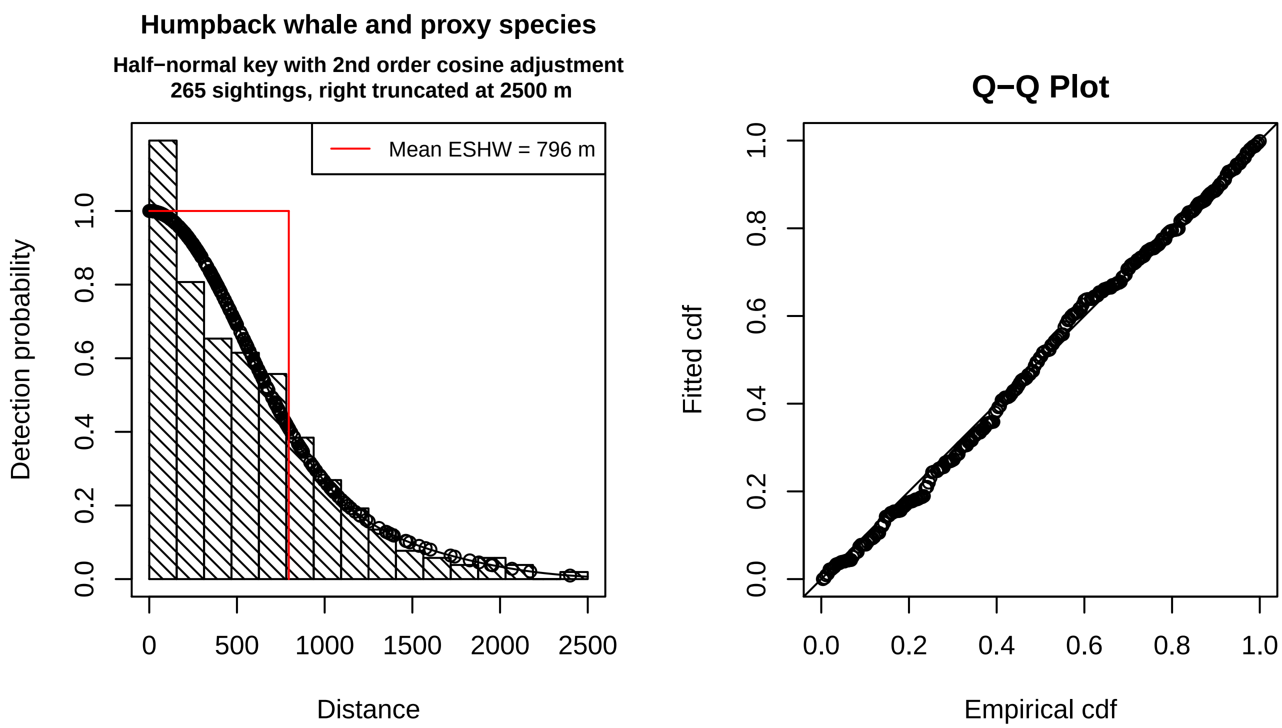

Figure 20: Detection function for CODA and SCANS II that was selected for the density model

Statistical output for this detection function:

```
Summary for ds object
Number of observations :  265
Distance range         :  0  -  2500
AIC                    :  3866.705

Detection function:
 Half-normal key function with cosine adjustment term of order 2

Detection function parameters
Scale Coefficients:
            estimate         se
(Intercept) 6.669731 0.05442969

Adjustment term parameter(s):
```

```
               estimate        se
cos, order 2 0.2899891 0.1074275


Monotonicity constraints were enforced.
                      Estimate          SE         CV
Average p             0.318228  0.01860599 0.05846748
N in covered region 832.736158 64.45598536 0.07740265

Monotonicity constraints were enforced.
```

Additional diagnostic plots:

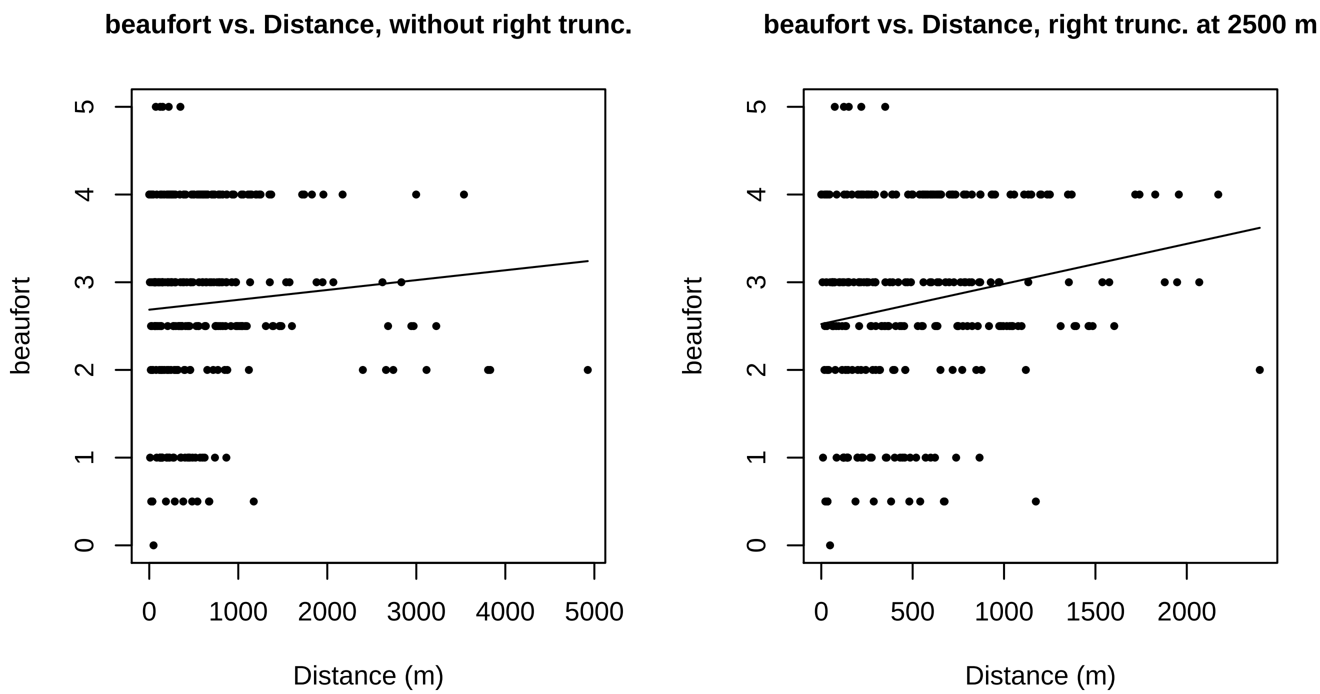

Figure 21: Scatterplots showing the relationship between Beaufort sea state and perpendicular sighting distance, for all sightings (left) and only those not right truncated (right). The line is a simple linear regression.

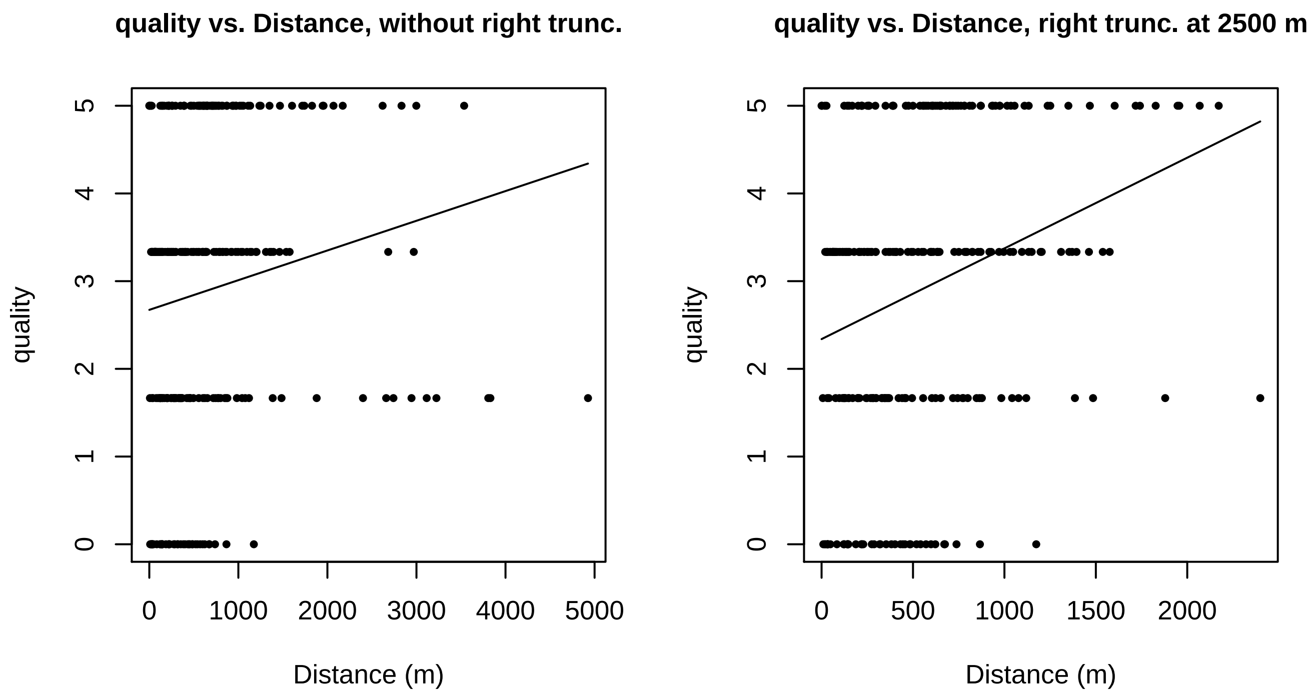

Figure 22: Scatterplots showing the relationship between the survey-specific index of the quality of observation conditions and perpendicular sighting distance, for all sightings (left) and only those not right truncated (right). Low values of the quality index correspond to better observation conditions. The line is a simple linear regression.

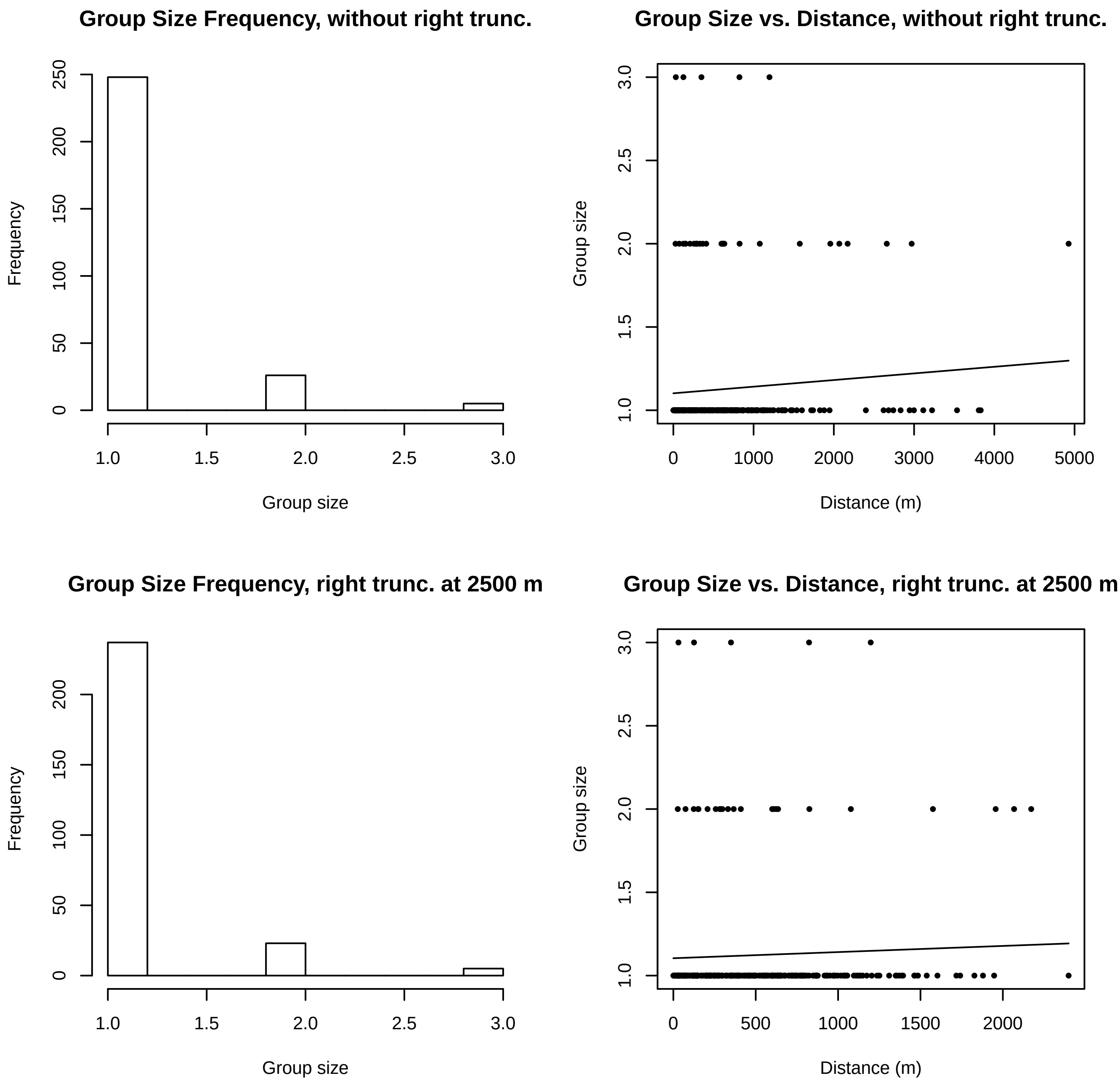

Figure 23: Histograms showing group size frequency and scatterplots showing the relationship between group size and perpendicular sighting distance, for all sightings (top row) and only those not right truncated (bottom row). In the scatterplot, the line is a simple linear regression.

Aerial Surveys

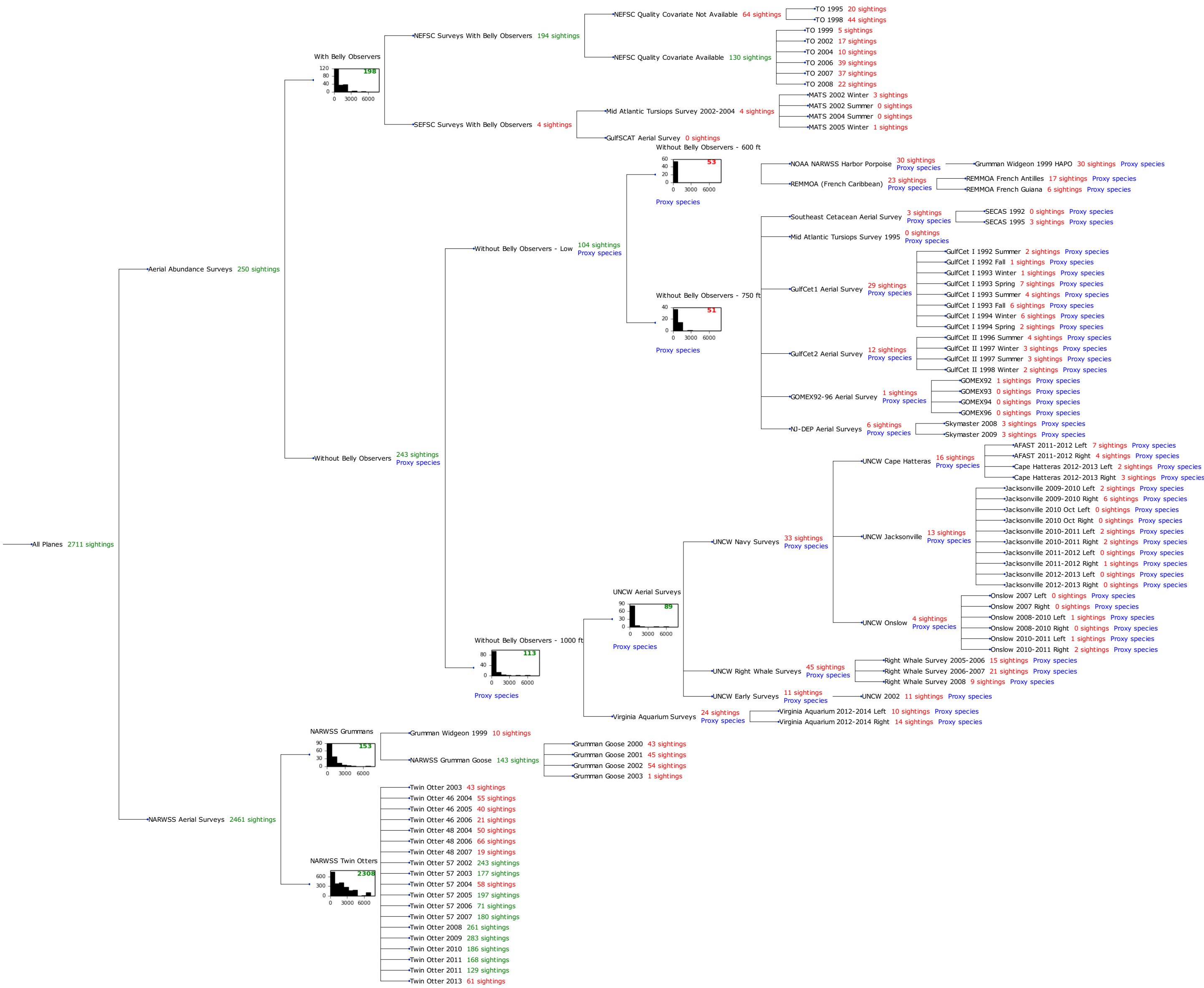

Figure 24: Detection hierarchy for aerial surveys

With Belly Observers

The sightings were right truncated at 2000m.

Covariate	Description
beaufort	Beaufort sea state.
size	Estimated size (number of individuals) of the sighted group.

Table 16: Covariates tested in candidate "multi-covariate distance sampling" (MCDS) detection functions.

Key	Adjustment	Order	Covariates	Succeeded	Δ AIC	Mean ESHW (m)

hn				Yes	0.00	924
hn	cos	2		Yes	1.49	867
hn			size	Yes	1.94	924
hn	cos	3		Yes	1.99	936
hr	poly	4		Yes	2.04	937
hr				Yes	2.18	988
hr	poly	2		Yes	2.27	914
hn	herm	4		No		
hn			beaufort	No		
hr			beaufort	No		
hr			size	No		
hn			beaufort, size	No		
hr			beaufort, size	No		

Table 17: Candidate detection functions for With Belly Observers. The first one listed was selected for the density model.

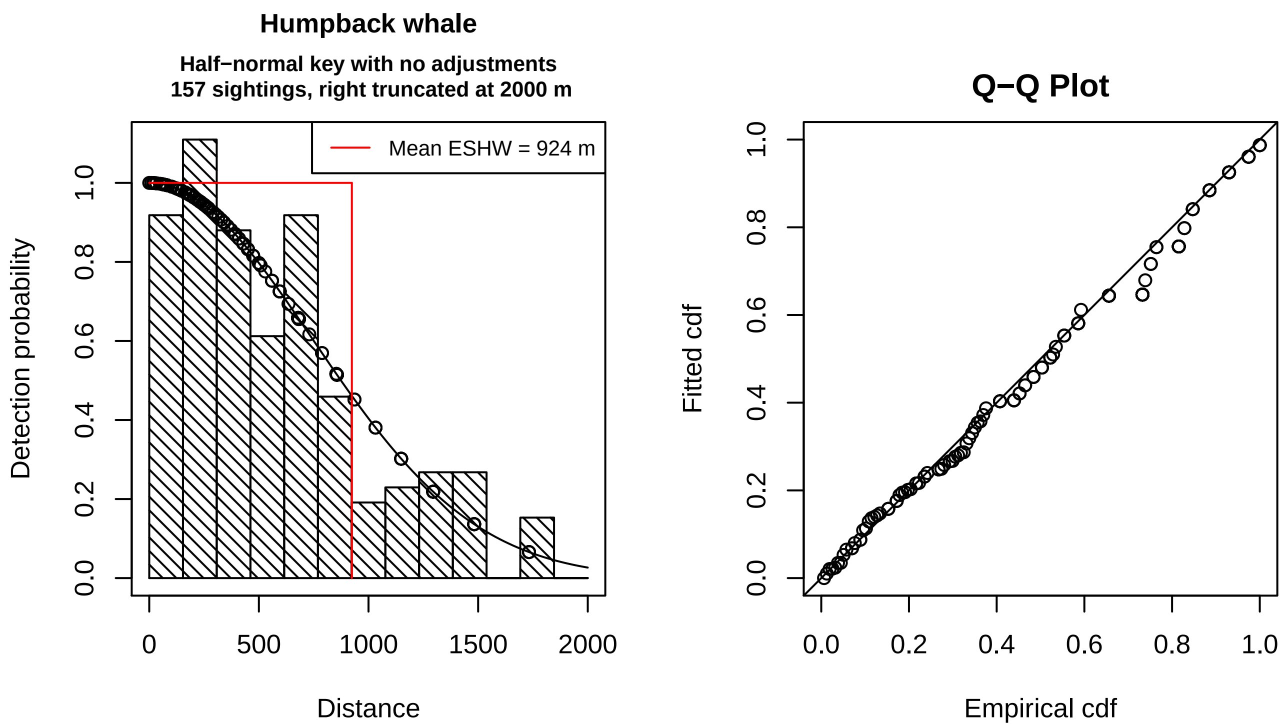

Figure 25: Detection function for With Belly Observers that was selected for the density model

Statistical output for this detection function:

```
Summary for ds object
Number of observations :  157
```

```
Distance range         :  0  -  2000
AIC                    :  2294.229

Detection function:
 Half-normal key function

Detection function parameters
Scale Coefficients:
            estimate         se
(Intercept) 6.610199 0.06334656

                       Estimate          SE         CV
Average p             0.4620808  0.02758566 0.05969878
N in covered region 339.7674296 28.40703886 0.08360730
```

Additional diagnostic plots:

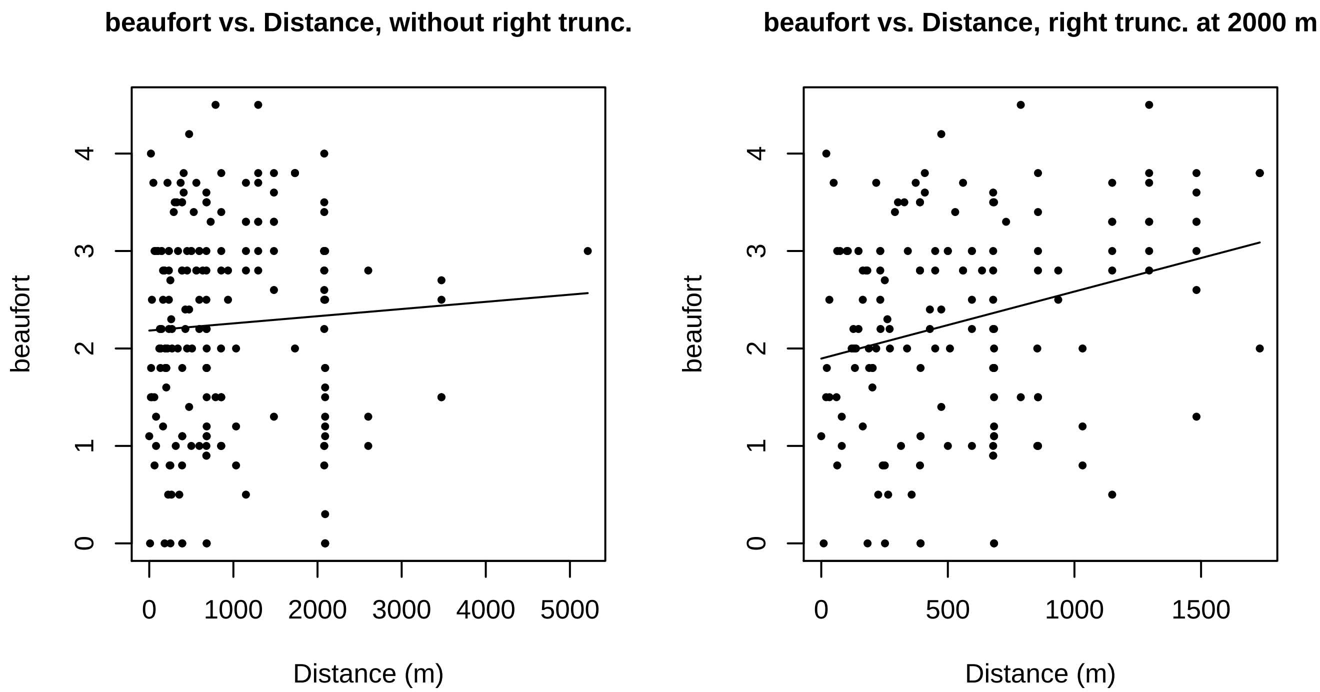

Figure 26: Scatterplots showing the relationship between Beaufort sea state and perpendicular sighting distance, for all sightings (left) and only those not right truncated (right). The line is a simple linear regression.

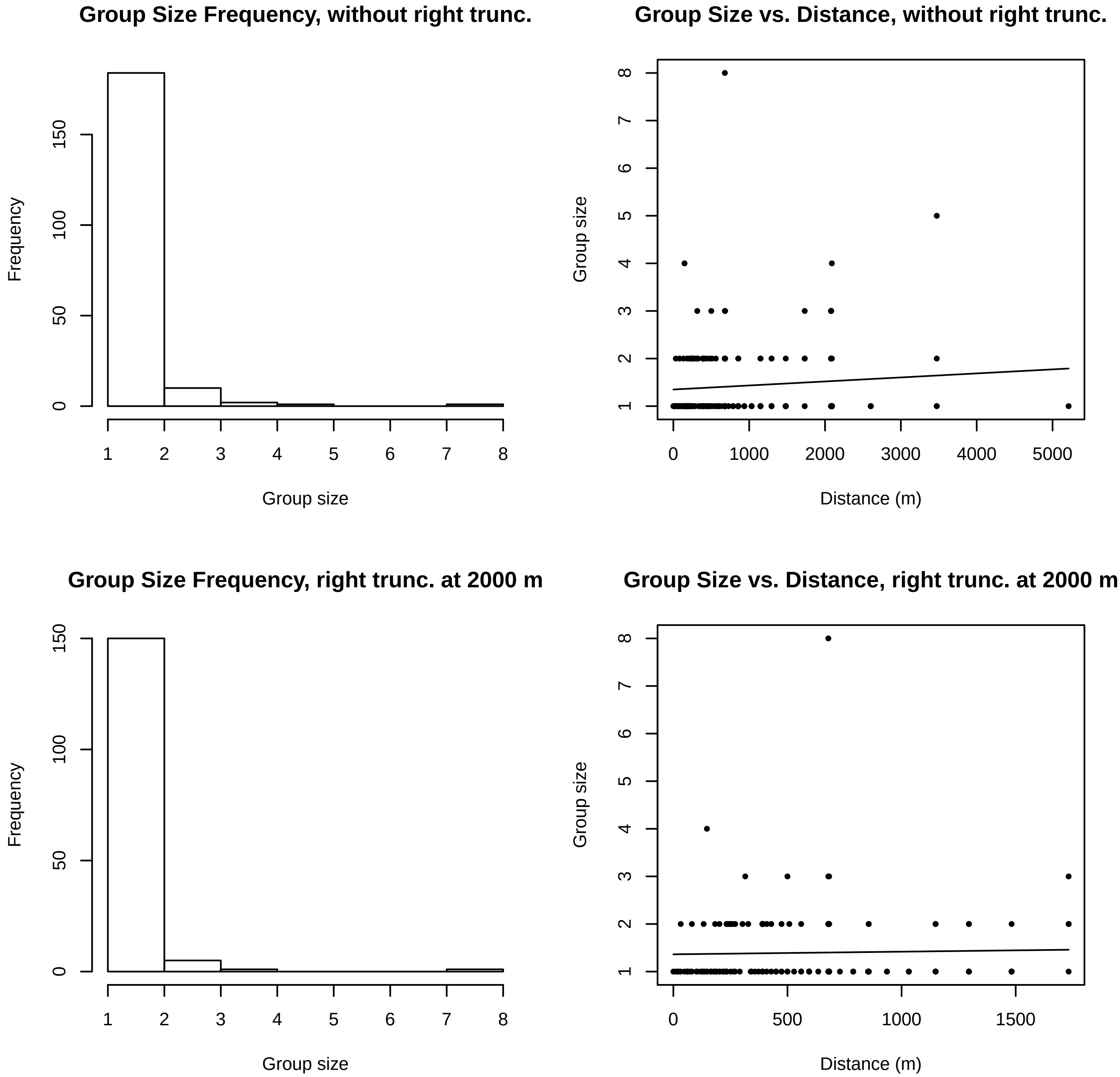

Figure 27: Histograms showing group size frequency and scatterplots showing the relationship between group size and perpendicular sighting distance, for all sightings (top row) and only those not right truncated (bottom row). In the scatterplot, the line is a simple linear regression.

Without Belly Observers - 600 ft

Because this taxon was sighted too infrequently to fit a detection function to its sightings alone, we fit a detection function to the pooled sightings of several other species that we believed would exhibit similar detectability. These "proxy species" are listed below.

Reported By Observer	Common Name	n
Balaenoptera	Balaenopterid sp.	2
Balaenoptera acutorostrata	Minke whale	8

Balaenoptera borealis	Sei whale	0
Balaenoptera borealis/edeni	Sei or Bryde's whale	0
Balaenoptera borealis/physalus	Fin or Sei whale	0
Balaenoptera edeni	Bryde's whale	0
Balaenoptera musculus	Blue whale	0
Balaenoptera physalus	Fin whale	15
Eubalaena glacialis	North Atlantic right whale	2
Eubalaena glacialis/Megaptera novaeangliae	Right or humpback whale	0
Megaptera novaeangliae	Humpback whale	16
Physeter macrocephalus	Sperm whale	10
Total		53

Table 18: Proxy species used to fit detection functions for Without Belly Observers - 600 ft. The number of sightings, n, is before truncation.

The sightings were right truncated at 600m. Due to a reduced frequency of sightings close to the trackline that plausibly resulted from the behavior of the observers and/or the configuration of the survey platform, the sightings were left truncted as well. Sightings closer than 32 m to the trackline were omitted from the analysis, and it was assumed that the the area closer to the trackline than this was not surveyed. This distance was estimated by inspecting histograms of perpendicular sighting distances.

Covariate	Description
beaufort	Beaufort sea state.
size	Estimated size (number of individuals) of the sighted group.

Table 19: Covariates tested in candidate "multi-covariate distance sampling" (MCDS) detection functions.

Key	Adjustment	Order	Covariates	Succeeded	Δ AIC	Mean ESHW (m)
hn				Yes	0.00	293
hr				Yes	1.14	318
hn			beaufort	Yes	1.57	293
hn	cos	3		Yes	1.65	311
hn	herm	4		Yes	1.93	291
hr			beaufort	Yes	1.97	326
hn	cos	2		Yes	1.97	283
hr	poly	4		Yes	3.14	318
hr	poly	2		Yes	3.14	318
hn			size	No		
hr			size	No		
hn			beaufort, size	No		
hr			beaufort, size	No		

Table 20: Candidate detection functions for Without Belly Observers - 600 ft. The first one listed was selected for the density model.

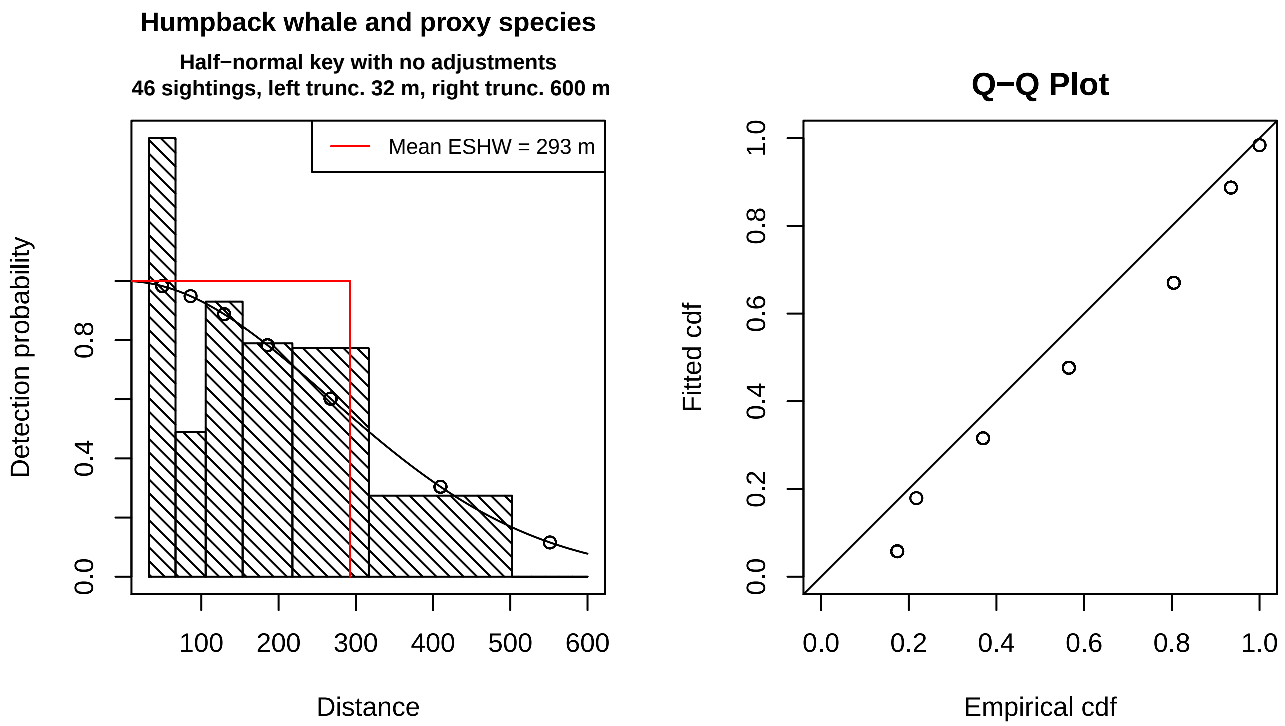

Figure 28: Detection function for Without Belly Observers - 600 ft that was selected for the density model

Statistical output for this detection function:

```
Summary for ds object
Number of observations :  46
Distance range         :  32.24668  -  600
AIC                    :  177.4011

Detection function:
 Half-normal key function

Detection function parameters
Scale Coefficients:
            estimate        se
(Intercept) 5.581559 0.1339955

                     Estimate          SE        CV
Average p            0.487738  0.06208134 0.1272842
N in covered region 94.312922 15.59372100 0.1653402
```

Additional diagnostic plots:

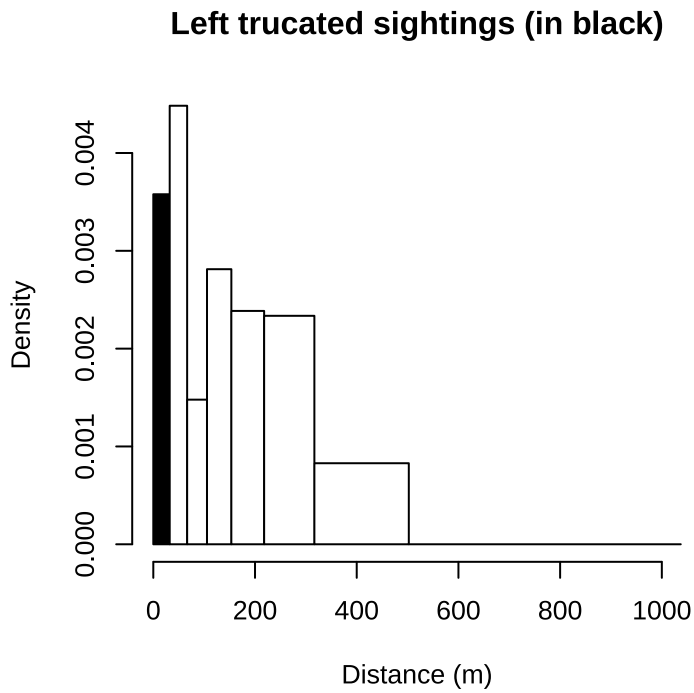

Figure 29: Density of sightings by perpendicular distance for Without Belly Observers - 600 ft. Black bars on the left show sightings that were left truncated.

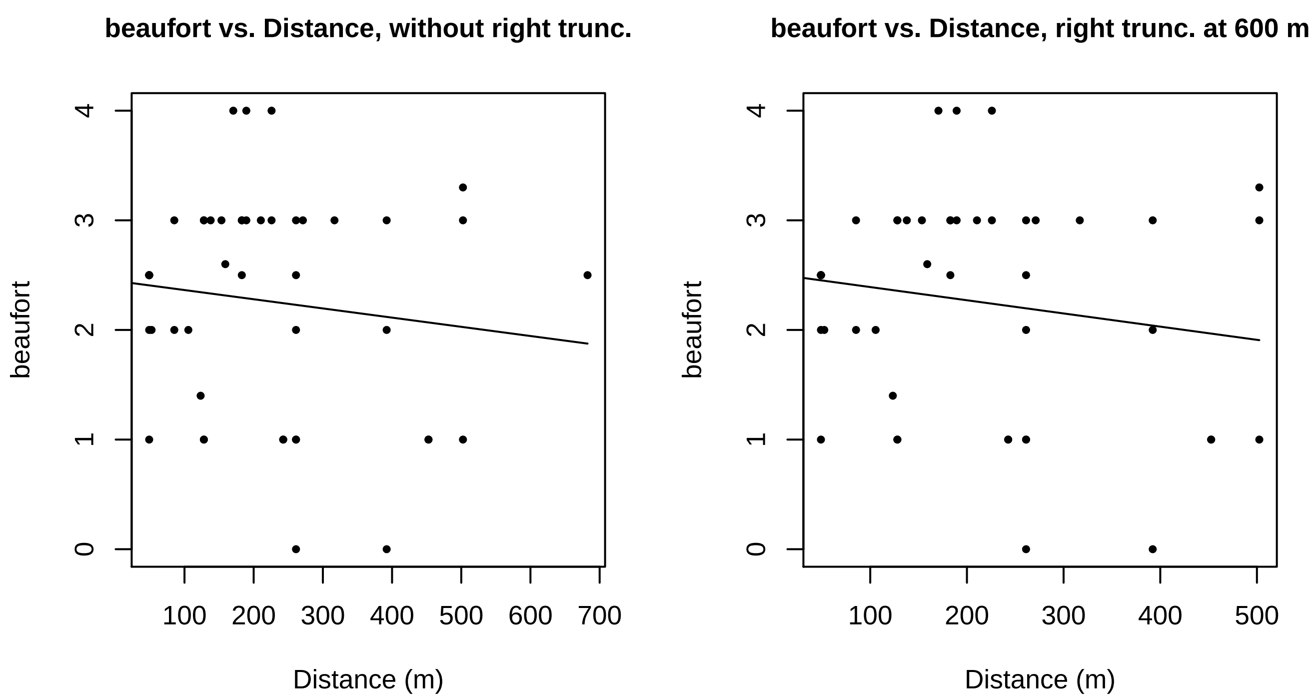

Figure 30: Scatterplots showing the relationship between Beaufort sea state and perpendicular sighting distance, for all sightings (left) and only those not right truncated (right). The line is a simple linear regression.

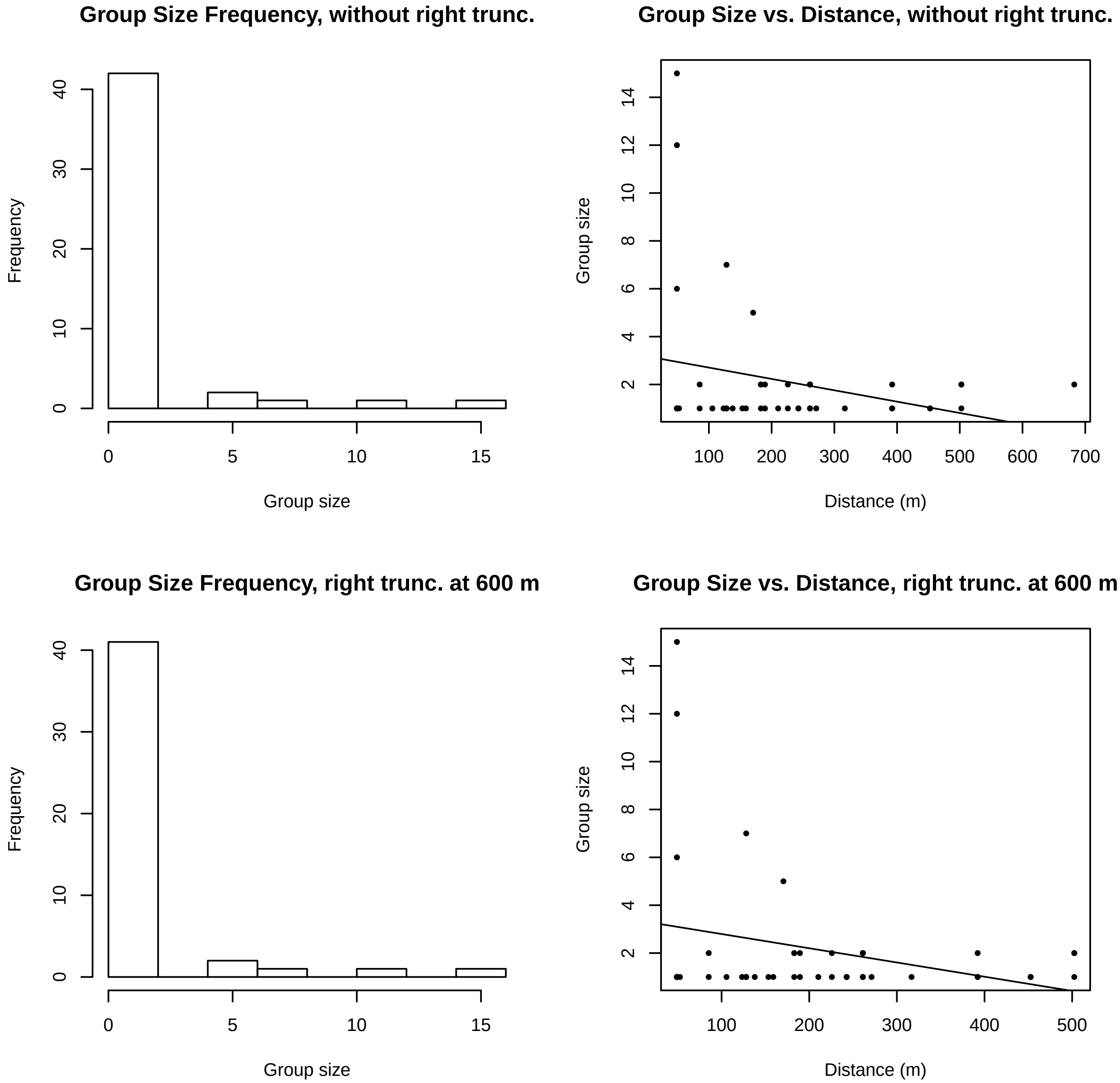

Figure 31: Histograms showing group size frequency and scatterplots showing the relationship between group size and perpendicular sighting distance, for all sightings (top row) and only those not right truncated (bottom row). In the scatterplot, the line is a simple linear regression.

Without Belly Observers - 750 ft

Because this taxon was sighted too infrequently to fit a detection function to its sightings alone, we fit a detection function to the pooled sightings of several other species that we believed would exhibit similar detectability. These "proxy species" are listed below.

Reported By Observer	Common Name	n
Balaenoptera	Balaenopterid sp.	1
Balaenoptera acutorostrata	Minke whale	0

Balaenoptera borealis	Sei whale	0
Balaenoptera borealis/edeni	Sei or Bryde's whale	2
Balaenoptera borealis/physalus	Fin or Sei whale	0
Balaenoptera edeni	Bryde's whale	3
Balaenoptera musculus	Blue whale	0
Balaenoptera physalus	Fin whale	2
Eubalaena glacialis	North Atlantic right whale	0
Eubalaena glacialis/Megaptera novaeangliae	Right or humpback whale	0
Megaptera novaeangliae	Humpback whale	6
Physeter macrocephalus	Sperm whale	37
Total		51

Table 21: Proxy species used to fit detection functions for Without Belly Observers - 750 ft. The number of sightings, n, is before truncation.

The sightings were right truncated at 600m. Due to a reduced frequency of sightings close to the trackline that plausibly resulted from the behavior of the observers and/or the configuration of the survey platform, the sightings were left truncted as well. Sightings closer than 40 m to the trackline were omitted from the analysis, and it was assumed that the the area closer to the trackline than this was not surveyed. This distance was estimated by inspecting histograms of perpendicular sighting distances. The vertical sighting angles were heaped at 10 degree increments, so the candidate detection functions were fitted using linear bins scaled accordingly.

Key	Adjustment	Order	Covariates	Succeeded	Δ AIC	Mean ESHW (m)
hn	cos	2		Yes	0.00	216
hr				Yes	0.59	251
hn	cos	3		Yes	2.31	255
hn	herm	4		Yes	2.46	316
hr	poly	2		Yes	2.59	251
hr	poly	4		Yes	2.66	249
hn				No		

Table 22: Candidate detection functions for Without Belly Observers - 750 ft. The first one listed was selected for the density model.

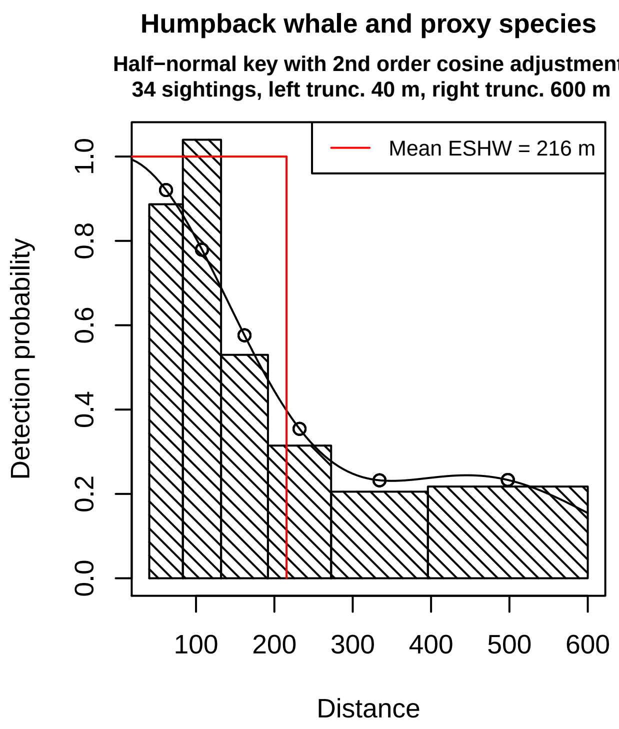

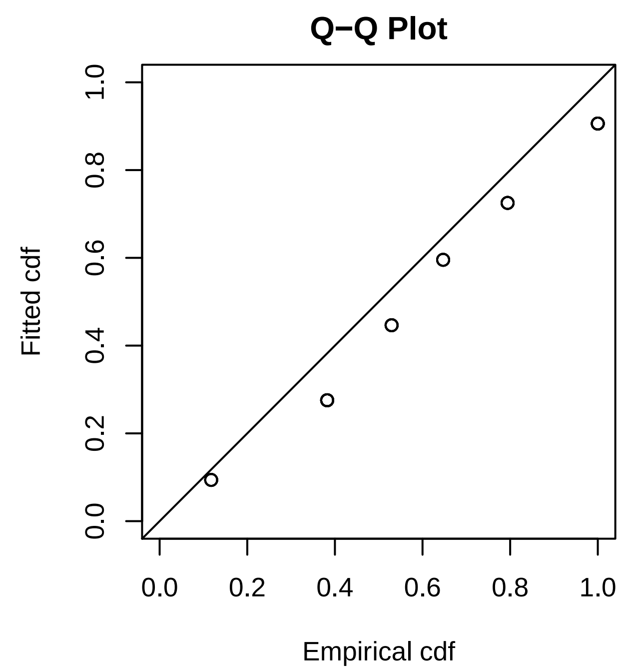

Figure 32: Detection function for Without Belly Observers - 750 ft that was selected for the density model

Statistical output for this detection function:

```
Summary for ds object
Number of observations :  34
Distance range         :  40.30835  -  600
AIC                    :  124.984

Detection function:
 Half-normal key function with cosine adjustment term of order 2

Detection function parameters
Scale Coefficients:
            estimate        se
(Intercept) 5.738324 0.1838281

Adjustment term parameter(s):
              estimate       se
cos, order 2 0.4333816 0.242253


Monotonicity constraints were enforced.
                      Estimate         SE        CV
Average p            0.3592782  0.0870934 0.2424122
N in covered region 94.6341978 26.3634680 0.2785829

Monotonicity constraints were enforced.
```

Additional diagnostic plots:

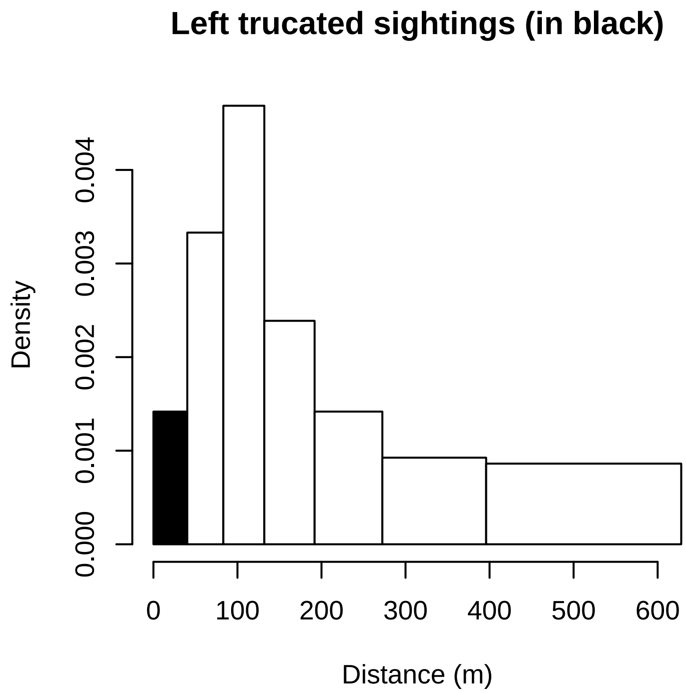

Figure 33: Density of sightings by perpendicular distance for Without Belly Observers - 750 ft. Black bars on the left show sightings that were left truncated.

Without Belly Observers - 1000 ft

Because this taxon was sighted too infrequently to fit a detection function to its sightings alone, we fit a detection function to the pooled sightings of several other species that we believed would exhibit similar detectability. These "proxy species" are listed below.

Reported By Observer	Common Name	n
Balaenoptera	Balaenopterid sp.	1
Balaenoptera acutorostrata	Minke whale	16
Balaenoptera borealis	Sei whale	0
Balaenoptera borealis/edeni	Sei or Bryde's whale	0
Balaenoptera borealis/physalus	Fin or Sei whale	0
Balaenoptera edeni	Bryde's whale	0
Balaenoptera musculus	Blue whale	0
Balaenoptera physalus	Fin whale	32
Eubalaena glacialis	North Atlantic right whale	34
Eubalaena glacialis/Megaptera novaeangliae	Right or humpback whale	0
Megaptera novaeangliae	Humpback whale	30
Total		113

Table 23: Proxy species used to fit detection functions for Without Belly Observers - 1000 ft. The number of sightings, n, is before truncation.

The sightings were right truncated at 1500m.

Covariate	Description
beaufort	Beaufort sea state.
quality	Survey-specific index of the quality of observation conditions, utilizing relevant factors other than Beaufort sea state (see methods).
size	Estimated size (number of individuals) of the sighted group.

Table 24: Covariates tested in candidate "multi-covariate distance sampling" (MCDS) detection functions.

Key	Adjustment	Order	Covariates	Succeeded	Δ AIC	Mean ESHW (m)
hr				Yes	0.00	434
hr	poly	4		Yes	1.58	424
hn	cos	2		Yes	1.71	462
hr	poly	2		Yes	1.92	427
hr			quality	Yes	1.96	433
hn	cos	3		Yes	3.64	418
hn				Yes	11.03	585
hn	herm	4		No		
hn			beaufort	No		
hr			beaufort	No		
hn			quality	No		
hn			size	No		
hr			size	No		
hn			beaufort, quality	No		
hr			beaufort, quality	No		
hn			beaufort, size	No		
hr			beaufort, size	No		
hn			quality, size	No		
hr			quality, size	No		
hn			beaufort, quality, size	No		
hr			beaufort, quality, size	No		

Table 25: Candidate detection functions for Without Belly Observers - 1000 ft. The first one listed was selected for the density model.

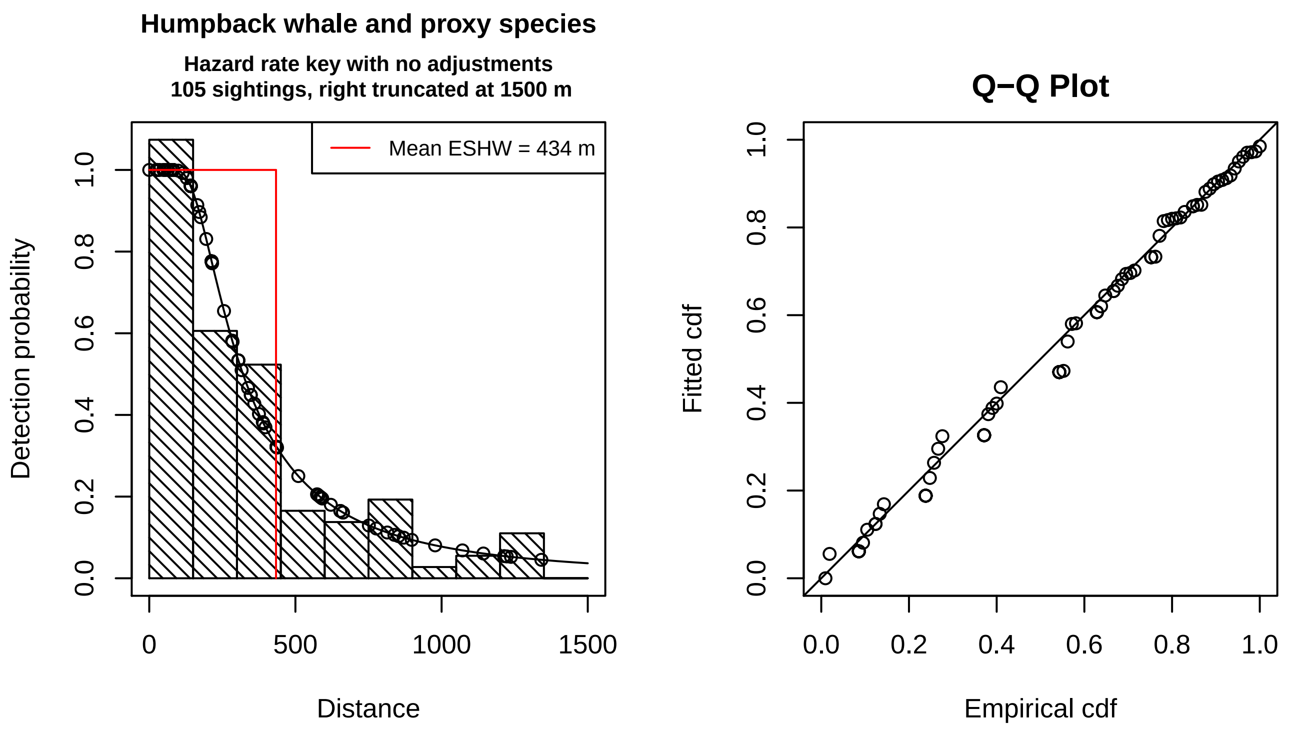

Figure 34: Detection function for Without Belly Observers - 1000 ft that was selected for the density model

Statistical output for this detection function:

```
Summary for ds object
Number of observations :  105
Distance range         :  0  -  1500
AIC                    :  1432.491

Detection function:
 Hazard-rate key function

Detection function parameters
Scale Coefficients:
            estimate        se
(Intercept) 5.576432 0.2232183

Shape parameters:
             estimate        se
(Intercept) 0.6374087 0.1752092

                       Estimate          SE        CV
Average p             0.2891295  0.03984493 0.1378100
N in covered region 363.1591175 58.28878285 0.1605048
```

Additional diagnostic plots:

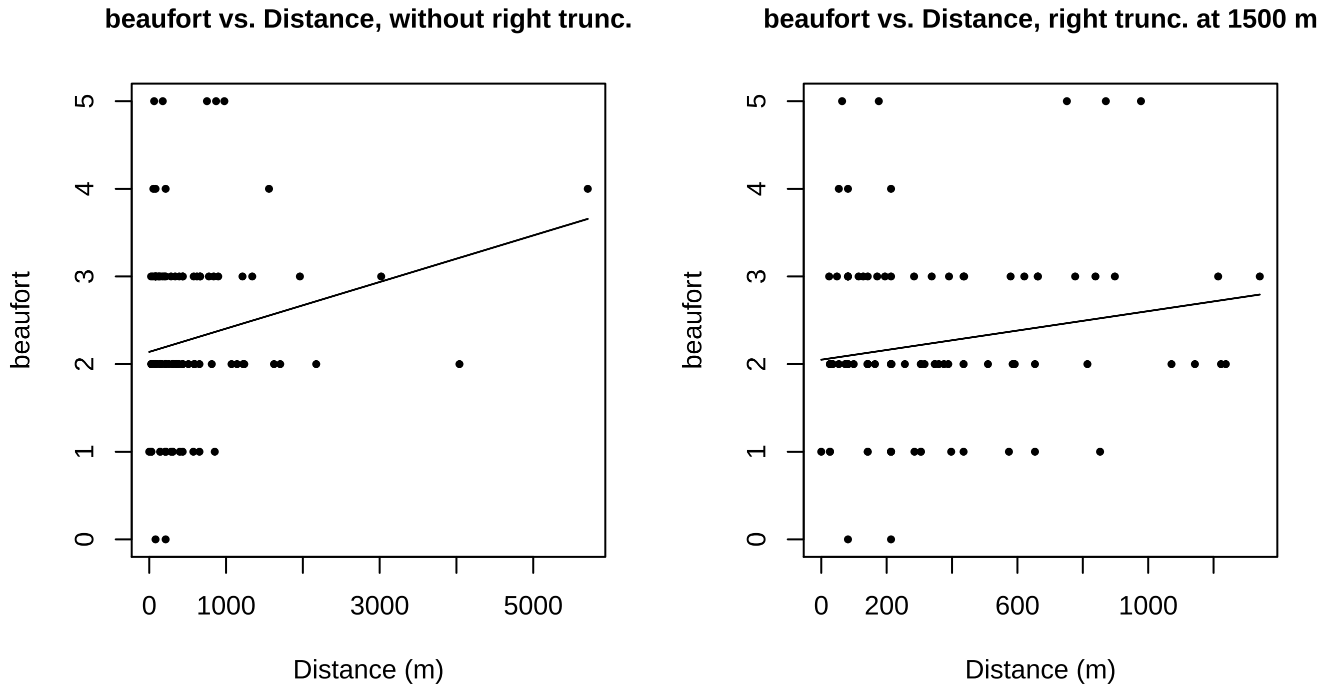

Figure 35: Scatterplots showing the relationship between Beaufort sea state and perpendicular sighting distance, for all sightings (left) and only those not right truncated (right). The line is a simple linear regression.

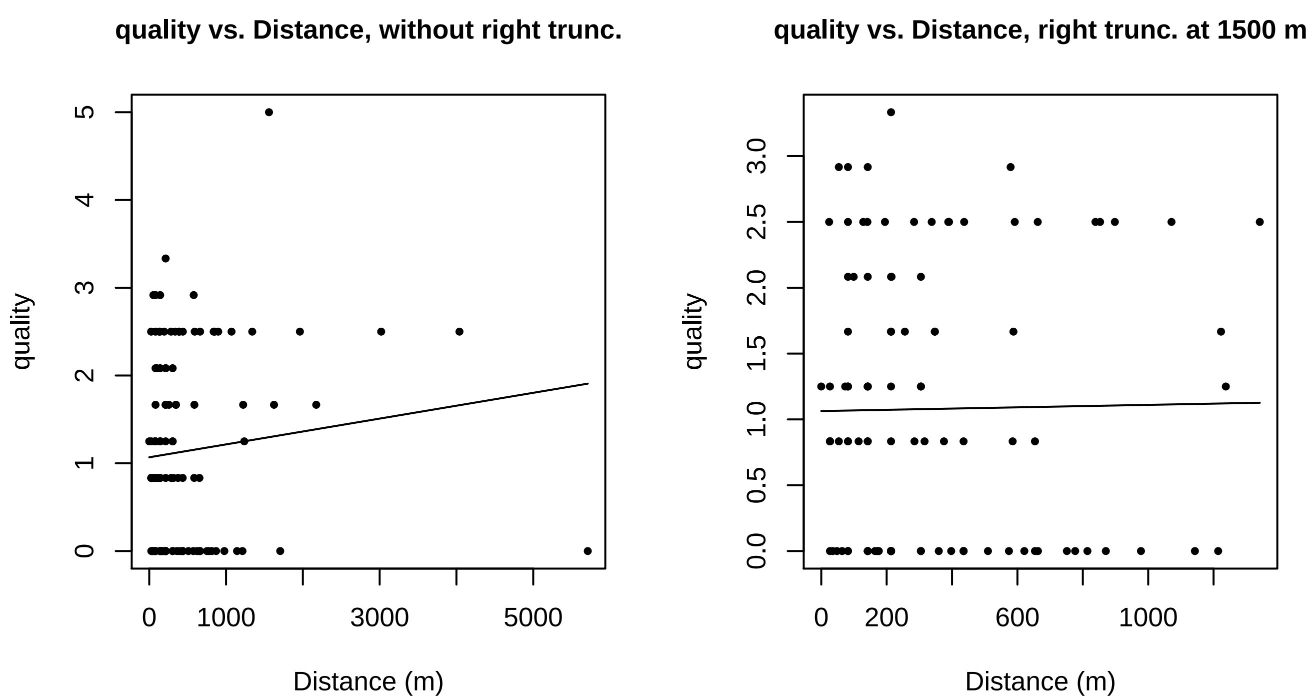

Figure 36: Scatterplots showing the relationship between the survey-specific index of the quality of observation conditions and perpendicular sighting distance, for all sightings (left) and only those not right truncated (right). Low values of the quality index correspond to better observation conditions. The line is a simple linear regression.

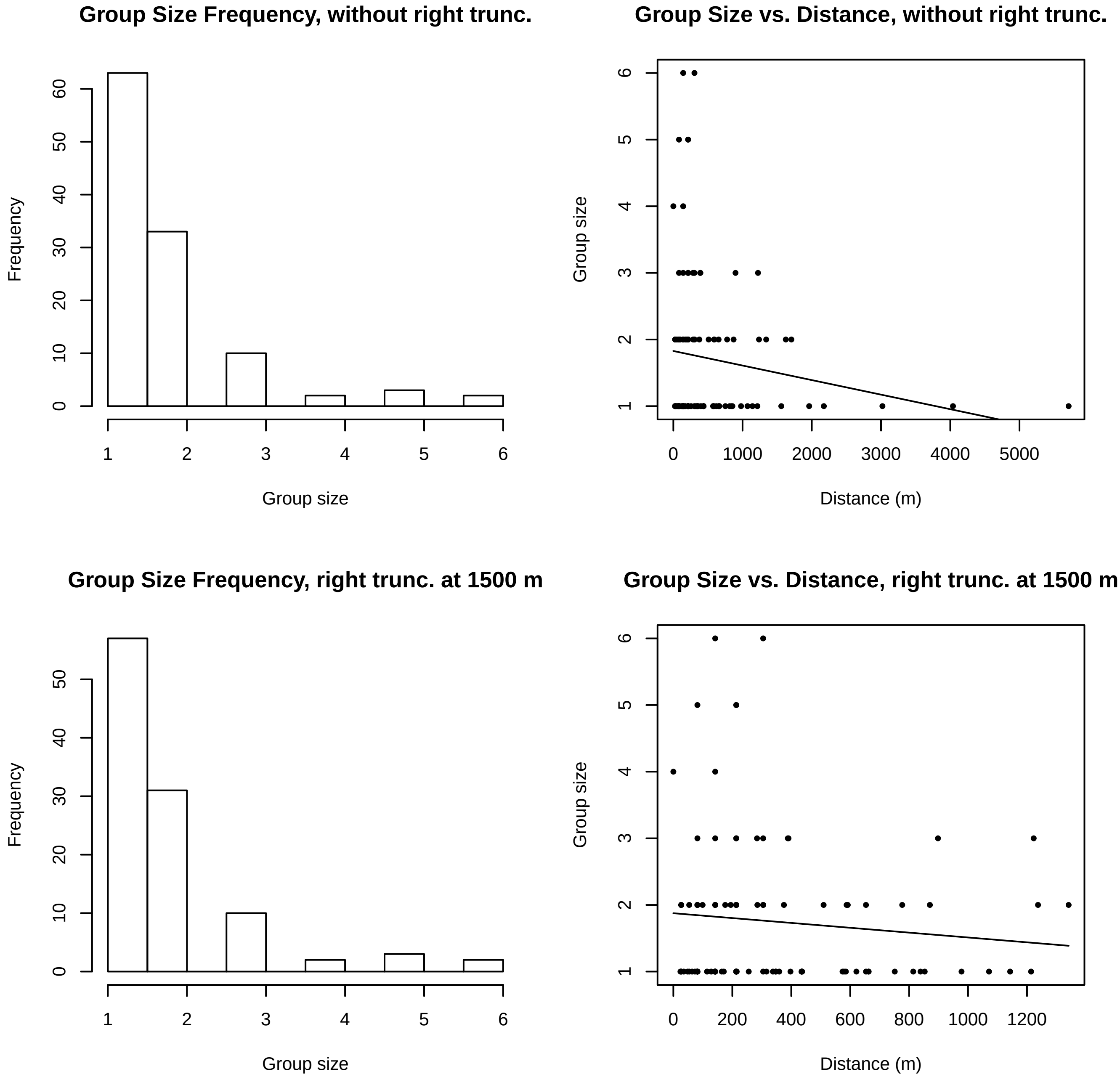

Figure 37: Histograms showing group size frequency and scatterplots showing the relationship between group size and perpendicular sighting distance, for all sightings (top row) and only those not right truncated (bottom row). In the scatterplot, the line is a simple linear regression.

UNCW Aerial Surveys

Because this taxon was sighted too infrequently to fit a detection function to its sightings alone, we fit a detection function to the pooled sightings of several other species that we believed would exhibit similar detectability. These "proxy species" are listed below.

Reported By Observer	Common Name	n
Balaenoptera	Balaenopterid sp.	1
Balaenoptera acutorostrata	Minke whale	15

Balaenoptera borealis	Sei whale	0
Balaenoptera borealis/edeni	Sei or Bryde's whale	0
Balaenoptera borealis/physalus	Fin or Sei whale	0
Balaenoptera edeni	Bryde's whale	0
Balaenoptera musculus	Blue whale	0
Balaenoptera physalus	Fin whale	19
Eubalaena glacialis	North Atlantic right whale	31
Eubalaena glacialis/Megaptera novaeangliae	Right or humpback whale	0
Megaptera novaeangliae	Humpback whale	23
Total		89

Table 26: Proxy species used to fit detection functions for UNCW Aerial Surveys. The number of sightings, n, is before truncation.

The sightings were right truncated at 1500m.

Covariate	Description
beaufort	Beaufort sea state.
quality	Survey-specific index of the quality of observation conditions, utilizing relevant factors other than Beaufort sea state (see methods).
size	Estimated size (number of individuals) of the sighted group.

Table 27: Covariates tested in candidate "multi-covariate distance sampling" (MCDS) detection functions.

Key	Adjustment	Order	Covariates	Succeeded	Δ AIC	Mean ESHW (m)
hn	cos	3		Yes	0.00	358
hr				Yes	0.01	397
hr	poly	4		Yes	0.85	391
hr	poly	2		Yes	1.03	386
hn	cos	2		Yes	1.24	409
hr			quality	Yes	1.55	396
hn				Yes	5.53	480
hn			quality	Yes	7.53	480
hn	herm	4		No		
hn			beaufort	No		
hr			beaufort	No		
hn			size	No		
hr			size	No		
hn			beaufort, quality	No		
hr			beaufort, quality	No		

hn	beaufort, size	No
hr	beaufort, size	No
hn	quality, size	No
hr	quality, size	No
hn	beaufort, quality, size	No
hr	beaufort, quality, size	No

Table 28: Candidate detection functions for UNCW Aerial Surveys. The first one listed was selected for the density model.

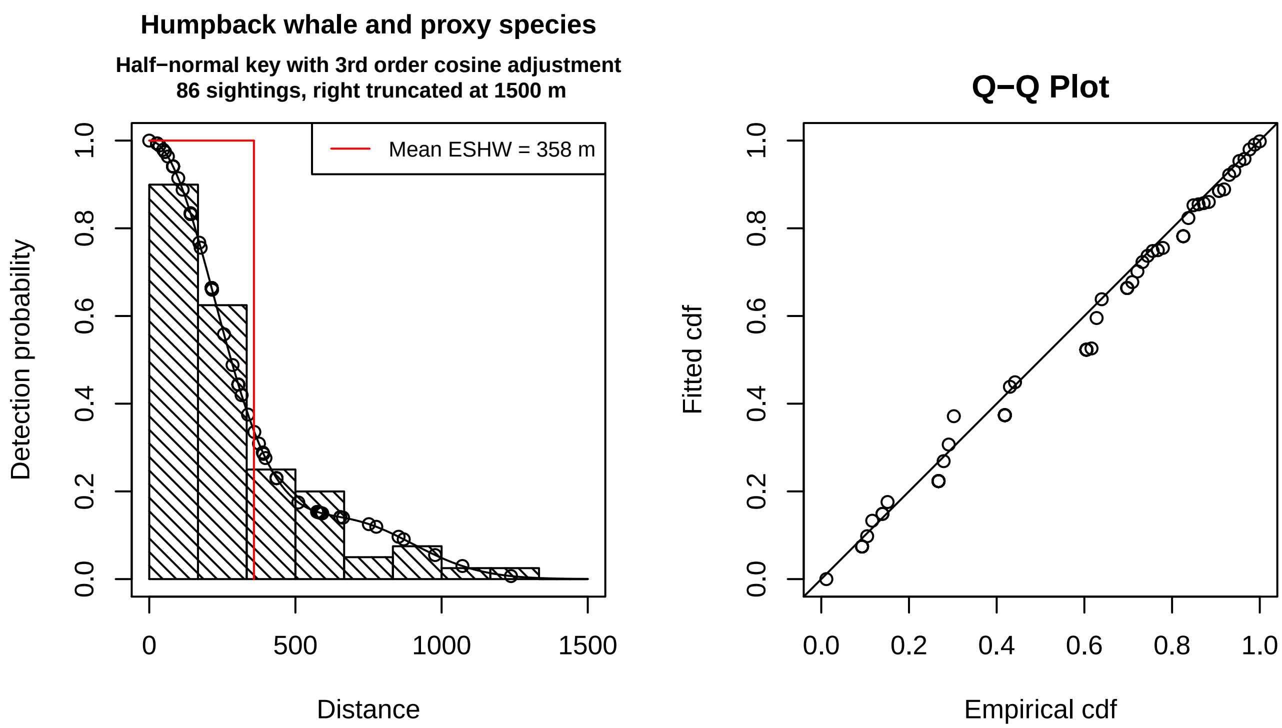

Figure 38: Detection function for UNCW Aerial Surveys that was selected for the density model

Statistical output for this detection function:

```
Summary for ds object
Number of observations :  86
Distance range         :  0  -  1500
AIC                    :  1144.166

Detection function:
 Half-normal key function with cosine adjustment term of order 3

Detection function parameters
Scale Coefficients:
            estimate         se
(Intercept) 6.006457 0.06897785

Adjustment term parameter(s):
```

```
               estimate        se
cos, order 3 0.4451317 0.1512901


Monotonicity constraints were enforced.
                        Estimate          SE        CV
Average p              0.2387636  0.02505434 0.1049337
N in covered region 360.1889026 50.76320966 0.1409350

Monotonicity constraints were enforced.
```

Additional diagnostic plots:

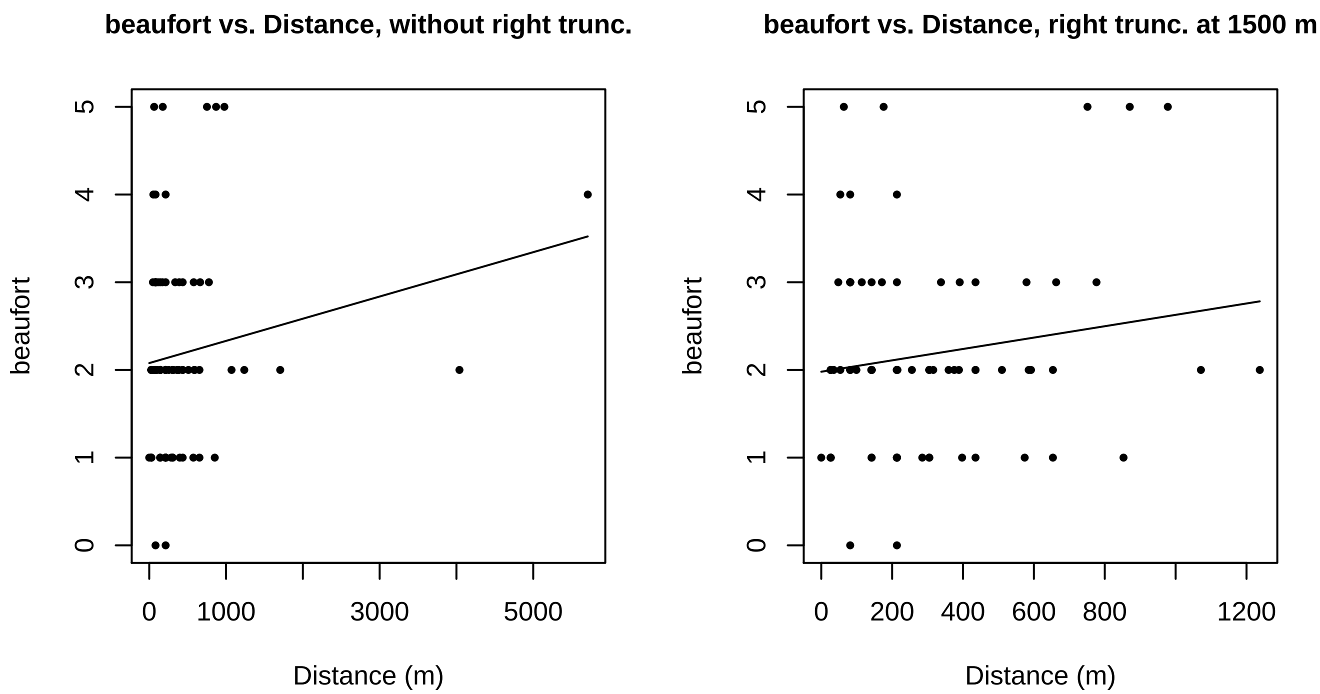

Figure 39: Scatterplots showing the relationship between Beaufort sea state and perpendicular sighting distance, for all sightings (left) and only those not right truncated (right). The line is a simple linear regression.

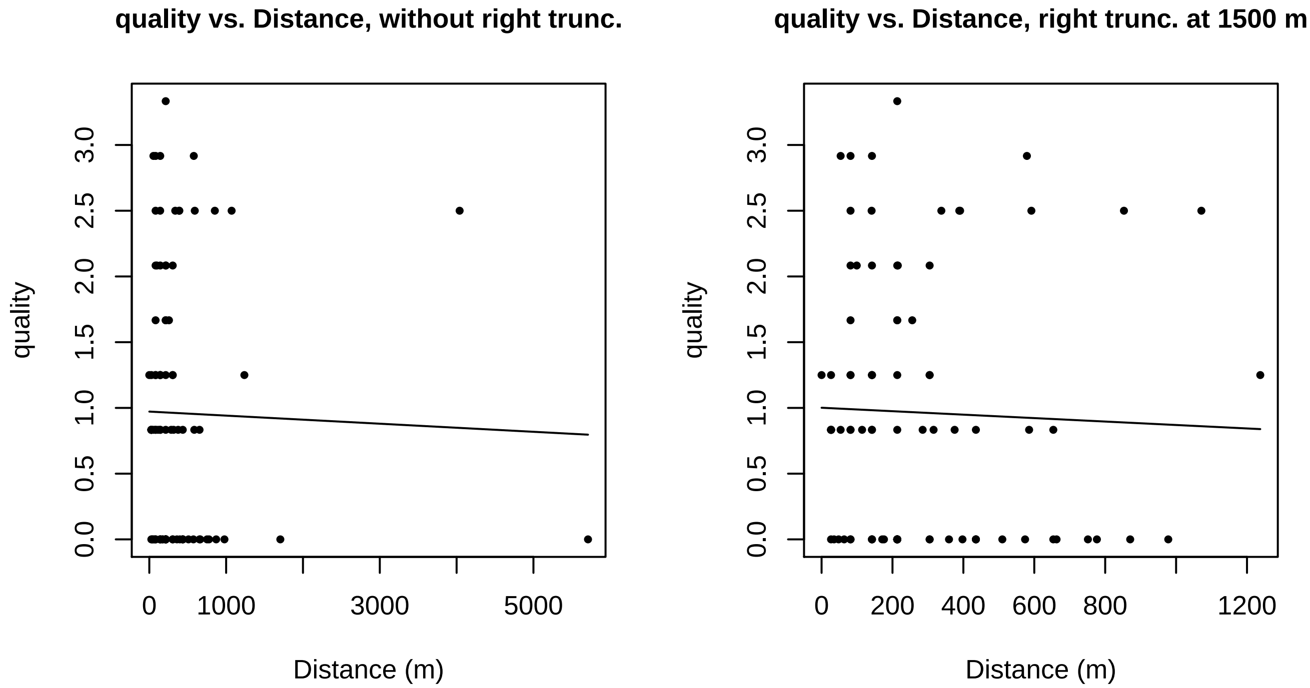

Figure 40: Scatterplots showing the relationship between the survey-specific index of the quality of observation conditions and perpendicular sighting distance, for all sightings (left) and only those not right truncated (right). Low values of the quality index correspond to better observation conditions. The line is a simple linear regression.

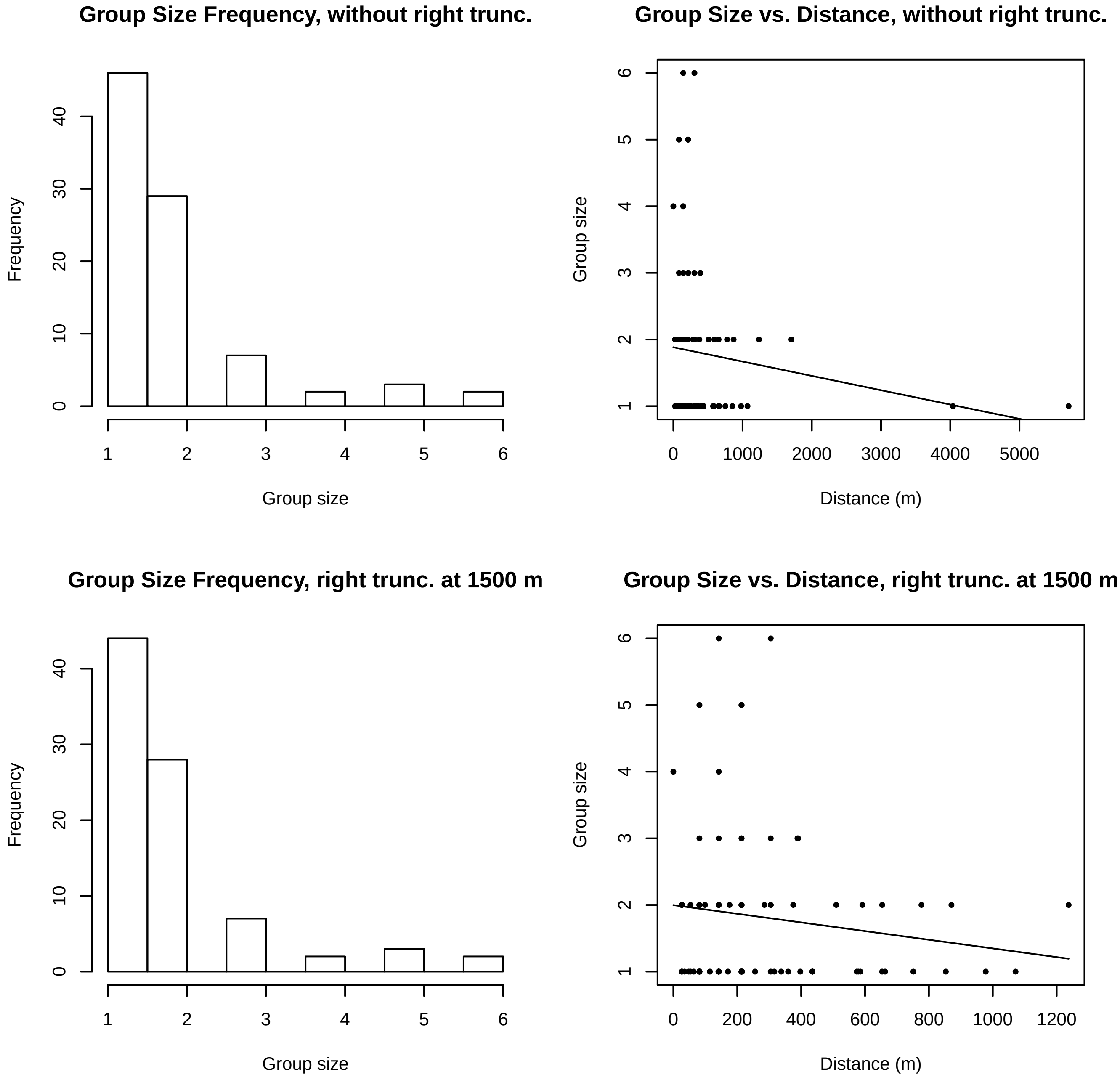

Figure 41: Histograms showing group size frequency and scatterplots showing the relationship between group size and perpendicular sighting distance, for all sightings (top row) and only those not right truncated (bottom row). In the scatterplot, the line is a simple linear regression.

NARWSS Grummans

The sightings were right truncated at 3000m. Due to a reduced frequency of sightings close to the trackline that plausibly resulted from the behavior of the observers and/or the configuration of the survey platform, the sightings were left truncted as well. Sightings closer than 107 m to the trackline were omitted from the analysis, and it was assumed that the the area closer to the trackline than this was not surveyed. This distance was estimated by inspecting histograms of perpendicular sighting distances.

Covariate	Description

beaufort	Beaufort sea state.
quality	Survey-specific index of the quality of observation conditions, utilizing relevant factors other than Beaufort sea state (see methods).
size	Estimated size (number of individuals) of the sighted group.

Table 29: Covariates tested in candidate “multi-covariate distance sampling” (MCDS) detection functions.

Key	Adjustment	Order	Covariates	Succeeded	Δ AIC	Mean ESHW (m)
hn	cos	2		Yes	0.00	944
hn				Yes	4.98	1186
hn			beaufort	Yes	5.09	1186
hn			quality	Yes	5.72	1185
hn	cos	3		Yes	6.04	1040
hn			beaufort, size	Yes	6.15	1188
hn			size	Yes	6.39	1189
hn			beaufort, quality	Yes	6.62	1184
hn			quality, size	Yes	7.23	1188
hn			beaufort, quality, size	Yes	7.84	1186
hn	herm	4		No		

Table 30: Candidate detection functions for NARWSS Grummans. The first one listed was selected for the density model.

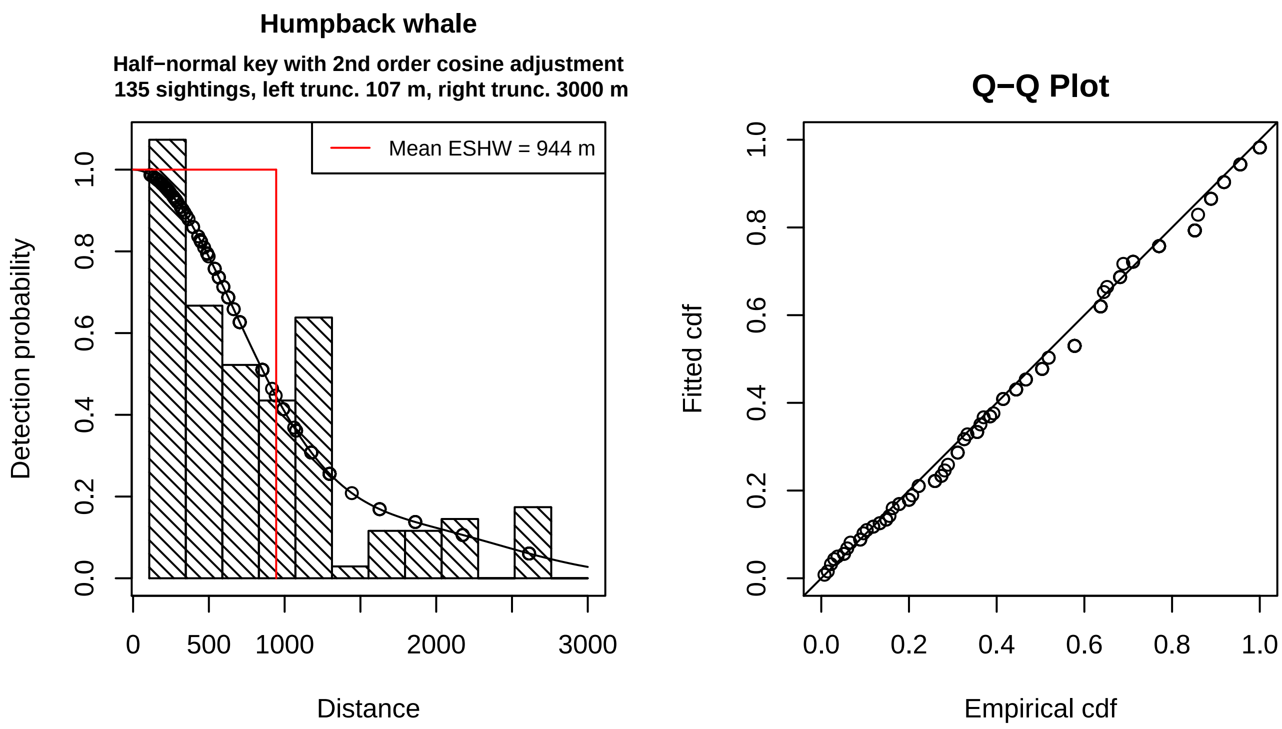

Figure 42: Detection function for NARWSS Grummans that was selected for the density model

Statistical output for this detection function:

```
Summary for ds object
Number of observations :  135
Distance range         :  106.5979  -  3000
AIC                    :  2050.203

Detection function:
 Half-normal key function with cosine adjustment term of order 2

Detection function parameters
Scale Coefficients:
            estimate         se
(Intercept)  7.02163 0.06899776

Adjustment term parameter(s):
             estimate        se
cos, order 2 0.355177 0.1235784


Monotonicity constraints were enforced.
                       Estimate          SE         CV
Average p             0.3147078  0.02979816 0.09468518
N in covered region 428.9693986 50.83155770 0.11849693

Monotonicity constraints were enforced.
```

Additional diagnostic plots:

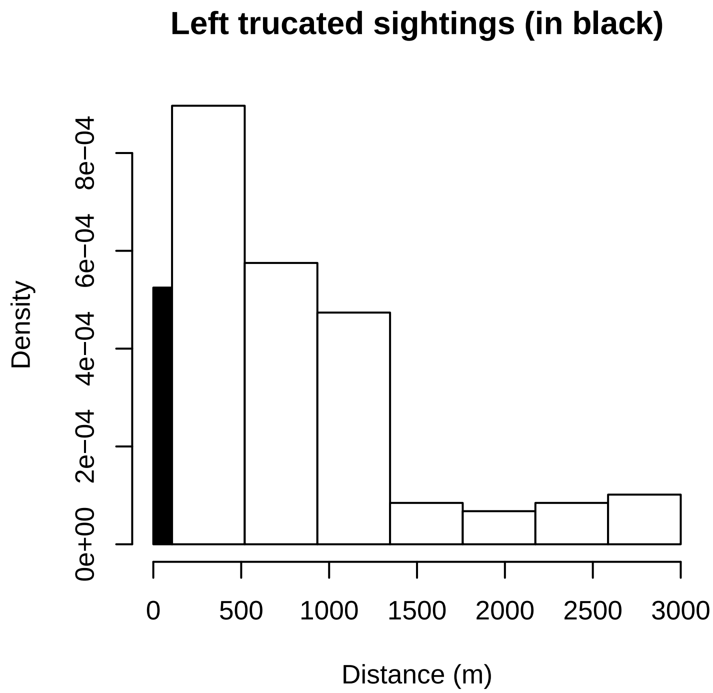

Figure 43: Density of sightings by perpendicular distance for NARWSS Grummans. Black bars on the left show sightings that were left truncated.

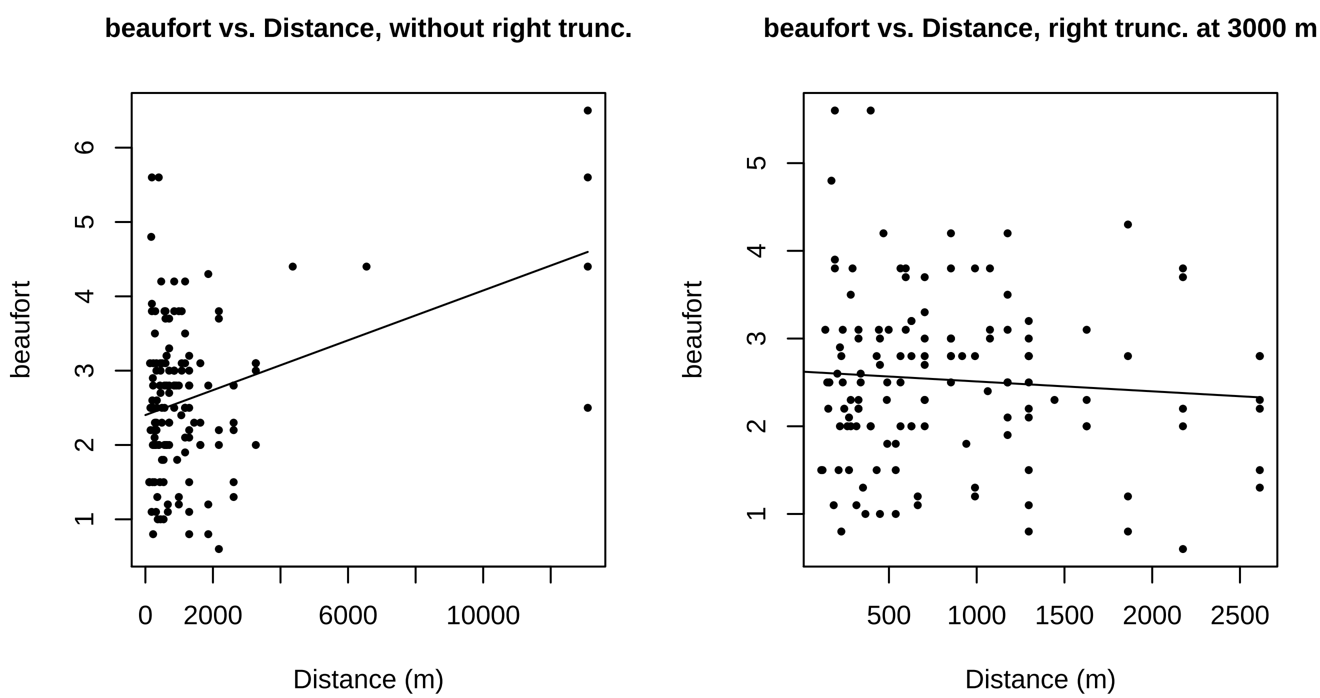

Figure 44: Scatterplots showing the relationship between Beaufort sea state and perpendicular sighting distance, for all sightings (left) and only those not right truncated (right). The line is a simple linear regression.

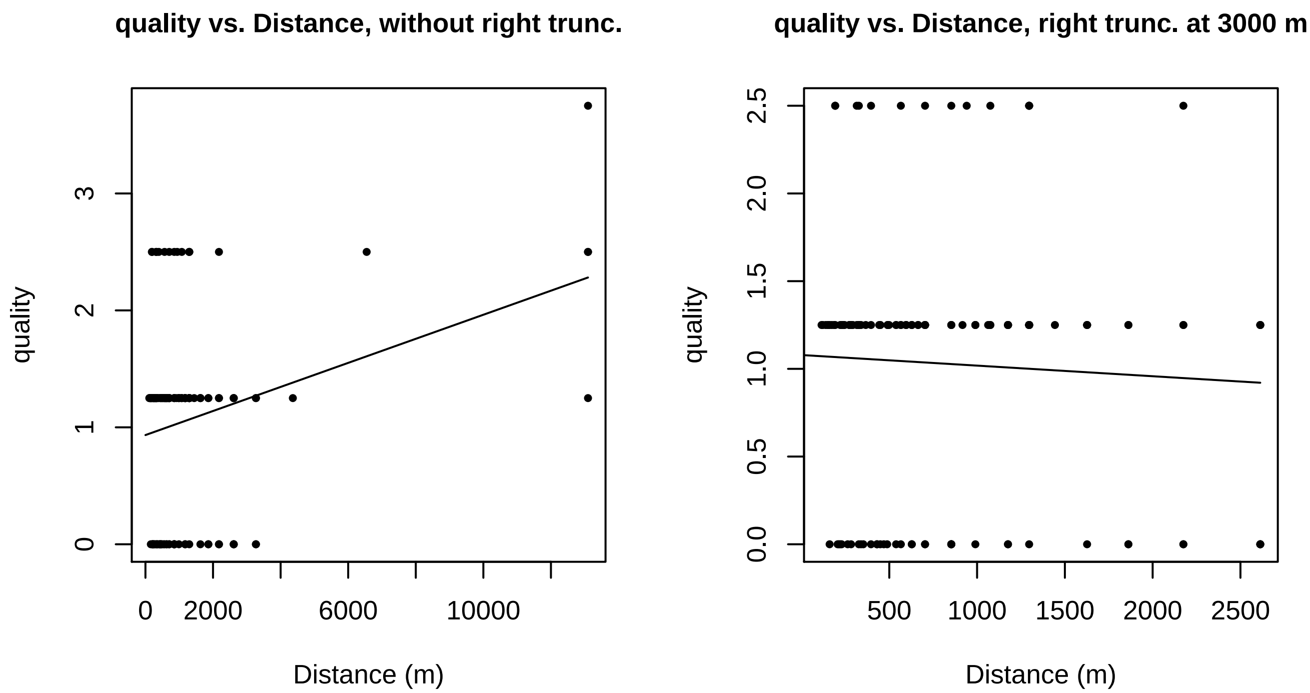

Figure 45: Scatterplots showing the relationship between the survey-specific index of the quality of observation conditions and perpendicular sighting distance, for all sightings (left) and only those not right truncated (right). Low values of the quality index correspond to better observation conditions. The line is a simple linear regression.

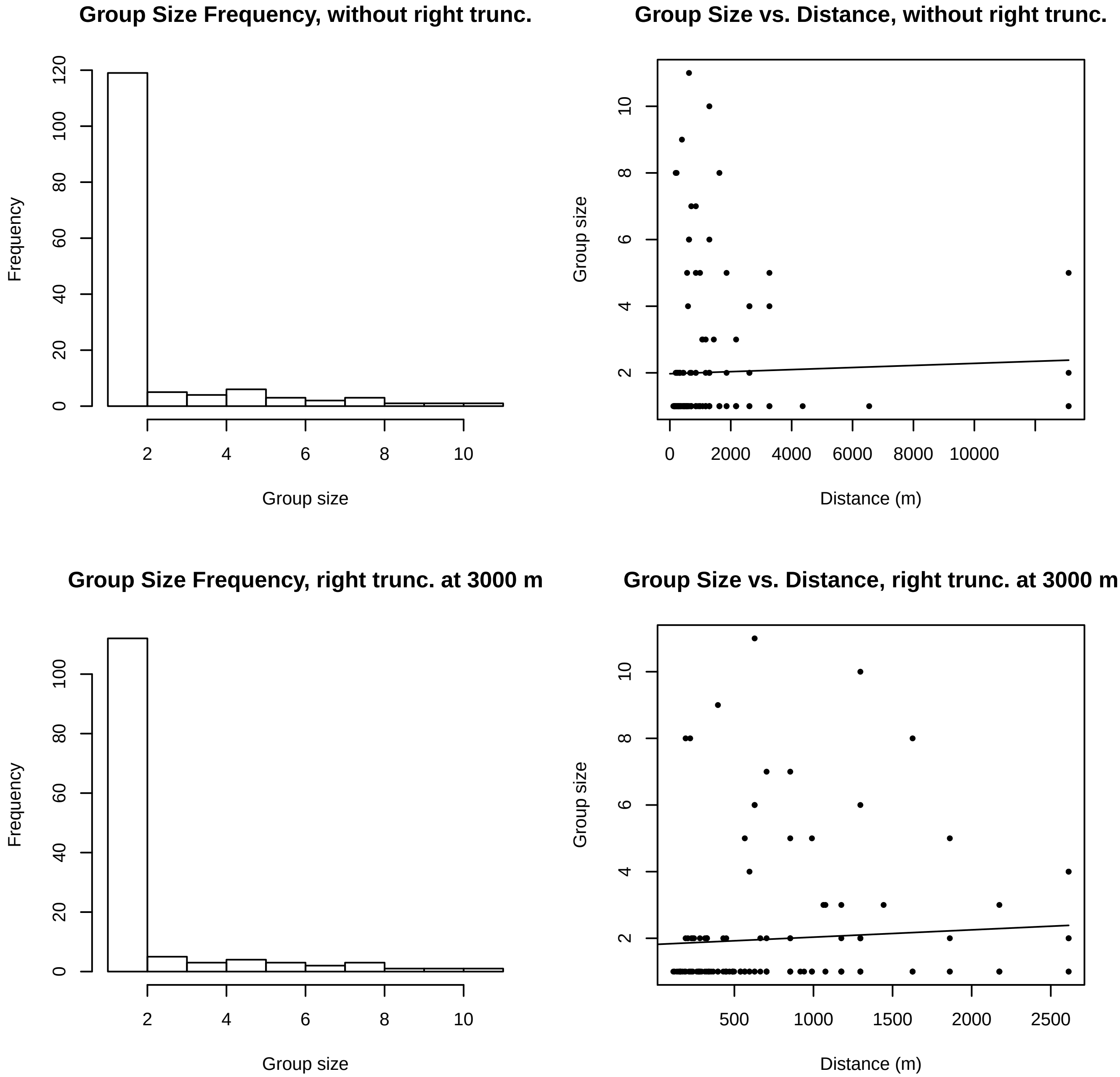

Figure 46: Histograms showing group size frequency and scatterplots showing the relationship between group size and perpendicular sighting distance, for all sightings (top row) and only those not right truncated (bottom row). In the scatterplot, the line is a simple linear regression.

NARWSS Twin Otters

The sightings were right truncated at 5000m. Due to a reduced frequency of sightings close to the trackline that plausibly resulted from the behavior of the observers and/or the configuration of the survey platform, the sightings were left truncted as well. Sightings closer than 107 m to the trackline were omitted from the analysis, and it was assumed that the the area closer to the trackline than this was not surveyed. This distance was estimated by inspecting histograms of perpendicular sighting distances. The vertical sighting angles were heaped at 10 degree increments up to 80 degrees and 1 degree increments thereafter, so the candidate detection functions were fitted using linear bins scaled accordingly.

Covariate	Description

beaufort	Beaufort sea state.
quality	Survey-specific index of the quality of observation conditions, utilizing relevant factors other than Beaufort sea state (see methods).
size	Estimated size (number of individuals) of the sighted group.

Table 31: Covariates tested in candidate "multi-covariate distance sampling" (MCDS) detection functions.

Key	Adjustment	Order	Covariates	Succeeded	Δ AIC	Mean ESHW (m)
hr	poly	4		Yes	0.00	2113
hn	cos	3		Yes	5.12	2244
hr	poly	2		Yes	5.12	2187
hn	cos	2		Yes	12.96	2394
hr			size	Yes	14.30	2280
hn				Yes	25.91	2649
hn	herm	4		Yes	26.51	2639
hr				Yes	27.09	2194
hn			beaufort	No		
hr			beaufort	No		
hn			quality	No		
hr			quality	No		
hn			size	No		
hn			beaufort, quality	No		
hr			beaufort, quality	No		
hn			beaufort, size	No		
hr			beaufort, size	No		
hn			quality, size	No		
hr			quality, size	No		
hn			beaufort, quality, size	No		
hr			beaufort, quality, size	No		

Table 32: Candidate detection functions for NARWSS Twin Otters. The first one listed was selected for the density model.

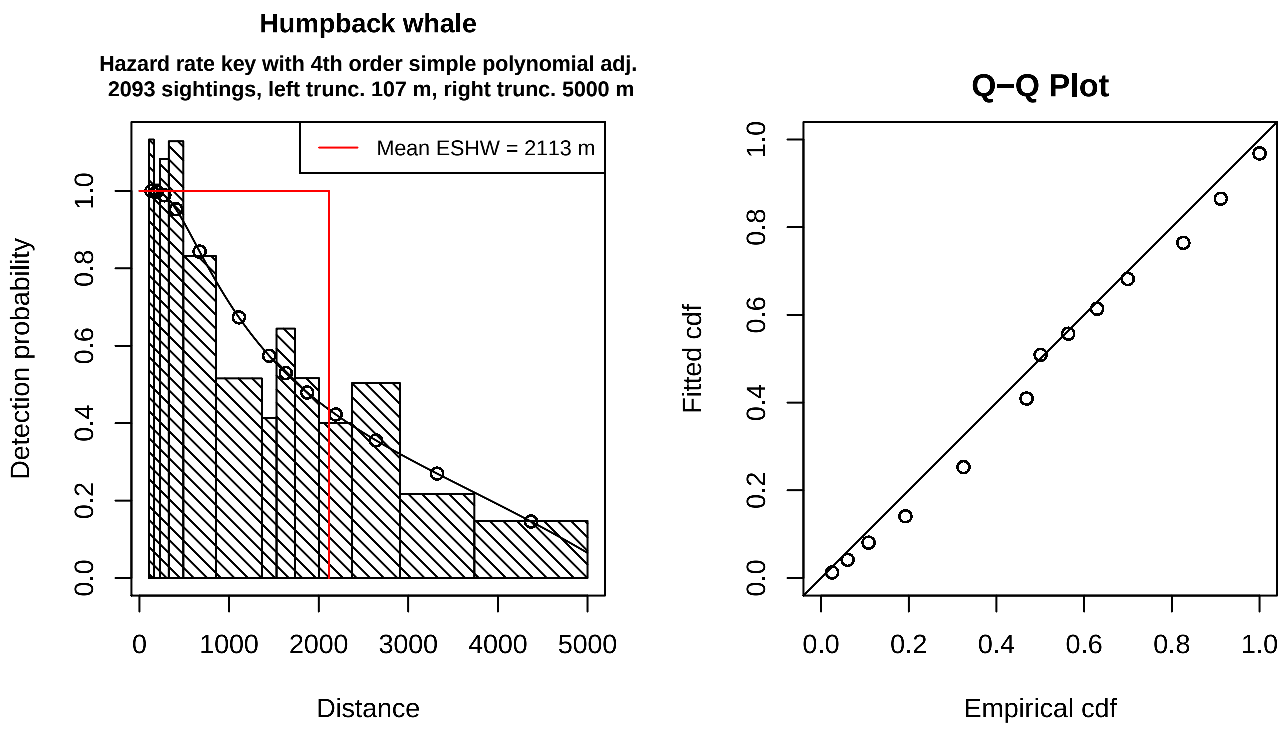

Figure 47: Detection function for NARWSS Twin Otters that was selected for the density model

Statistical output for this detection function:

```
Summary for ds object
Number of observations :  2093
Distance range         :  106.5979  -  5000
AIC                    :  10313.32

Detection function:
 Hazard-rate key function with simple polynomial adjustment term of order 4

Detection function parameters
Scale Coefficients:
            estimate        se
(Intercept) 7.127614 0.1420639

Shape parameters:
                estimate        se
(Intercept) 1.313404e-08 0.1294258

Adjustment term parameter(s):
                estimate        se
poly, order 4 -0.7058236 0.1244022


Monotonicity constraints were enforced.
                        Estimate           SE         CV
Average p              0.4226137   0.02549883 0.06033603
N in covered region 4952.5137804 309.93012447 0.06258037

Monotonicity constraints were enforced.
```

Additional diagnostic plots:

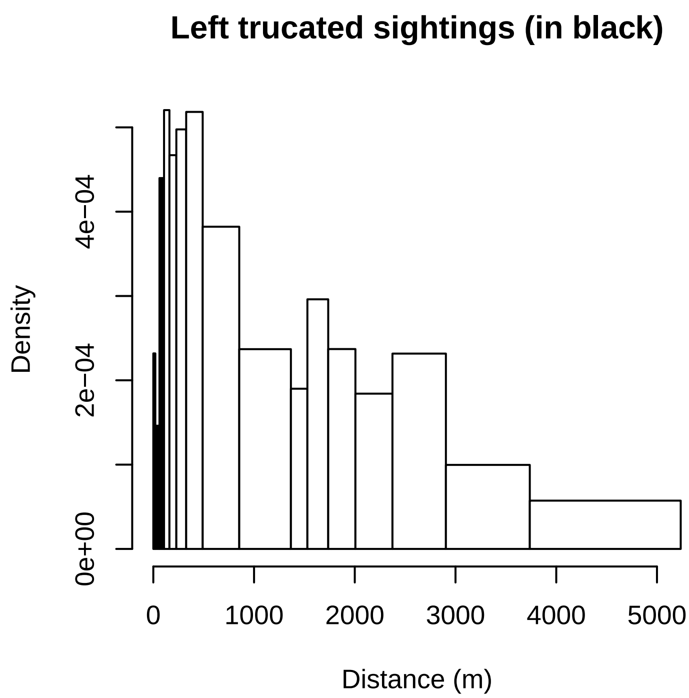

Figure 48: Density of sightings by perpendicular distance for NARWSS Twin Otters. Black bars on the left show sightings that were left truncated.

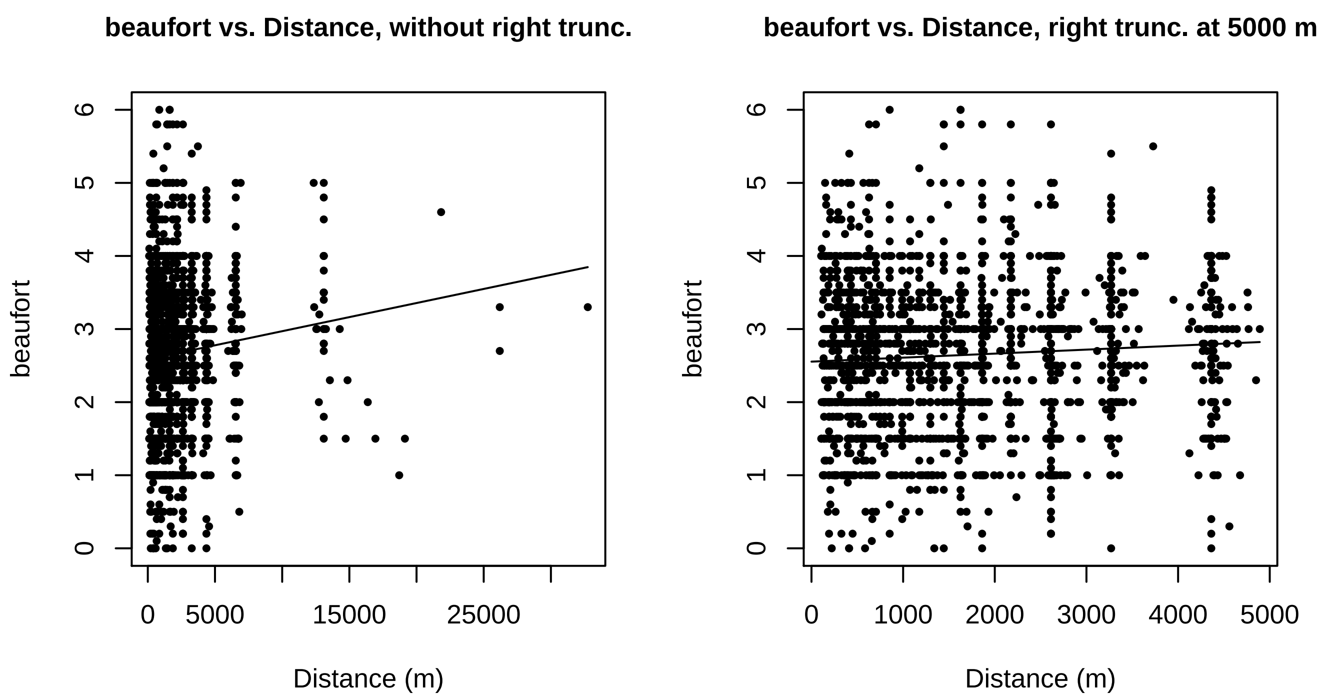

Figure 49: Scatterplots showing the relationship between Beaufort sea state and perpendicular sighting distance, for all sightings (left) and only those not right truncated (right). The line is a simple linear regression.

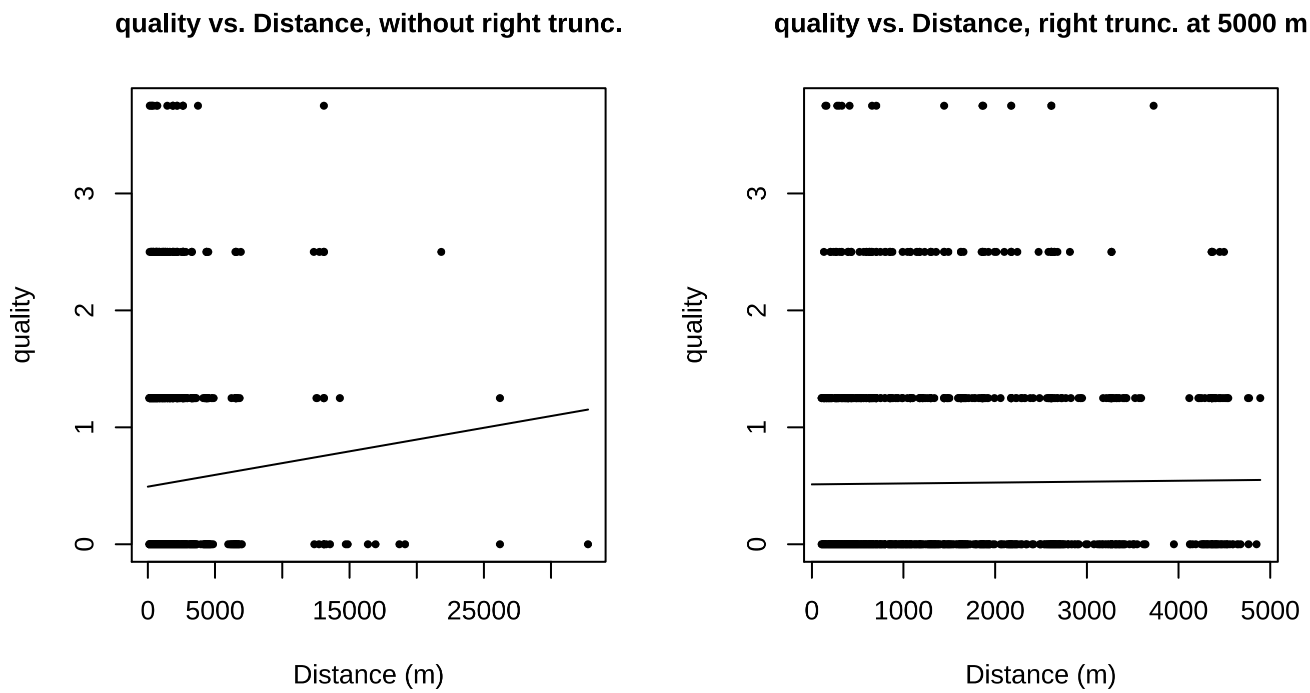

Figure 50: Scatterplots showing the relationship between the survey-specific index of the quality of observation conditions and perpendicular sighting distance, for all sightings (left) and only those not right truncated (right). Low values of the quality index correspond to better observation conditions. The line is a simple linear regression.

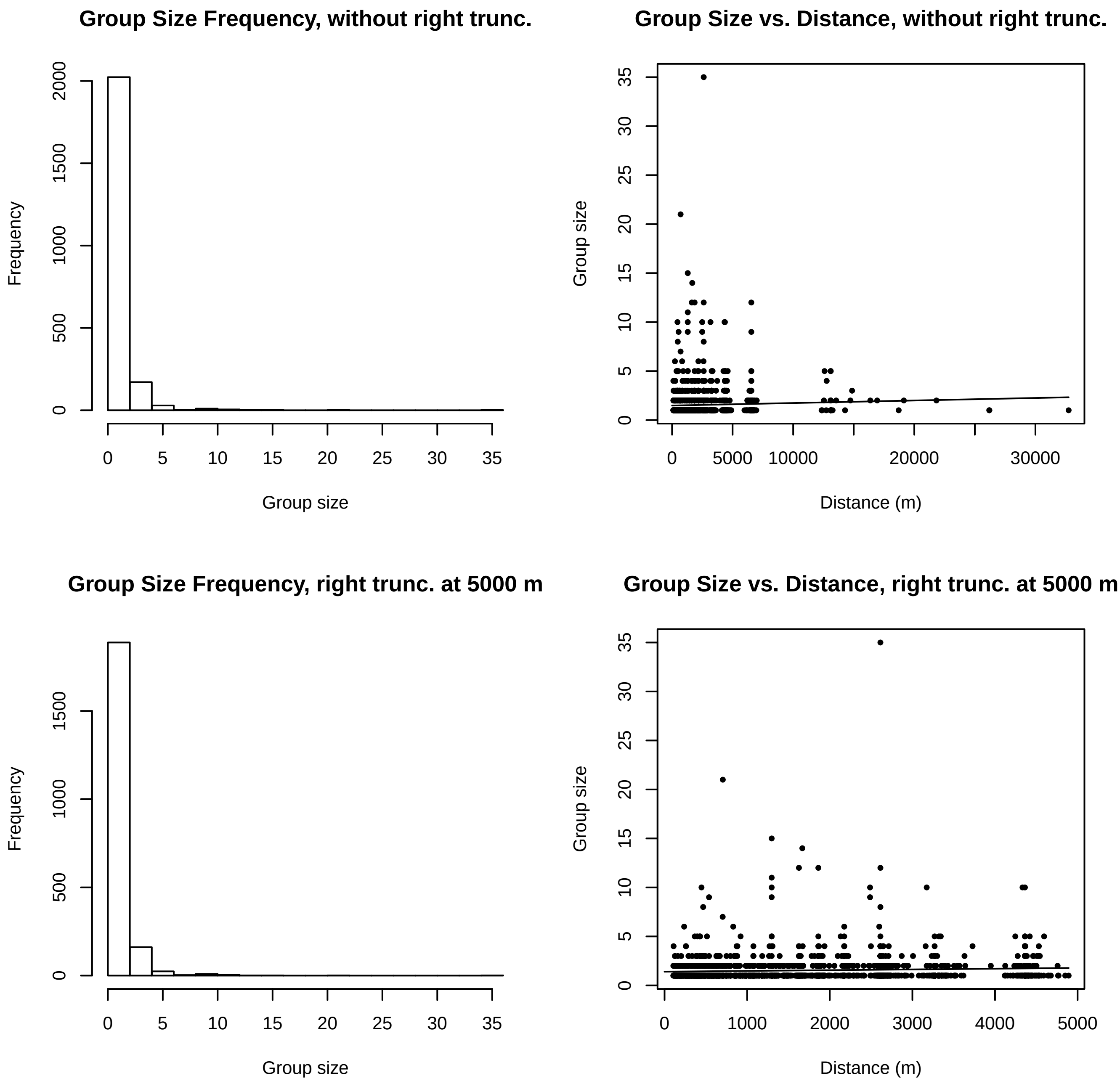

Figure 51: Histograms showing group size frequency and scatterplots showing the relationship between group size and perpendicular sighting distance, for all sightings (top row) and only those not right truncated (bottom row). In the scatterplot, the line is a simple linear regression.

g(0) Estimates

Platform	Surveys	Group Size	*g(0)*	Biases Addressed	Source
Shipboard	Binocular Surveys	Any	0.921	Perception	Barlow and Forney (2007)
Shipboard	NEFSC Endeavor	Any	0.88	Perception	Palka (2006)
Shipboard	Naked Eye Surveys	Any	0.38	Perception	Palka (2006)
Aerial	All	Any	0.451	Both	Heide-Jorgensen et al. (2012)

Table 33: Estimates of *g(0)* used in this density model.

Palka (2006) provided a survey-specific g(0) estimate (0.88) for humpbacks sighted on NOAA NEFSC's 2004 Endeavor shipboard survey. This survey used a dual- team methodology to account for perception bias. It did not account for availability bias, but availability bias is not expected to be significant for humpbacks, which are not a particularly long diving whale. We used Palka's g(0) estimate for the lower team, which was the primary team and the one for which we had sightings.

No other shipboard binocular surveys estimated g(0). For these we utilized Barlow and Forney's (2007) estimate (0.921), produced from several years of dual-team surveys in the Pacific ocean that used similar binoculars and protocols to the surveys in our study. Like Palka's, this estimate accounted for perception bias but not availability bias. We preferred it to Palka's because the latter was obtained from a very low number of sightings (~5).

As above, Palka (2006) provided a survey-specific g(0) estimate (0.38) for humpbacks sighted on NOAA NEFSC's 1999 Abel-J naked eye shipboard survey. We used the estimate for the upper team, which was the primary team and the one for which we had sightings. We also used this estimate with the European naked eye surveys, which did not publish g(0) estimates. (The European surveys were not used in the East Coast model documented here, but may have been used in the AFTT model. Please consult the AFTT model documentation for more information.)

Heide-Jorgensen et al. (2012) estimated the availability bias (0.46) and perception bias (0.98) components of g(0) for diving humpbacks at a West Greenland feeding ground, seen from a Twin Otter aircraft with bubble windows and a center observer in the copilot's seat, flying at 213 m altitude at 167 km/hr. For aerial surveys, we preferred this estimate to Palka (2006) because it was specific to humpbacks (Palka estimated g(0)=0.53 for all large whales pooled together).

Density Models

North Atlantic humpback whales undergo an annual migration in which they migrate to high latitudes in summer to feed and return low latitudes in winter to breed and calve (Mattila et al. 1989, 1994). In our study area, humpbacks feed in the Gulf of Maine during summer and breed in the West Indies in the winter (Robbins 2007). The survey data indicated that humpbacks are present in the Gulf of Maine throughout the year, although most appeared to depart during the fall and return during spring, with a relatively small number remaining to overwinter. The surveys also reported humpbacks southwest of Cape Cod and down the mid-Atlantic shelf in fall, winter, and spring. The mid-Atlantic may represent a supplementary winter feeding ground for juvenile and mature humpbacks (Wiley et al. 1995; Swingle et al. 1993).

In version 2 of our humpback models, we split the year into four seasons. This decision originated with a belief that the spring/summer half of the year should be split into two distinct seasons because: 1) starting in July, no humpbacks were reported southwest of the Nantucket Shoals by the surveys available to us at that time; 2) Robbins (2007, Fig. 3.2) reported a dramatic jump in humpback encounter rates going from June to July; 3) the survey data extended far into Canadian waters starting in July, but there was none in prior months. Proceeding from those these, we split the year into four seasons: winter (Dec-Mar), spring (Apr-Jun), summer (Jul-Sep), and fall (Oct-Nov). But when we predicted those models, we found that the predicted spatial distributions of humpbacks in spring, summer, and fall were all very similar. Also, we subsequently integrated the NJ DEP surveys, which reported humpbacks near New Jersey the months of August-November, indicating that humpbacks were utilizing areas south of the Gulf of Maine in fall months. Given the similarity in our spring, summer, and fall predictions, for we changed our model to only use two seasons: summer and winter.

As with version 2, we designated April the first month of summer because 1) Robbins (2007, Table 3.2) reported that the earliest sighting dates of female and male migrants arriving at the Gulf of Maine feeding grounds were 20 March and 19

April, respectively. Also the sightings reported by our surveys showed distinctly more sightings in April than in March, while February and March were similar to each other, as were April and May (see maps in Temporal Variability section).

Also as with version 2, we designated December as the first month of winter because 1) Robbins (2007, Table 3.3) reported that the last sighting dates of female and male migrants in the Gulf of Maine were 19 and 9 December, and 2) December is the first month in which our surveys reported significant numbers of humpbacks along the southeast coast.

Winter

In winter, relatively few humpbacks were sighted, but they were distributed throughout the study area, with many close to shore but some as far off shore as eastern Georges Bank, and one deeper than the shelf break off the Florida coast. We speculate that these sightings constitute a mixture of humpbacks overwintering and migrating. Obvious aggregations appear in the Gulf of Maine and around Cape Hatteras. The mid-Atlantic may represent a supplementary winter feeding ground for juvenile and mature humpbacks (Wiley et al. 1995; Swingle et al. 1993). Acoustic studies (see Discussion) reported humpbacks near the shelf break in Onslow Bay, North Carolina and Jacksonville, Florida; the visual surveys also reported sightings on those regions.

Although there appeared to be more sightings in the Gulf of Maine than in the mid-Atlantic, we couldn't discern a distinct difference in the distribution patterns between the two areas, and the literature did not conclusively indicate there was an important difference between whales present in the two areas. Thus we modeled the entire east coast as a single model, grouping the northern and southern surveys together. We excluded Canadian waters, as we had no surveys in Canada in winter and were reluctant to extrapolate our model into Canadian waters.

In March, 2015, we reviewed our version 9 models with J. Robbins. She expressed support for our decision to group the northern and southern data into a single model, explaining that most of sightings were probably of overwintering juvenile humpbacks and that she considered it unlikely that there was a significant difference between humpbacks in the two areas, at least that could be elucidated by our models.

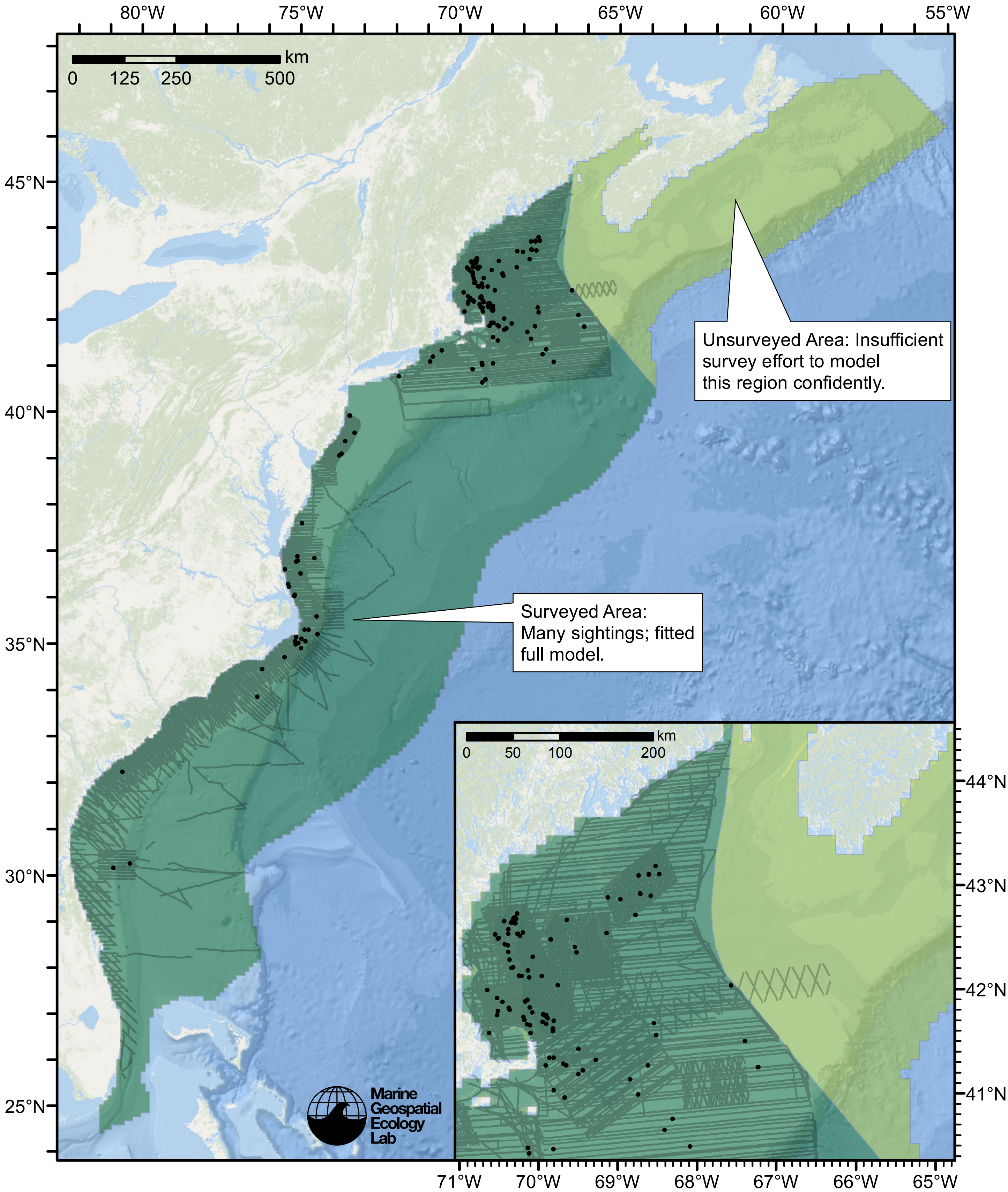

Figure 52: Humpback whale density model schematic for Winter season. All on-effort sightings are shown, including those that were truncated when detection functions were fitted.

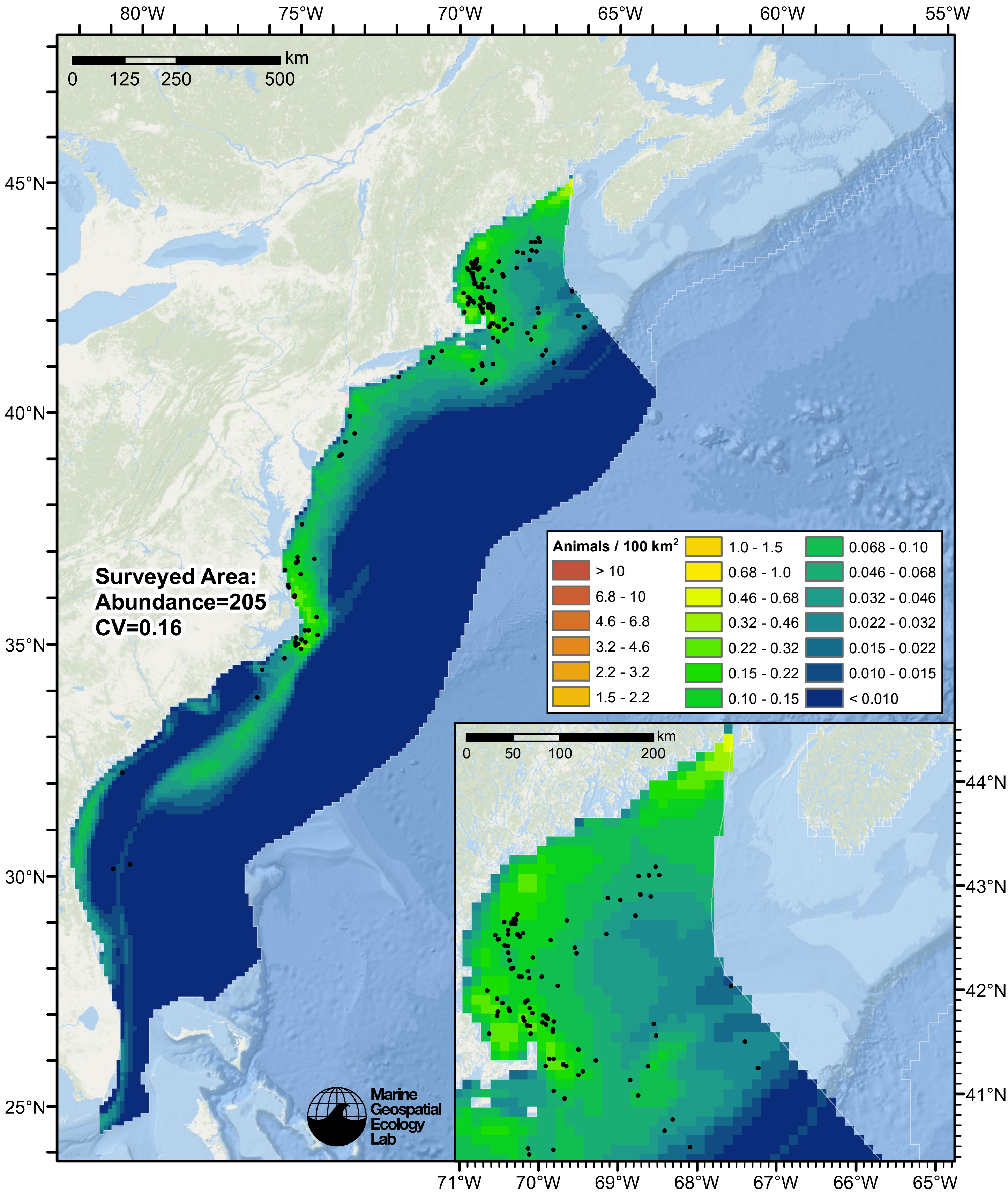

Figure 53: Humpback whale density predicted by the Winter season climatological model that explained the most deviance. Pixels are 10x10 km. The legend gives the estimated individuals per pixel; breaks are logarithmic. The same scale is used for all seasons. Abundance for each region was computed by summing the density cells occuring in that region.

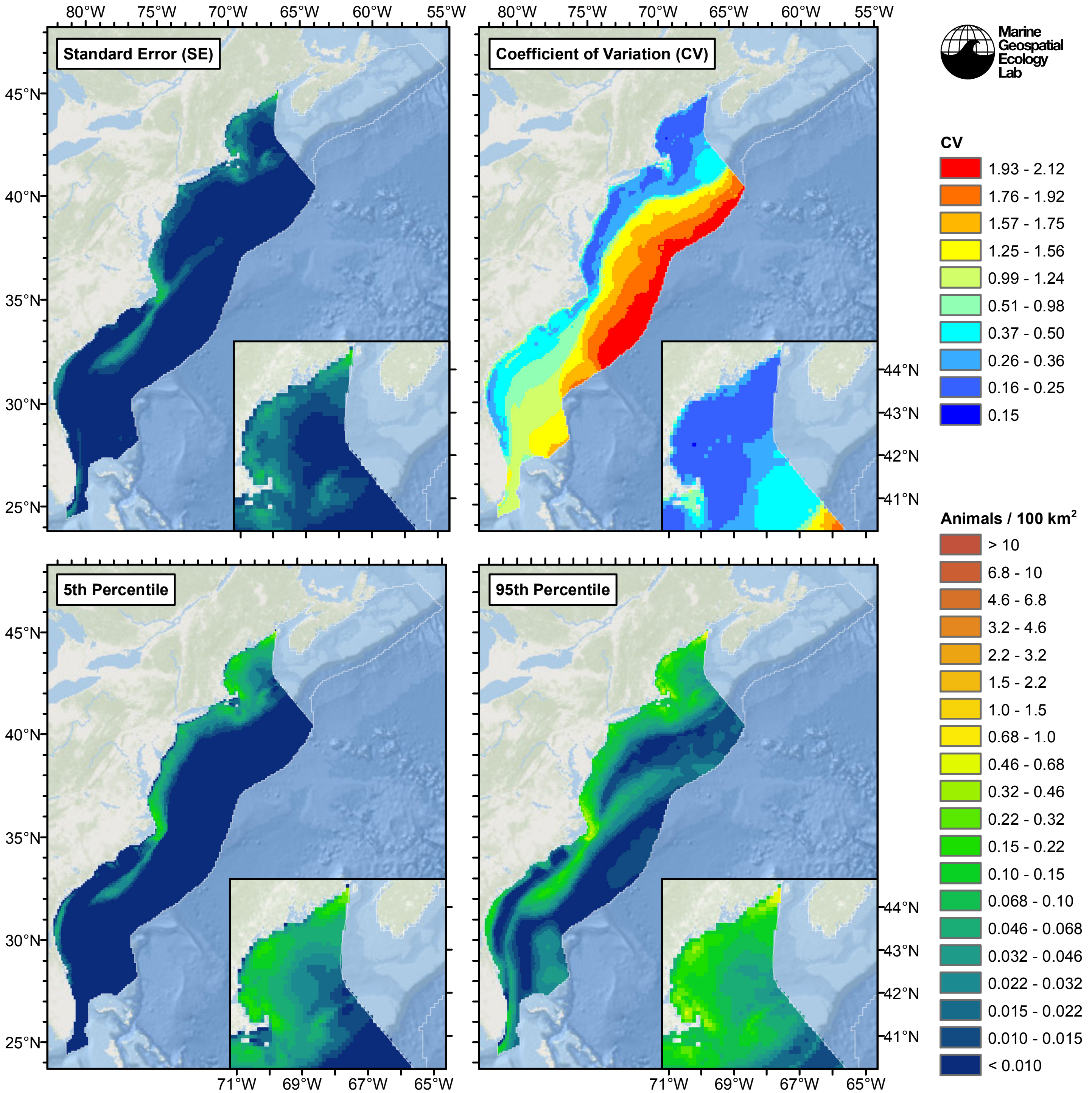

Figure 54: Estimated uncertainty for the Winter season climatological model that explained the most deviance. These estimates only incorporate the statistical uncertainty estimated for the spatial model (by the R mgcv package). They do not incorporate uncertainty in the detection functions, g(0) estimates, predictor variables, and so on.

Surveyed Area

Statistical output

```
Rscript.exe: This is mgcv 1.8-2. For overview type 'help("mgcv-package")'.


Family: Tweedie(p=1.213)
```

```
Link function: log

Formula:
abundance ~ offset(log(area_km2)) + s(log10(Depth), bs = "ts",
    k = 5) + s(sqrt(DistToShore/1000), bs = "ts", k = 5) + s(I(ClimDistToFront2^(1/3)),
    bs = "ts", k = 5) + s(log10(pmax(ClimEKE, 1e-04)), bs = "ts",
    k = 5) + s(ClimChl1, bs = "ts", k = 5)

Parametric coefficients:
            Estimate Std. Error t value Pr(>|t|)
(Intercept)  -8.1186     0.1797  -45.19   <2e-16 ***
---
Signif. codes:  0 '***' 0.001 '**' 0.01 '*' 0.05 '.' 0.1 ' ' 1

Approximate significance of smooth terms:
                                edf Ref.df     F  p-value
s(log10(Depth))              2.7145      4 7.830 2.82e-08 ***
s(sqrt(DistToShore/1000))    0.9061      4 1.578 0.006493 **
s(I(ClimDistToFront2^(1/3)))  0.9966      4 2.985 0.000244 ***
s(log10(pmax(ClimEKE, 1e-04))) 1.1188      4 6.879 5.36e-08 ***
s(ClimChl1)                  2.7342      4 9.222 1.56e-09 ***
---
Signif. codes:  0 '***' 0.001 '**' 0.01 '*' 0.05 '.' 0.1 ' ' 1

R-sq.(adj) =  0.00482   Deviance explained = 18.4%
-REML = 1093.6  Scale est. = 21.42     n = 31668

All predictors were significant. This is the final model.
Creating term plots.
Diagnostic output from gam.check():

Method: REML   Optimizer: outer newton
full convergence after 9 iterations.
Gradient range [-0.0006943249,0.0002064049]
(score 1093.577 & scale 21.42037).
Hessian positive definite, eigenvalue range [0.3541158,824.1048].
Model rank =  21 / 21

Basis dimension (k) checking results. Low p-value (k-index<1) may
indicate that k is too low, especially if edf is close to k'.

                                k'   edf k-index p-value
s(log10(Depth))              4.000 2.715   0.776    0.04
s(sqrt(DistToShore/1000))    4.000 0.906   0.744    0.00
s(I(ClimDistToFront2^(1/3)))  4.000 0.997   0.787    0.08
s(log10(pmax(ClimEKE, 1e-04))) 4.000 1.119   0.804    0.88
s(ClimChl1)                  4.000 2.734   0.765    0.04
```

Predictors retained during the model selection procedure: Depth, DistToShore, ClimDistToFront2, ClimEKE, ClimChl1

Predictors dropped during the model selection procedure: Slope, DistTo125m, ClimSST

Model term plots

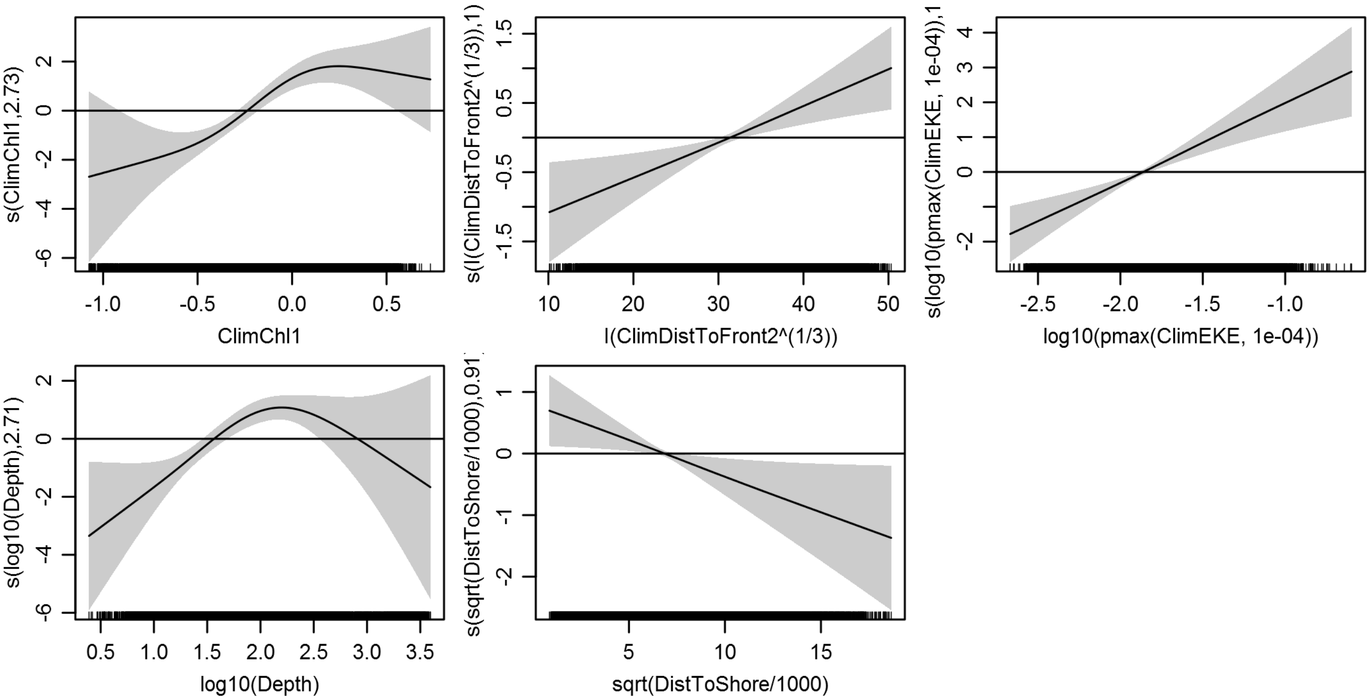

Diagnostic plots

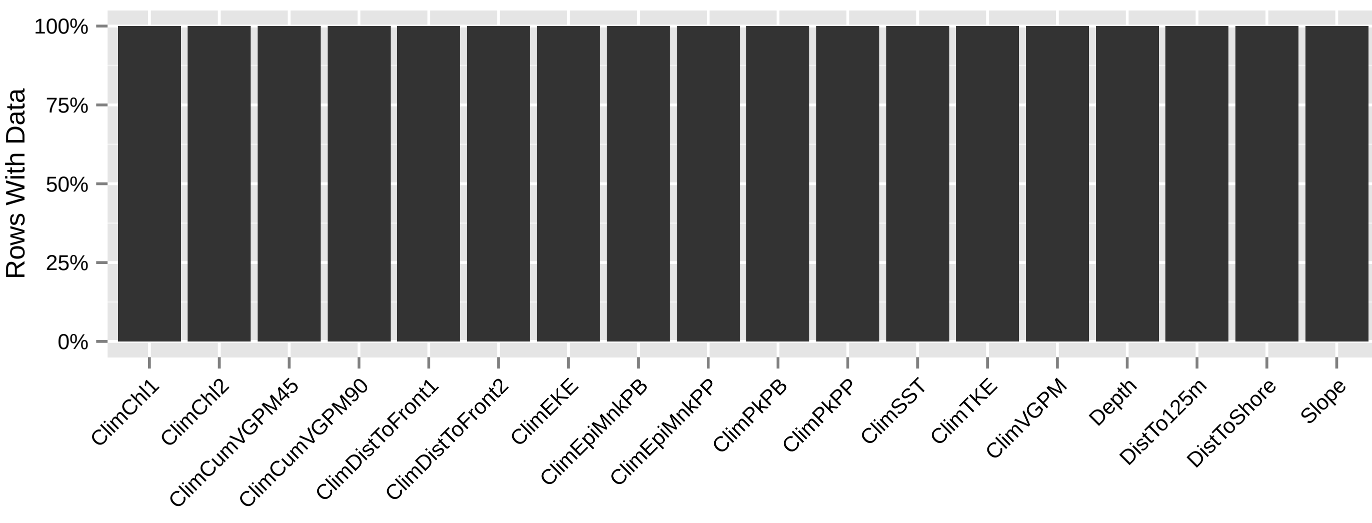

Figure 55: Segments with predictor values for the Humpback whale Climatological model, Winter season, Surveyed Area. This plot is used to assess how many segments would be lost by including a given predictor in a model.

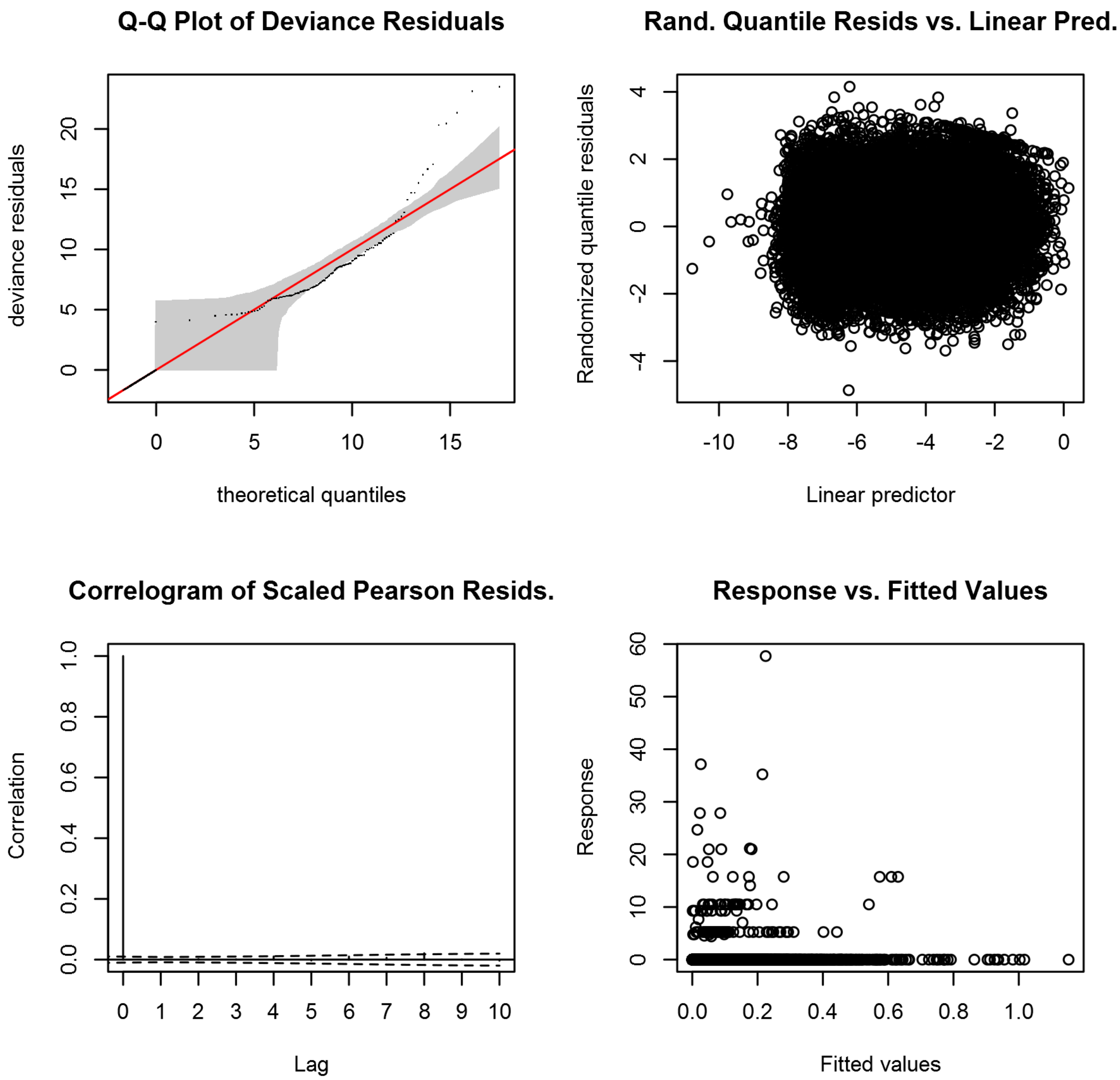

Figure 56: Statistical diagnostic plots for the Humpback whale Climatological model, Winter season, Surveyed Area.

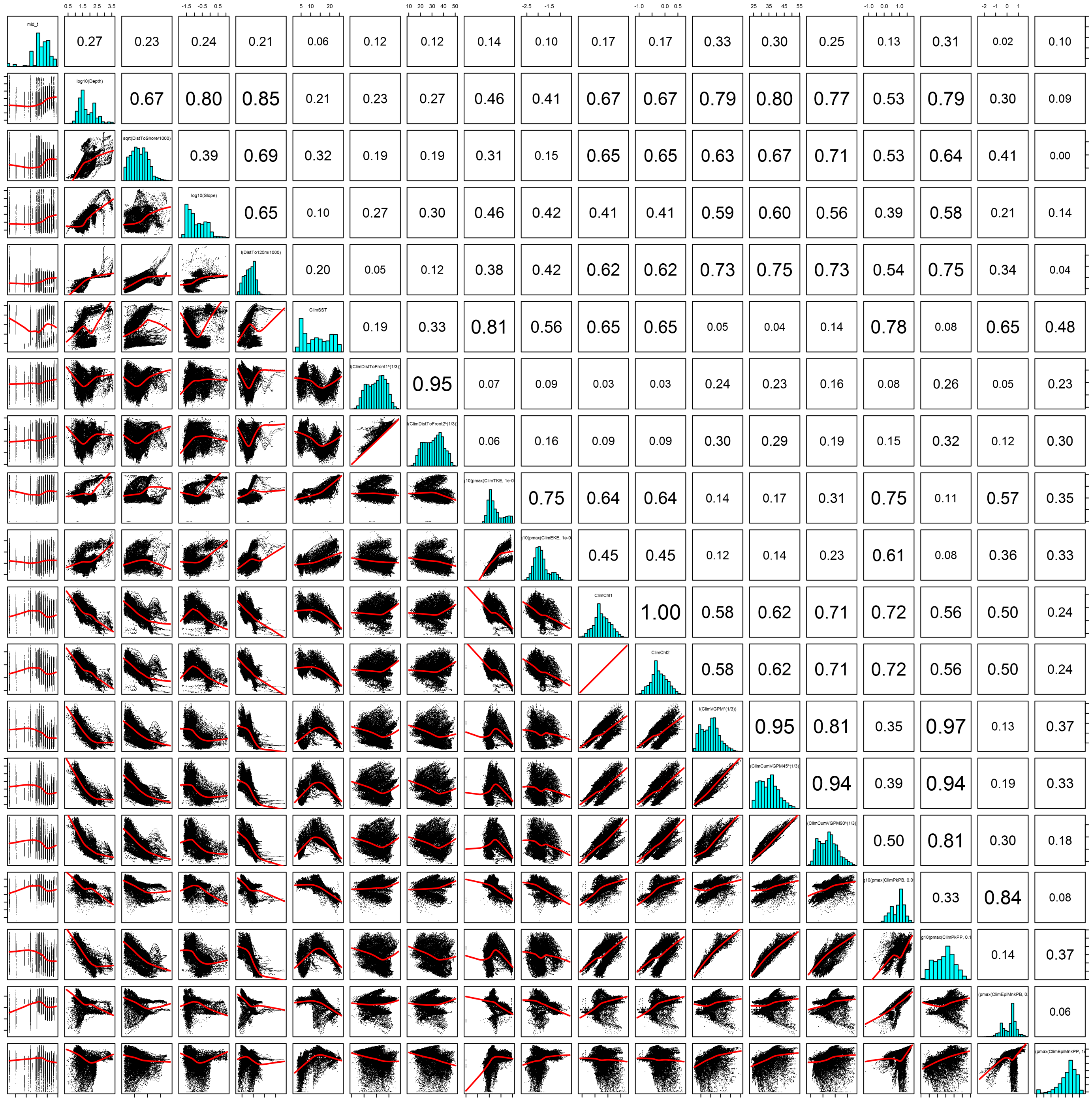

Figure 57: Scatterplot matrix for the Humpback whale Climatological model, Winter season, Surveyed Area. This plot is used to inspect the distribution of predictors (via histograms along the diagonal), simple correlation between predictors (via pairwise Pearson coefficients above the diagonal), and linearity of predictor correlations (via scatterplots below the diagonal). This plot is best viewed at high magnification.

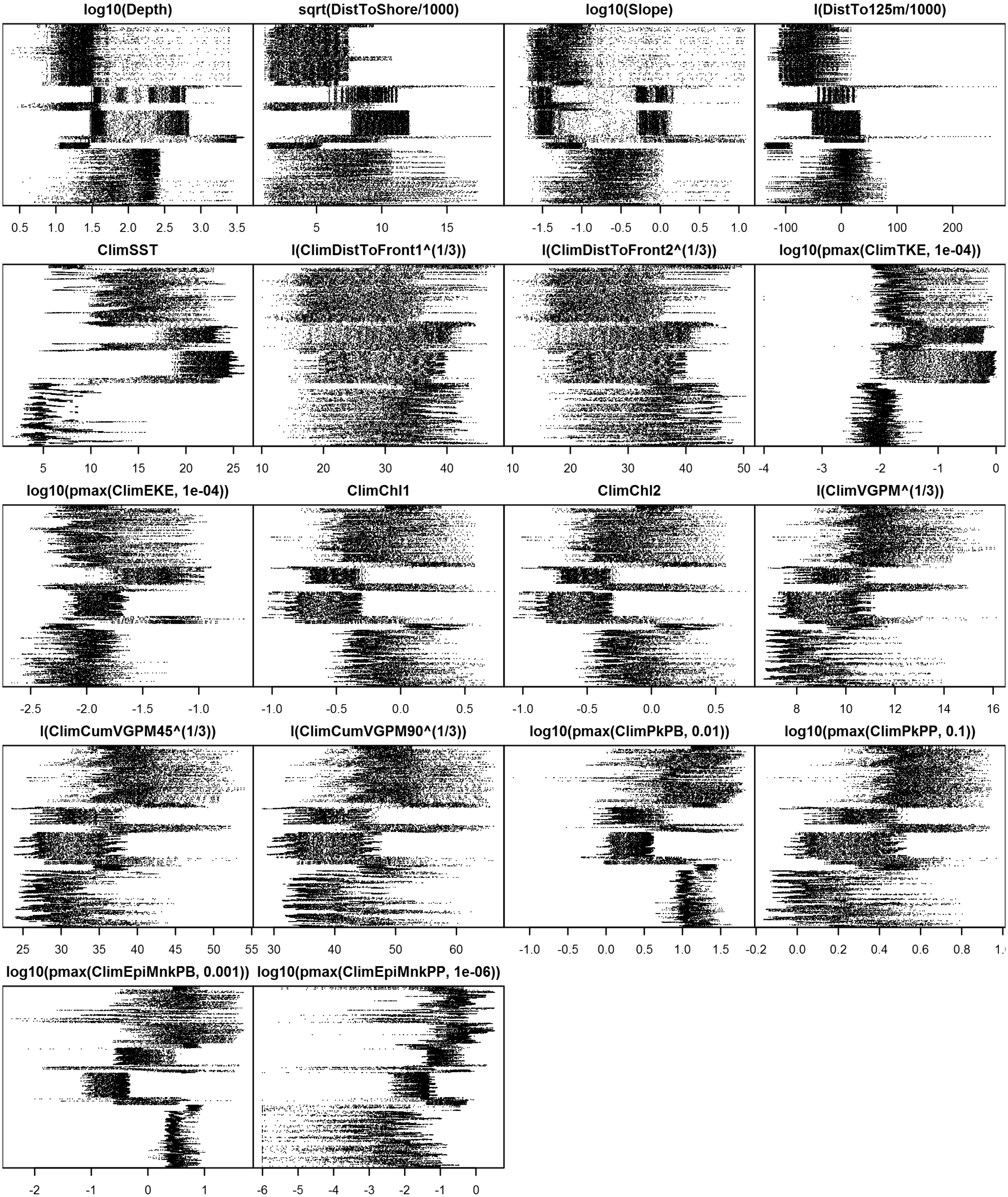

Figure 58: Dotplot for the Humpback whale Climatological model, Winter season, Surveyed Area. This plot is used to check for suspicious patterns and outliers in the data. Points are ordered vertically by transect ID, sequentially in time.

Unsurveyed Area

Density was not modeled for this region.

Contemporaneous Model

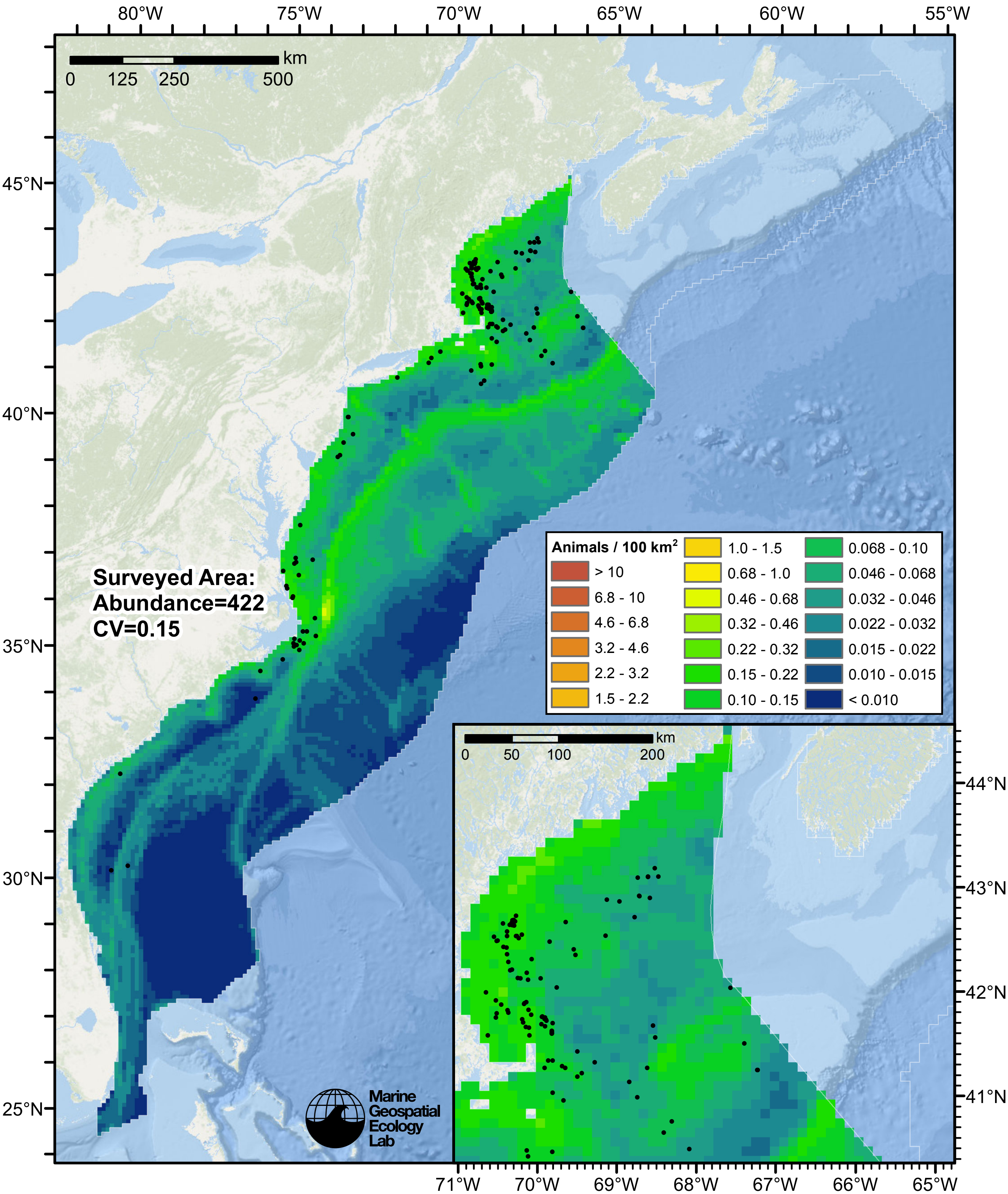

Figure 59: Humpback whale density predicted by the Winter season contemporaneous model that explained the most deviance. Pixels are 10x10 km. The legend gives the estimated individuals per pixel; breaks are logarithmic. The same scale is used for all seasons. Abundance for each region was computed by summing the density cells occuring in that region.

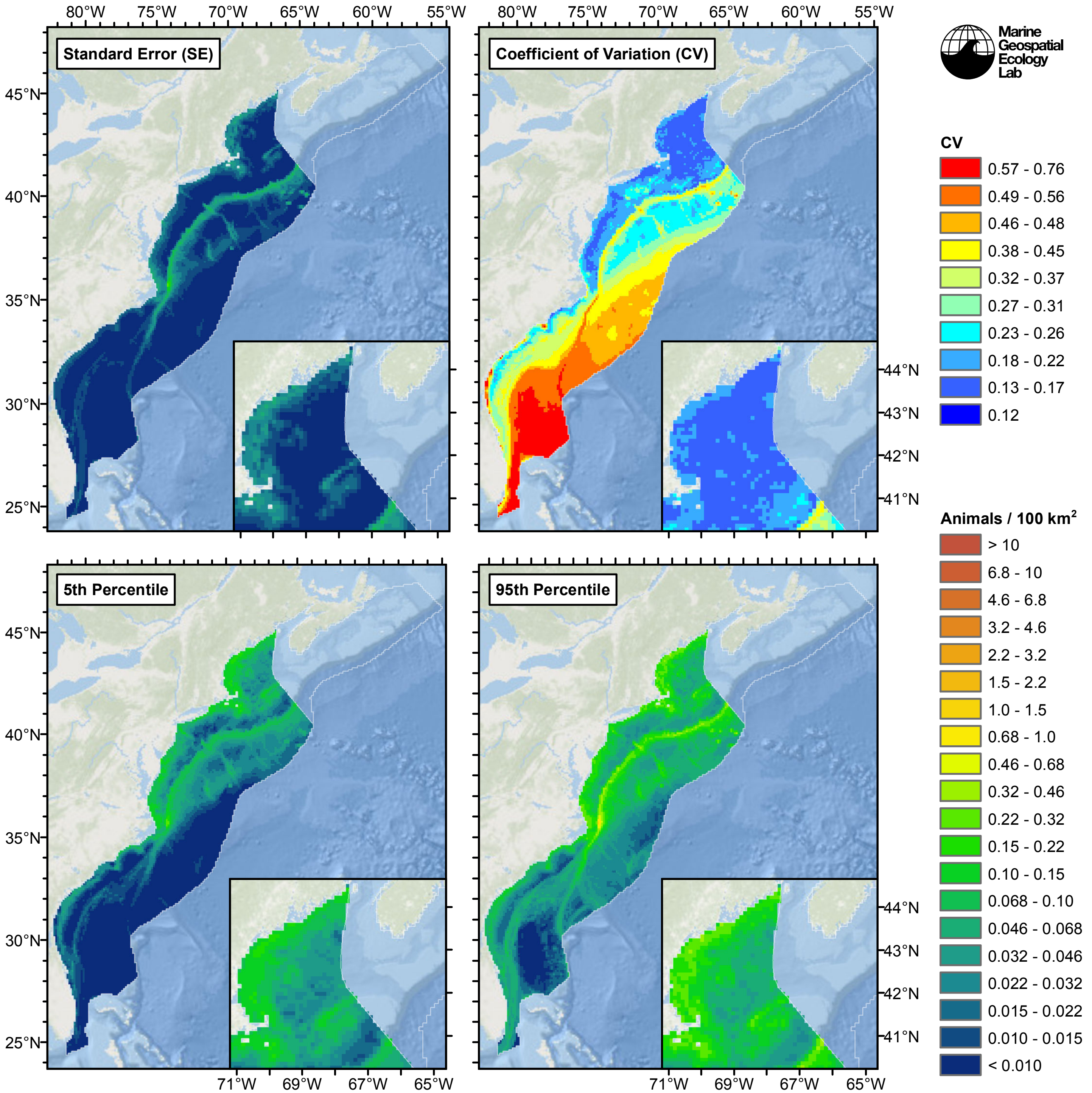

Figure 60: Estimated uncertainty for the Winter season contemporaneous model that explained the most deviance. These estimates only incorporate the statistical uncertainty estimated for the spatial model (by the R mgcv package). They do not incorporate uncertainty in the detection functions, g(0) estimates, predictor variables, and so on.

Surveyed Area

Statistical output

```
Rscript.exe: This is mgcv 1.8-2. For overview type 'help("mgcv-package")'.


Family: Tweedie(p=1.212)
```

```
Link function: log

Formula:
abundance ~ offset(log(area_km2)) + s(log10(Slope), bs = "ts",
    k = 5) + s(SST, bs = "ts", k = 5) + s(log10(pmax(TKE, 1e-04)),
    bs = "ts", k = 5) + s(I(CumVGPM90^(1/3)), bs = "ts", k = 5)

Parametric coefficients:
            Estimate Std. Error t value Pr(>|t|)
(Intercept)  -7.7599     0.1532  -50.64   <2e-16 ***
---
Signif. codes:  0 '***' 0.001 '**' 0.01 '*' 0.05 '.' 0.1 ' ' 1

Approximate significance of smooth terms:
                              edf Ref.df      F  p-value
s(log10(Slope))            1.2011      4  7.485 2.32e-08 ***
s(SST)                     1.0251      4  4.011 1.64e-05 ***
s(log10(pmax(TKE, 1e-04))) 0.9511      4  2.066  0.00208 **
s(I(CumVGPM90^(1/3)))      3.0246      4 14.128 9.25e-14 ***
---
Signif. codes:  0 '***' 0.001 '**' 0.01 '*' 0.05 '.' 0.1 ' ' 1

R-sq.(adj) =  0.00601   Deviance explained = 15.4%
-REML = 1097.8  Scale est. = 21.657    n = 30357

All predictors were significant. This is the final model.
Creating term plots.
Diagnostic output from gam.check():

Method: REML   Optimizer: outer newton
full convergence after 10 iterations.
Gradient range [-0.0001414761,3.013027e-05]
(score 1097.813 & scale 21.65738).
Hessian positive definite, eigenvalue range [0.225054,835.2719].
Model rank =  17 / 17

Basis dimension (k) checking results. Low p-value (k-index<1) may
indicate that k is too low, especially if edf is close to k'.

                              k'   edf k-index p-value
s(log10(Slope))            4.000 1.201   0.773    0.17
s(SST)                     4.000 1.025   0.749    0.04
s(log10(pmax(TKE, 1e-04))) 4.000 0.951   0.772    0.12
s(I(CumVGPM90^(1/3)))      4.000 3.025   0.779    0.54

Predictors retained during the model selection procedure: Slope, SST, TKE, CumVGPM90

Predictors dropped during the model selection procedure: Depth, DistToShore, DistTo125m,
DistToFront2
```

Model term plots

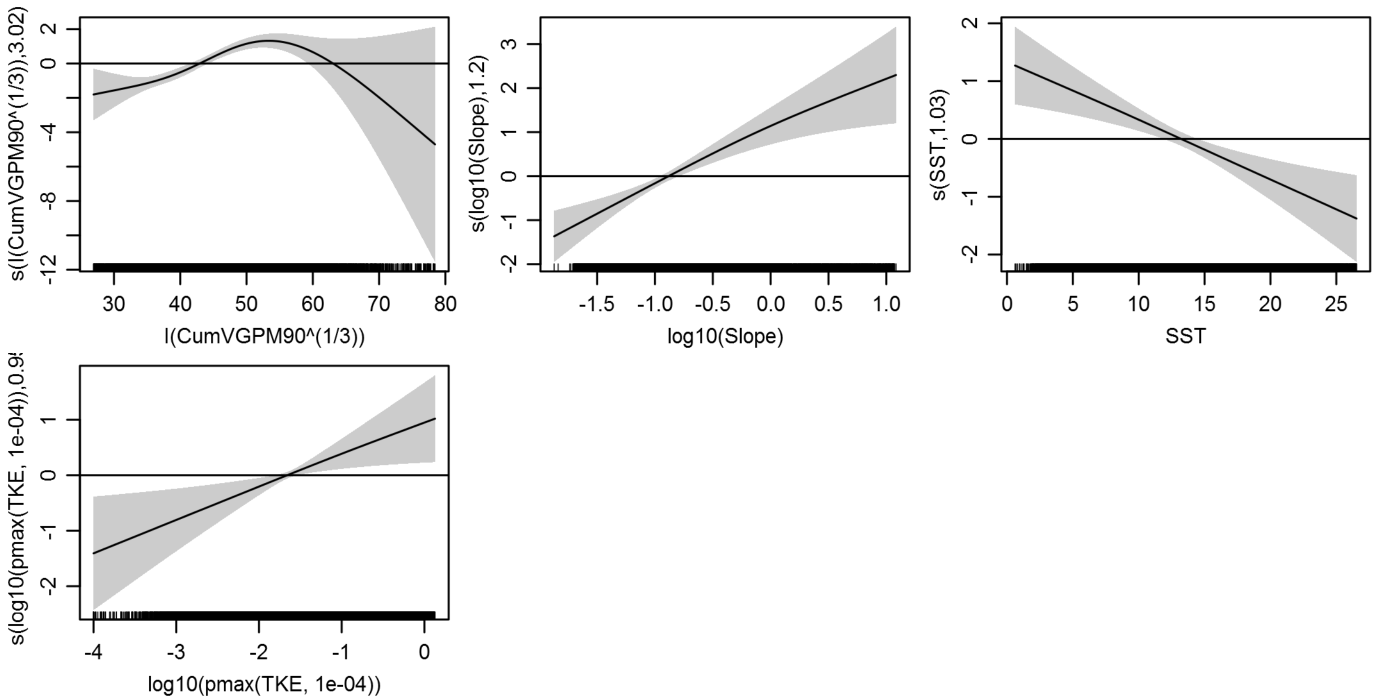

Diagnostic plots

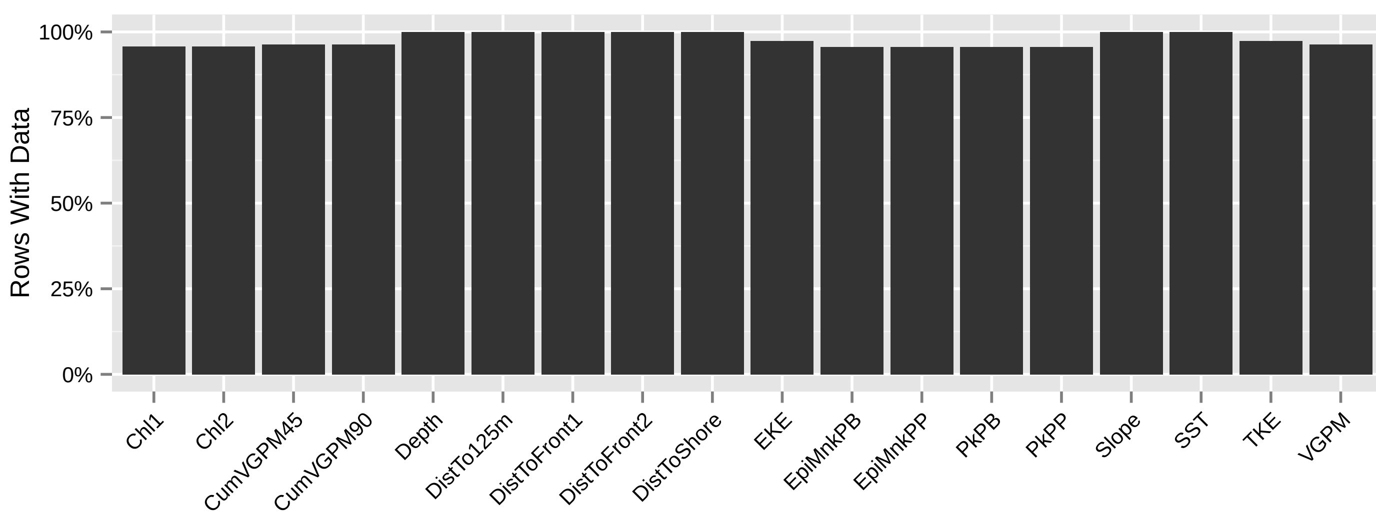

Figure 61: Segments with predictor values for the Humpback whale Contemporaneous model, Winter season, Surveyed Area. This plot is used to assess how many segments would be lost by including a given predictor in a model.

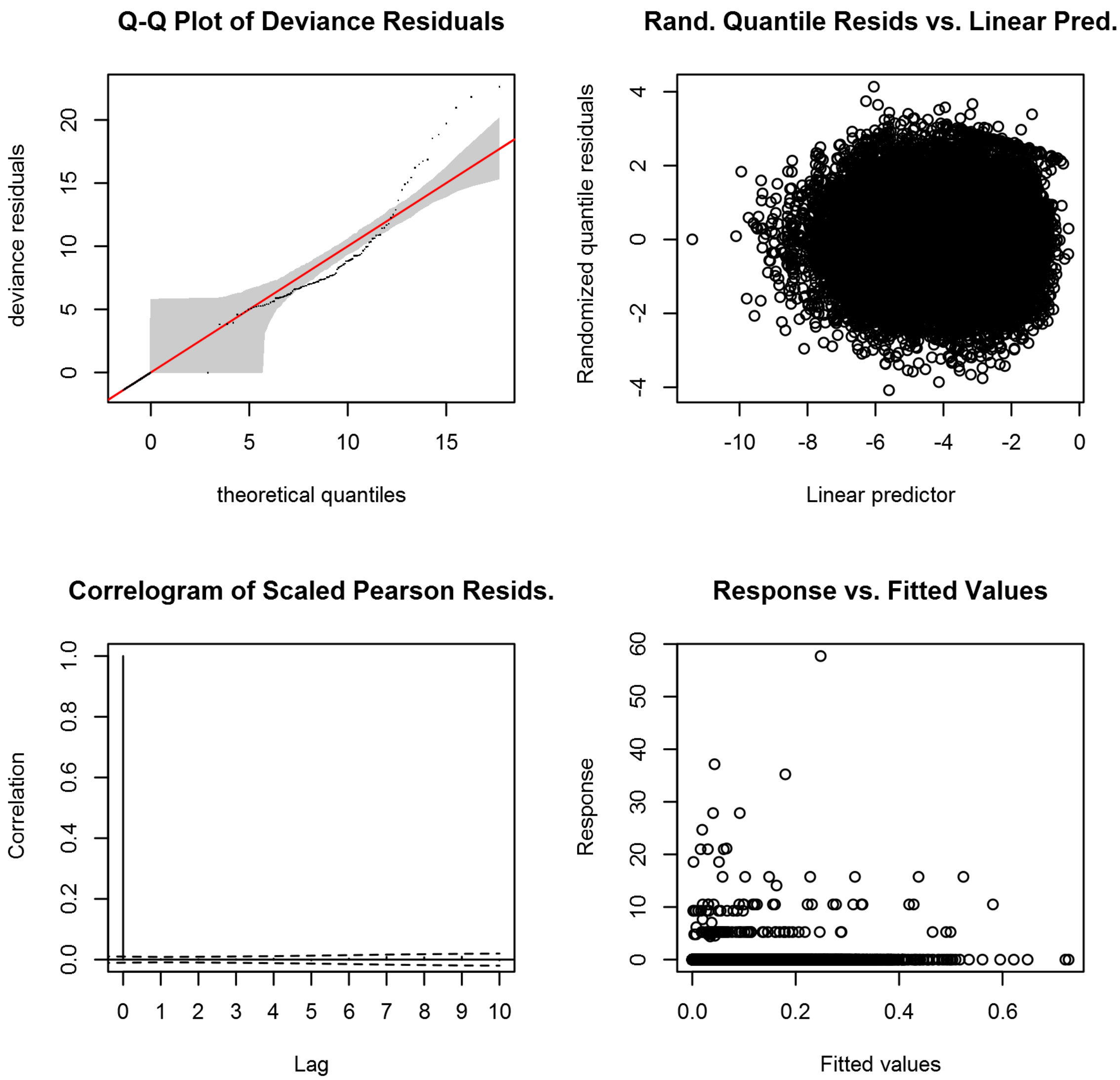

Figure 62: Statistical diagnostic plots for the Humpback whale Contemporaneous model, Winter season, Surveyed Area.

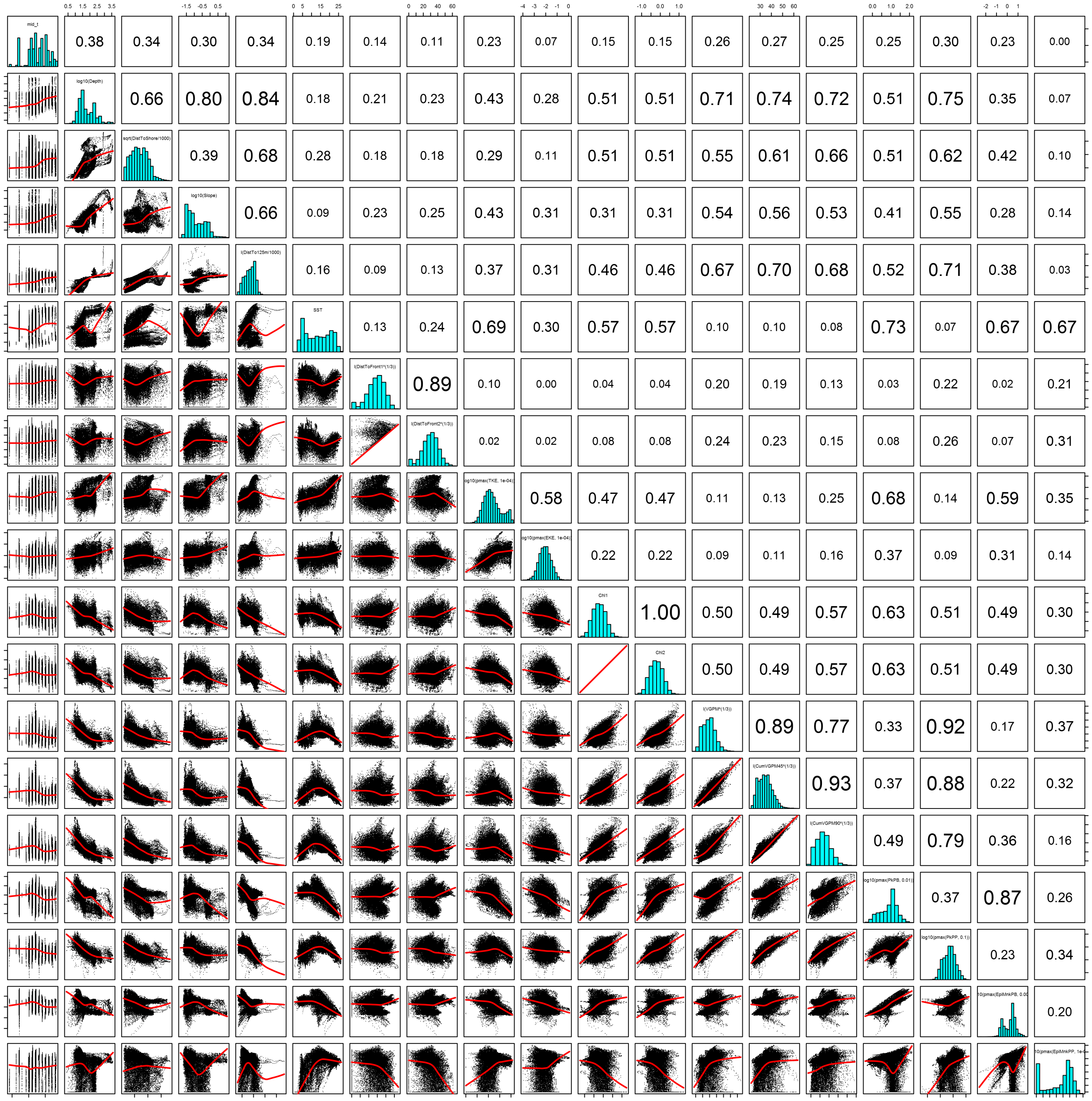

Figure 63: Scatterplot matrix for the Humpback whale Contemporaneous model, Winter season, Surveyed Area. This plot is used to inspect the distribution of predictors (via histograms along the diagonal), simple correlation between predictors (via pairwise Pearson coefficients above the diagonal), and linearity of predictor correlations (via scatterplots below the diagonal). This plot is best viewed at high magnification.

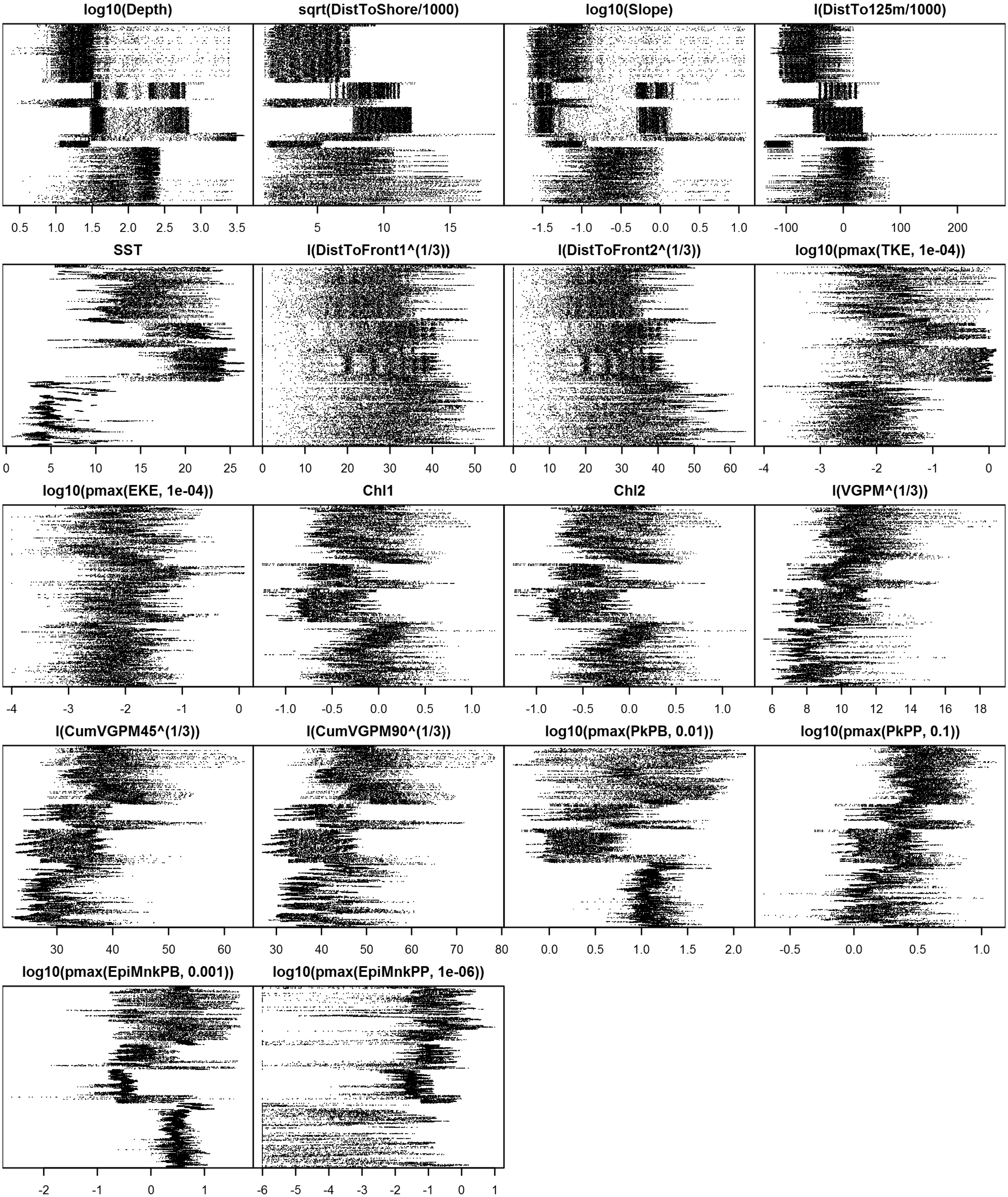

Figure 64: Dotplot for the Humpback whale Contemporaneous model, Winter season, Surveyed Area. This plot is used to check for suspicious patterns and outliers in the data. Points are ordered vertically by transect ID, sequentially in time.

Unsurveyed Area

Density was not modeled for this region.

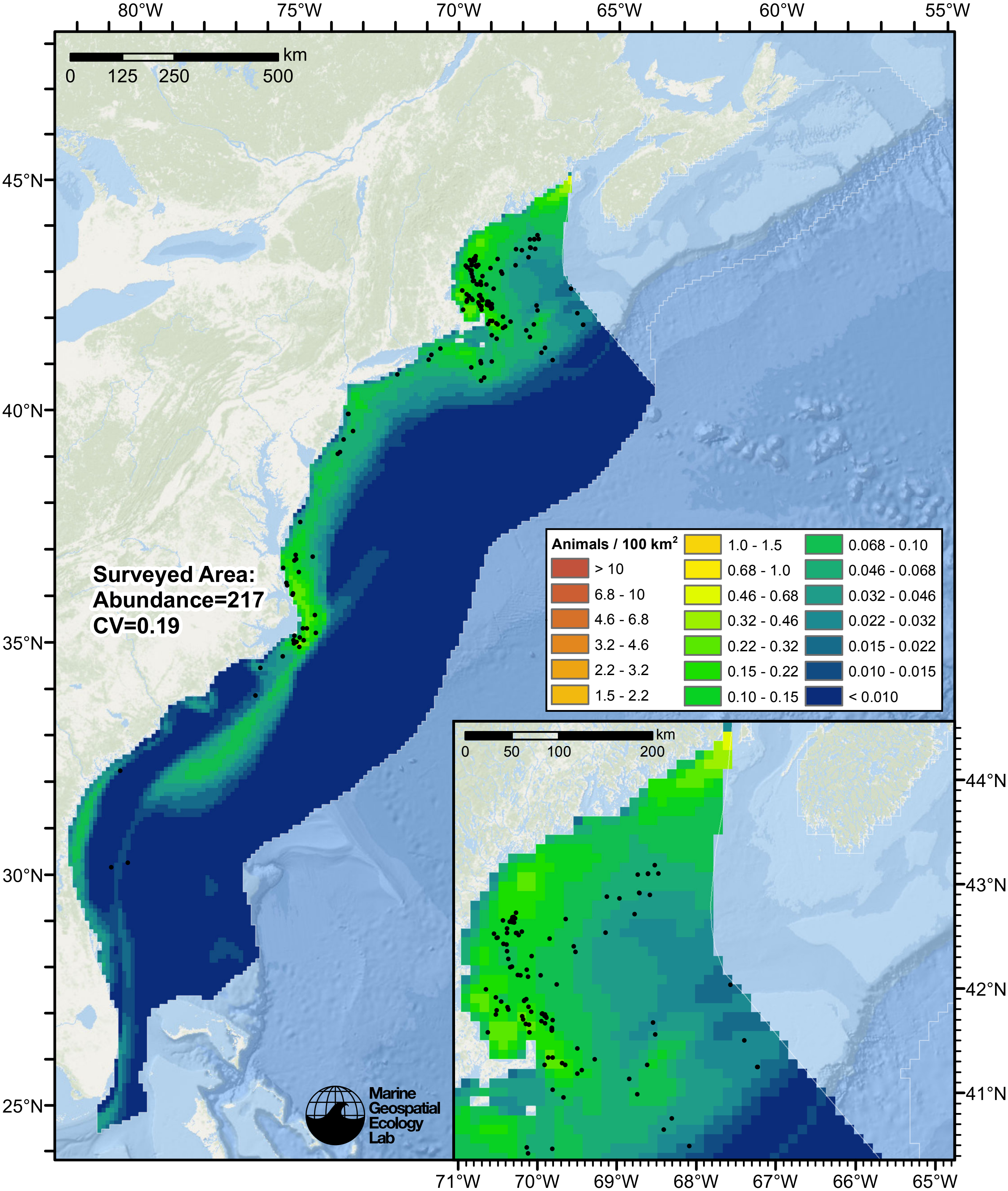

Figure 65: Humpback whale density predicted by the Winter season climatological same segments model that explained the most deviance. Pixels are 10x10 km. The legend gives the estimated individuals per pixel; breaks are logarithmic. The same scale is used for all seasons. Abundance for each region was computed by summing the density cells occuring in that region.

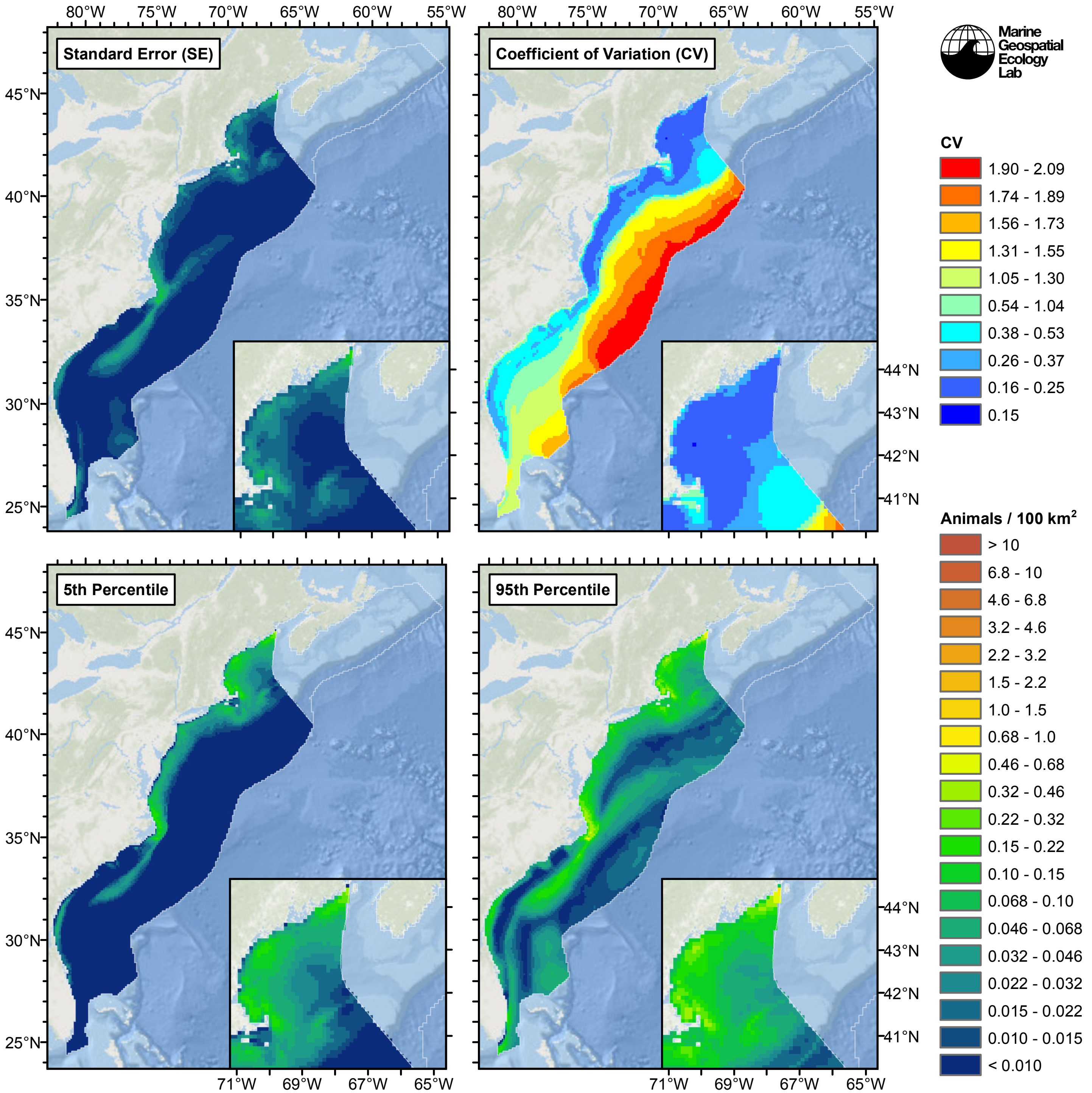

Figure 66: Estimated uncertainty for the Winter season climatological same segments model that explained the most deviance. These estimates only incorporate the statistical uncertainty estimated for the spatial model (by the R mgcv package). They do not incorporate uncertainty in the detection functions, g(0) estimates, predictor variables, and so on.

Surveyed Area

Statistical output

```
Rscript.exe: This is mgcv 1.8-2. For overview type 'help("mgcv-package")'.


Family: Tweedie(p=1.214)
```

```
Link function: log

Formula:
abundance ~ offset(log(area_km2)) + s(log10(Depth), bs = "ts",
    k = 5) + s(sqrt(DistToShore/1000), bs = "ts", k = 5) + s(I(ClimDistToFront2^(1/3)),
    bs = "ts", k = 5) + s(log10(pmax(ClimEKE, 1e-04)), bs = "ts",
    k = 5) + s(ClimChl1, bs = "ts", k = 5)

Parametric coefficients:
            Estimate Std. Error t value Pr(>|t|)
(Intercept)   -8.049      0.178  -45.23   <2e-16 ***
---
Signif. codes:  0 '***' 0.001 '**' 0.01 '*' 0.05 '.' 0.1 ' ' 1

Approximate significance of smooth terms:
                                edf Ref.df     F  p-value
s(log10(Depth))              2.6793      4 7.422 6.86e-08 ***
s(sqrt(DistToShore/1000))    0.9053      4 1.529 0.007312 **
s(I(ClimDistToFront2^(1/3)))  0.9976      4 3.002 0.000234 ***
s(log10(pmax(ClimEKE, 1e-04))) 1.1232      4 6.917 4.91e-08 ***
s(ClimChl1)                  2.7803      4 9.144 2.10e-09 ***
---
Signif. codes:  0 '***' 0.001 '**' 0.01 '*' 0.05 '.' 0.1 ' ' 1

R-sq.(adj) =  0.00475   Deviance explained = 17.8%
-REML =   1092  Scale est. = 21.454    n = 30357

All predictors were significant. This is the final model.
Creating term plots.
Diagnostic output from gam.check():

Method: REML   Optimizer: outer newton
full convergence after 9 iterations.
Gradient range [-0.0007552073,0.0002292819]
(score 1091.975 & scale 21.45443).
Hessian positive definite, eigenvalue range [0.3492334,819.8543].
Model rank =  21 / 21

Basis dimension (k) checking results. Low p-value (k-index<1) may
indicate that k is too low, especially if edf is close to k'.

                                k'   edf k-index p-value
s(log10(Depth))              4.000 2.679   0.803    0.06
s(sqrt(DistToShore/1000))    4.000 0.905   0.811    0.21
s(I(ClimDistToFront2^(1/3)))  4.000 0.998   0.806    0.04
s(log10(pmax(ClimEKE, 1e-04))) 4.000 1.123   0.786    0.04
s(ClimChl1)                  4.000 2.780   0.790    0.05
```

Predictors retained during the model selection procedure: Depth, DistToShore, ClimDistToFront2, ClimEKE, ClimChl1

Predictors dropped during the model selection procedure: Slope, DistTo125m, ClimSST

Model term plots

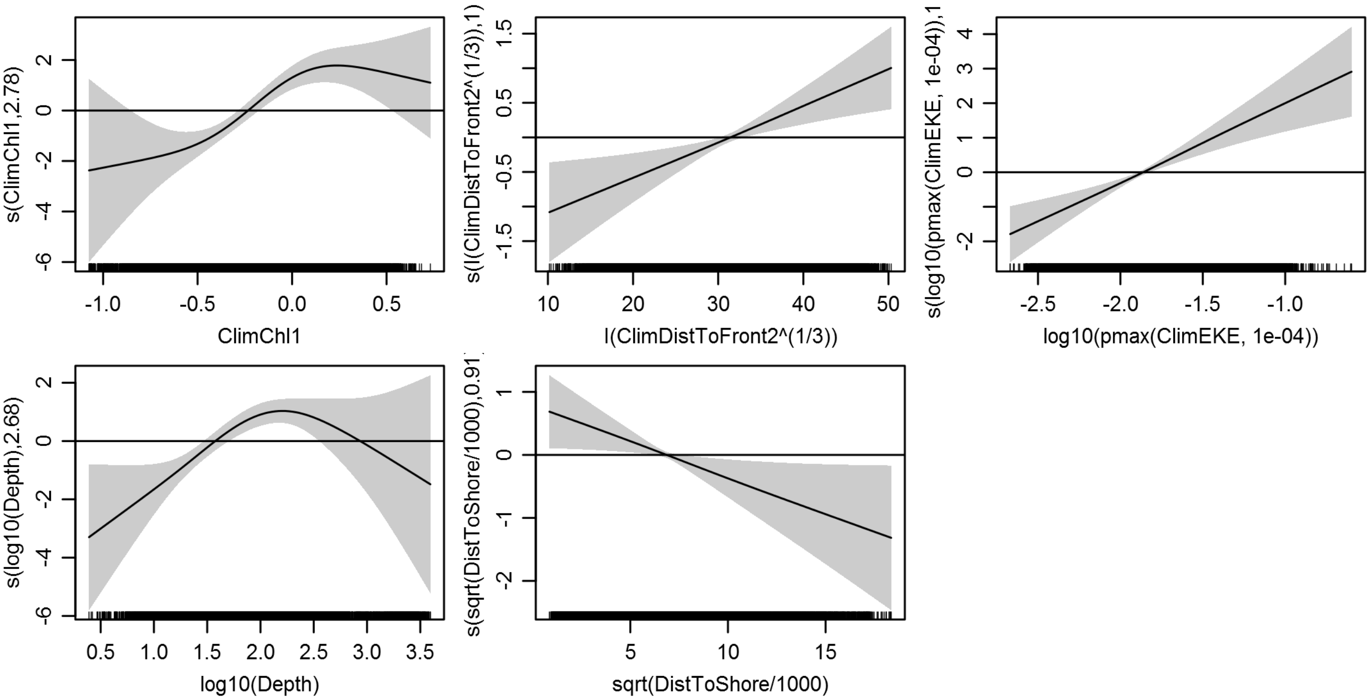

Diagnostic plots

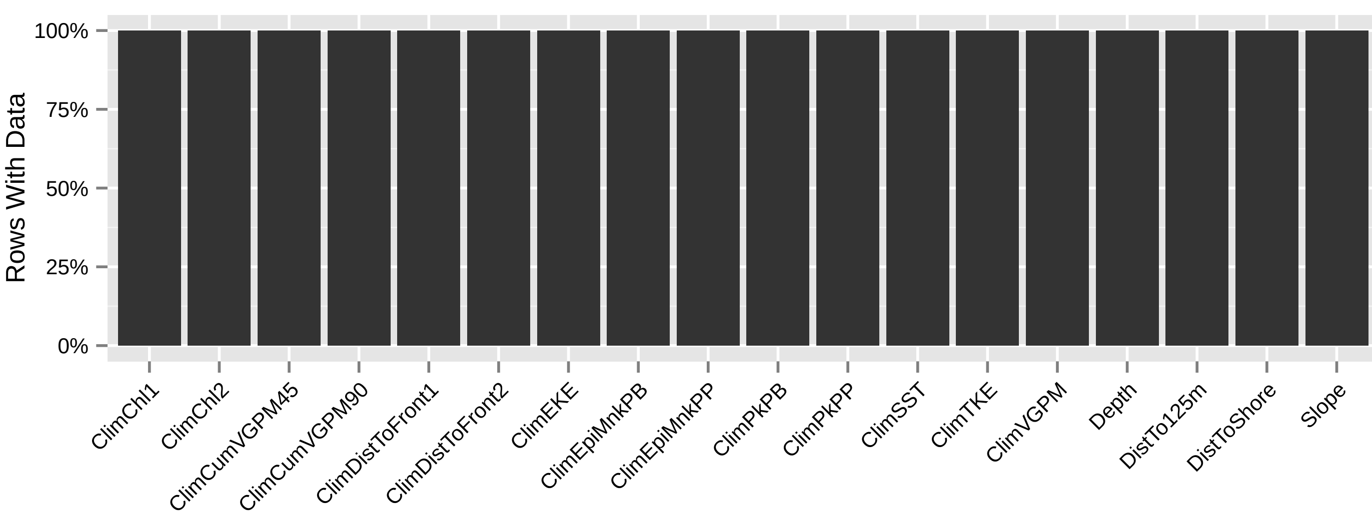

Figure 67: Segments with predictor values for the Humpback whale Climatological model, Winter season, Surveyed Area. This plot is used to assess how many segments would be lost by including a given predictor in a model.

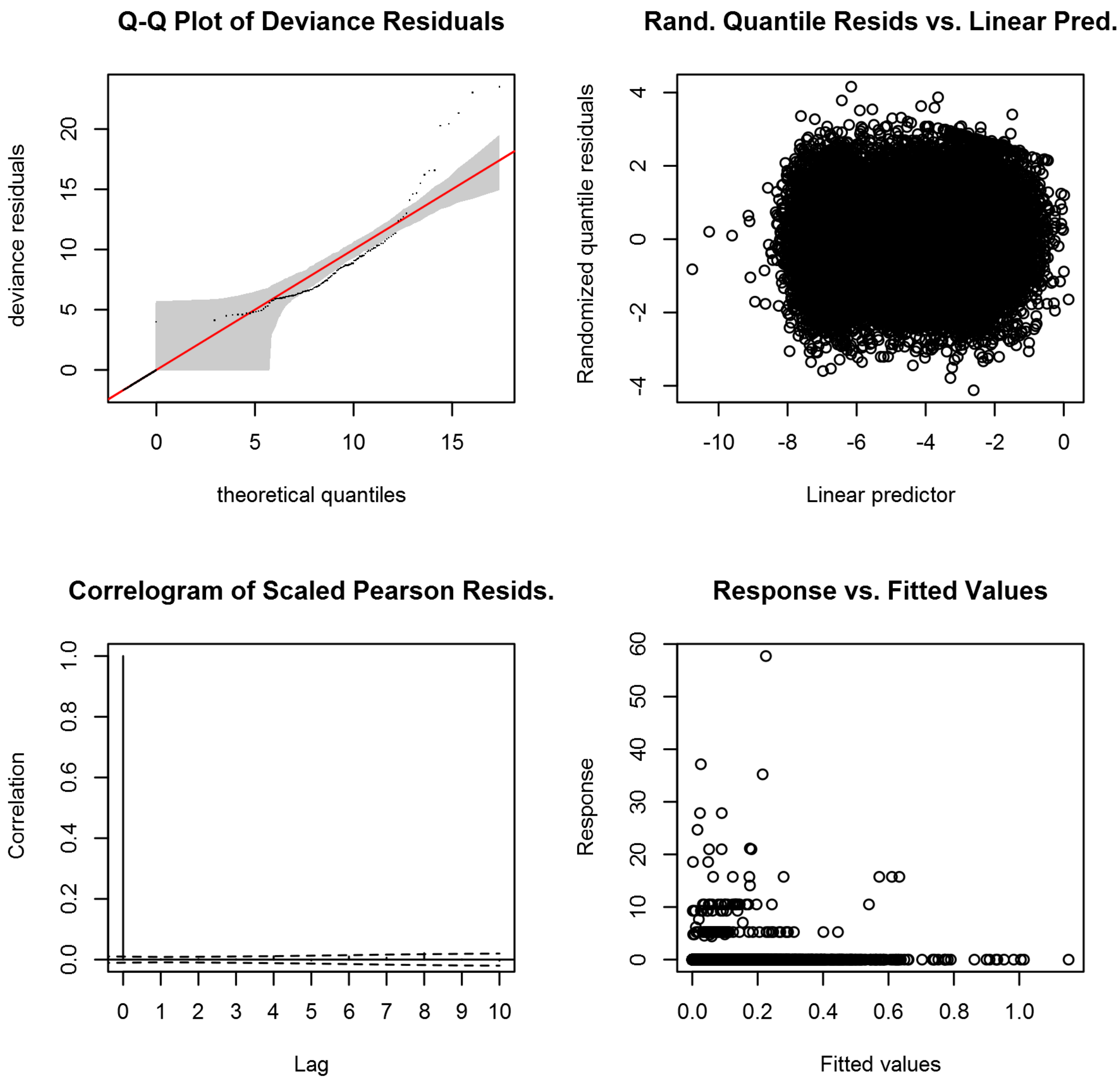

Figure 68: Statistical diagnostic plots for the Humpback whale Climatological model, Winter season, Surveyed Area.

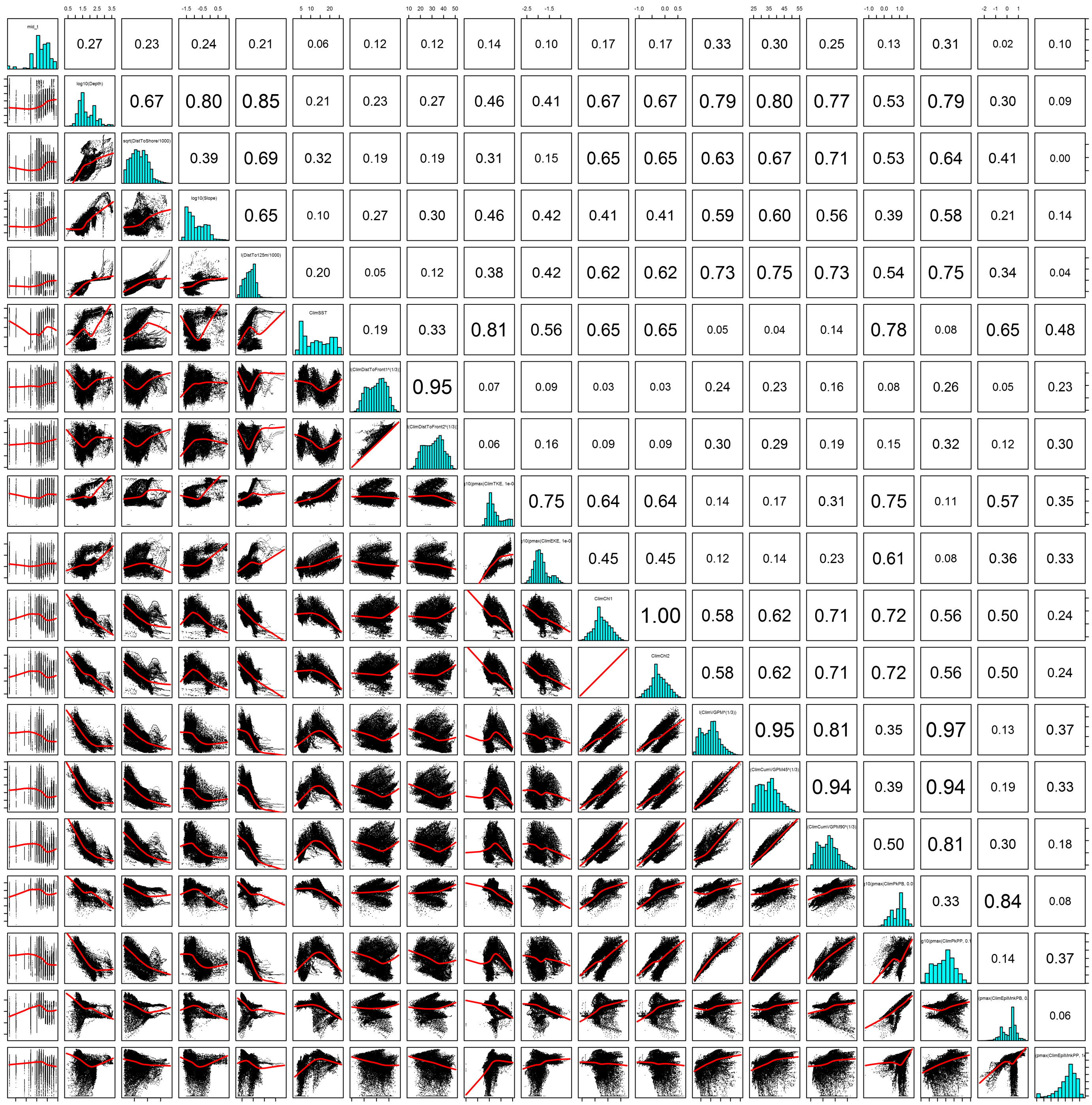

Figure 69: Scatterplot matrix for the Humpback whale Climatological model, Winter season, Surveyed Area. This plot is used to inspect the distribution of predictors (via histograms along the diagonal), simple correlation between predictors (via pairwise Pearson coefficients above the diagonal), and linearity of predictor correlations (via scatterplots below the diagonal). This plot is best viewed at high magnification.

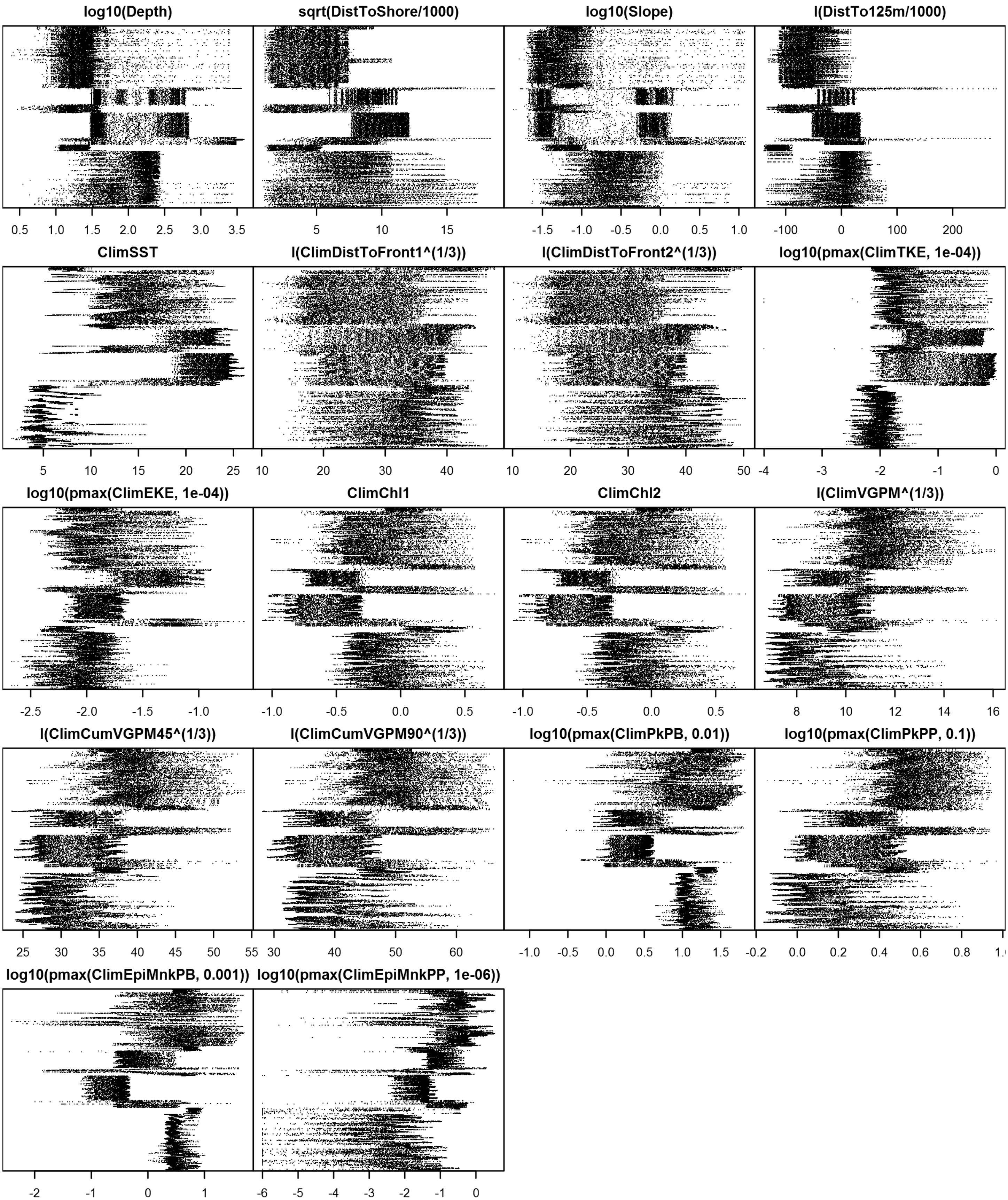

Figure 70: Dotplot for the Humpback whale Climatological model, Winter season, Surveyed Area. This plot is used to check for suspicious patterns and outliers in the data. Points are ordered vertically by transect ID, sequentially in time.

Unsurveyed Area

Density was not modeled for this region.

Summer

In this season, the entire study area was surveyed extensively (although the majority of effort occurred during the July-August period). We divided the study area at the north wall of the Gulf Stream, separating the highly productive northern region, representing probable feeding habitat, from the less productive southern region, which we assumed is essentially unoccupied during this season.

In March, 2015, we reviewed our version 9 models with J. Robbins. She expressed support this geographic split and our assumption that the southern area is unoccupied during summer.

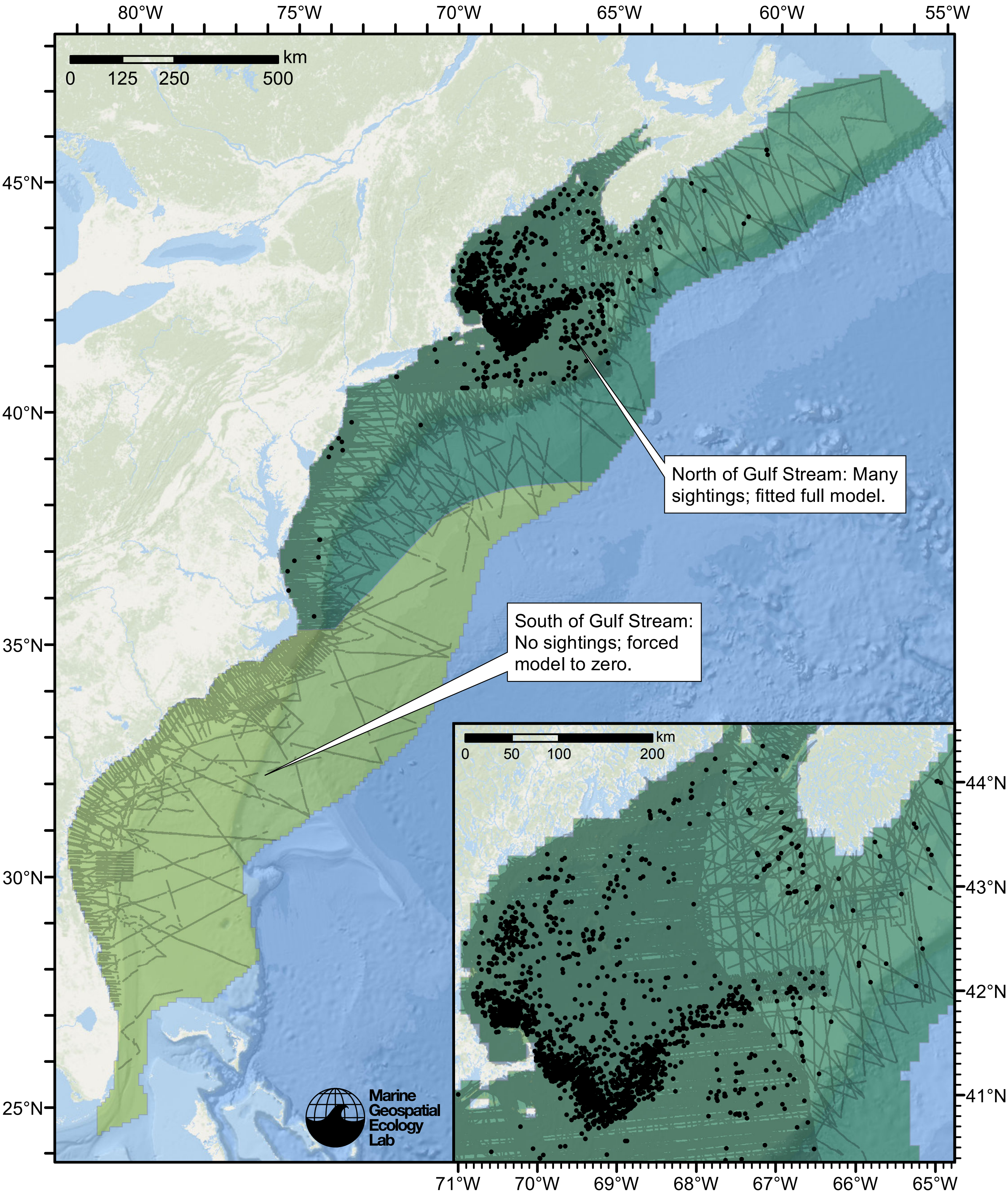

Figure 71: Humpback whale density model schematic for Summer season. All on-effort sightings are shown, including those that were truncated when detection functions were fitted.

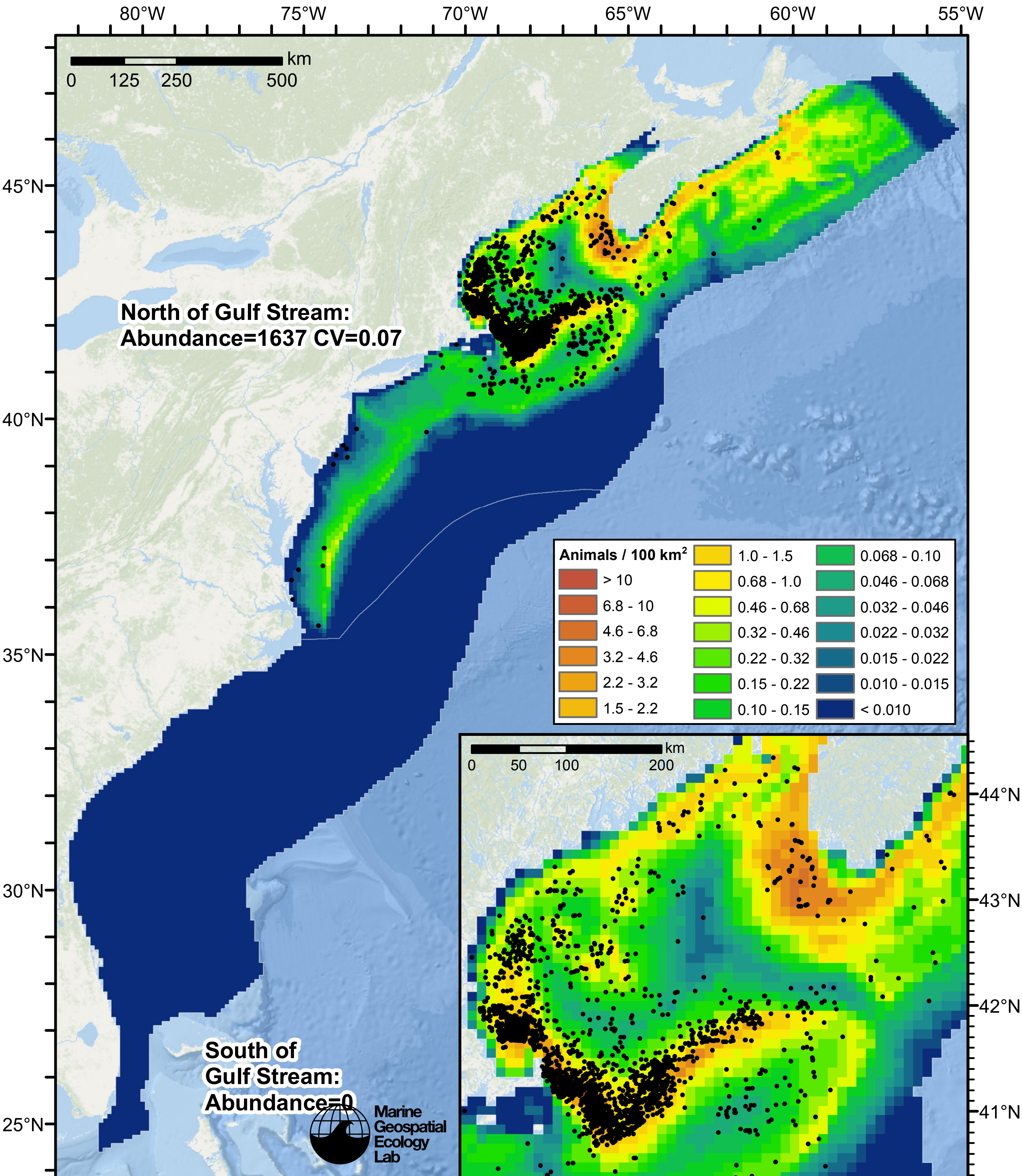

Figure 72: Humpback whale density predicted by the Summer season climatological model that explained the most deviance. Pixels are 10x10 km. The legend gives the estimated individuals per pixel; breaks are logarithmic. The same scale is used for all seasons. Abundance for each region was computed by summing the density cells occuring in that region.

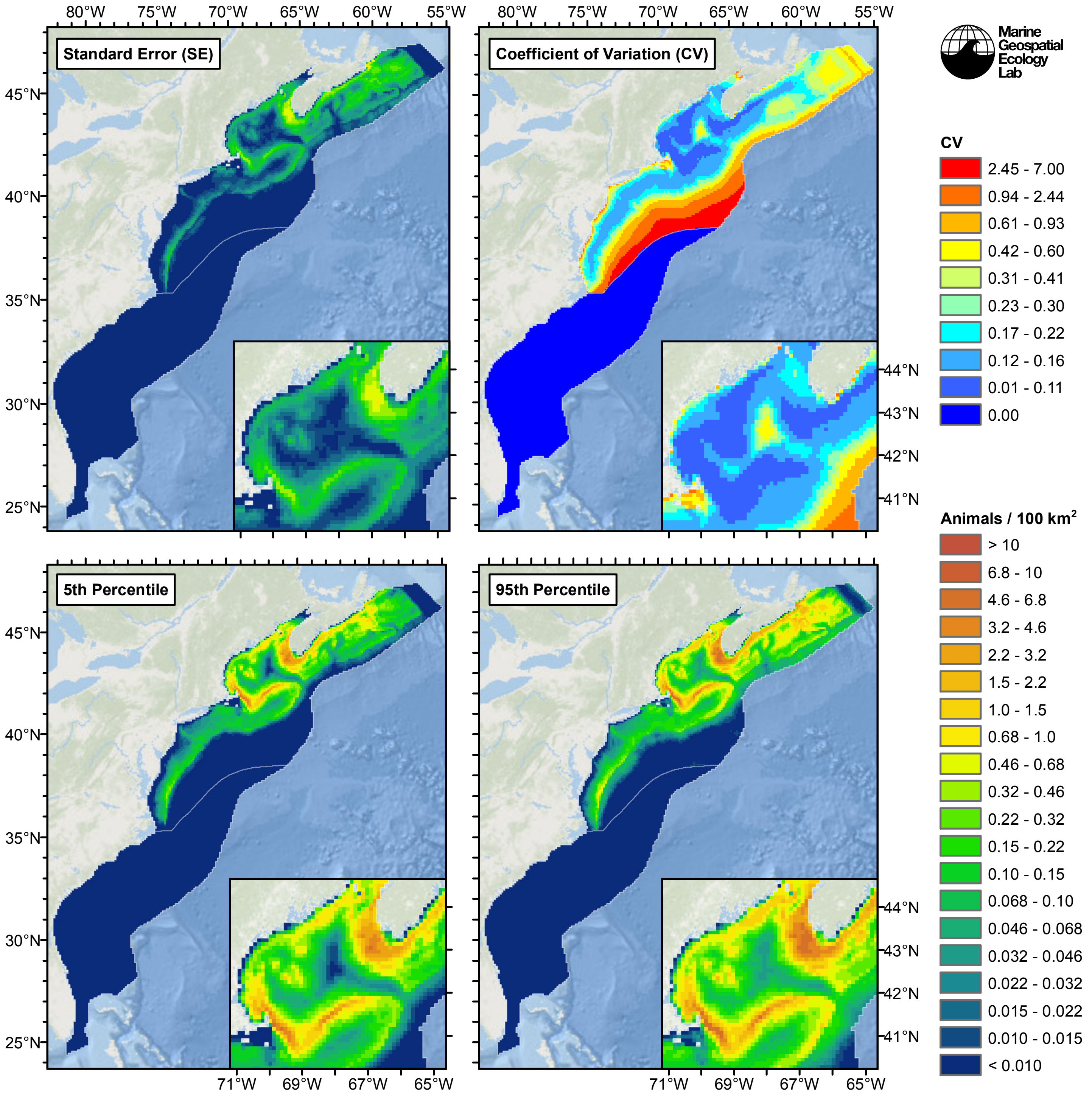

Figure 73: Estimated uncertainty for the Summer season climatological model that explained the most deviance. These estimates only incorporate the statistical uncertainty estimated for the spatial model (by the R mgcv package). They do not incorporate uncertainty in the detection functions, g(0) estimates, predictor variables, and so on.

North of Gulf Stream

Statistical output

```
Rscript.exe: This is mgcv 1.8-2. For overview type 'help("mgcv-package")'.


Family: Tweedie(p=1.266)
```

```
Link function: log

Formula:
abundance ~ offset(log(area_km2)) + s(log10(Depth), bs = "ts",
    k = 5) + s(log10(Slope), bs = "ts", k = 5) + s(I(DistTo125m/1000),
    bs = "ts", k = 5) + s(I(DistTo300m/1000), bs = "ts", k = 5) +
    s(ClimSST, bs = "ts", k = 5) + s(I(ClimDistToFront2^(1/3)),
    bs = "ts", k = 5) + s(log10(pmax(ClimEKE, 1e-04)), bs = "ts",
    k = 5) + s(log10(pmax(ClimPkPB, 0.01)), bs = "ts", k = 5)

Parametric coefficients:
            Estimate Std. Error t value Pr(>|t|)
(Intercept)  -6.8012     0.1052  -64.66   <2e-16 ***
---
Signif. codes:  0 '***' 0.001 '**' 0.01 '*' 0.05 '.' 0.1 ' ' 1

Approximate significance of smooth terms:
                                 edf Ref.df       F  p-value
s(log10(Depth))                3.883      4  74.053  < 2e-16 ***
s(log10(Slope))                1.109      4   6.732 1.16e-07 ***
s(I(DistTo125m/1000))          3.669      4  57.300  < 2e-16 ***
s(I(DistTo300m/1000))          3.805      4 112.972  < 2e-16 ***
s(ClimSST)                     3.688      4  24.741  < 2e-16 ***
s(I(ClimDistToFront2^(1/3)))   2.770      4   3.966 0.000396 ***
s(log10(pmax(ClimEKE, 1e-04))) 3.395      4  32.922  < 2e-16 ***
s(log10(pmax(ClimPkPB, 0.01))) 2.981      4  12.367 1.29e-11 ***
---
Signif. codes:  0 '***' 0.001 '**' 0.01 '*' 0.05 '.' 0.1 ' ' 1

R-sq.(adj) =  0.0566   Deviance explained = 32.3%
-REML =  11137  Scale est. = 16.377    n = 50288

All predictors were significant. This is the final model.
Creating term plots.
Diagnostic output from gam.check():

Method: REML   Optimizer: outer newton
full convergence after 15 iterations.
Gradient range [-0.002447077,0.00433836]
(score 11137.07 & scale 16.37671).
Hessian positive definite, eigenvalue range [0.1213168,6356.395].
Model rank =  33 / 33

Basis dimension (k) checking results. Low p-value (k-index<1) may
indicate that k is too low, especially if edf is close to k'.

                                  k'   edf k-index p-value
s(log10(Depth))                4.000 3.883   0.798    0.10
s(log10(Slope))                4.000 1.109   0.807    0.30
s(I(DistTo125m/1000))          4.000 3.669   0.750    0.00
s(I(DistTo300m/1000))          4.000 3.805   0.806    0.30
s(ClimSST)                     4.000 3.688   0.792    0.06
s(I(ClimDistToFront2^(1/3)))   4.000 2.770   0.812    0.45
s(log10(pmax(ClimEKE, 1e-04))) 4.000 3.395   0.832    0.96
s(log10(pmax(ClimPkPB, 0.01))) 4.000 2.981   0.806    0.31

Predictors retained during the model selection procedure: Depth, Slope, DistTo125m, DistTo300m,
ClimSST, ClimDistToFront2, ClimEKE, ClimPkPB
```

```
Predictors dropped during the model selection procedure:
```

Model term plots

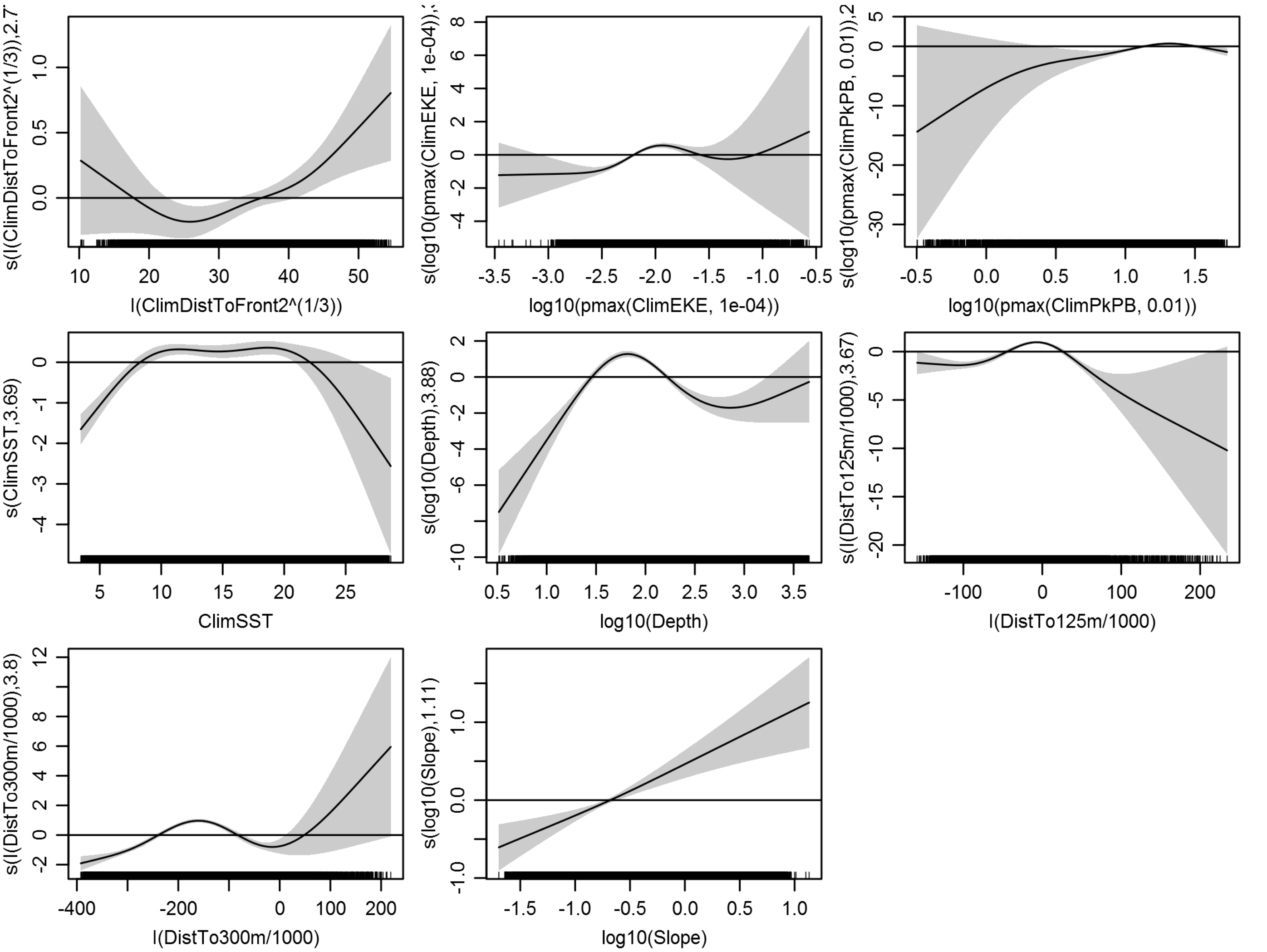

Diagnostic plots

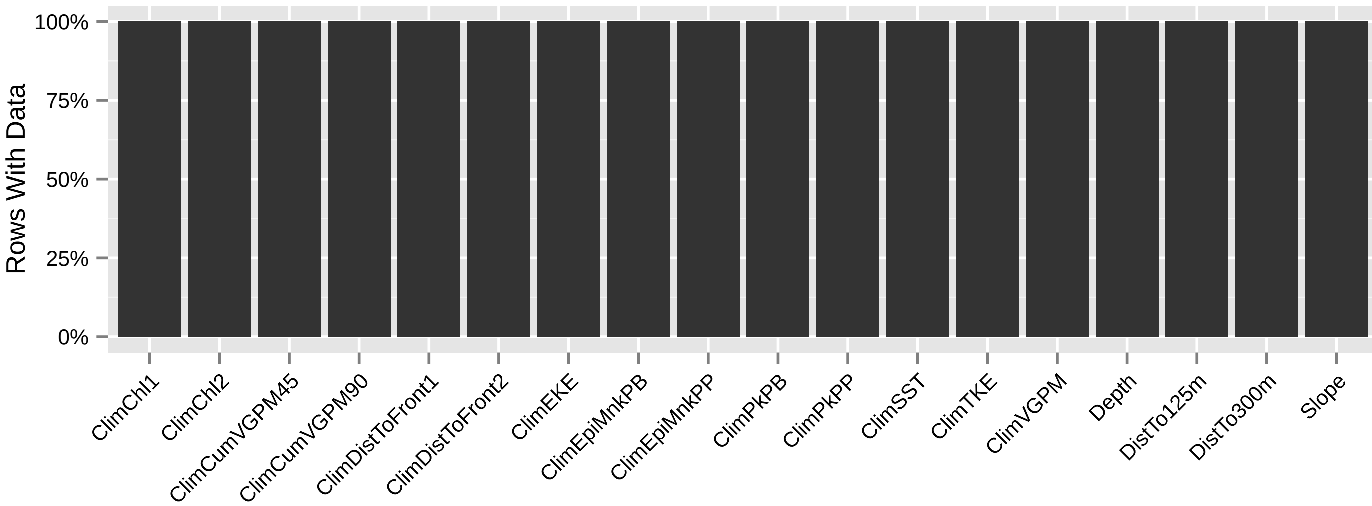

Figure 74: Segments with predictor values for the Humpback whale Climatological model, Summer season, North of Gulf Stream. This plot is used to assess how many segments would be lost by including a given predictor in a model.

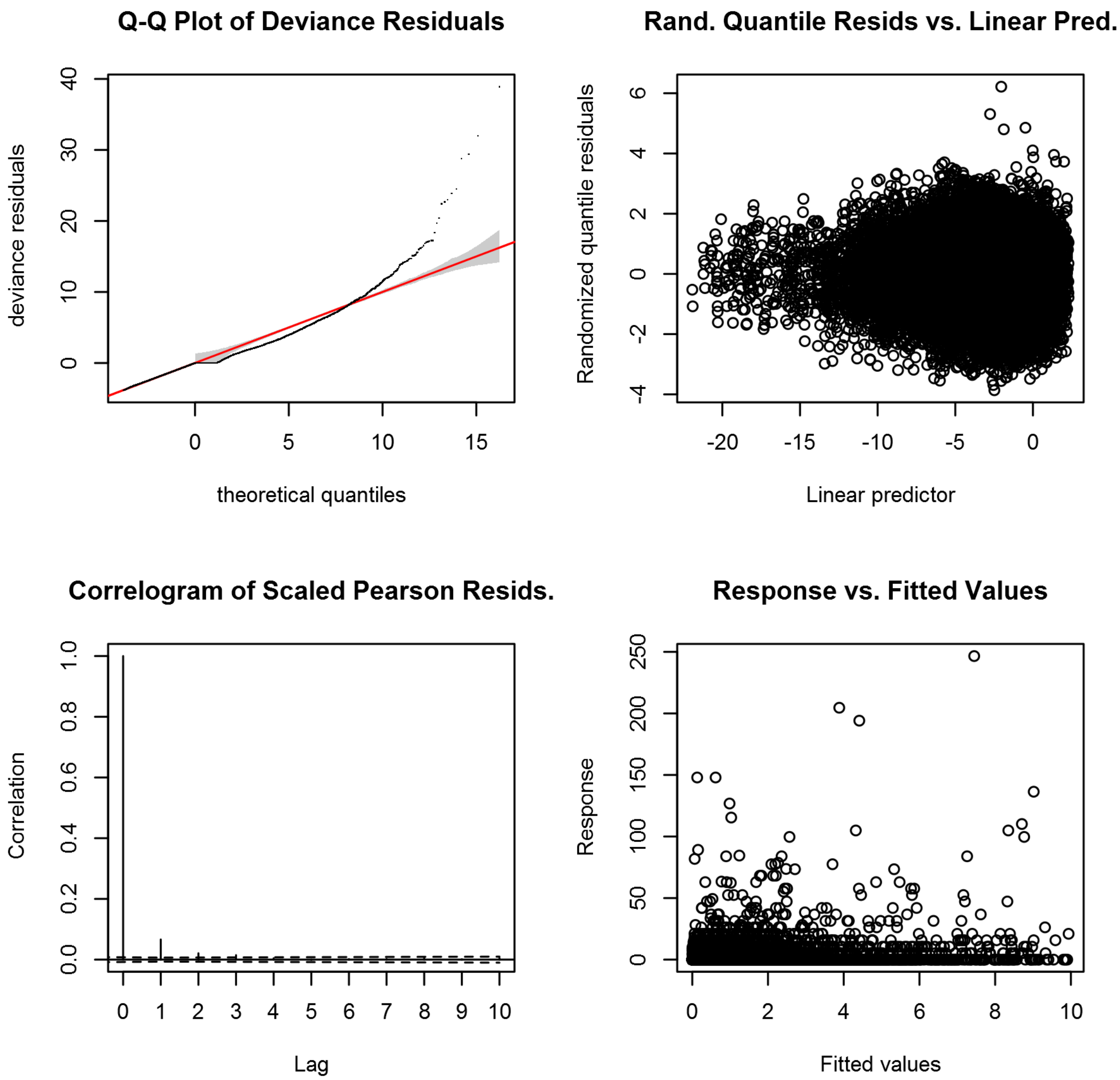

Figure 75: Statistical diagnostic plots for the Humpback whale Climatological model, Summer season, North of Gulf Stream.

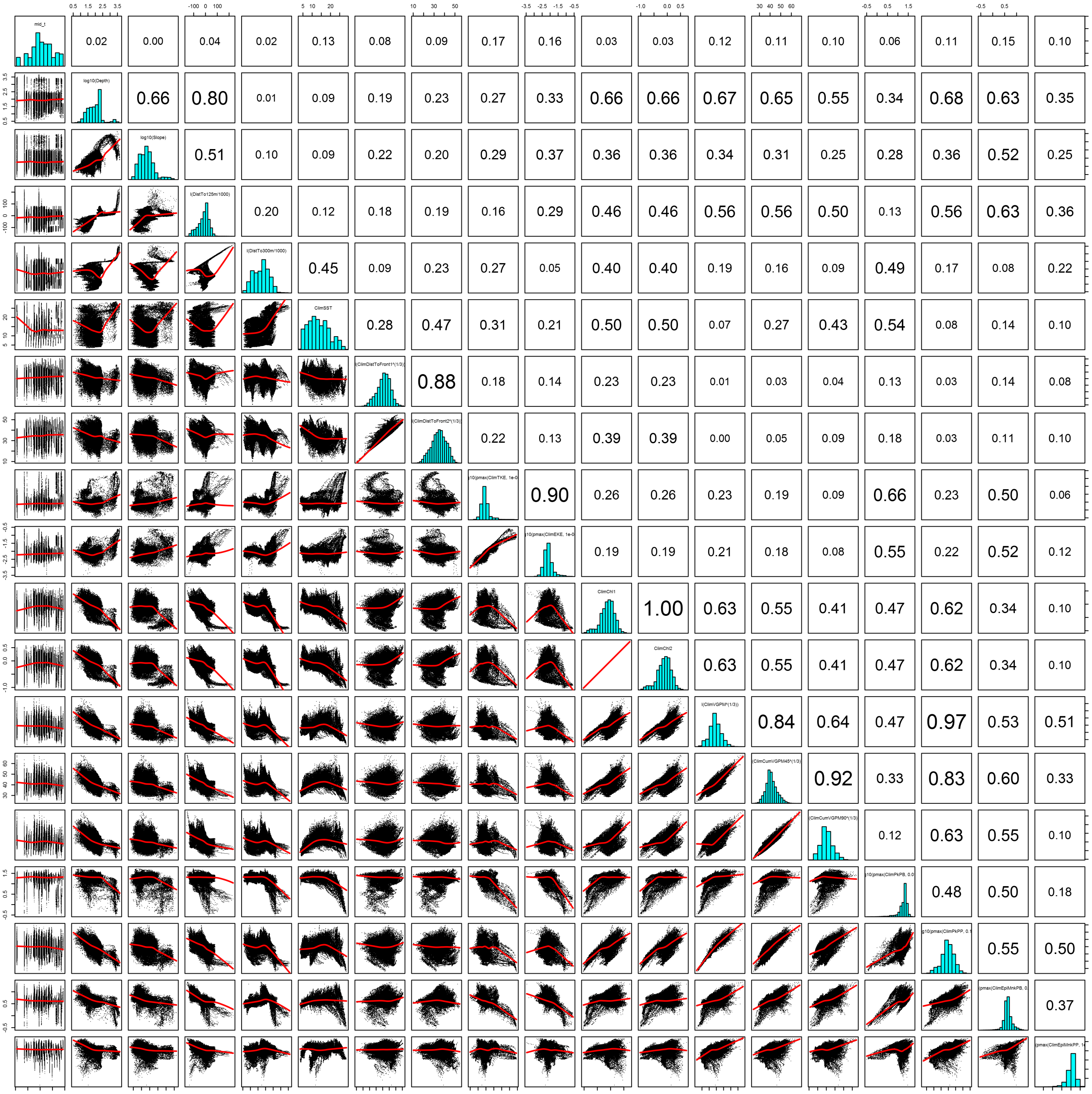

Figure 76: Scatterplot matrix for the Humpback whale Climatological model, Summer season, North of Gulf Stream. This plot is used to inspect the distribution of predictors (via histograms along the diagonal), simple correlation between predictors (via pairwise Pearson coefficients above the diagonal), and linearity of predictor correlations (via scatterplots below the diagonal). This plot is best viewed at high magnification.

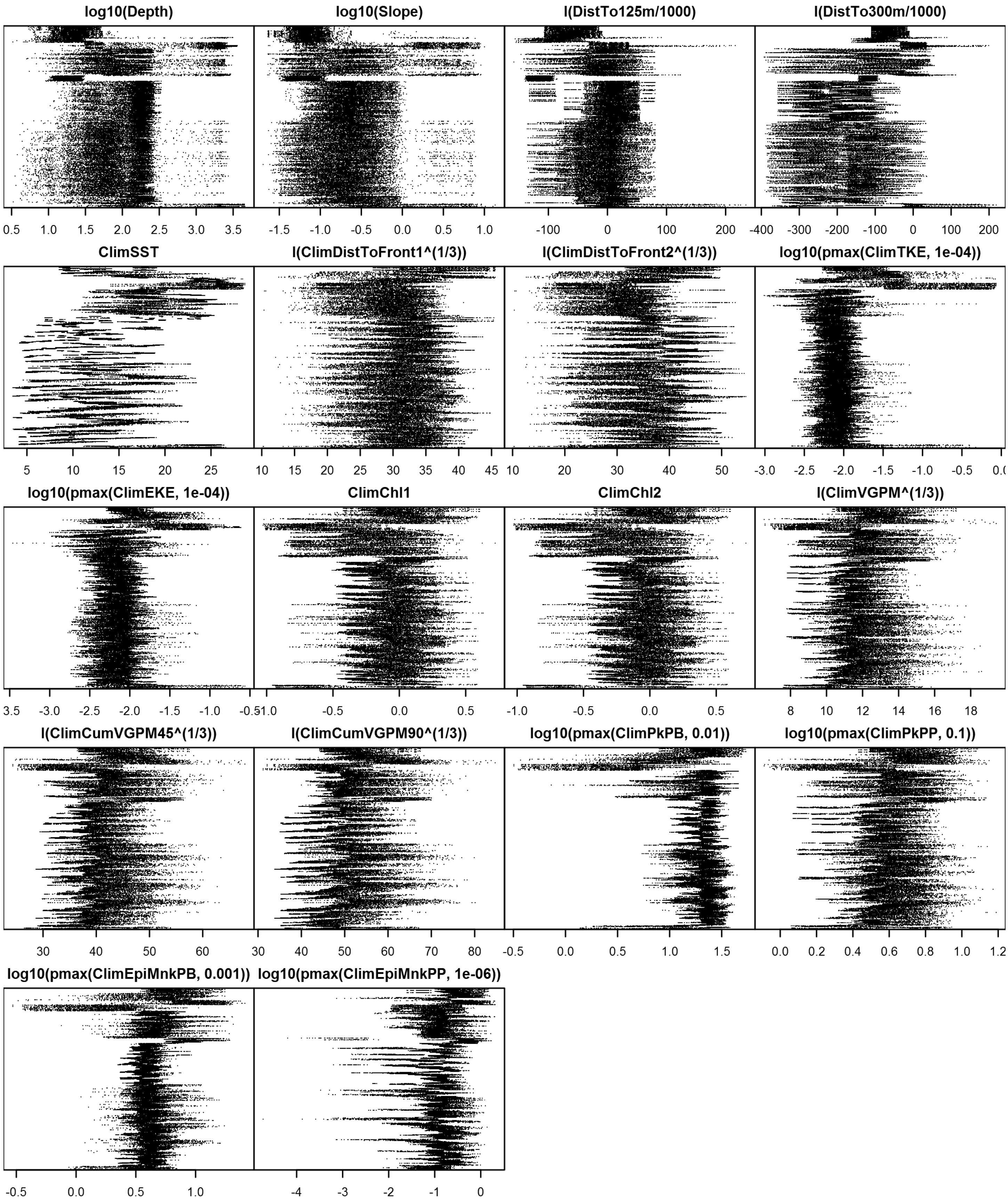

Figure 77: Dotplot for the Humpback whale Climatological model, Summer season, North of Gulf Stream. This plot is used to check for suspicious patterns and outliers in the data. Points are ordered vertically by transect ID, sequentially in time.

South of Gulf Stream

Density assumed to be 0 in this region.

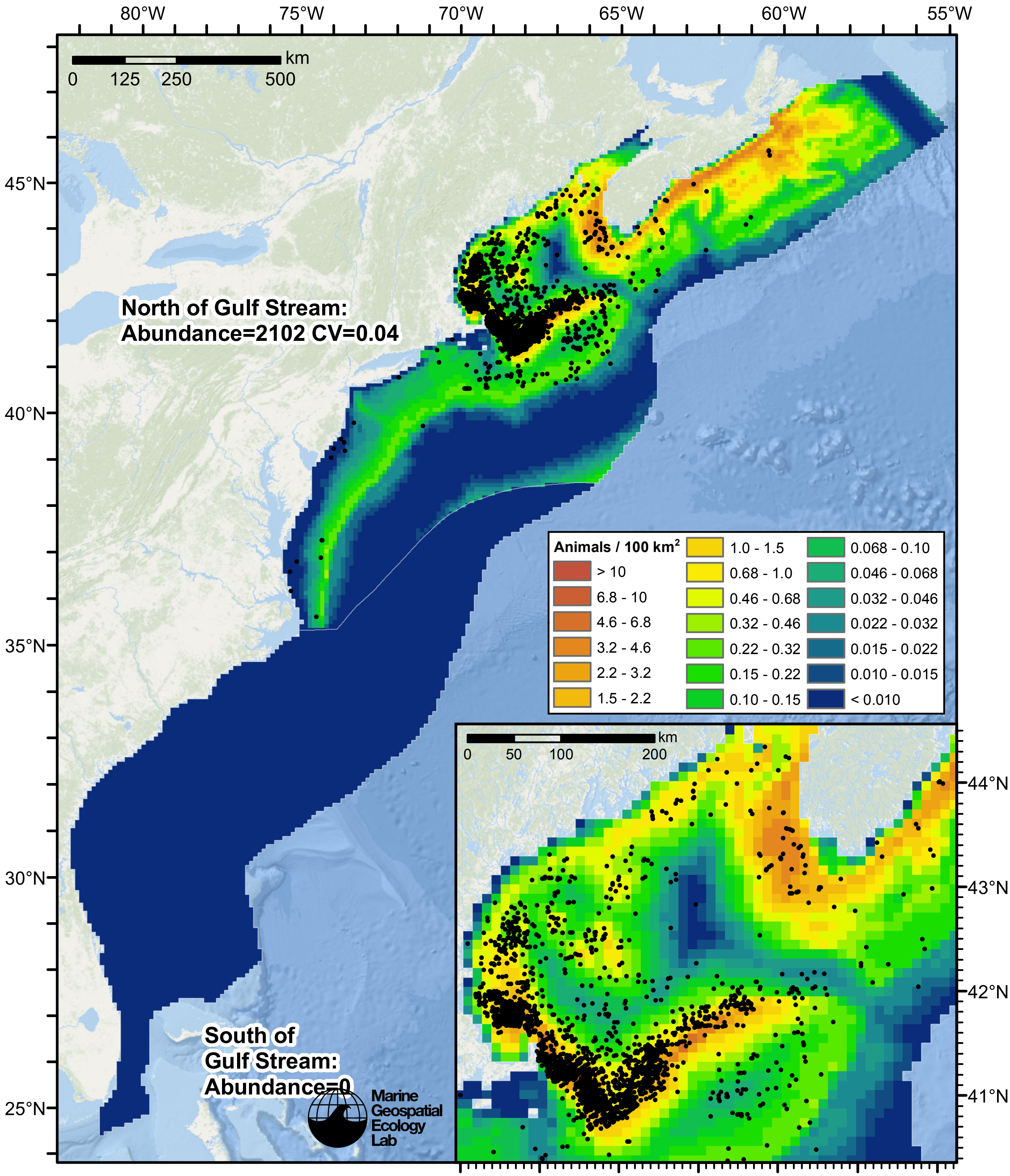

Figure 78: Humpback whale density predicted by the Summer season contemporaneous model that explained the most deviance. Pixels are 10x10 km. The legend gives the estimated individuals per pixel; breaks are logarithmic. The same scale is used for all seasons. Abundance for each region was computed by summing the density cells occuring in that region.

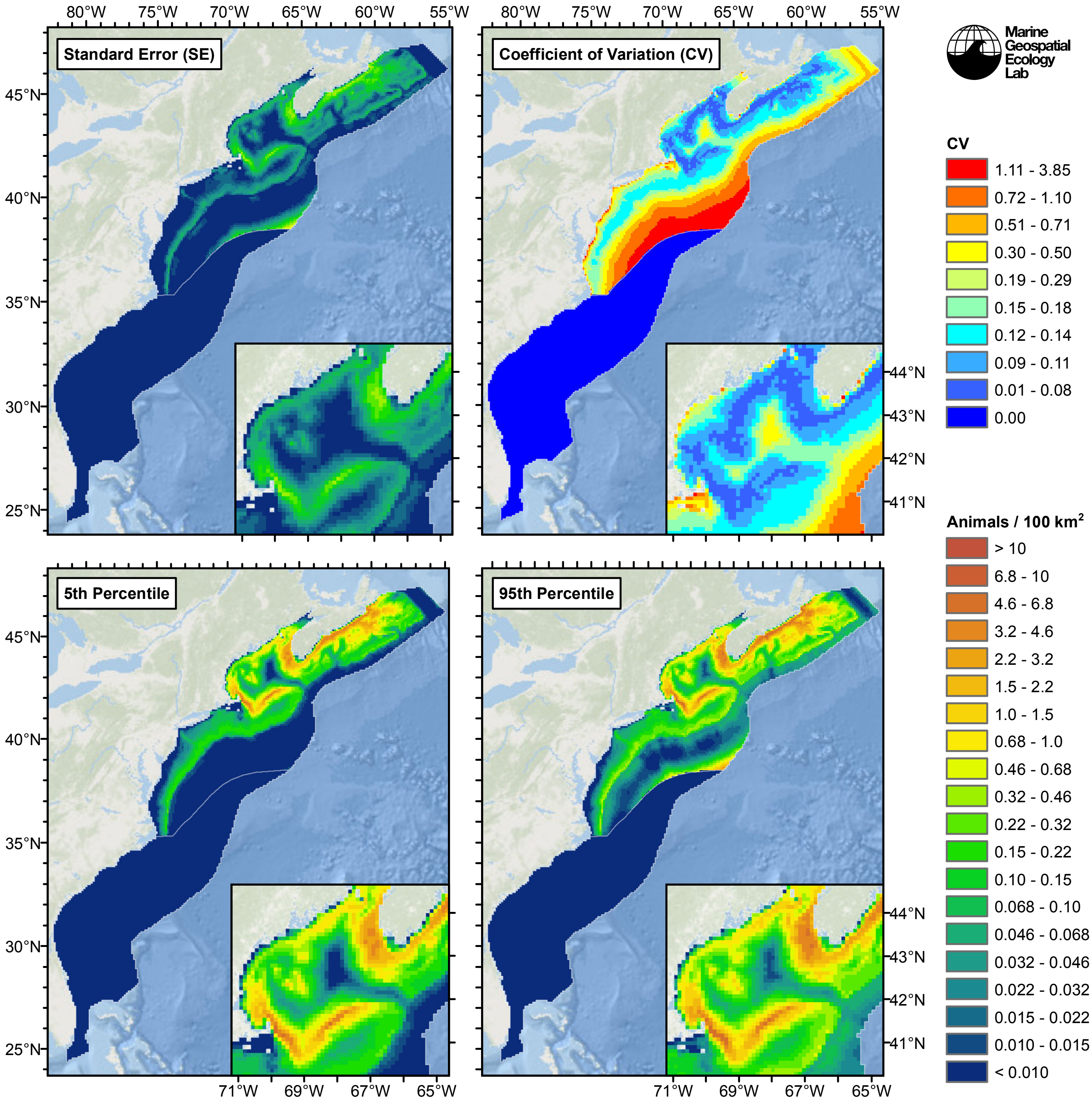

Figure 79: Estimated uncertainty for the Summer season contemporaneous model that explained the most deviance. These estimates only incorporate the statistical uncertainty estimated for the spatial model (by the R mgcv package). They do not incorporate uncertainty in the detection functions, g(0) estimates, predictor variables, and so on.

North of Gulf Stream

Statistical output

```
Rscript.exe: This is mgcv 1.8-2. For overview type 'help("mgcv-package")'.


Family: Tweedie(p=1.272)
```

```
Link function: log

Formula:
abundance ~ offset(log(area_km2)) + s(log10(Depth), bs = "ts",
    k = 5) + s(log10(Slope), bs = "ts", k = 5) + s(I(DistTo125m/1000),
    bs = "ts", k = 5) + s(I(DistTo300m/1000), bs = "ts", k = 5) +
    s(SST, bs = "ts", k = 5) + s(log10(pmax(EKE, 1e-04)), bs = "ts",
    k = 5)

Parametric coefficients:
            Estimate Std. Error t value Pr(>|t|)
(Intercept) -6.70009    0.06824  -98.19   <2e-16 ***
---
Signif. codes:  0 '***' 0.001 '**' 0.01 '*' 0.05 '.' 0.1 ' ' 1

Approximate significance of smooth terms:
                              edf Ref.df       F  p-value
s(log10(Depth))            3.8750      4  71.252  < 2e-16 ***
s(log10(Slope))            0.9851      4   3.521 0.000101 ***
s(I(DistTo125m/1000))      3.8321      4  79.654  < 2e-16 ***
s(I(DistTo300m/1000))      3.8797      4 120.215  < 2e-16 ***
s(SST)                     3.8471      4  28.177  < 2e-16 ***
s(log10(pmax(EKE, 1e-04))) 0.9340      4   2.132 0.002086 **
---
Signif. codes:  0 '***' 0.001 '**' 0.01 '*' 0.05 '.' 0.1 ' ' 1

R-sq.(adj) =  0.0495   Deviance explained = 30.6%
-REML =  11173  Scale est. = 16.809    n = 49799

All predictors were significant. This is the final model.
Creating term plots.
Diagnostic output from gam.check():

Method: REML   Optimizer: outer newton
full convergence after 12 iterations.
Gradient range [-0.008188195,0.007688735]
(score 11173.46 & scale 16.80884).
Hessian positive definite, eigenvalue range [0.3845055,6292.771].
Model rank =  25 / 25

Basis dimension (k) checking results. Low p-value (k-index<1) may
indicate that k is too low, especially if edf is close to k'.

                              k'   edf k-index p-value
s(log10(Depth))            4.000 3.875   0.801    0.20
s(log10(Slope))            4.000 0.985   0.805    0.28
s(I(DistTo125m/1000))      4.000 3.832   0.804    0.28
s(I(DistTo300m/1000))      4.000 3.880   0.801    0.22
s(SST)                     4.000 3.847   0.784    0.02
s(log10(pmax(EKE, 1e-04))) 4.000 0.934   0.787    0.04
```

Predictors retained during the model selection procedure: Depth, Slope, DistTo125m, DistTo300m, SST, EKE

Predictors dropped during the model selection procedure: DistToFront1

Model term plots

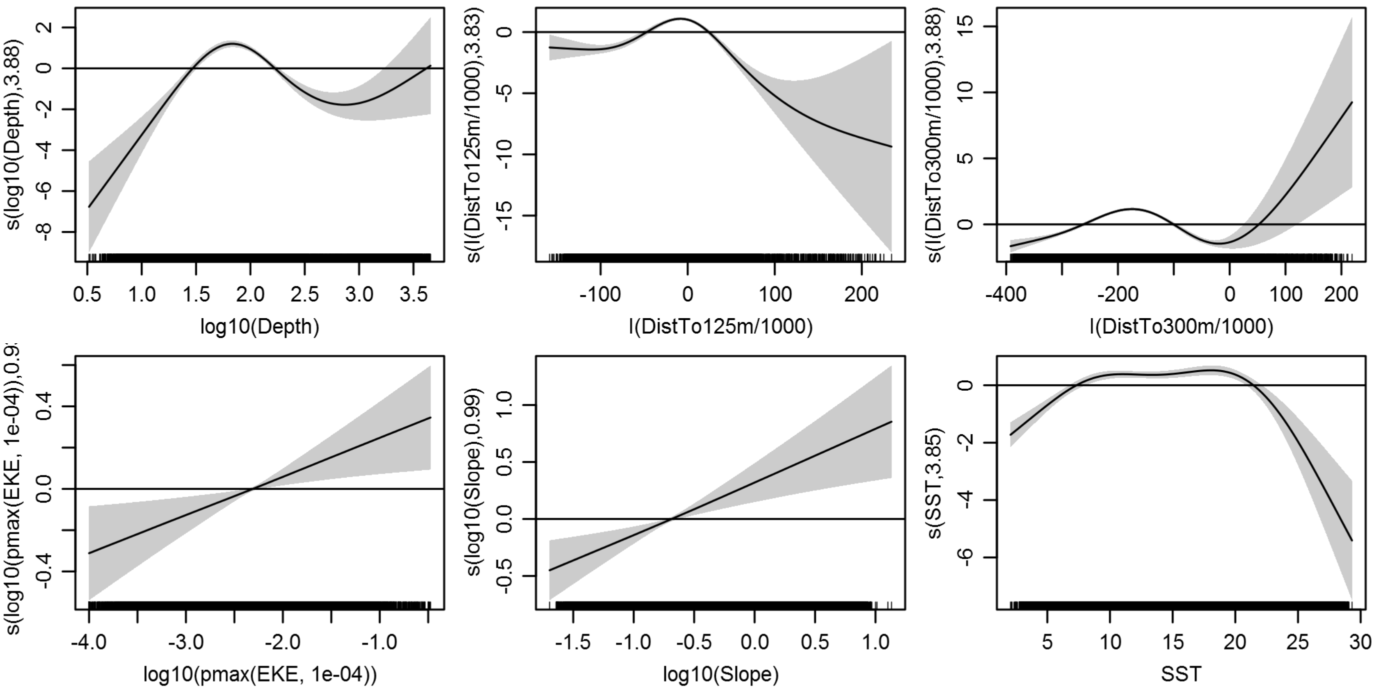

Diagnostic plots

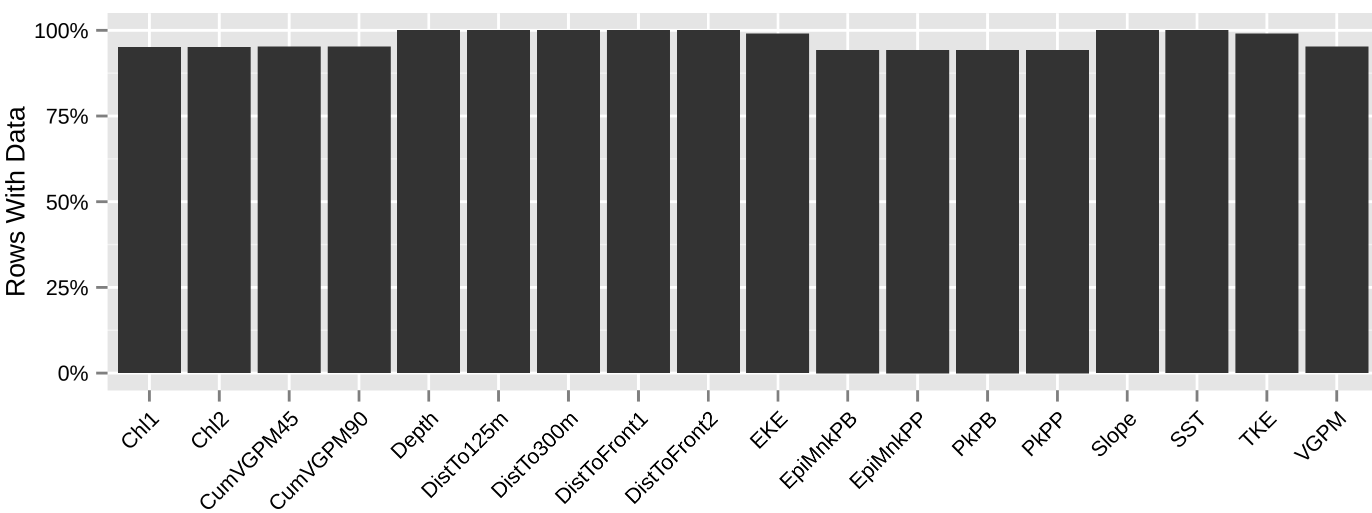

Figure 80: Segments with predictor values for the Humpback whale Contemporaneous model, Summer season, North of Gulf Stream. This plot is used to assess how many segments would be lost by including a given predictor in a model.

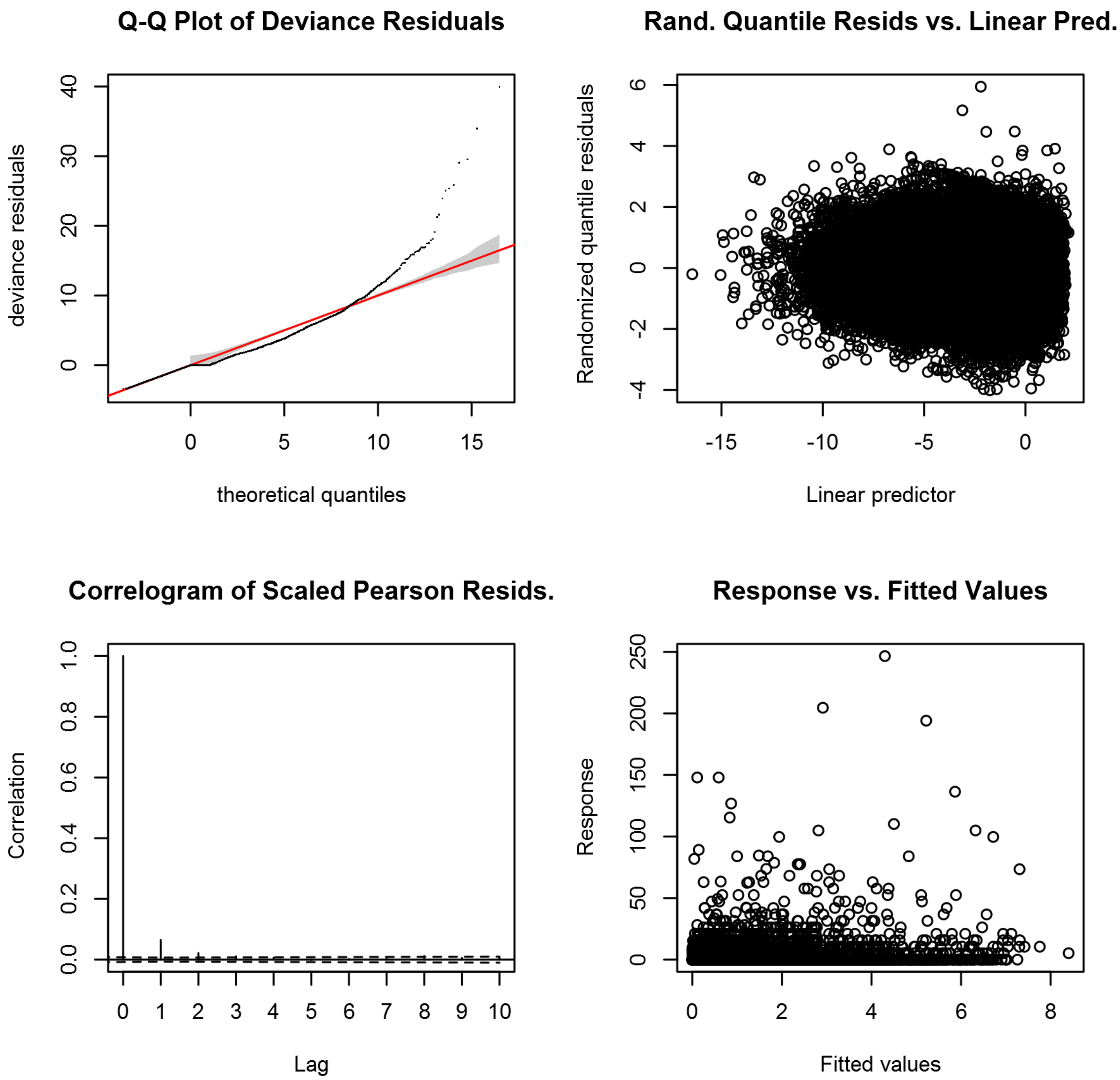

Figure 81: Statistical diagnostic plots for the Humpback whale Contemporaneous model, Summer season, North of Gulf Stream.

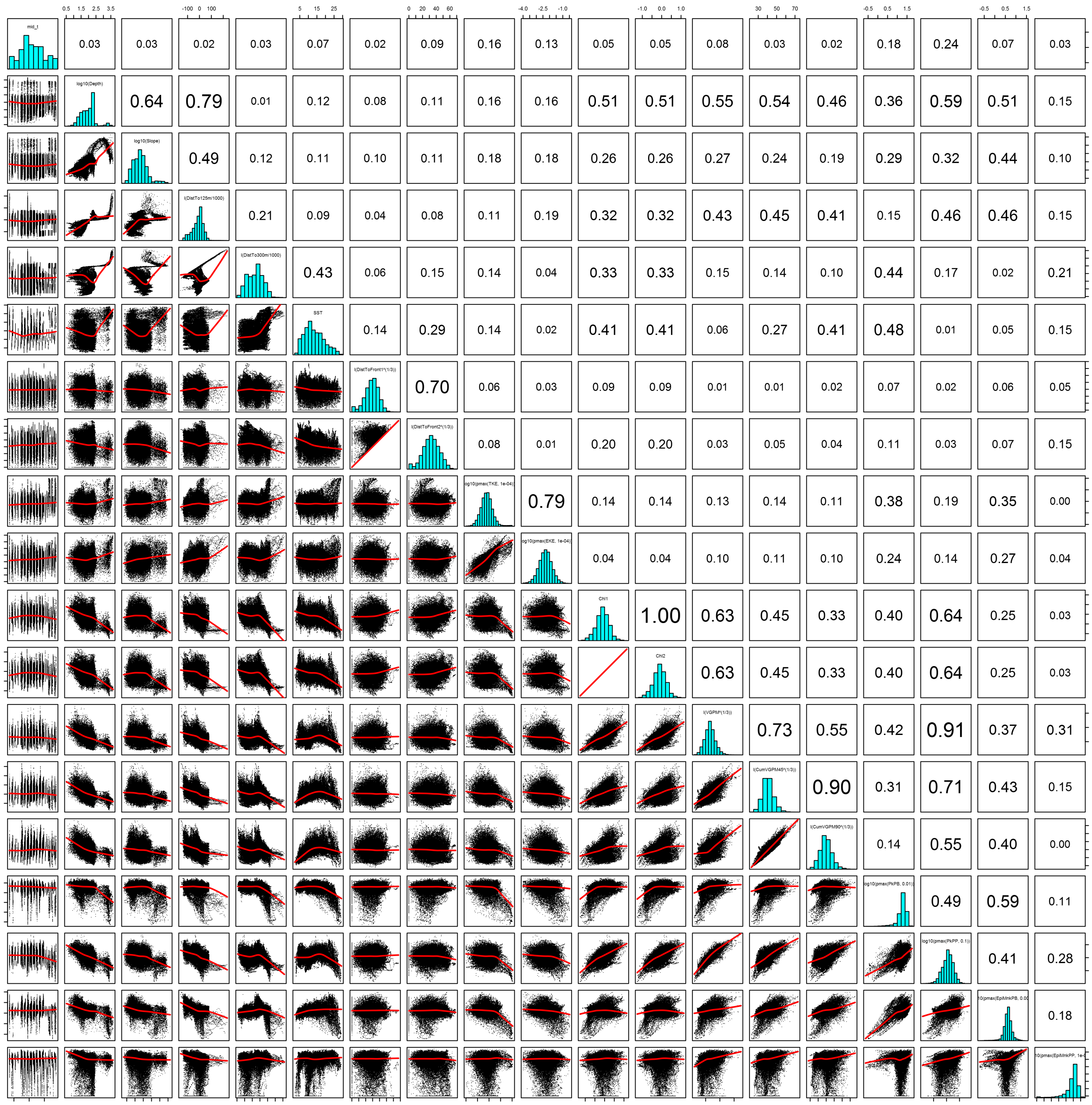

Figure 82: Scatterplot matrix for the Humpback whale Contemporaneous model, Summer season, North of Gulf Stream. This plot is used to inspect the distribution of predictors (via histograms along the diagonal), simple correlation between predictors (via pairwise Pearson coefficients above the diagonal), and linearity of predictor correlations (via scatterplots below the diagonal). This plot is best viewed at high magnification.

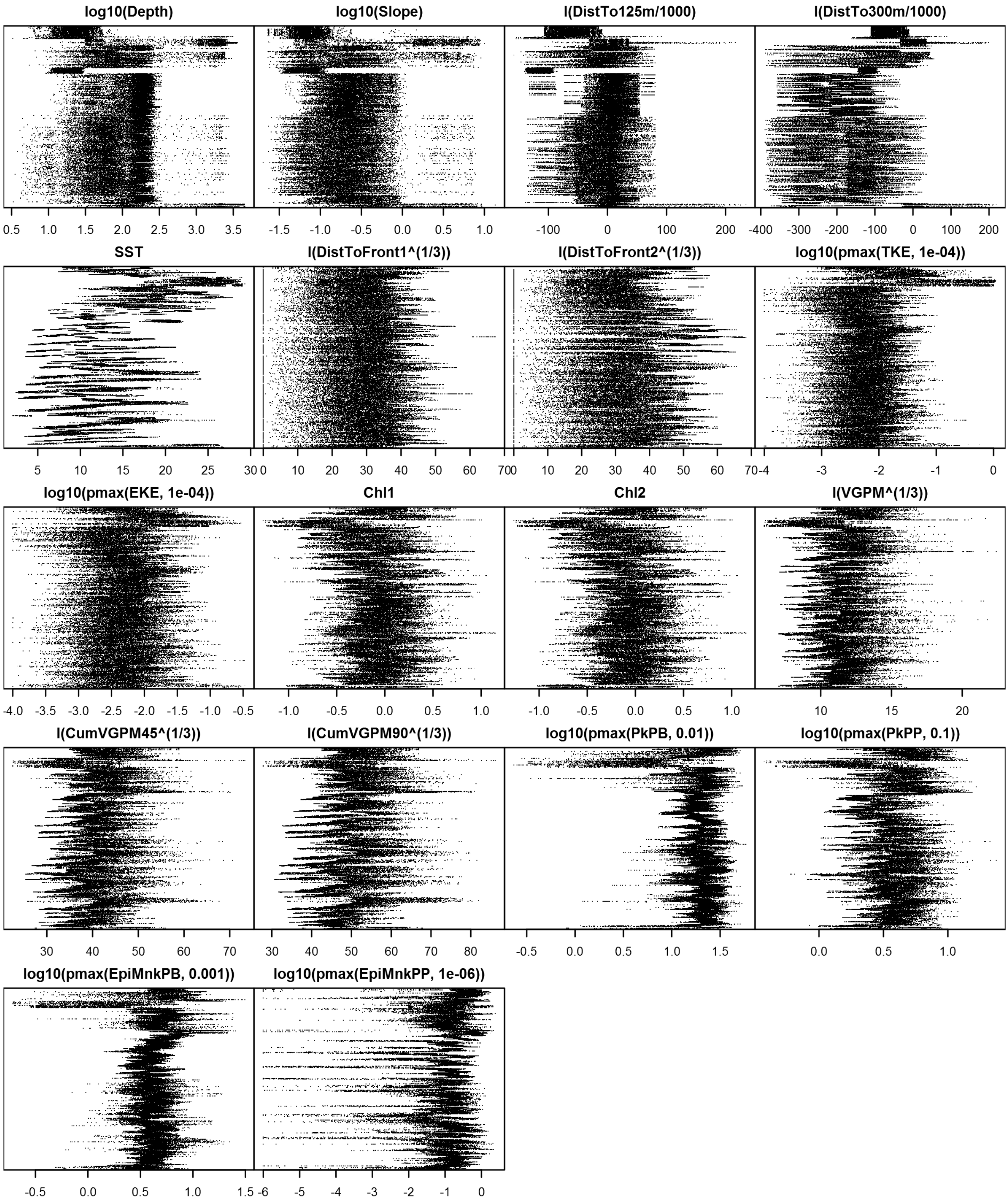

Figure 83: Dotplot for the Humpback whale Contemporaneous model, Summer season, North of Gulf Stream. This plot is used to check for suspicious patterns and outliers in the data. Points are ordered vertically by transect ID, sequentially in time.

South of Gulf Stream

Density assumed to be 0 in this region.

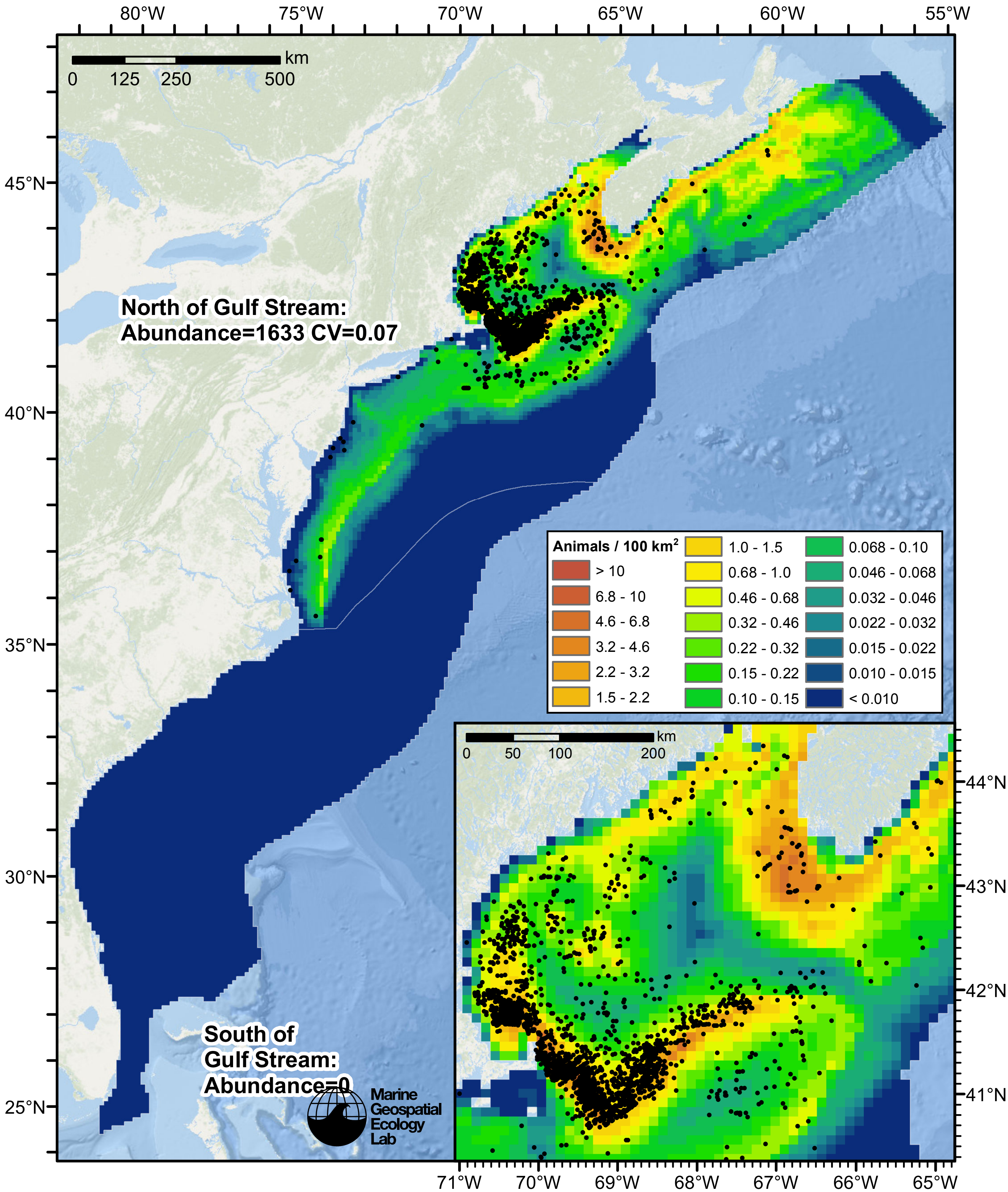

Figure 84: Humpback whale density predicted by the Summer season climatological same segments model that explained the most deviance. Pixels are 10x10 km. The legend gives the estimated individuals per pixel; breaks are logarithmic. The same scale is used for all seasons. Abundance for each region was computed by summing the density cells occuring in that region.

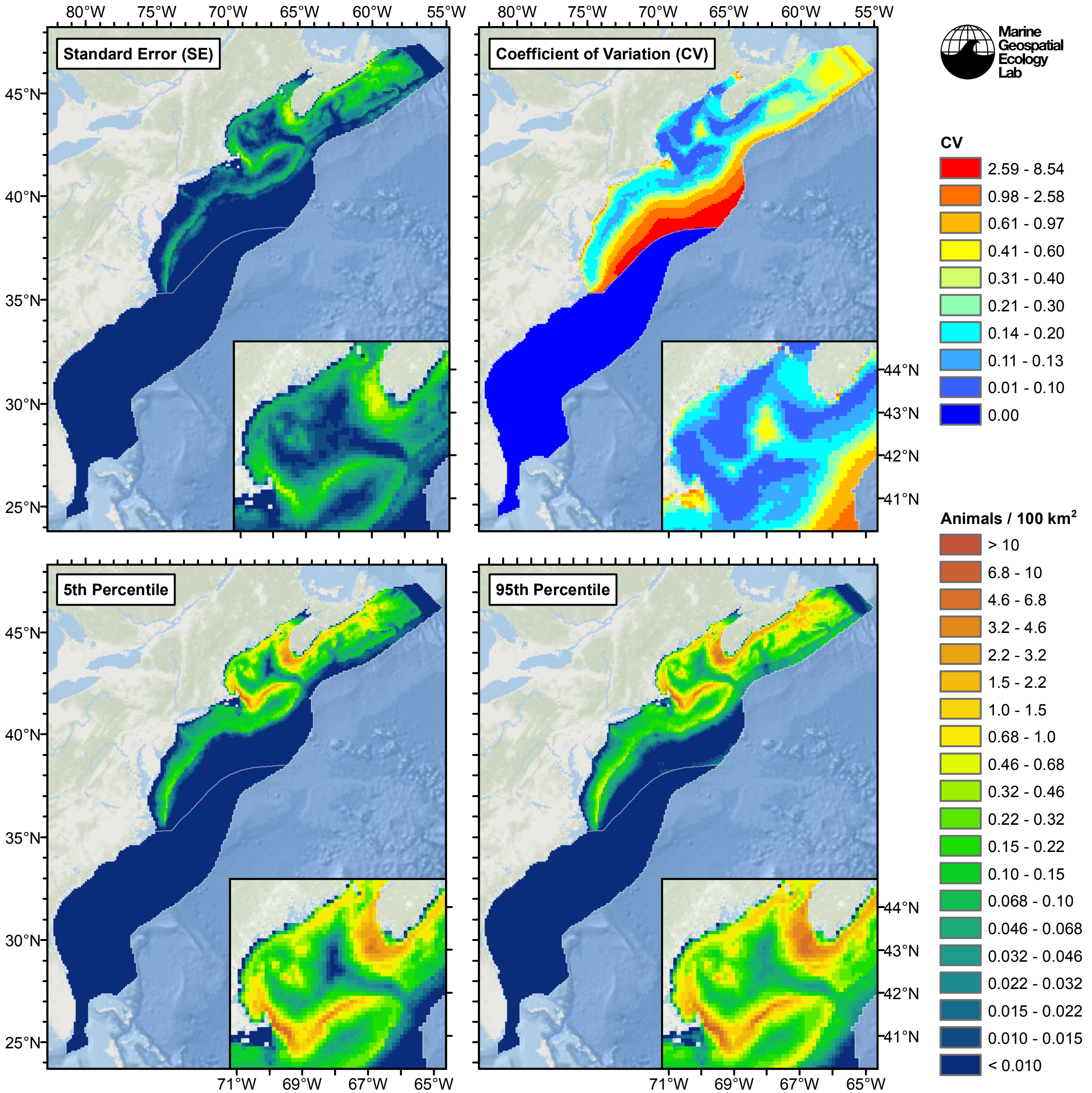

Figure 85: Estimated uncertainty for the Summer season climatological same segments model that explained the most deviance. These estimates only incorporate the statistical uncertainty estimated for the spatial model (by the R mgcv package). They do not incorporate uncertainty in the detection functions, g(0) estimates, predictor variables, and so on.

North of Gulf Stream

Statistical output

```
Rscript.exe: This is mgcv 1.8-2. For overview type 'help("mgcv-package")'.


Family: Tweedie(p=1.268)
```

```
Link function: log

Formula:
abundance ~ offset(log(area_km2)) + s(log10(Depth), bs = "ts",
    k = 5) + s(log10(Slope), bs = "ts", k = 5) + s(I(DistTo125m/1000),
    bs = "ts", k = 5) + s(I(DistTo300m/1000), bs = "ts", k = 5) +
    s(ClimSST, bs = "ts", k = 5) + s(log10(pmax(ClimEKE, 1e-04)),
    bs = "ts", k = 5)

Parametric coefficients:
            Estimate Std. Error t value Pr(>|t|)
(Intercept) -6.70681    0.07492  -89.52   <2e-16 ***
---
Signif. codes:  0 '***' 0.001 '**' 0.01 '*' 0.05 '.' 0.1 ' ' 1

Approximate significance of smooth terms:
                                edf Ref.df       F  p-value
s(log10(Depth))               3.887      4  78.100  < 2e-16 ***
s(log10(Slope))               1.045      4   5.562 1.26e-06 ***
s(I(DistTo125m/1000))         3.571      4  56.435  < 2e-16 ***
s(I(DistTo300m/1000))         3.767      4 116.979  < 2e-16 ***
s(ClimSST)                    3.844      4  26.599  < 2e-16 ***
s(log10(pmax(ClimEKE, 1e-04))) 3.410      4  29.374  < 2e-16 ***
---
Signif. codes:  0 '***' 0.001 '**' 0.01 '*' 0.05 '.' 0.1 ' ' 1

R-sq.(adj) =  0.0563   Deviance explained = 31.5%
-REML =  11135  Scale est. = 16.506    n = 49799

All predictors were significant. This is the final model.
Creating term plots.
Diagnostic output from gam.check():

Method: REML   Optimizer: outer newton
full convergence after 13 iterations.
Gradient range [-0.000490583,0.000439745]
(score 11134.63 & scale 16.50598).
Hessian positive definite, eigenvalue range [0.3793321,6338.475].
Model rank =  25 / 25

Basis dimension (k) checking results. Low p-value (k-index<1) may
indicate that k is too low, especially if edf is close to k'.

                                 k'   edf k-index p-value
s(log10(Depth))               4.000 3.887   0.769    0.02
s(log10(Slope))               4.000 1.045   0.789    0.28
s(I(DistTo125m/1000))         4.000 3.571   0.766    0.01
s(I(DistTo300m/1000))         4.000 3.767   0.763    0.00
s(ClimSST)                    4.000 3.844   0.771    0.01
s(log10(pmax(ClimEKE, 1e-04))) 4.000 3.410   0.775    0.06

Predictors retained during the model selection procedure: Depth, Slope, DistTo125m, DistTo300m,
ClimSST, ClimEKE

Predictors dropped during the model selection procedure: ClimDistToFront2
```

Model term plots

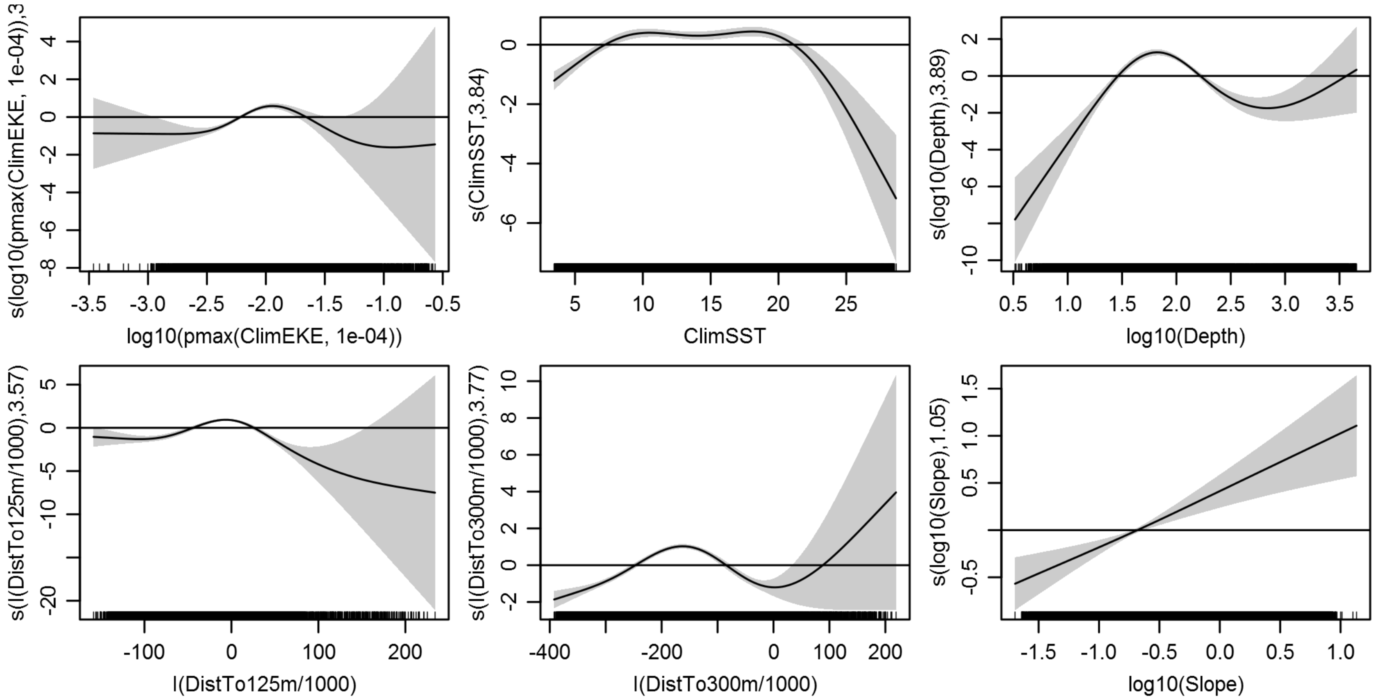

Diagnostic plots

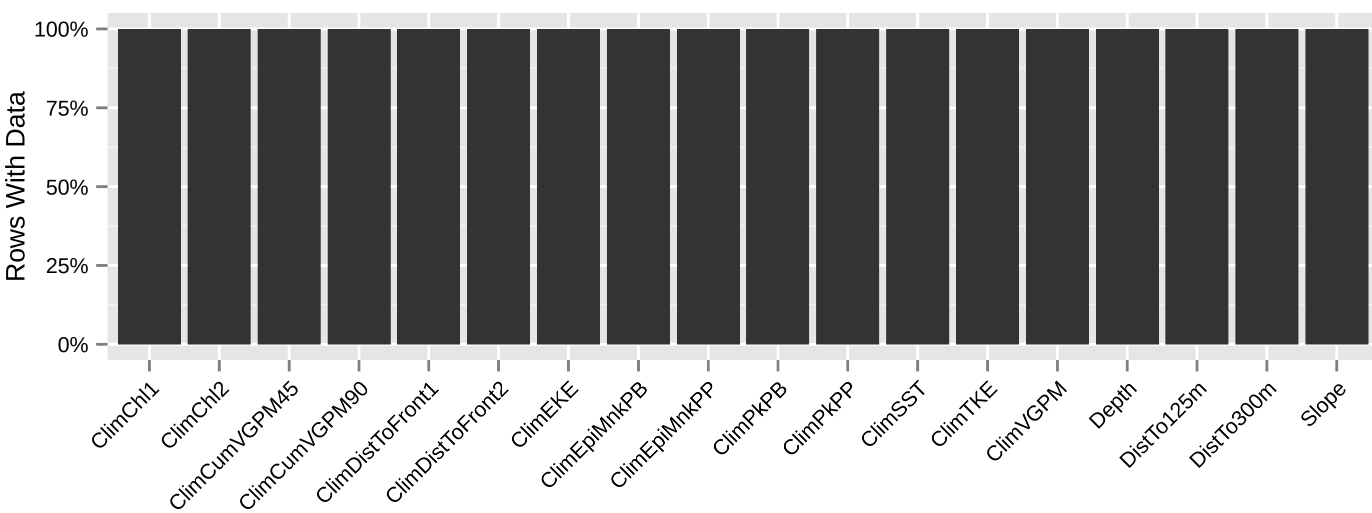

Figure 86: Segments with predictor values for the Humpback whale Climatological model, Summer season, North of Gulf Stream. This plot is used to assess how many segments would be lost by including a given predictor in a model.

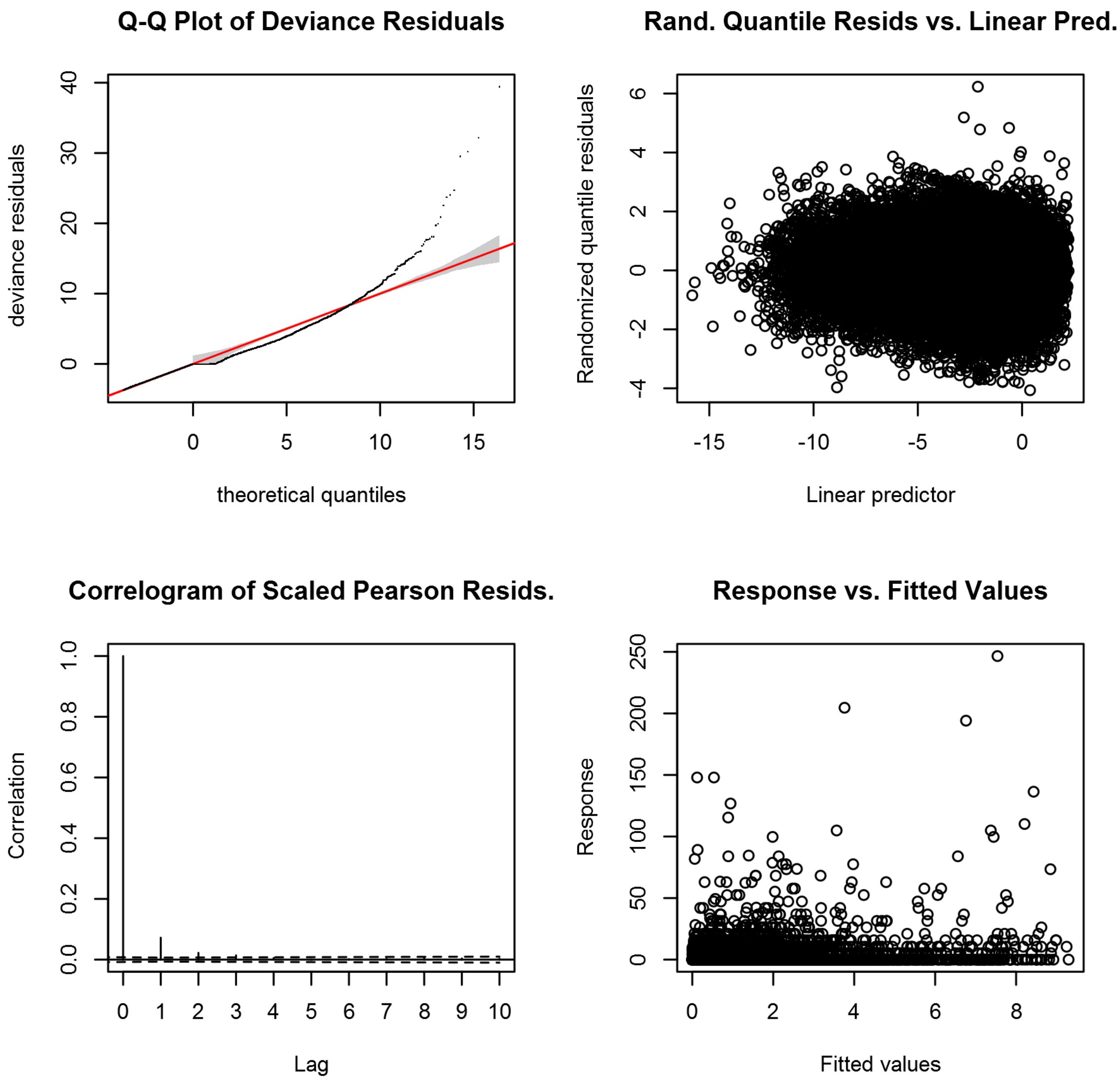

Figure 87: Statistical diagnostic plots for the Humpback whale Climatological model, Summer season, North of Gulf Stream.

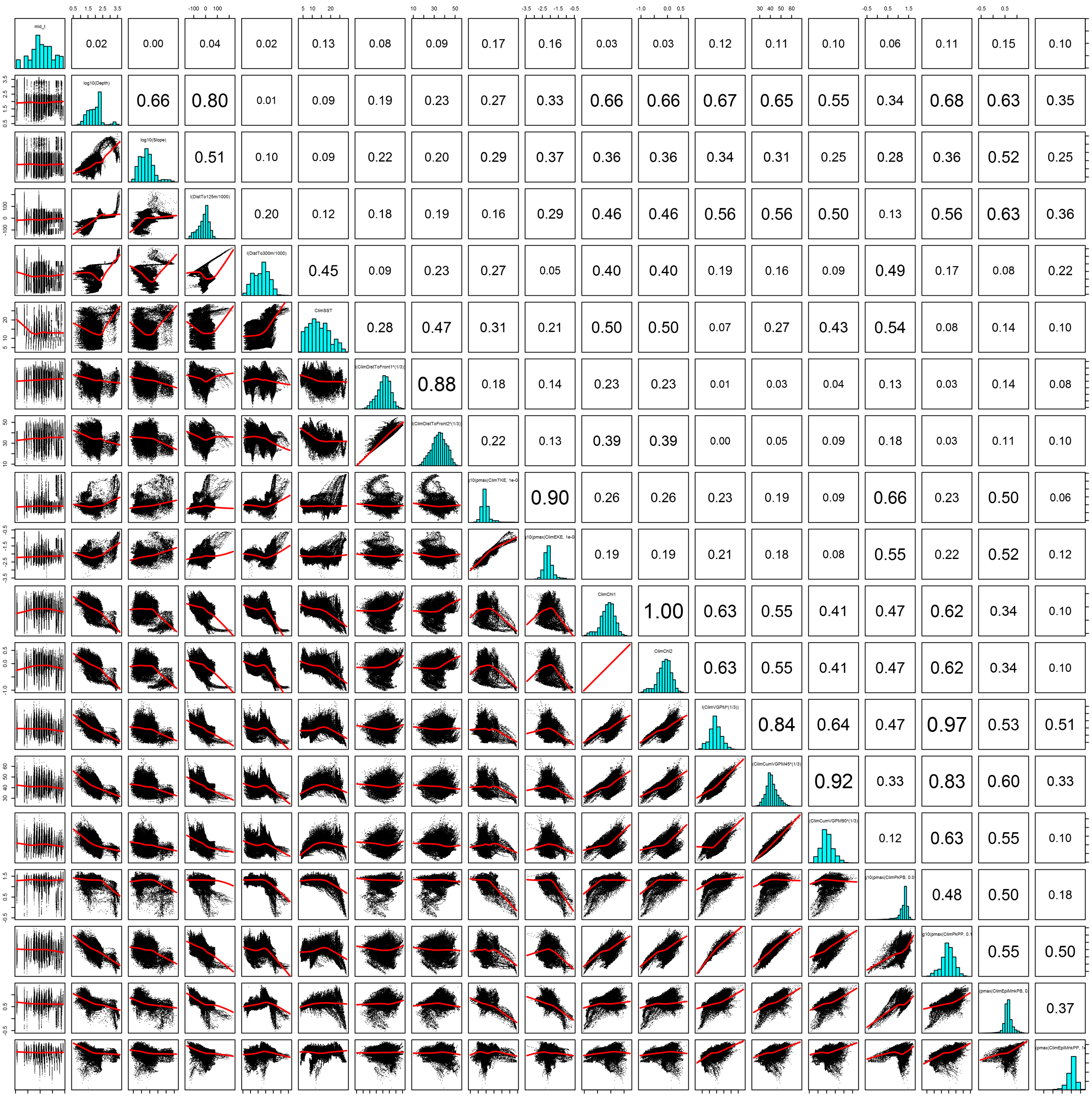

Figure 88: Scatterplot matrix for the Humpback whale Climatological model, Summer season, North of Gulf Stream. This plot is used to inspect the distribution of predictors (via histograms along the diagonal), simple correlation between predictors (via pairwise Pearson coefficients above the diagonal), and linearity of predictor correlations (via scatterplots below the diagonal). This plot is best viewed at high magnification.

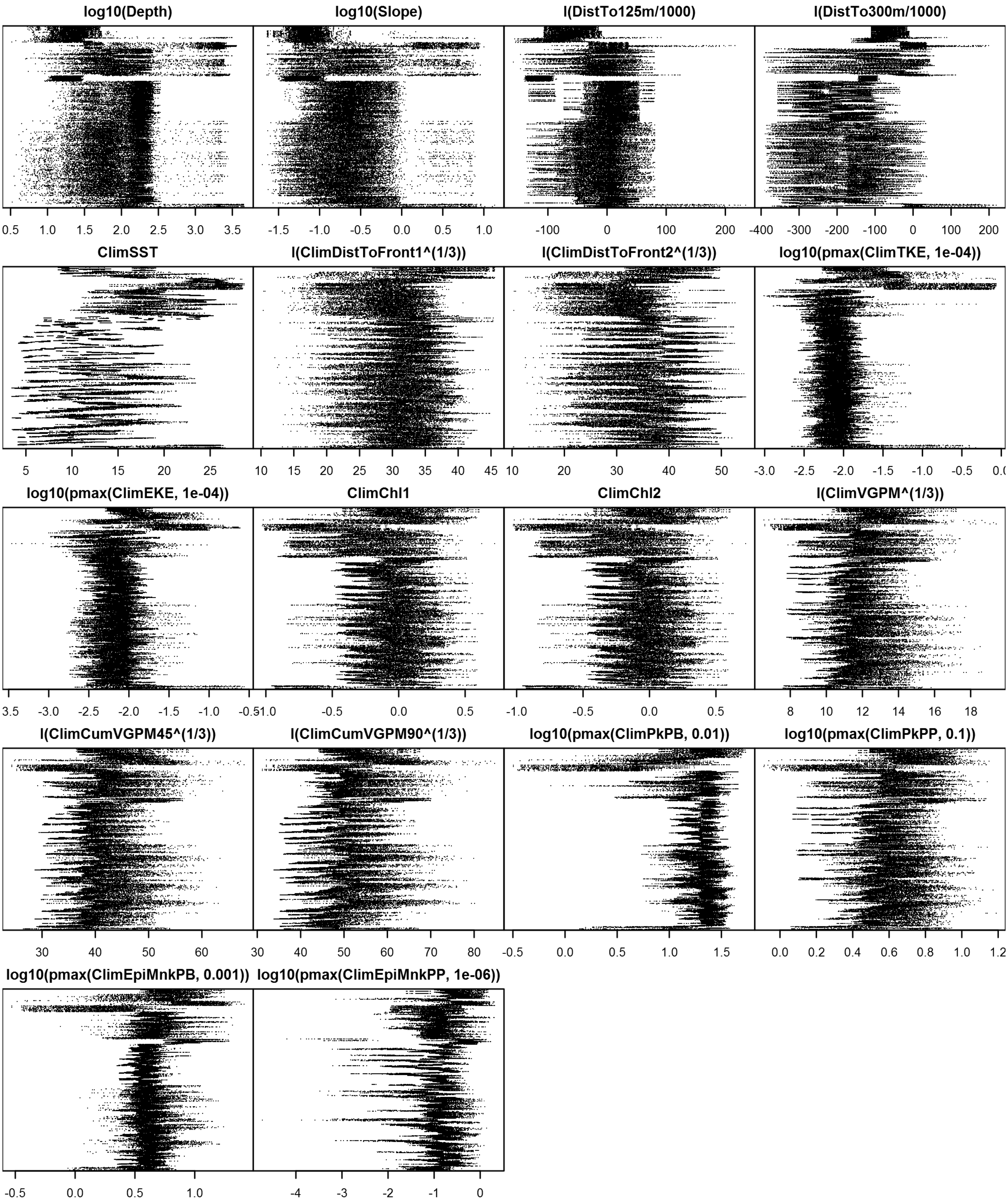

Figure 89: Dotplot for the Humpback whale Climatological model, Summer season, North of Gulf Stream. This plot is used to check for suspicious patterns and outliers in the data. Points are ordered vertically by transect ID, sequentially in time.

South of Gulf Stream

Density assumed to be 0 in this region.

Model Comparison

Spatial Model Performance

The table below summarizes the performance of the candidate spatial models that were tested. For each season, the first model contained only physiographic predictors. Subsequent models added additional suites of predictors of based on when they became available via remote sensing.

For each model, three versions were fitted; the % Dev Expl columns give the % deviance explained by each one. The "climatological" models were fitted to 8-day climatologies of the environmental predictors. Because the environmental predictors were always available, no segments were lost, allowing these models to consider the maximal amount of survey data. The "contemporaneous" models were fitted to day-of-sighting images of the environmental predictors; these were smoothed to reduce data loss due to clouds, but some segments still failed to retrieve environmental values and were lost. Finally, the "climatological same segments" models fitted climatological predictors to the segments retained by the contemporaneous model, so that the explantory power of the two types of predictors could be directly compared. For each of the three models, predictors were selected independently via shrinkage smoothers; thus the three models did not necessarily utilize the same predictors.

Predictors derived from ocean currents first became available in January 1993 after the launch of the TOPEX/Poseidon satellite; productivity predictors first became available in September 1997 after the launch of the SeaWiFS sensor. Contemporaneous and climatological same segments models considering these predictors usually suffered data loss. Date Range shows the years spanned by the retained segments. The Segments column gives the number of segments retained; % Lost gives the percentage lost.

Season	Predictors	Climatol % Dev Expl	Contemp % Dev Expl	Climatol Same Segs % Dev Expl	Segments	% Lost	Date Range
Winter							
	Phys	10.6			31668		1992-2014
	Phys+SST	15.6	14.3	15.6	31668	0.0	1992-2014
	Phys+SST+Curr	16.7	10.6	16.7	31668	0.0	1992-2014
	Phys+SST+Curr+Prod	18.4	15.4	17.8	30357	4.1	1999-2013
Summer							
	Phys	29.3			50288		1995-2014
	Phys+SST	30.4	30.6	30.4	50288	0.0	1995-2014
	Phys+SST+Curr	31.6	30.6	31.5	49799	1.0	1995-2013
	Phys+SST+Curr+Prod	32.3	30.5	31.5	47409	5.7	1998-2013

Table 34: Deviance explained by the candidate density models.

Abundance Estimates

The table below shows the estimated mean abundance (number of animals) within the study area, for the models that explained the most deviance for each model type. Mean abundance was calculated by first predicting density maps for a series of time steps, then computing the abundance for each map, and then averaging the abundances. For the climatological models, we used 8-day climatologies, resulting in 46 abundance maps. For the contemporaneous models, we used daily images, resulting in 365 predicted abundance maps per year that the prediction spanned. The Dates column gives the dates to which the estimates apply. For our models, these are the years for which both survey data and remote sensing data were available.

The Assumed g(0)=1 column specifies whether the abundance estimate assumed that detection was certain along the survey trackline. Studies that assumed this did not correct for availability or perception bias, and therefore underestimated abundance. The In our models column specifies whether the survey data from the study was also used in our models. If not, the study provides a completely independent estimate of abundance.

Season	Dates	Model or study	Estimated abundance	CV	Assumed g(0)=1	In our models
Winter						
	1992-2014	Climatological model*	205	0.16	No	
	1999-2013	Contemporaneous model	422	0.15	No	
	1992-2014	Climatological same segments model	217	0.19	No	
Summer						
	1995-2014	Climatological model*	1637	0.07	No	
	1995-2013	Contemporaneous model	2102	0.04	No	
	1995-2014	Climatological same segments model	1633	0.07	No	
	Jun-Aug 2011	Central Virginia to lower Bay of Fundy (Waring et al. 2014)	335	0.42	No	No
	Jun-Oct 2008	Gulf of Maine and Bay of Fundy photo ID mark- recapture estimate (J. Robbins, pers. comm. cited in Waring et al. 2014)	823			
	August 2006	Southern Gulf of Maine to upper Bay of Fundy and Gulf of St. Lawrence (Waring et al. 2014)	847	0.55	No	Yes
	Jun-Aug 2004	Maryland to Bay of Fundy (Waring et al. 2013)	359	0.75	No	Yes

Table 35: Estimated mean abundance within the study area. We selected the model marked with * as our best estimate of the abundance and distribution of this taxon. For comparison, independent abundance estimates from NOAA technical reports and/or the scientific literature are shown. Please see the Discussion section below for our evaluation of our models compared to the other estimates. Our coefficients of variation (CVs) underestimate the true uncertainty in our estimates, as they only incorporated the uncertainty of the GAM stage of our models. Other sources of uncertainty include the detection functions and g(0) estimates. It was not possible to incorporate these into our CVs without undertaking a computationally-prohibitive bootstrap; we hope to attempt that in a future version of our models.

Density Maps

Climatological Model

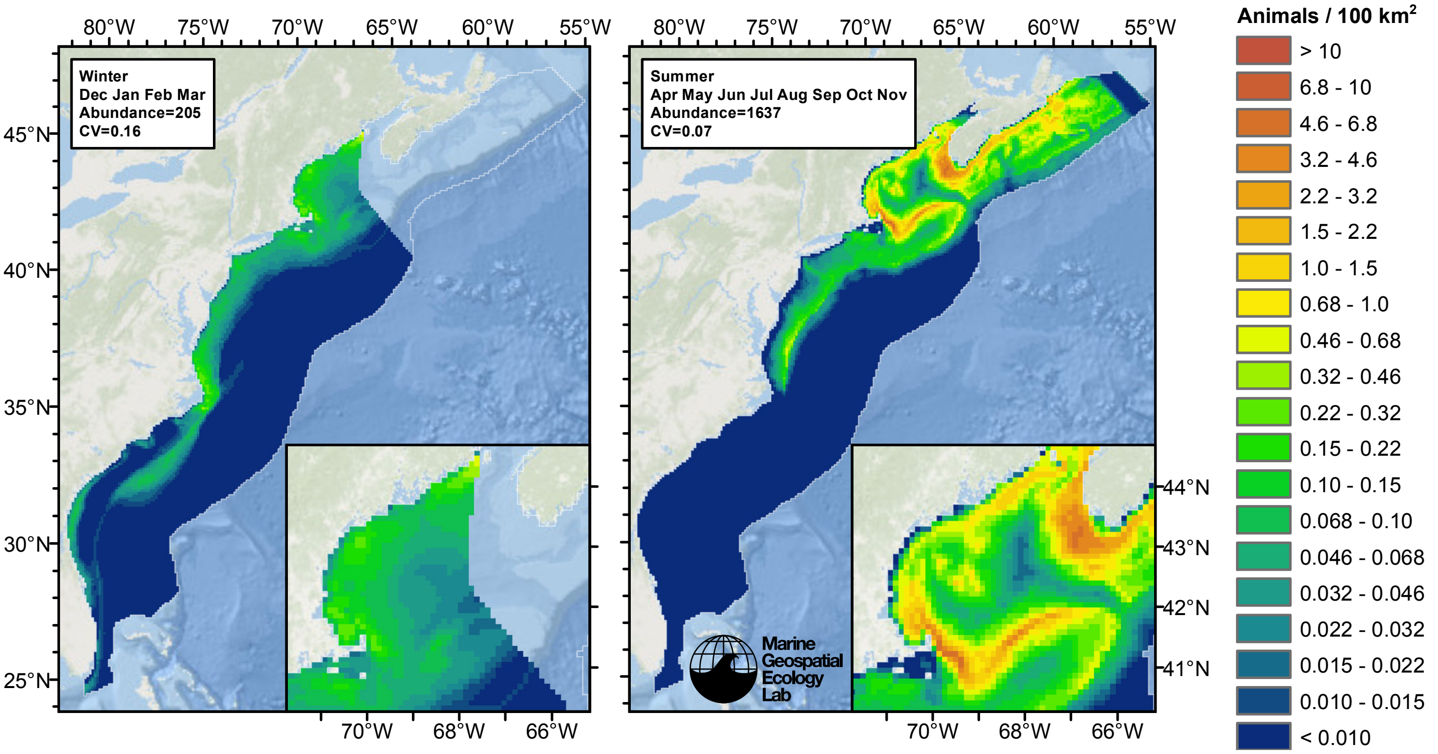

Figure 90: Humpback whale density and abundance predicted by the climatological model that explained the most deviance. Regions inside the study area (white line) where the background map is visible are areas we did not model (see text).

Contemporaneous Model

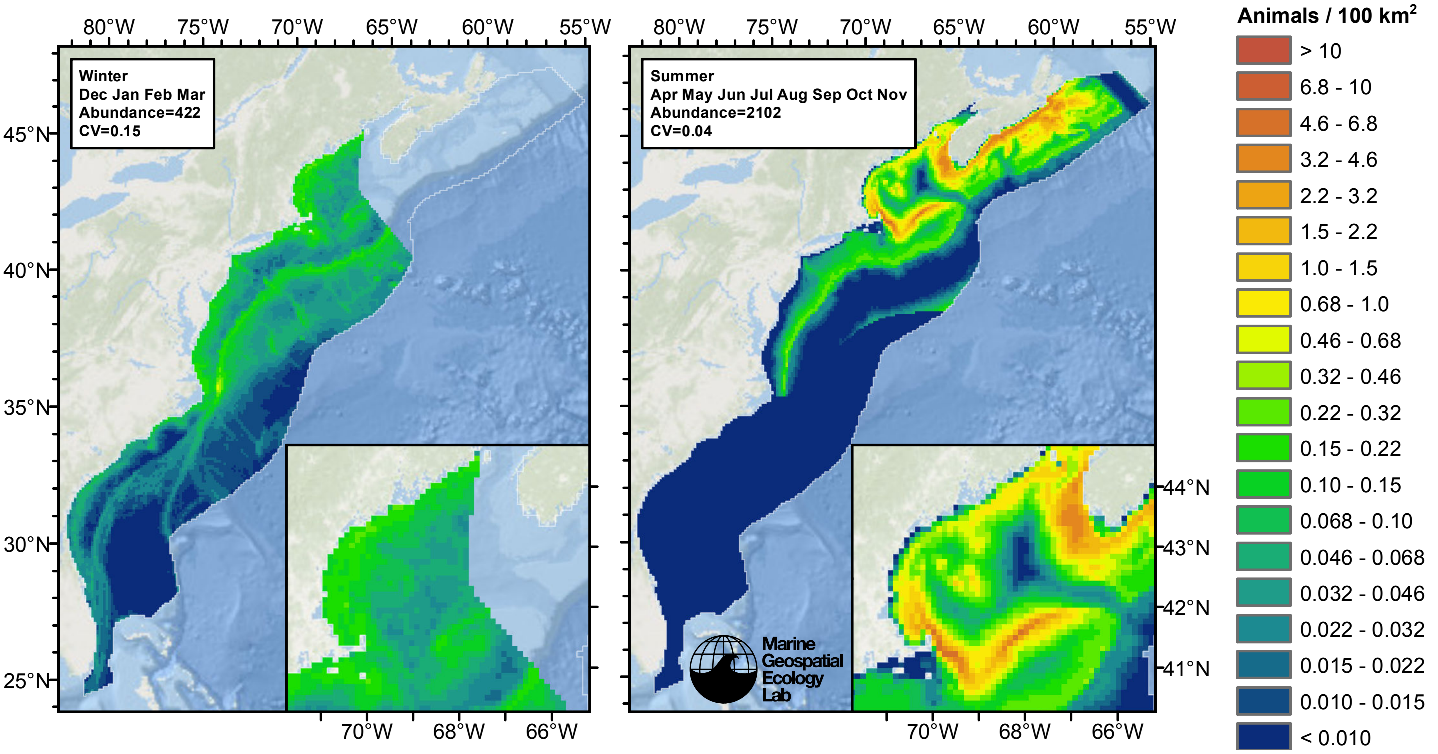

Figure 91: Humpback whale density and abundance predicted by the contemporaneous model that explained the most deviance. Regions inside the study area (white line) where the background map is visible are areas we did not model (see text).

Climatological Same Segments Model

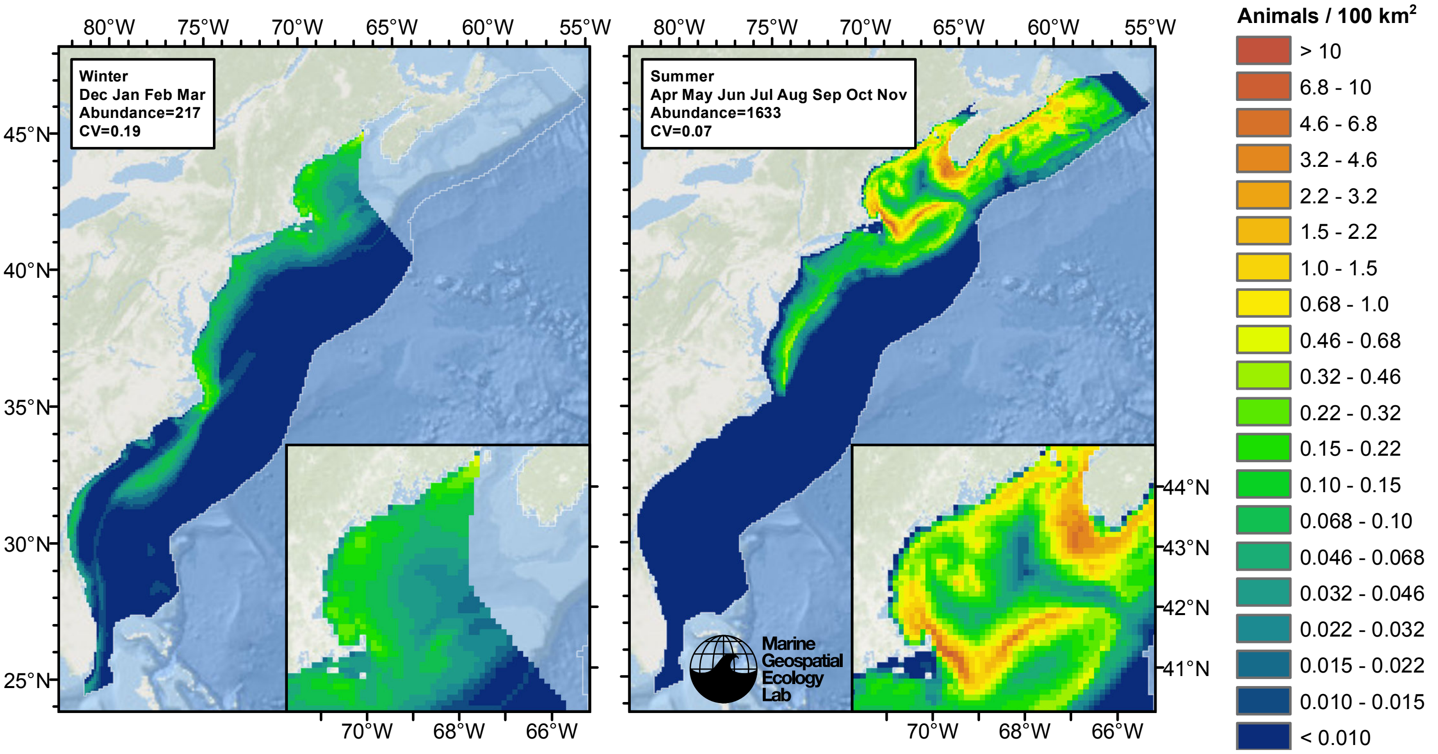

Figure 92: Humpback whale density and abundance predicted by the climatological same segments model that explained the most deviance. Regions inside the study area (white line) where the background map is visible are areas we did not model (see text).

Temporal Variability

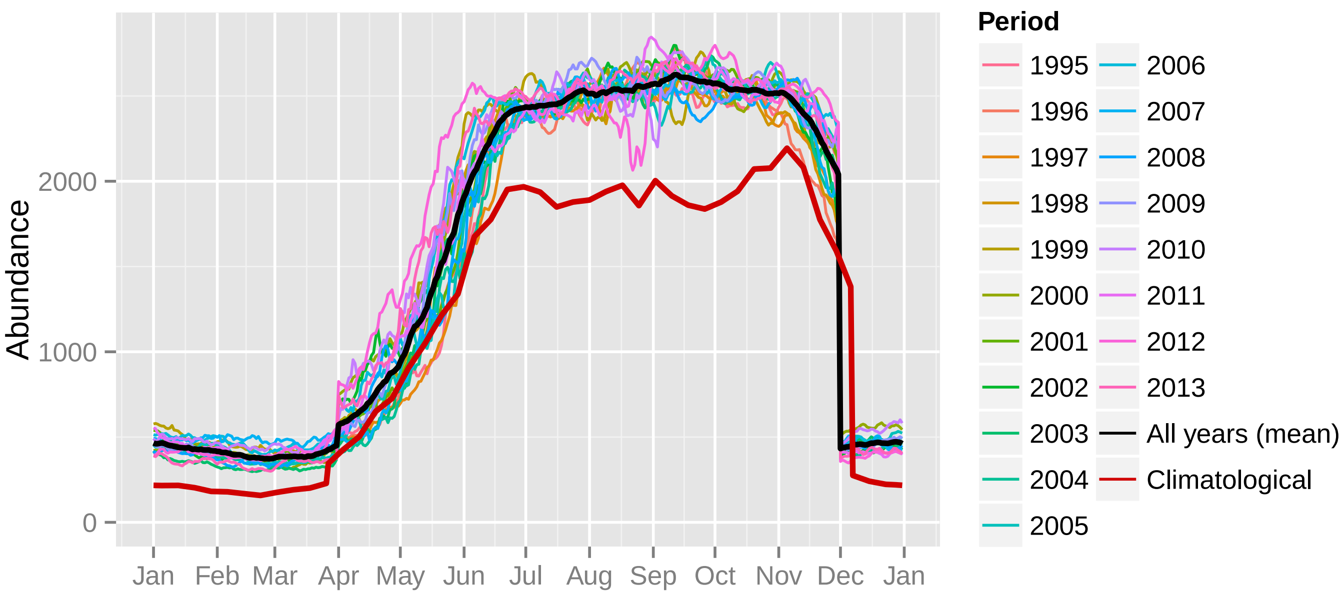

Figure 93: Comparison of Humpback whale abundance predicted at a daily time step for different time periods. Individual years were predicted using contemporaneous models. "All years (mean)" averages the individual years, giving the mean annual abundance of the contemporaneous model. "Climatological" was predicted using the climatological model. The results for the climatological same segments model are not shown.

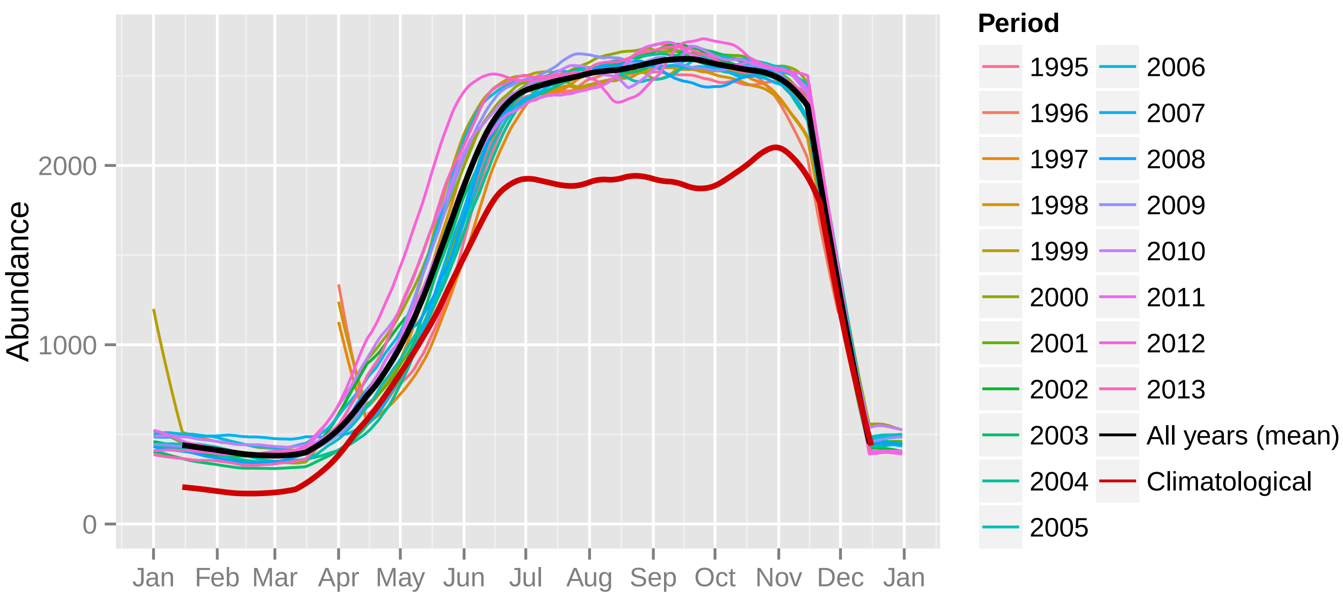

Figure 94: The same data as the preceding figure, but with a 30-day moving average applied.

Climatological Model

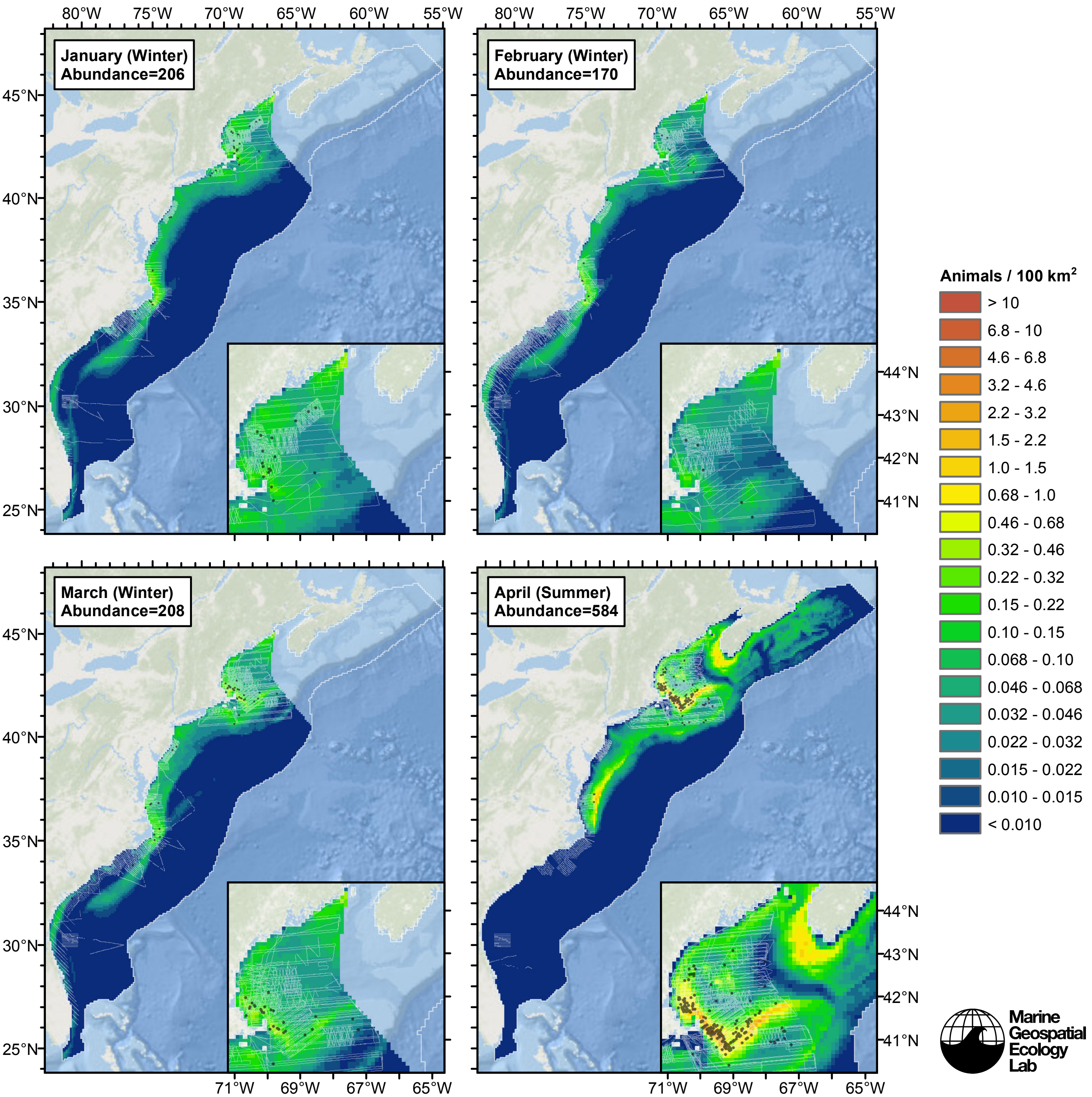

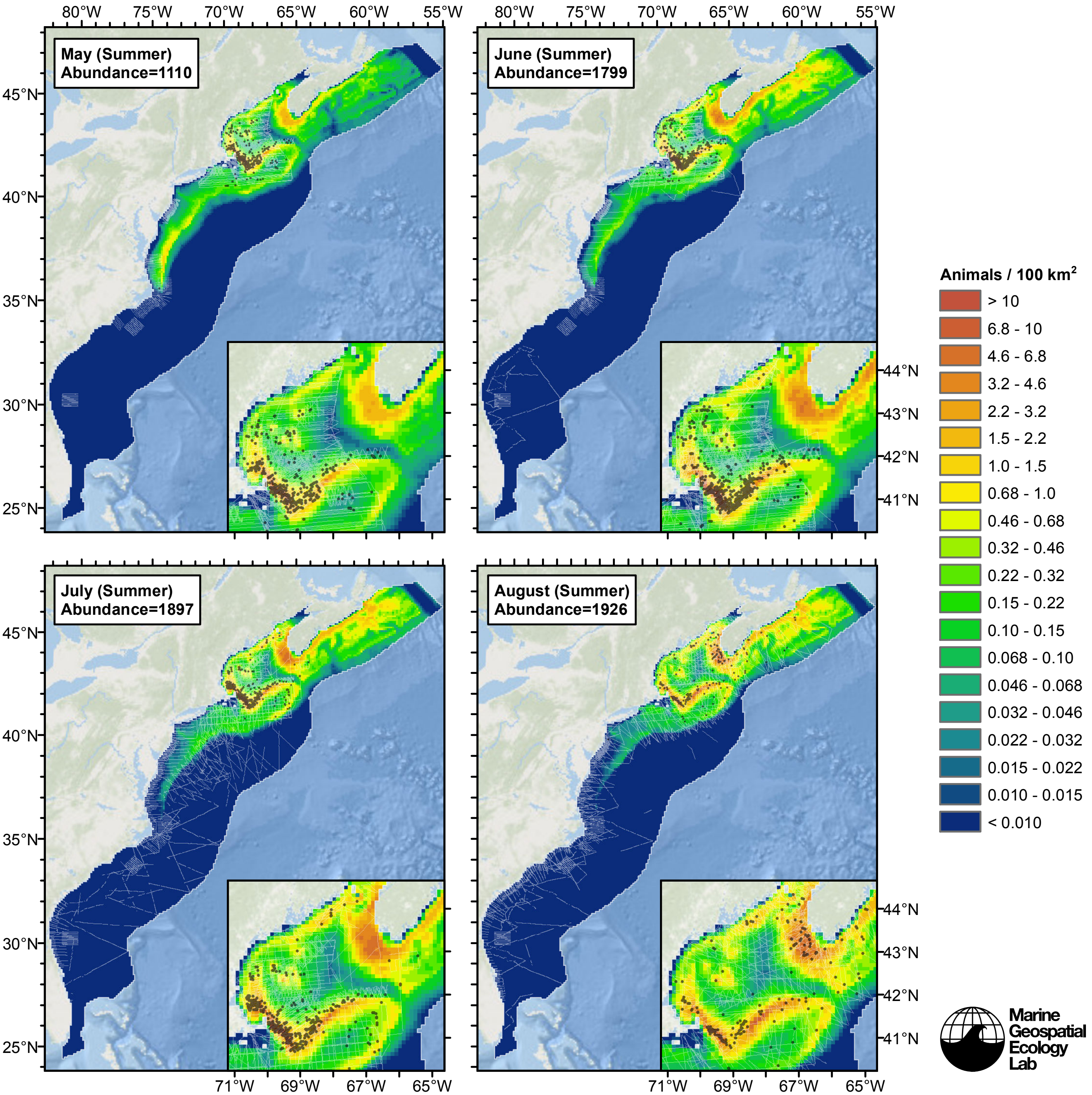
May (Summer)
Abundance=1110
June (Summer)
Abundance=1799
July (Summer)
Abundance=1897
August (Summer)
Abundance=1926
80°W
75°W
70°W
65°W
60°W
55°W
45°N
40°N
35°N
30°N
25°N
44°N
43°N
42°N
41°N
71°W
69°W
67°W
65°W
Animals / 100 km²
> 10
6.8 - 10
4.6 - 6.8
3.2 - 4.6
2.2 - 3.2
1.5 - 2.2
1.0 - 1.5
0.68 - 1.0
0.46 - 0.68
0.32 - 0.46
0.22 - 0.32
0.15 - 0.22
0.10 - 0.15
0.068 - 0.10
0.046 - 0.068
0.032 - 0.046
0.022 - 0.032
0.015 - 0.022
0.010 - 0.015
< 0.010
Marine Geospatial Ecology Lab

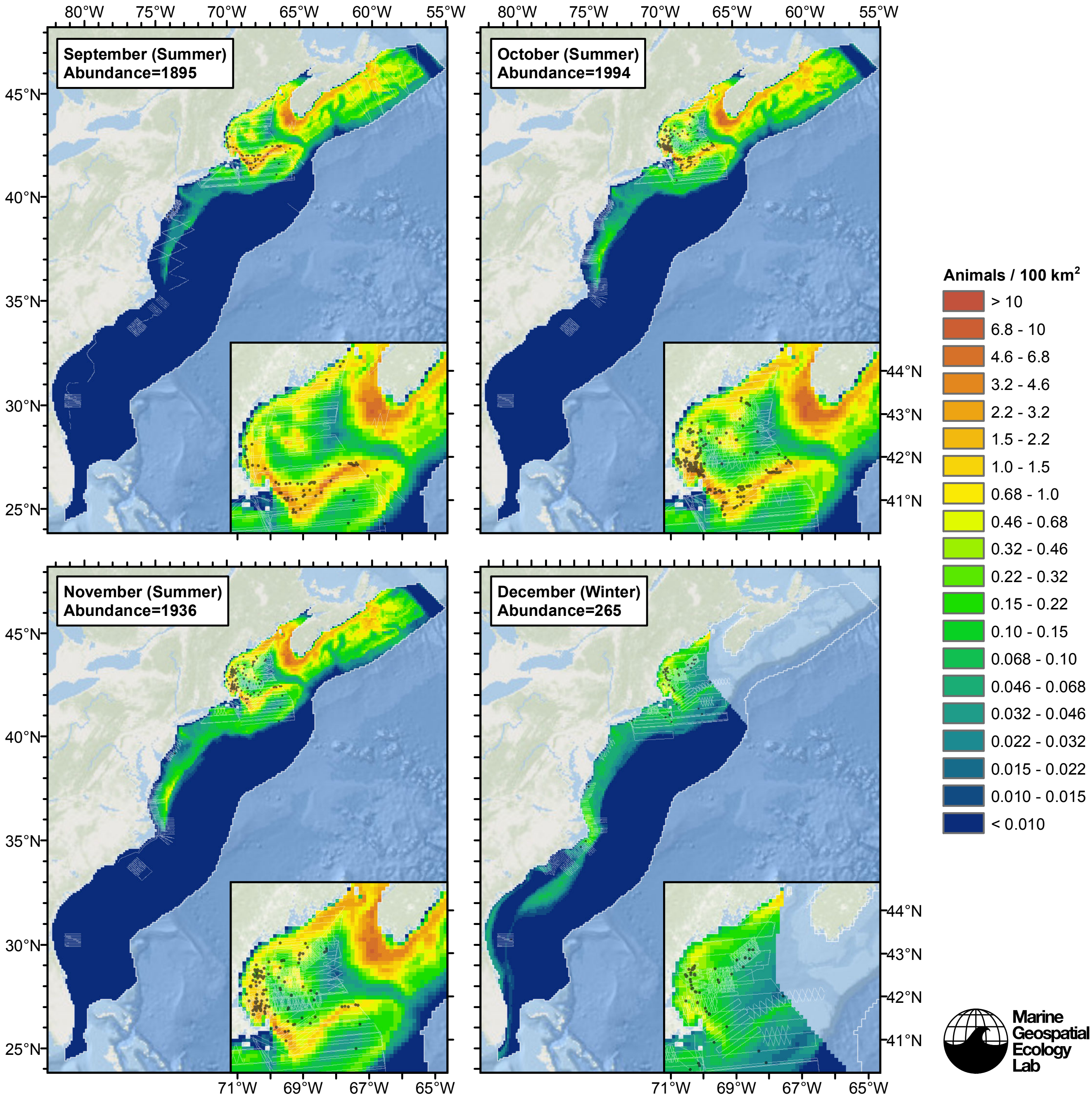

September (Summer)
Abundance=1895
October (Summer)
Abundance=1994
November (Summer)
Abundance=1936
December (Winter)
Abundance=265
80°W
75°W
70°W
65°W
60°W
55°W
45°N
40°N
35°N
30°N
25°N
44°N
43°N
42°N
41°N
71°W
69°W
67°W
65°W
Animals / 100 km²
> 10
6.8 - 10
4.6 - 6.8
3.2 - 4.6
2.2 - 3.2
1.5 - 2.2
1.0 - 1.5
0.68 - 1.0
0.46 - 0.68
0.32 - 0.46
0.22 - 0.32
0.15 - 0.22
0.10 - 0.15
0.068 - 0.10
0.046 - 0.068
0.032 - 0.046
0.022 - 0.032
0.015 - 0.022
0.010 - 0.015
< 0.010
Marine Geospatial Ecology Lab

Contemporaneous Model

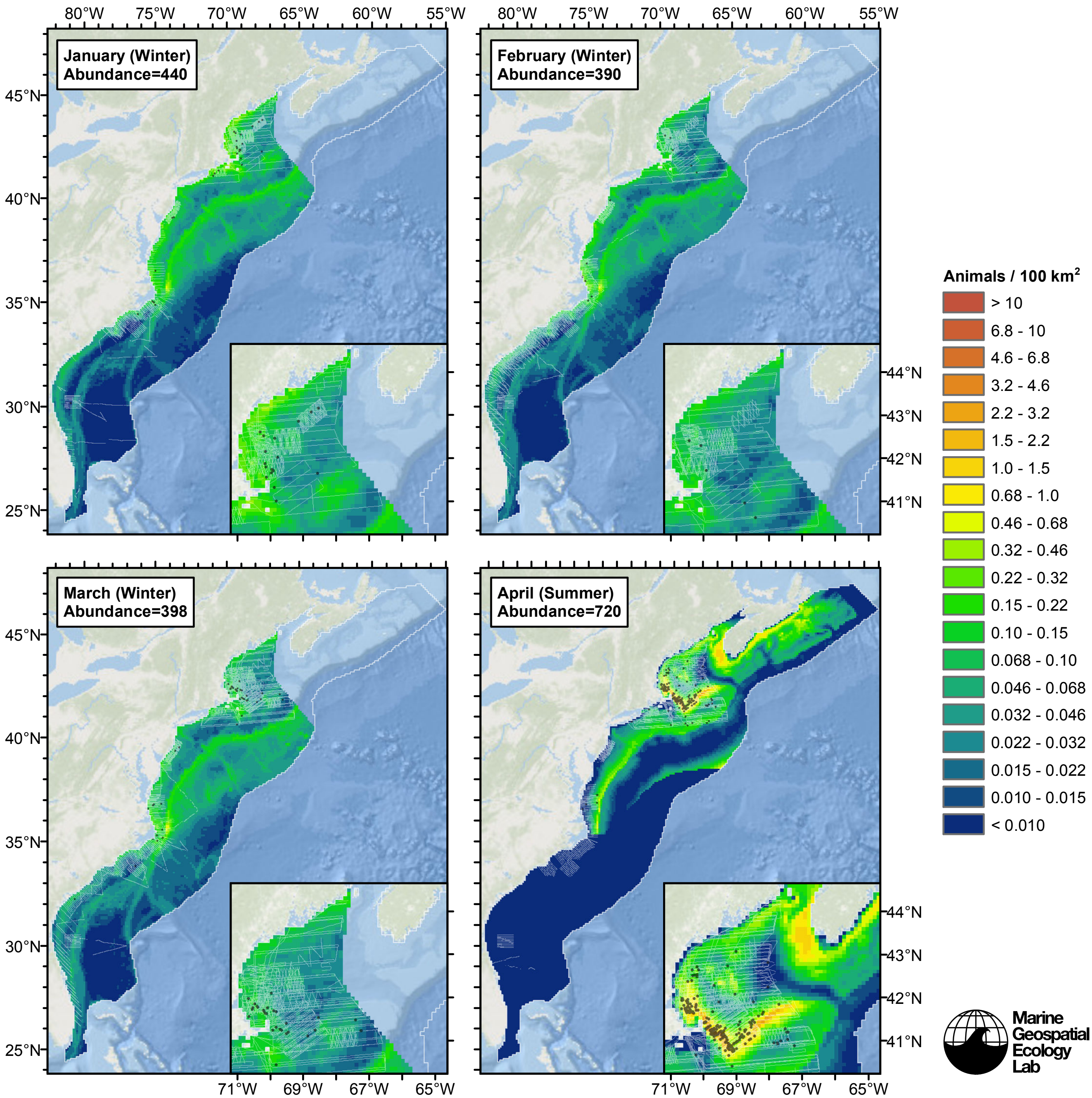

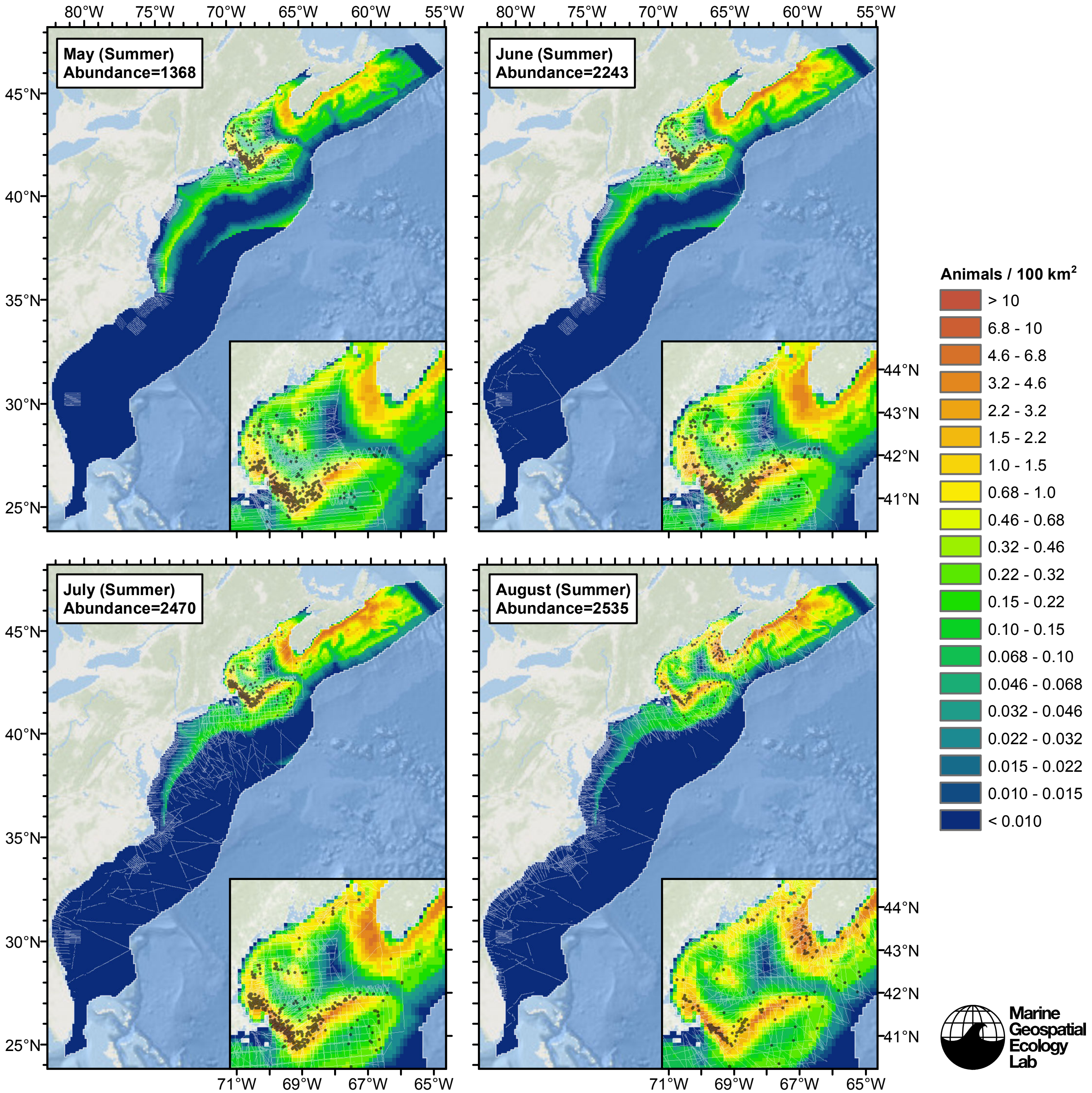

May (Summer)
Abundance=1368
June (Summer)
Abundance=2243
July (Summer)
Abundance=2470
August (Summer)
Abundance=2535
80°W
75°W
70°W
65°W
60°W
55°W
45°N
40°N
35°N
30°N
25°N
44°N
43°N
42°N
41°N
71°W
69°W
67°W
65°W
Animals / 100 km^2
> 10
6.8 - 10
4.6 - 6.8
3.2 - 4.6
2.2 - 3.2
1.5 - 2.2
1.0 - 1.5
0.68 - 1.0
0.46 - 0.68
0.32 - 0.46
0.22 - 0.32
0.15 - 0.22
0.10 - 0.15
0.068 - 0.10
0.046 - 0.068
0.032 - 0.046
0.022 - 0.032
0.015 - 0.022
0.010 - 0.015
< 0.010
Marine
Geospatial
Ecology
Lab

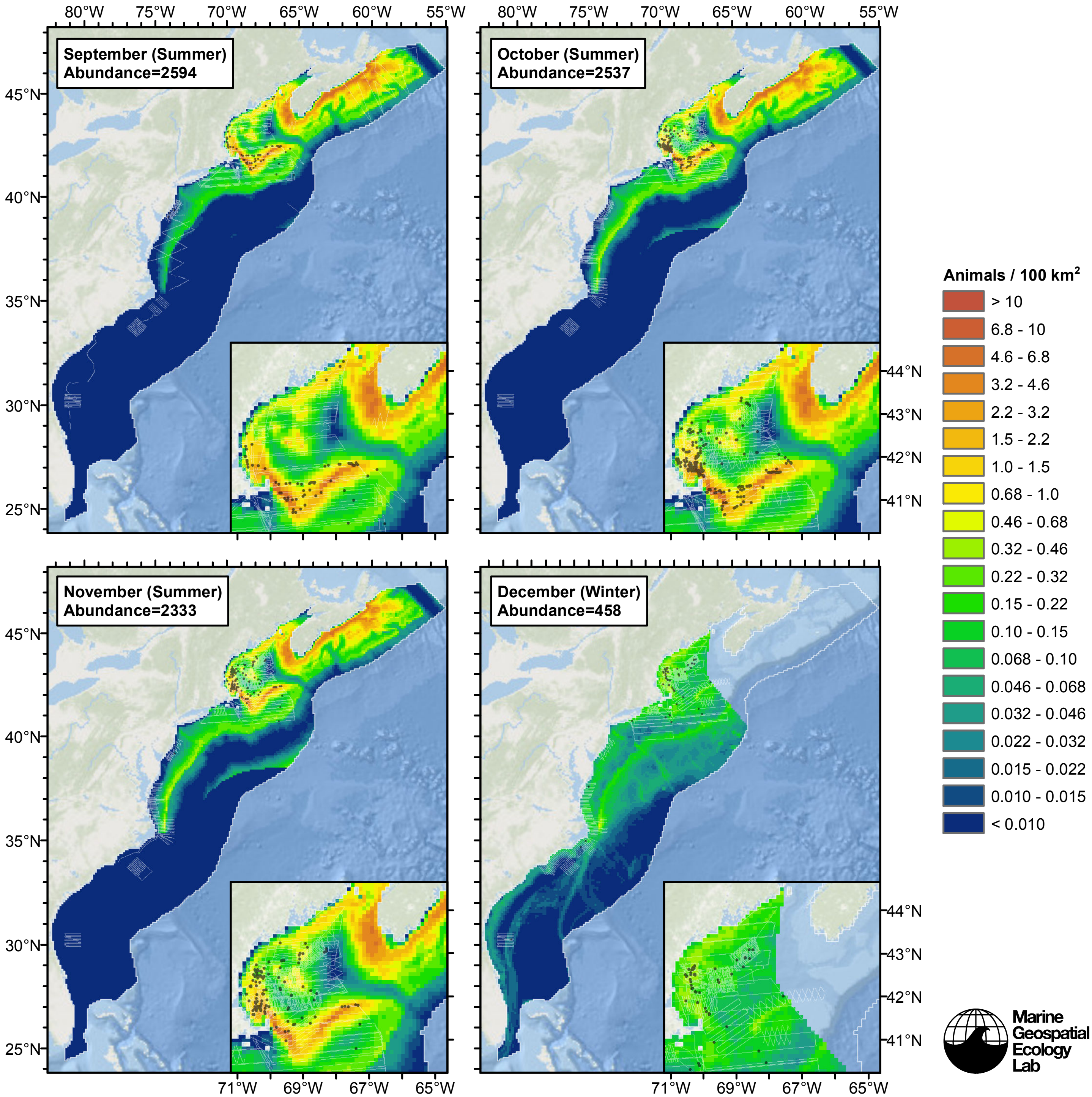
September (Summer)
Abundance=2594
October (Summer)
Abundance=2537
November (Summer)
Abundance=2333
December (Winter)
Abundance=458
80°W
75°W
70°W
65°W
60°W
55°W
45°N
40°N
35°N
30°N
25°N
44°N
43°N
42°N
41°N
71°W
69°W
67°W
65°W
Animals / 100 km²
> 10
6.8 - 10
4.6 - 6.8
3.2 - 4.6
2.2 - 3.2
1.5 - 2.2
1.0 - 1.5
0.68 - 1.0
0.46 - 0.68
0.32 - 0.46
0.22 - 0.32
0.15 - 0.22
0.10 - 0.15
0.068 - 0.10
0.046 - 0.068
0.032 - 0.046
0.022 - 0.032
0.015 - 0.022
0.010 - 0.015
< 0.010
Marine Geospatial Ecology Lab

Climatological Same Segments Model

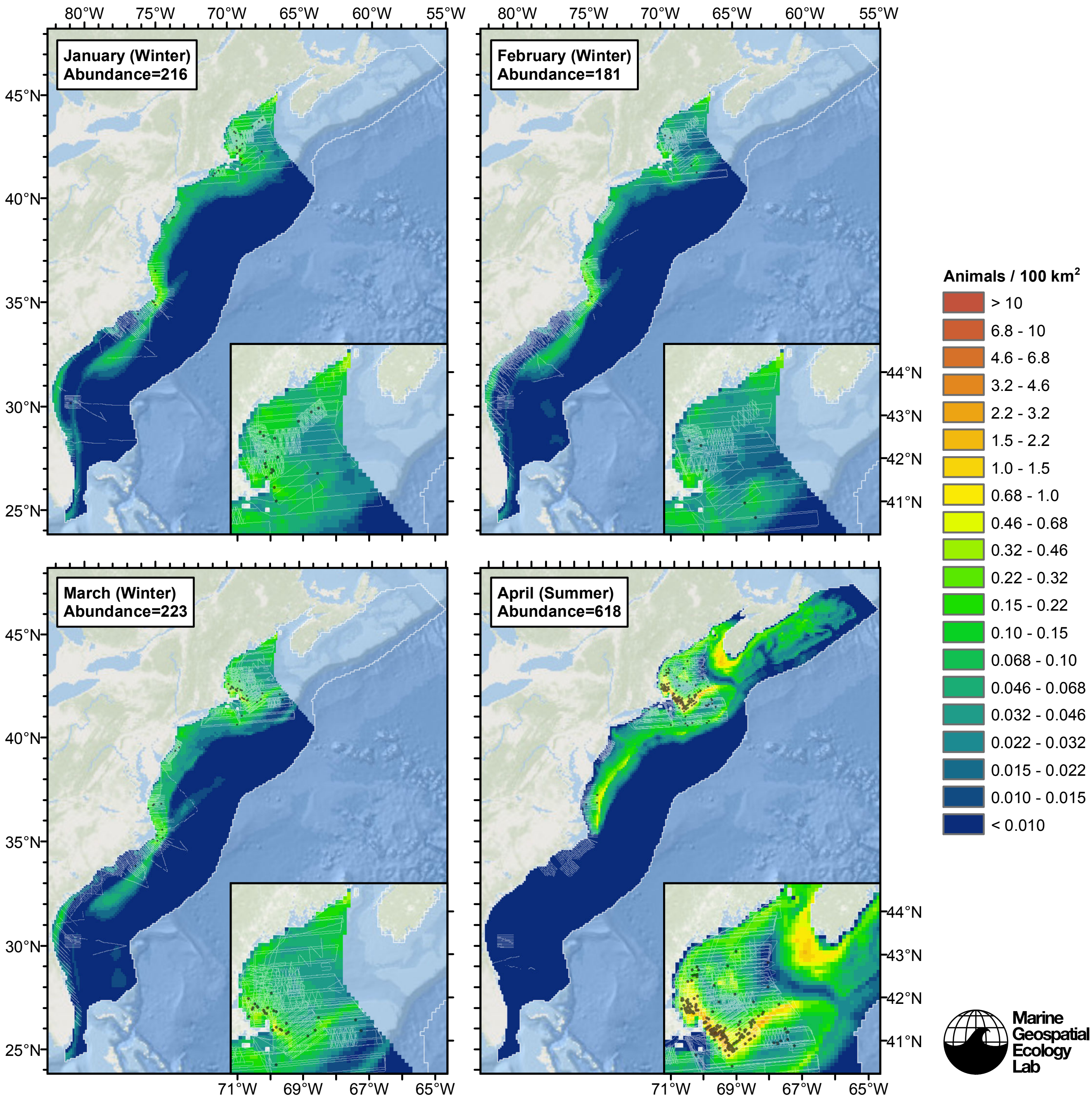

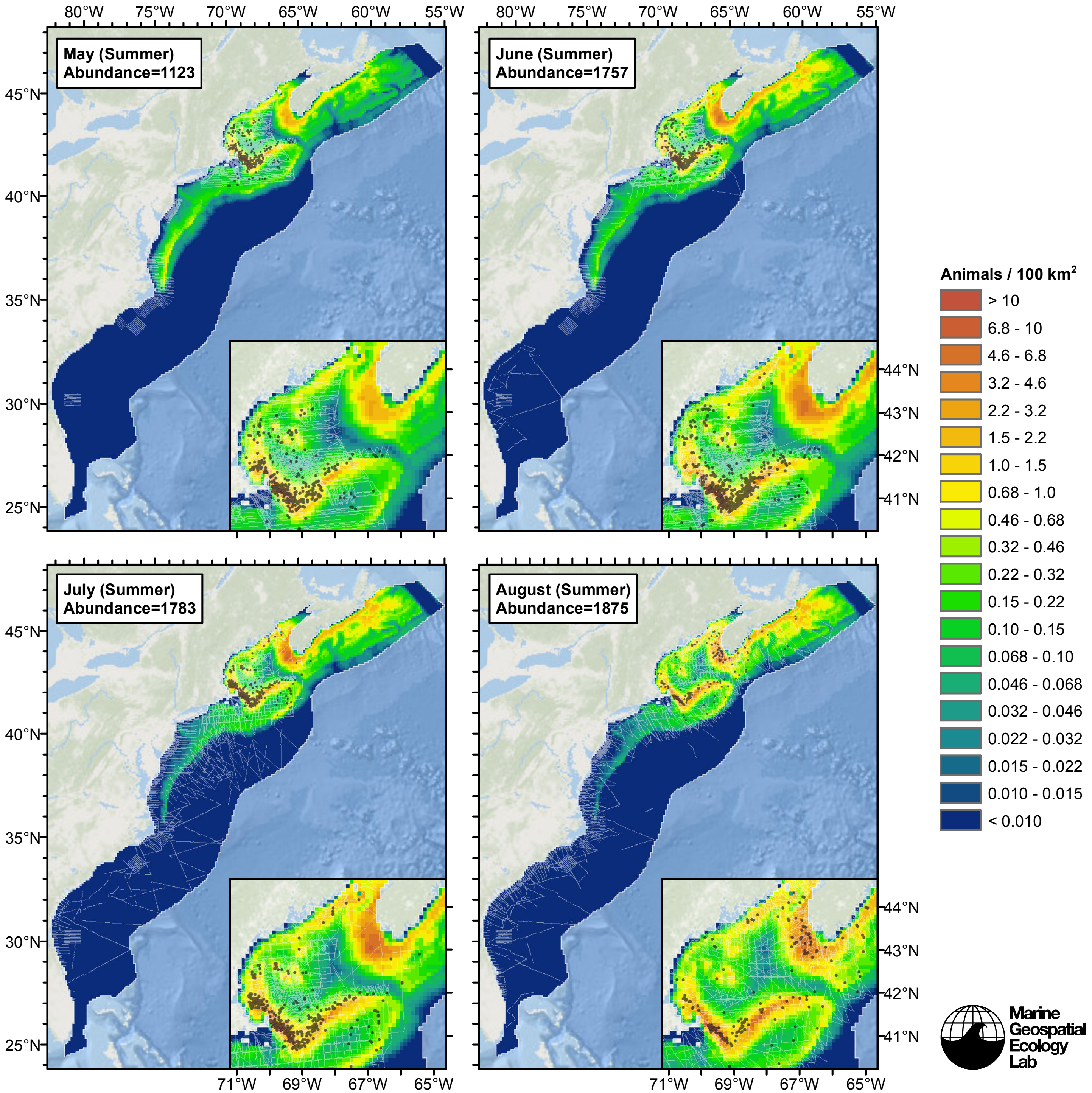
May (Summer)
Abundance=1123
June (Summer)
Abundance=1757
July (Summer)
Abundance=1783
August (Summer)
Abundance=1875
80°W 75°W 70°W 65°W 60°W 55°W
45°N 40°N 35°N 30°N 25°N
44°N 43°N 42°N 41°N
71°W 69°W 67°W 65°W
Animals / 100 km²
> 10
6.8 - 10
4.6 - 6.8
3.2 - 4.6
2.2 - 3.2
1.5 - 2.2
1.0 - 1.5
0.68 - 1.0
0.46 - 0.68
0.32 - 0.46
0.22 - 0.32
0.15 - 0.22
0.10 - 0.15
0.068 - 0.10
0.046 - 0.068
0.032 - 0.046
0.022 - 0.032
0.015 - 0.022
0.010 - 0.015
< 0.010
Marine Geospatial Ecology Lab

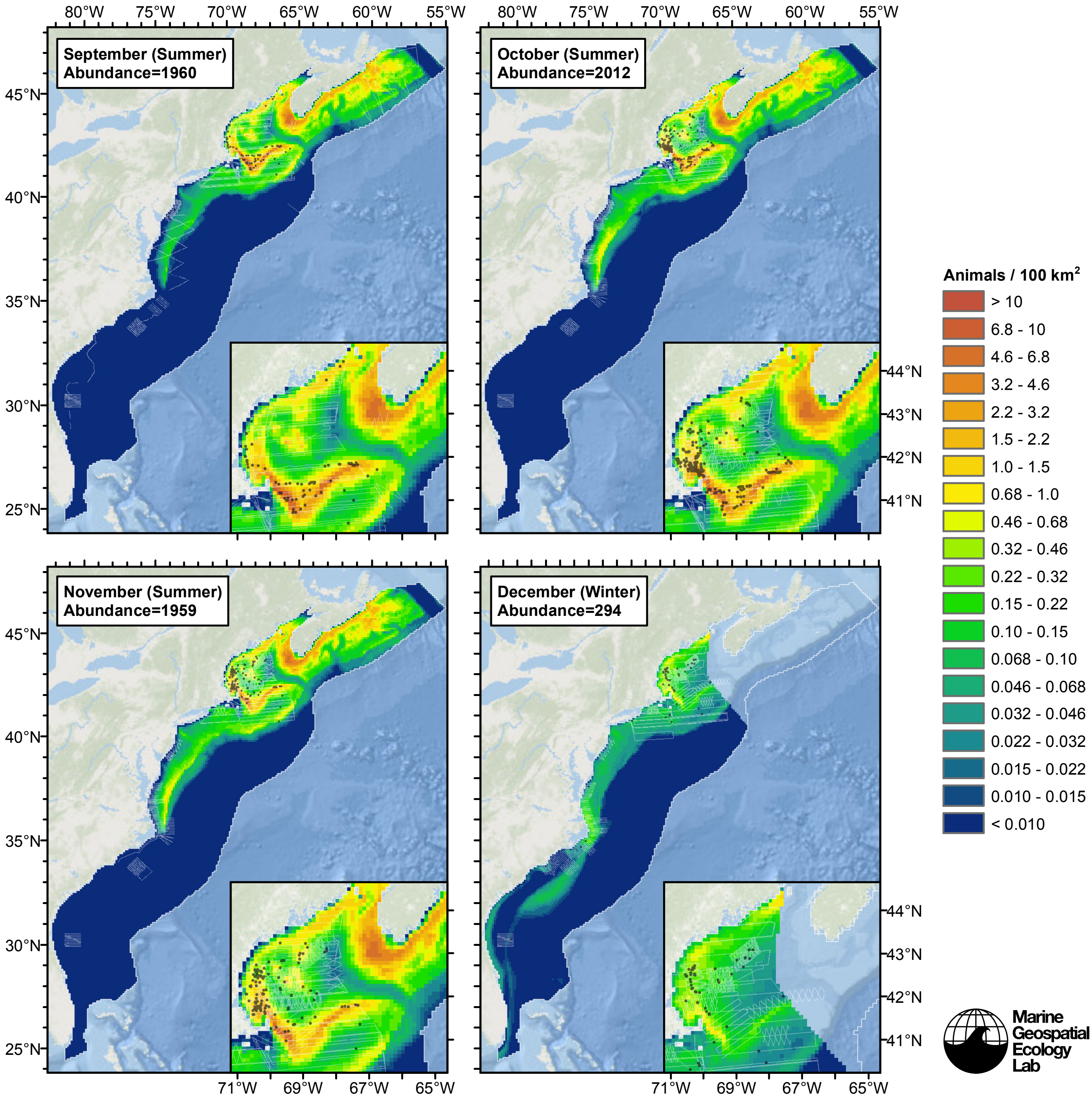

Discussion

Winter

In this season, the two climatological models outperformed the contemporaneous models for each suite of predictors we tested. The two climatological models predicted humpbacks on the shelf throughout the study area, but not off the shelf. In contrast, the contemporaneous model predicted them both on and off the shelf, in roughly same the density.

This latter off-shelf prediction is not supported by our data: although survey effort was sparse in winter, no sightings were reported off the shelf in any season, except near the shelf break. CETAP (1982) conducted several years of surveys in all seasons, both on and off the shelf, and reported no off-shelf sightings away from the shelf break in any season. Finally, Kennedy et al. (2014) tracked several humpbacks by satellite during their migrations from Caribbean breeding grounds to northern feeding grounds and classified their behavioral states as either "transit" or "area restricted search" (ARS) at 12 h intervals. Although the sample size is small, all of the humpbacks exhibited consistent linear travel from the breeding to feeding grounds during their migrations. Of ~13 whales tracked at least partially during migration, only three switched from transit behavior to ARS, with a total of only six 12 h intervals classified as ARS between them. This evidence collectively suggests that humpbacks do not occupy waters far off-shelf during winter except while transiting these waters during migration.

Given the lower explanatory power of the contemporaneous model and its unsupported prediction of abundance off the shelf, we selected the climatological model that considered all segments as our best estimate of humpback distribution and abundance during this season. We chose this model over the climatological model that considered the same segments as the contemporaneous model because the latter model considered fewer segments, to no obvious advantage.

In the southeast, aerial surveys and acoustic monitoring studies were conducted simultaneously in three U.S. Navy exercise areas. While the acoustic data could not be incorporated into our models, it can be used to evaluate our season definitions. At Onslow Bay, North Carolina, acoustic monitoring detected humpbacks close to the deep side of the shelf in November-April (Hodge and Read 2014). An instrument deployed in deeper waters farther from the shelf break ("Site E") did not detect humpbacks from August-December, the only months it was deployed (Debich et al. 2014). Instruments were not deployed on the shallow side of the shelf break at Onslow Bay. A similar study near Cape Hatteras deployed an instrument on the deep side of the shelf break during March and April and did not report any humpbacks (Stanistreet et al. 2013). Finally, a similar study near Jacksonville, Florida deployed instruments on both sides of the shelf break and reported humpbacks on the shallow side in March, with one song in April (Johnson et al. 2014).

While these data generally support our season definitions, the acoustic and visual datasets together suggest that humpback migrations may be spread out over a long period of time, with different groups of whales departing at different times, or that migrations might start at different times in different years. For example, the acoustic data show humpbacks present as far south as Jacksonville in April, yet the visual surveys show an obvious and dramatic increase in humpback sightings in the Gulf of Maine at the same time. This highlights a central difficulty with our density models: different classes of whales (e.g. juveniles and adults) probably respond to the environment differently, but we lack the information to classify and model them separately. Instead, we assume that the entire population switches behavioral modes at the same time each year (e.g. switching from migration and overwintering to foraging at the March/April boundary) and fit different models based on seasons. Our models may adequately capture the overall distribution of humpbacks but they cannot account for outliers such as individuals still in Jacksonville in April.

Summer

In this season, the three models explained nearly the same amount of deviance when only physiographic and SST-related predictors were considered. When we added predictors related to ocean currents and productivity, the climatological models showed more improvement than the contemporaneous model in terms of explained deviance.

The mean abundance estimated by each of the three models was higher than that estimated by most of the other studies we identified (Table 35), but the geographic coverage of the other studies varied widely, making a direct comparison problematic. The minimum population estimate from the most recent NOAA stock assessment report (Waring et al. 2014) was 823, taken from J. Robbins' (2010) photo ID study. Our estimates were substantially higher, at about 1600 for the climatological models and 2100 for the contemporaneous model.

When we reviewed our results with Robbins in March 2015, she noted that her estimate of 823 only covered the Gulf of Maine while ours also encompassed the Scotian Shelf. While she could not offer an estimate for the Scotian Shelf, she believed our estimate of about 1600 was roughly reasonable for the two regions combined.

In any case, the Scotian Shelf represents an area of relative higher uncertainty. The main spatial difference between our climatological models and our contemporaneous model occurred along the Scotian Shelf, close to shore. This area accounts for the bulk of the difference in the abundance estimates. The two comparative estimates that we obtained for this region from the literature were even farther apart than our models: Palka (2006) estimated 847 humpbacks for the Gulf of Maine and the Scotian Shelf combined, while Lawson and Gosselin (2011, cited by Waring et al. 2014) estimated 2612 for the Scotian Shelf alone. (We were not able to examine this latter estimate in detail, as the paper was not available to us.)

We made several attempts to contact J. Lawson regarding the Canadian TNASS survey used to produce the latter estimate, in the hope of incorporating it into our models to address this question, but we received no response. We remain hopeful that a collaboration can be established in the future, and that the Canadian TNASS data may be incorporated into a new version of our models.

Until then, we consider the climatological model that included all segments our best estimate of humpback distribution and abundance during this season, on the basis of explaining the most deviance while considering the most segments, and because the contemporaneous model predicted a patch of abundance in April-June north of the Gulf Stream far off the shelf that we believe is probably wrong (see maps in the Temporal Variability section). We chose the all-segments climatological model over the model that considered the same segments as the contemporaneous model because the latter model considered fewer segments, to no obvious advantage, and explained less deviance. (We note that the two models' predictions were very similar.)

References

Barlow J, Forney KA (2007) Abundance and density of cetaceans in the California Current ecosystem. Fish. Bull. 105: 509-526.

CETAP (1982) A characterization of marine mammals and turtles in the mid-and north Atlantic areas of the US outer continental shelf. Final Report. Bureau of Land Management, Washington, DC. Ref. AA551-CT8-48.

Chelton DB, Schlax MG, Samelson RM (2011) Global observations of nonlinear mesoscale eddies. Prog. Oceanogr. 91: 167-216.

Debich AJ, Baumann-Pickering A, Sirovic A, Buccowich JS, Gentes ZE, et al. (2014) Passive Acoustic Monitoring for Marine Mammals in the Cherry Point OPAREA 2011-2012. MPL Technical Memorandum #545. Marine Physical Laboratory, Scripps Institution of Oceanography, University of California San Diego, La Jolla, California. 83 p. Available online: http://www.navymarinespeciesmonitoring.us/index.php/download_file/view/660/

Heide-Jorgensen MP, Laidre KL, Hansen RG, Burt ML, Simon M, et al (2012) Rate of increase and current abundance of humpback whales in West Greenland. Journal of Cetacean Research and Management 12: 1-14.

Hodge L, Reed A (2014) Passive Acoustic Monitoring for Marine Mammals in Onslow Bay (multiple documents). Reports by the Duke University Marine Laboratory, Beaufort, North Carolina. Available online: http://www.navymarinespeciesmonitoring.us/reading-room/atlantic/ under Technical Reports.

Johnson SC, Sirovic A, Buccowich JS, Debich AJ, Roche LK, et al. (2014) Passive Acoustic Monitoring for Marine Mammals in the Jacksonville Range Complex 2010. MPL Technical Memorandum #548. Marine Physical Laboratory, Scripps Institution of Oceanography, University of California San Diego, La Jolla, California. 26 p. Available online: http://www.navymarinespeciesmonitoring.us/index.php/download_file/view/660/

Kennedy AS, Zerbini AN, Vazquez OV, Gandilhon N, Clapham PJ, Adam O (2014) Local and migratory movements of humpback whales (Megaptera novaeangliae) satellite-tracked in the North Atlantic Ocean. Can. J. Zool. 92:9-18.

Mattila DK, Clapham PJ, Katona SK, Stone GS (1989) Population composition of humpback whales, Megaptera novaeangliae, on Silver Bank, 1984. Can J Zool. 67: 281-285.

Palka DL (2006) Summer Abundance Estimates of Cetaceans in US North Atlantic Navy Operating Areas. US Dept Commer, Northeast Fish Sci Cent Ref Doc. 06-03: 41 p.

Robbins J (2007) Structure and dynamics of the Gulf of Maine humpback whale population. PhD Thesis, University of St. Andrews, Scotland.

Stanistreet J, Hodge L, Reed A (2013) Passive Acoustic Monitoring for Marine Mammals at Site A in the Cape Hatteras Survey Area, March - April 2012. A report by the Duke University Marine Laboratory, Beaufort, North Carolina. 13 p. Available online: http://www.navymarinespeciesmonitoring.us/index.php/download_file/view/471/

Swingle WM, Barco SG, Pitchford TD, Mclellan WA, Pabst D (1993) Appearance of juvenile humpback whales feeding in the nearshore waters of Virginia. Marine Mammal Science 9: 309-315.

Waring GT, Josephson E, Maze-Foley K, Rosel PE, eds. (2013) U.S. Atlantic and Gulf of Mexico Marine Mammal Stock Assessments – 2012. NOAA Tech Memo NMFS NE 223; 419 p.

Waring GT, Josephson E, Maze-Foley K, Rosel PE, eds. (2014) U.S. Atlantic and Gulf of Mexico Marine Mammal Stock Assessments – 2013. NOAA Tech Memo NMFS NE 228; 464 p.

Wiley DN, Asmutis RA, Pichford TD, Gannon DP (1995) Stranding and mortality of humpback whales, Megaptera novaeangliae, in the mid-Atlantic and southeast United States, 1985-1992. Fishery Bulletin 93: 196-205.